

1-1-2008

Air void characteristics of air-entrained self-consolidating concrete

Mary Ellen Barfield
University of Nevada, Las Vegas

Follow this and additional works at: <https://digitalscholarship.unlv.edu/rtds>

Repository Citation

Barfield, Mary Ellen, "Air void characteristics of air-entrained self-consolidating concrete" (2008). *UNLV Retrospective Theses & Dissertations*. 2369.
<http://dx.doi.org/10.25669/5vu4-nnaw>

This Thesis is protected by copyright and/or related rights. It has been brought to you by Digital Scholarship@UNLV with permission from the rights-holder(s). You are free to use this Thesis in any way that is permitted by the copyright and related rights legislation that applies to your use. For other uses you need to obtain permission from the rights-holder(s) directly, unless additional rights are indicated by a Creative Commons license in the record and/or on the work itself.

This Thesis has been accepted for inclusion in UNLV Retrospective Theses & Dissertations by an authorized administrator of Digital Scholarship@UNLV. For more information, please contact digitalscholarship@unlv.edu.

AIR VOID CHARACTERISTICS OF AIR-ENTRAINED
SELF-CONSOLIDATING CONCRETE

by

Mary Ellen Barfield

Bachelor of Science
United States Air Force Academy
2004

A thesis submitted in partial fulfillment
of the requirement for the

**Master of Science Degree in Engineering
Department of Civil and Environmental Engineering
Howard R. Hughes College of Engineering**

**Graduate College
University of Nevada, Las Vegas
August 2008**

UMI Number: 1460526

INFORMATION TO USERS

The quality of this reproduction is dependent upon the quality of the copy submitted. Broken or indistinct print, colored or poor quality illustrations and photographs, print bleed-through, substandard margins, and improper alignment can adversely affect reproduction.

In the unlikely event that the author did not send a complete manuscript and there are missing pages, these will be noted. Also, if unauthorized copyright material had to be removed, a note will indicate the deletion.

UMI[®]

UMI Microform 1460526

Copyright 2009 by ProQuest LLC.

All rights reserved. This microform edition is protected against unauthorized copying under Title 17, United States Code.

ProQuest LLC
789 E. Eisenhower Parkway
PO Box 1346
Ann Arbor, MI 48106-1346

Copyright by Mary Ellen Barfield 2008
All rights reserved



Thesis Approval
The Graduate College
University of Nevada, Las Vegas

May 30, 2008

The Thesis prepared by

Mary Ellen Barfield


Entitled

Air Void Characteristics of Air-Entrained Self-Consolidating Concrete


is approved in partial fulfillment of the requirements for the degree of

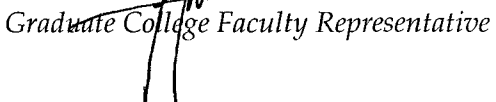
Master of Science in Engineering


Examination Committee Chair


Dean of the Graduate College


Examination Committee Member


Examination Committee Member


Graduate College Faculty Representative


Examination Committee Member

ABSTRACT

Air Void Characteristics of Air-Entrained Self-Consolidating Concrete

by

Mary Ellen Barfield

Dr. Nader Ghafoori, Examination Committee Chair
Professor and Chairman of Civil and Environmental Engineering Department
University of Nevada, Las Vegas

The purpose of this study was to determine the influence of admixture source, slump flow, hauling time and remediation on the air void characteristics of air-entrained self-consolidating concrete (SCC). The first phase of the investigation focused on the effects of four different admixture manufacturers and three distinct slump flows on the fresh flow properties and air void characteristics of SCC. The second phase evaluated the effects of eight hauling times and two forms of remediation on the air void characteristics of three SCC mixtures. The type of high range water reducing admixture and the type of air-entraining agent used significantly influenced the flow properties and air void characteristics of the trial self-consolidating concrete. The air void characteristics deteriorated with increasing slump flow. With increased hauling time, the slump flow decreased and the air void characteristics improved. Remediation typically deteriorated the air void system of self-consolidated concretes when compared to that of the companion non-remediated mixtures.

TABLE OF CONTENTS

ABSTRACT	iii
LIST OF TABLES.....	viii
LIST OF FIGURES	x
ACKNOWLEDGEMENTS.....	xii
CHAPTER 1 INTRODUCTION	1
1.1 Background on Self-Consolidating Concrete	1
1.1.1 Characterization of Self-Consolidating Concrete Mixtures	3
1.1.1.1 Fresh Properties	3
1.1.1.2 Admixtures	4
1.1.1.2.1 High Range Water Reducing Admixtures	4
1.1.1.2.2 Viscosity Modifying Admixtures	7
1.1.1.2.3 Air-Entraining Admixtures.....	7
1.1.1.2.4 Admixture Interactions.....	11
1.2 Frost Durability and Air Void Production.....	11
1.2.1 Mechanisms of Freezing and Thawing Deterioration in Concrete.....	11
1.2.2 Requirements for Freeze-Thaw Durability	13
1.2.2.1 Specific Surface and Spacing Factor of Air Voids.....	13
1.2.2.2 Methods of Measuring Air in Concrete.....	16
1.2.2.2.1 Measuring Total Air Content	18
1.2.2.2.2 Measuring Air Void Characteristics.....	19
1.2.3 Air Void Production	20
1.2.3.1 Effect of AEA Type on Air Void Production.....	21
1.2.3.2 Effects of Slump Flow on Air Void Production	24
1.2.3.3 Effects of Admixture Interactions on Air Void Production	26
1.3 Hauling Time and Air Void Stability	27
1.3.1 Background on Slump Loss.....	28
1.3.2 Effects of Hauling Time on Air Content	29
1.3.3 Definition of Air Void Stability.....	30
1.3.4 Effects of Hauling Time on Air Void Stability	30
1.3.5 Effects of Retempering on Air Void Stability	32
1.4 Research Objectives	33
1.5 Research Significance.....	34

CHAPTER 2 EXPERIMENTAL PROGRAM.....	36
2.1 Mixture Proportioning	36
2.1.1 Cement and Fly Ash	37
2.1.2 Aggregate.....	37
2.1.3 Admixtures	41
2.1.3.1 High Range Water Reducing Admixtures (HRWR)	41
2.1.3.2 Viscosity Modifying Admixtures (VMA)	42
2.1.3.3 Air-Entraining Admixtures (AEA).....	43
2.2 Test Equipment.....	43
2.2.1 Concrete Mixer	43
2.2.2 Air Void Analyzer	45
2.2.2.1 AVA Testing Procedures.....	46
2.2.2.2 Accuracy and Correlation of Results.....	50
2.2.2.3 Advantages and Disadvantages of the Air Void Analyzer	52
2.2.3 Air Content Test	53
2.3 Test Program.....	53
2.3.1 Mixing Sequence	54
2.3.2 SCC Test Methods.....	56
2.3.2.1 Slump Flow and T ₅₀ Tests	56
2.3.2.2 J-Ring Passing Ability Test	57
2.3.2.3 Dynamic Segregation Resistance Test	58
2.3.3 Phase I Procedures.....	59
2.3.3.1 Determination of Optimum Admixture Dosage	60
2.3.3.2 Target Fresh Properties.....	60
2.3.3.3 Hardened Properties	61
2.3.4 Phase II Procedures	62
2.3.4.1 Target Remediation Properties	64
CHAPTER 3 PHASE I: MIXTURE OPTIMIZATION OF AIR-ENTRAINED SELF-CONSOLIDATING CONCRETES.....	66
3.1 Optimized HRWR and VMA Admixture Dosages	66
3.2 Fresh Properties	68
3.2.1 Effects of Admixture Source	71
3.2.2 Effects of Slump Flow.....	73
3.2.3 Predictive Equations of Admixture Dosages.....	75
3.2.4 Air Content	79
3.2.4.1 Effects of Admixture Source on Air Content	79
3.2.4.2 Effects of Slump Flow on Air Content.....	81
3.3 Air Void Characteristics	82
3.3.1 Effects of Admixture Source on Air Void Characteristics.....	84
3.3.2 Effects of Slump Flow on Air Void Characteristics.....	85
3.3.3 Predictive Equations of Air Void Characteristics.....	86
3.3.4 Correlation of Total Air Content to AVA Air Content	87
3.4 Compressive Strength.....	89
3.5 Conclusions	91

CHAPTER 4	PHASE II: EFFECTS OF HAULING TIME ON FRESHLY-MIXED SELF-CONSOLIDATING CONCRETE.....	95
4.1	Effects of Hauling Time on Flow Properties.....	96
4.1.1	Predictive Equations of Slump Flow.....	98
4.1.2	Effects of Hauling Time on Air Content.....	99
4.1.2.1	Effects of Slump Flow on Air Content.....	101
4.1.2.2	Mechanism of the Salt-Type AEA.....	103
4.1.2.3	Entrapped Air.....	104
4.2	Effects of Hauling Time on Air Void Characteristics.....	105
4.2.1	Air Void Distributions.....	108
4.2.2	Effect of AEA Dosage on Air Void Characteristics.....	110
4.2.3	Effect of Slump Flow on Air Void Characteristics.....	111
4.2.4	Predictive Equations of Air Void Characteristics.....	112
4.3	Conclusions.....	112
CHAPTER 5	PHASE II: EFFECTS OF REMEDIATION ON SELF-CONSOLIDATING CONCRETE.....	115
5.1	Remediation A: Overdosing and Under-Dosing Admixtures.....	116
5.1.1	Mixture Proportioning and Fresh Properties.....	116
5.1.2	Admixture Dosages.....	122
5.1.3	Air Void Characteristics.....	127
5.2	Remediation B: Retempering.....	131
5.2.1	Mixture Proportioning and Fresh Properties.....	132
5.2.2	Admixture Dosages.....	135
5.2.3	Air Void Characteristics.....	138
5.3	Comparison of Remediation Techniques.....	142
5.3.1	Admixture Dosages.....	143
5.3.2	Air Content.....	148
5.3.3	Air Void Characteristics.....	150
5.4	Conclusions.....	152
CHAPTER 6	CONCLUSIONS AND RECOMMENDATIONS.....	157
6.1	Effects of Admixture Source and Slump Flow on SCC.....	157
6.1.1	Effects of Admixture Source.....	157
6.1.1.1	High Range Water Reducing Admixture Source.....	157
6.1.1.2	Air-Entraining Admixture Source.....	158
6.1.2	Effects of Slump Flow.....	159
6.1.2.1	Air Void Characteristics.....	160
6.1.2.2	Compressive Strength.....	161
6.2	Effects of Hauling Time on SCC.....	161
6.2.1	Fresh Properties.....	161
6.2.2	Air Void Characteristics.....	163
6.3	Effects of Hauling Time and Remediation on SCC.....	163
6.3.1	Remediation A: Overdosing.....	164
6.3.2	Remediation B: Retempering.....	165
6.3.3	Comparison of Remediation Techniques.....	167

6.3.3.1	Admixture dosages	167
6.3.3.2	Air Content	167
6.3.3.3	Air Void Characteristics	168
6.4	Recommendations on Future Research	168
APPENDIX A CONVERSIONS		170
APPENDIX B ADDITIONAL TABLES AND FIGURES		171
REFERENCES		194
VITA		199

LIST OF TABLES

Table 1.1	Classification and performance characteristics of common air-entraining admixtures	9
Table 1.2	Total air content for frost-resistant concrete (ACI 318-05, Table 4.2.1.).....	16
Table 1.3	Requirements for special exposure conditions (ACI 318-05, Table 4.2.2).....	17
Table 2.1	Basic mixture proportions (excluding admixtures)	37
Table 2.2	Chemical and physical properties of Portland cement and fly ash	38
Table 2.3	Aggregate physical properties	40
Table 2.4	Selected high range water reducers	42
Table 2.5	Selected viscosity modifying admixtures	42
Table 2.6	Selected air-entraining admixtures	43
Table 2.7	Visual Stability Index (ASTM C 1611).....	59
Table 2.8	Mixture identification	59
Table 2.9	Phase I target fresh properties	61
Table 2.10	Phase II Remediation Target Fresh Properties	64
Table 3.1	Phase I mixture constituents and proportions.....	67
Table 3.2	Phase I fresh properties.....	68
Table 3.3	VMA-to-HRWR dosage ratios	72
Table 3.4	Average fresh properties by source	73
Table 3.5	HRWR and VMA predictive equations.....	75
Table 3.6	Statistical data for HRWR and VMA equations.....	75
Table 3.7	Statistical data for AEA dosage predictive equation	77
Table 3.8	Actual and calculated HRWR and VMA dosages (ml/kg cementitious materials)	78
Table 3.9	Actual and calculated AEA dosages (ml/kg cementitious materials).....	78
Table 3.10	Statistical data for predictive equations of air void characteristics	87
Table 3.11	Actual and calculated air void characteristics	88
Table 3.12	Phase I compressive strength results	89
Table 3.13	Phase I comparison of admixture manufacturers	93
Table 4.1	Fresh properties of SCC with hauling time	96
Table 4.2	Predictive equations for final slump flow with hauling time	98
Table 4.3	Trend line equations for prediction of air content	102
Table 4.4	Percent entrapped air (AVA % air > 0.35 mm).....	105
Table 4.5	Air void characteristics with respect to hauling time	106
Table 5.1	Target fresh properties for Phase II remediation	116
Table 5.2	B-SF22 Phase II remediation A mixture constituents and proportions ...	117
Table 5.3	B-SF25 Phase II remediation A mixture constituents and proportions ...	118
Table 5.4	B-SF28 Phase II remediation A mixture constituents and proportions ...	119

Table 5.5	B-SF22 Remediation A fresh properties	120
Table 5.6	B-SF25 Remediation A fresh properties	121
Table 5.7	B-SF28 Remediation A fresh properties	121
Table 5.8	Predictive equations for overdosing HRWR from source B	123
Table 5.9	Remediation A: Change in air void characteristics from $t_h = 10$ min.	129
Table 5.10	Remediation A: Change in air void characteristics from respective hauling times.....	130
Table 5.11	Statistical data for predictive equations for remediation A air void characteristics	131
Table 5.12	B-SF22 Remediation B fresh properties.....	133
Table 5.13	B-SF25 Remediation B fresh properties.....	133
Table 5.14	B-SF28 Remediation B fresh properties.....	133
Table 5.15	Remediation B predictive equations of air content	135
Table 5.16	B-SF22 retempered admixture dosages.....	136
Table 5.17	B-SF25 retempered admixture dosages.....	136
Table 5.18	B-SF28 retempered admixture dosages.....	136
Table 5.19	Remediation B: Change in air void characteristics from $t_h = 10$ min.	140
Table 5.20	Remediation B: Change in air void characteristics from respective hauling times.....	141
Table 5.21	Statistical data of predictive equations for remediation B air void characteristics	143
Table 5.22	559 mm slump flow remediation dosage comparison (ml/kg cm)	144
Table 5.23	635 mm slump flow remediation dosage comparison (ml/kg cm)	145
Table 5.24	711 mm slump flow remediation dosage comparison (ml/kg cm)	145
Table 5.25	Statistical data for predictive equations of HRWR remediation dosages.....	147
Table 5.26	559 mm slump flow - calculated versus actual HRWR remediation dosages.....	147
Table 5.27	635 mm slump flow - calculated versus actual HRWR remediation dosages.....	148
Table 5.28	711 mm slump flow - calculated versus actual HRWR remediation dosages.....	148
Table 5.29	Change in air void characteristics from initial mixing time ($t_h = 10$ min.) to average of all hauling times	150
Table 5.30	Change in air void characteristics from respective hauling times	151
Table 5.31	Comparison of remediation techniques	154

LIST OF FIGURES

Figure 1.1	Examples of materials used in regular concrete and self-consolidating concrete by absolute volume (Kosmatka, Kerkhoff and Panarese, 2002).....	3
Figure 1.2	Polycarboxylate molecule (adapted from Daczko and Kerns, 2008)	6
Figure 1.3	Chemical structure of a polycarboxylate polymer (Rixom and Mailvaganam, 1999)	6
Figure 1.4	Air-entrainment molecule schematic: (a) surfactant, (b) distribution of surfactant on air-water interface (from Du and Folliard, 2003; Mindess and Young, 1981).....	10
Figure 1.5	Illustration of spacing factor (Crawford, Wathne and Mullarky, 2003)....	14
Figure 1.6	Correlation between freeze-thaw durability and air content (Cordon and Merrill, 1963).....	17
Figure 1.7	Polished section of air-entrained concrete as seen through a microscope (Kosmatka et al., 2002).....	20
Figure 1.8	AEAs at the cement-air-water interface (adapted from Rixom and Mailvaganam, 1999)	21
Figure 1.9	Chemical compositions of typical AEA agents: abietic acid, the primary component of wood-derived acid salts (left) and orthododecylbenzene sulfonate, the primary component of synthetic detergents (right) (Rixom and Mailvaganam, 1999)	22
Figure 1.10	Theoretical relationship between air content and slump flow (not to scale).....	26
Figure 1.11	Relationship between time, air content and slump of concrete (Kosmatka et al., 2002).....	31
Figure 2.1	Coarse aggregate gradation	39
Figure 2.2	Fine aggregate gradation	40
Figure 2.3	Optimum volumetric coarse-to-fine aggregate ratio	41
Figure 2.4	Laboratory concrete mixer.....	44
Figure 2.5	Concrete mixer speed control box	45
Figure 2.6	Sampling SCC with attachment.....	46
Figure 2.7	Adding water (left) and removing air bubbles (right)	47
Figure 2.8	Magnetic stirring rod (left) and attaching mortar sample to piston (right)	48
Figure 2.9	Adding viscous release liquid to riser column.....	48
Figure 2.10	Bubbles rising in Air Void Analyzer	49
Figure 2.11	Air Void Analyzer test set up	50
Figure 2.12	Spacing factor correlation between ASTM C 457 and AVA (Magura, 1996).....	51
Figure 2.13	Volumetric air content roll-a-meter	54

Figure 2.14	Mixing and hauling sequence	55
Figure 2.15	Slump flow measurement – average of D_1 and D_2 is taken.....	56
Figure 2.16	J-Ring test demonstrating good passing ability	58
Figure 2.17	Compression test machine	62
Figure 3.1	Phase I admixture dosages with respect to manufacturer.....	69
Figure 3.2	Phase I admixture dosages with respect to slump flow.....	70
Figure 3.3	Chemical structure of a polycarboxylate polymer (SIKA ViscoCrete, 2008).....	72
Figure 3.4	Phase I air void characteristics: specific surface (top) and spacing factor (bottom).....	83
Figure 3.5	Phase I air content correlation between Air Void Analyzer and ASTM C 173	88
Figure 3.6	28-day average compressive strength results	90
Figure 4.1	Effects of hauling time on slump flow	97
Figure 4.2	Air content with respect to hauling time	100
Figure 4.3	Volumetric air content versus slump flow.....	102
Figure 4.4	Entrapped air content with respect to slump flow	106
Figure 4.5	Effects of hauling time on air void characteristics	107
Figure 4.6	Typical air void distribution of B-SF22 at 10 minutes (left) and at 90 minutes (right)	109
Figure 4.7	Typical air void distribution of B-SF25 at 10 minutes (left) and at 90 minutes (right)	109
Figure 4.8	Typical air void distribution of B-SF28 at 10 minutes (left) and at 90 minutes (right)	110
Figure 5.1	Remediation A dosage of HRWR admixture with hauling time	123
Figure 5.2	Remediation A: change in HRWR vs. slump loss of all mixtures	124
Figure 5.3	Remediation A dosage of VMA with hauling time	125
Figure 5.4	Remediation A dosage of AEA with hauling time	126
Figure 5.5	Remediation A air void characteristics.....	128
Figure 5.6	Remediation B volumetric air content.....	134
Figure 5.7	Remediation B admixture dosages	137
Figure 5.8	Remediation B: change in HRWR dosage vs. slump loss of all mixtures	138
Figure 5.9	Remediation B air void characteristics.....	139
Figure 5.10	Comparison of total admixture dosages of remediation techniques A and B.....	144
Figure 5.11	Air content comparison of remediation techniques	149
Figure 5.12	Comparison of remediation techniques: predictive equations of air void specific surface (top) and spacing factor (bottom)	153

ACKNOWLEDGEMENTS

I would like to thank my advisor, Dr. Nader Ghafoori for his guidance on this research project and willingness to always listen to my ideas. His focus on excellence allowed me to accomplish more than I wanted to.

Of great importance was the daily help I received from Hamidou Diawara and Patrick Moorehead. Hamidou completed over one year of research in SCC that served as the basis for my project. I would like to thank Hamidou for his willingness to share ideas, offer suggestions or lend a hand in the lab. Without Patrick, his cheery disposition and ability to carry more rocks than I could, I would have never mixed so much concrete. He allowed me to worry about the results, although I always appreciated his input. I would also like to thank Allen Sampson for his tireless efforts to repair the roll-a-meter, among other things.

Finally, I would like to thank my husband, Oliver. Without his support and love of a concrete-covered wife, I would have never been able to complete this research.

CHAPTER 1

INTRODUCTION

Self-consolidating concrete (SCC) was first developed in the 1980's in Japan, quickly spread into Europe, and is most recently being utilized in the United States. This type of concrete, also referred to as self-compacting concrete, has the ability to flow and consolidate under its own weight and is especially designed for areas of heavy reinforcement or complicated formwork. In addition to being highly flowable, the SCC mixture must be cohesive enough to fill any size or shape without segregation or bleeding.

Self-consolidating concrete can be used in various cast-in-place and pre-cast applications where it may be exposed to water and cold temperatures. As a result, it must exhibit the proper freeze-thaw durability properties for those applications under severe conditions. The production of an air-entrained SCC mixture with the proper air void characteristics is critical to ensuring the concrete's long-term durability and resistance to subsequent deterioration.

1.1 Background on Self-Consolidating Concrete

SCC was initially developed in order to reduce the occurrence of under- and over-consolidation in concrete. Insufficient consolidation is detrimental to the overall strength of a concrete structure due to the increase of entrapped air and surface flaws. These defects are especially prevalent near rebar and areas confined by formwork.

Excessive vibration can result in segregation, external and internal bleeding, and the destruction of the air void system, which can affect both the strength and durability of a concrete structure (Bonen and Shah, 2005). To combat these adverse effects that come with mechanical consolidation, SCC was developed to be highly flowable, thus eliminating all problems associated with manually vibrating conventional concrete. The self-consolidation properties also provide a better aesthetic appeal of the finished product due to less bug holes and surface imperfections. There is an improved work environment for employees when placing the concrete due to the lack of noisy vibration equipment. Finally, construction time and cost required for the placement of the concrete is reduced.

Despite all of these positive characteristics and myriad applications in reinforced concrete structural elements, there are some drawbacks to using SCC over conventional concrete. Self-consolidating concrete is typically reserved for difficult pouring situations due to the higher cost of materials, increased dosage of admixtures, complexity of mixture designs, and increased formwork pressure. It can be difficult to maintain SCC at the desired slump flow levels over an extended period of time without the use of a set retarder. Stringent quality control is required for the materials incorporated into an SCC mixture, which may cause contractors to not choose SCC over conventional concrete. In order to reduce costs, SCC has been successfully tested in a variety of different ways that are more economical than the typical SCC mixture. For example, Bosilijkov, Duh and Žarnić (2005) have effectively used less desirable aggregates, and Nehdi, Pardhan and Koshowski (2004) have successfully used a high volume of replacement composite cements in SCC mixtures.

1.1.1 Characterization of Self-Consolidating Concrete Mixtures

1.1.1.1 Fresh Properties

Self-consolidating concrete is characterized by its fresh properties, which are achieved through its unique mixture design. A good SCC mixture should have the following fresh properties: a) high deformability, b) high flow ability, c) resistance to segregation, and d) passing ability (ability to flow through reinforcing bars and other confined spaces) (Bonen and Shah, 2005). Specialized tests have been developed to measure the fresh properties of SCC mixtures, which are described in Section 2.3.2.

The desired flow ability is achieved by altering the concrete mixture proportions. When compared to conventional concrete, SCC mixtures typically contain an increased cement content and an increased percentage of fine materials, as shown in Figure 1.1 (*ME 03-10*, 2003). These fine materials generally come in the form of additional cement or supplementary cementitious materials such as fly ash or silica fume. Changing the

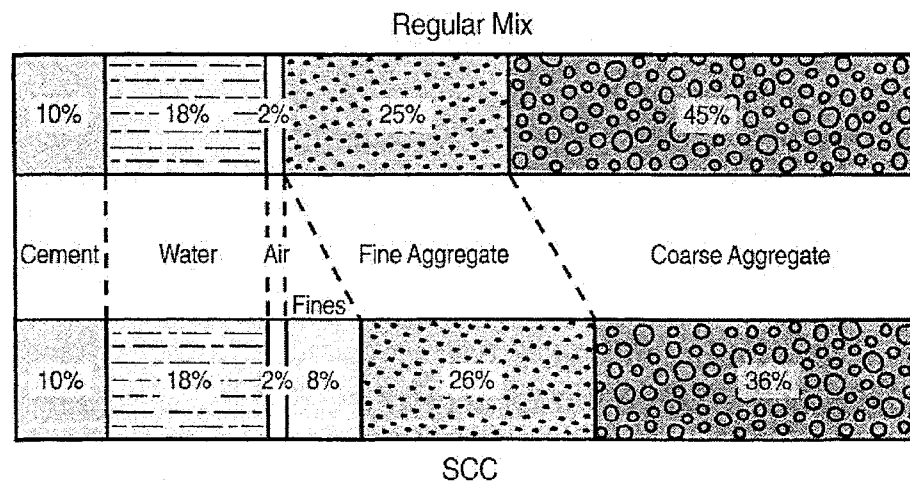


Figure 1.1 Examples of materials used in regular concrete and self-consolidating concrete by absolute volume (Kosmatka, Kerkhoff and Panarese, 2002)

aggregate volume, coarse-to-fine aggregate ratio and the composition of other ingredients can also highly modify the flow characteristics.

One of the main challenges in determining the proportions for an SCC mixture is to maintain stability while achieving the necessary filling and flowing capabilities (Bonen and Shah, 2005). The stability of a mixture is directly related to its viscosity, which is controlled by the content of free water, the superplasticizer, and the volume of the solids in the concrete (Bonen and Shah, 2005). The two main types of SCC, powder-type and VMA-type, are proportioned differently to achieve similar flow characteristics. The powder-type SCC incorporates high amounts of cementitious materials added to the mixture to maintain the proper viscosity, while the VMA-type uses a viscosity modifying admixture (VMA) (Kosmatka et al., 2002). An SCC mixture can also be characterized as a combination of the powder and VMA-types, called moderate-type SCC. The HRWR, VMA and cementitious materials are balanced to achieve the required flow properties.

1.1.1.2 Admixtures

One of the key characterizations of a self-consolidating concrete mixture is the use of admixtures. As previously stated, a high range water reducer, or superplasticizer, is required in all cases to achieve the high flow ability of the concrete. In some cases, a viscosity modifying admixture is also required to achieve stability and resistance to aggregate segregation and bleeding. Finally, an air-entraining admixture is necessary to create a proper air void matrix and to stabilize the air voids.

1.1.1.2.1 High Range Water Reducing Admixtures

High range water reducing admixtures (HRWR), or superplasticizers, are essential to creating self-consolidating concrete mixtures. They create a highly flowable concrete

by increasing the slump characteristics without adding more water. Four types of commonly used superplasticizers are: sulfonated melamine-formaldehyde condensates, sulfonated naphthalene-formaldehyde condensates, naphthalene-lingosulphonate, and polycarboxylate polymers (Rixom and Mailvaganam, 1999). While producing the essential flow characteristics of SCC, the addition of a HRWR admixture can negatively cause segregation, excessive bleeding, loss of entrained air, and a reduction of compressive strength (Dodson, 1990).

The type of HRWR most commonly used has evolved over time as technology has improved the effectiveness and ability to reduce water in a given mixture. The main mechanism by which a superplasticizer reduces the amount of water needed to produce high flow ability is to adsorb onto the surface of cement particles (Rixom and Mailvaganam, 1999). The adsorption limits the amount of clumping that can occur between the cement particles. The HRWR essentially disperses all elements in the mixture. Many factors can affect the effectiveness of a superplasticizer, but primarily it is related to the size of the cement particles. The finer the cement, the more surface area is available for the HRWR admixture to adsorb to, and thus a higher dosage is necessary to create an equally flowable mixture. In this investigation, the only type of HRWR admixture utilized is the polycarboxylate superplasticizer.

The basic structure of a HRWR polycarboxylate admixture on the molecular level is that of a comb polymer, as seen in Figure 1.2. The main component of the HRWR molecule acts like a backbone with many long strands of side chains that look like a comb. The binding sites of a polycarboxylate are anionic, which bond with the positive charge of the cement particle. The side chains act as a physical impediment to

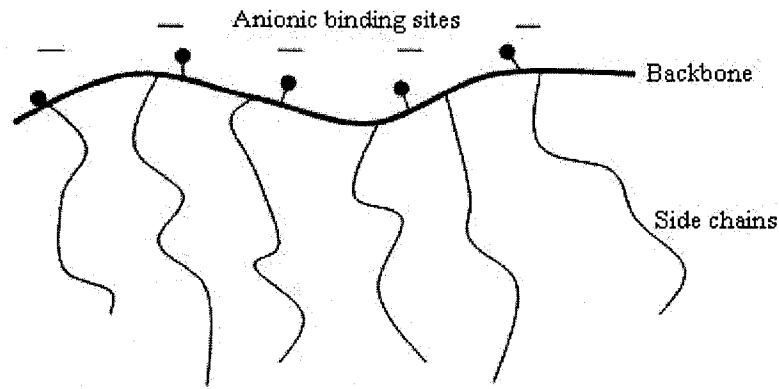


Figure 1.2 Polycarboxylate molecule (adapted from Daczko and Kerns, 2008)

“reagglomeration of the dispersed cement grains,” thus allowing the paste of the concrete to flow freely (Daczko and Kerns, 2008). An electrostatic repulsion caused by the negative charge induced by the superplasticizer on the cement particle also causes the cement particles to disperse and repulse each other.

While different manufacturers use the same basic polycarboxylate molecule in the HRWR, they will not necessarily behave in the same manner or require the same dosage to achieve a similar slump flow. The basic chemical structure of a polycarboxylate HRWR can be seen in Figure 1.3, with an acid component acting as the binding site to the cement particles, and the ester component acting as the side chain. The behavior of

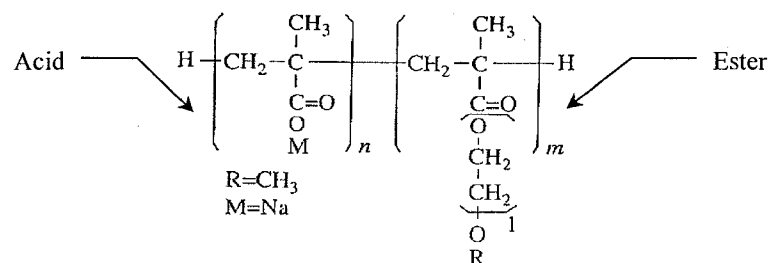


Figure 1.3 Chemical structure of a polycarboxylate polymer (Rixom and Mailvaganam, 1999)

the HRWR can be modified by adjusting the ratio of acid and ester in the molecule by changing the modulus n and m . The higher the acid component, the more binding sites are available for the HRWR to adsorb to the cement. With a higher the ester component, the adsorption occurs more gradually, and thus fluidity retention increases.

1.1.1.2.2 Viscosity Modifying Admixtures

The addition of a viscosity modifying admixture (VMA), also referred to as an anti-washout admixture, increases viscosity, and reduces segregation, bleeding and sedimentation in SCC. Cellulose derivatives and polysaccharides (welan gums) of microbial sources are commonly used as VMAs in concrete (Khayat, 1995). In general, a viscosity modifying admixture like welan gum and other cellulose derivatives work to increase the viscosity of water by affixing itself to the water molecules. Viscosity modifiers are generally long-chain polymers which bond to the periphery of the water molecules when added to a concrete mixture, thus “fixing part of the mixing water” (Khayat and Assaad, 2002). Additionally, the VMA molecules can intertwine and develop attractive forces towards each other, further blocking the flow of water in the cement paste, causing it to have a more viscous or gel-like behavior. VMA molecules can disassociate and align in high rates of flow, thus causing a decrease in the apparent viscosity of the mixture.

1.1.1.2.3 Air-Entraining Admixtures

Air-entrained concrete was developed in the mid-1930s, and is recommended today for nearly all concretes to improve freeze-thaw resistance when exposed to water and deicing chemicals (Kosmatka et al., 2002). The total air content by volume of the concrete is often the only specification for a mixture, but certain air void parameters that

describe the size and spacing of the air voids must be attained as well to secure adequate freeze-thaw durability. The air-entraining admixture stabilizes bubbles formed during the mixing process, enhances the incorporation of bubbles of various sizes, impedes bubble coalescence, and anchors bubbles to cement and aggregate particles. Entraining air into a concrete mixture is a complex process that is affected by many factors such as temperature, cement chemistry, supplementary cementitious materials, aggregate size and volume, slump flow, mixing action, and time (Du and Folliard, 2003).

Most air-entraining admixtures consist of one or more of the following materials: wood resin (Vinsol resin), sulfonated hydrocarbons, fatty and resinous acids, or synthetic detergents. Classifications and performance characteristics of common air-entraining admixtures can be seen in Table 1.1. Most air-entraining admixtures are surface-acting agents, or surfactants, which are molecules with a hydrophilic head and a hydrophobic tail, as seen in Figure 1.4(a). When AEAs are added to concrete, they form a film at the air void-water phase interface, as seen in Figure 1.4(b). In order to be an effective AEA, the film must have sufficient elasticity to resist internal and external pressures in its environment in fresh concrete.

The action created by the mixer enfolds and stirs air into the concrete paste. The quantity and size of the air voids in concrete are continually changing during mixing. The stability of the air voids in fresh concrete with respect to mixing time is important because concrete is usually handled in some way prior to placement in its final location. The film created by the AEA must resist deterioration over time and inhibit bubble coalescence (joining or merging) by transmitting air across the air-to-water interface.

Table 1.1 Classification and performance characteristics of common air-entraining admixtures (Kosmatka et al., 2002)

Classification	Chemical description	Notes and performance characteristics
Wood-derived acid salts Vinsol resin	Alkali or alkanolamine salt of: A mixture of tricyclic acids, phenolics, and terpenes.	Quick air generation. Minor air gain with initial mixing. Air loss with prolonged mixing. Mid-sized air bubbles formed. Compatible with most other admixtures.
Wood rosin	Tricyclic acids-major component.	Same as above.
Tall oil	Tricyclic acids-minor component. Fatty acid-major component. Tricyclic acids-minor component.	Slower air generation. Air may increase with prolonged mixing. Smallest air bubbles of all agents. Compatible with most other admixtures.
Vegetable oil acids	Coconut fatty acids, alkanolamine salt.	Slower air generation than wood rosins. Moderate air loss with mixing. Coarser air bubbles relative to wood rosins. Compatible with most other admixtures.
Synthetic detergents	Alkyl-aryl sulfonates and sulfates (i.e. sodium dodecylbenzenesulfonate).	Quick air generation. Minor air loss with mixing. Coarser bubbles. May be incompatible with some HRWR. Also applicable to cellular concretes.
Synthetic workability acids	Alkyl-aryl ethoxylates.	Primarily used in masonry mortars.
Miscellaneous	Alkali-alkanolamine acid salts of lingosulfonate. Oxygenated petroleum residues. Proteinaceous materials. Animal tallow.	All these are rarely used as concrete air-entraining agents in current practice.

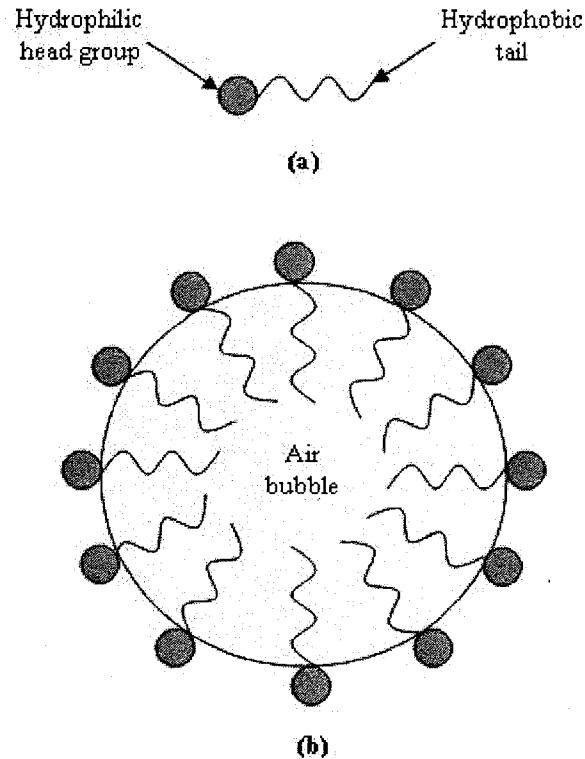


Figure 1.4 Air-entrainment molecule schematic: (a) surfactant, (b) distribution of surfactant on air-water interface (from Du and Folliard, 2003; Mindess and Young, 1981)

Many factors besides the actions of the air-entrainment are involved in producing concrete with a stable air void system. In conventional concrete, the air content and air void characteristics will generally decrease as the cement content increases (Kosmatka et al., 2002). An increase in cement fineness will also result in a decrease in the amount of air entrained. The size of coarse aggregate has been shown to have a significant effect on the amount of entrained air, in that the AEA dosage requirement decreases with an increase in the maximum size of aggregate. The increase of fine aggregate causes more air to be entrained for a given amount of air entraining admixture. Finally, the type of mixer, the energy of mixing, and the volume of concrete loaded into the mixer will have an effect on the amount of air entrained and size of bubbles (Du and Folliard, 2003).

1.1.1.2.4 Admixture Interactions

The chemical interaction between various admixtures becomes a paramount aspect of this investigation, since the admixtures work on the molecular level to disrupt or improve the performance of SCC. The HRWR and VMA essentially work against each other: the HRWR produces flowable concrete, while the VMA increases its viscosity and slows down the rate and extent of flow. A viscosity modifying admixture is typically necessary at the larger slump flow levels to maintain a stable concrete mixture resistant to segregation and bleeding. Air-entrainment can also significantly reduce the viscosity of SCC, “which in turn can lower the cohesiveness and resistance to segregation” (Khayat, 2000). In contrast, air-entrainment can also reduce the occurrence of internal and external bleeding (Kosmatka et al., 2002). The HRWR and VMA also have a considerable effect on the air content and characteristics of the air voids due to disruption of the air-entraining action, as is discussed in Section 1.2.3.3.

1.2 Frost Durability and Air Void Production

1.2.1 Mechanisms of Freezing and Thawing Deterioration in Concrete

Freezing and thawing in the environment can cause massive scaling and crumbling of concrete with exposure to moist or wet conditions. The resistance of hardened concrete to freezing and thawing can be greatly enhanced by incorporating intentionally entrained air voids in the concrete, even when deicing chemicals are involved. As the water in concrete freezes, it produces osmotic and hydraulic pressures in the capillaries and pores of the cement paste and aggregate (Kosmatka et al., 2002). If the pressure exceeds the tensile strength of the paste or aggregate, the void will dilate and

rupture. Over time, the cumulative effect of successive freeze-thaw cycles causes deterioration of concrete, which can be described as scaling, cracking and crumbling.

The hydraulic pressures in concrete are caused by the 9% expansion of water when it freezes; during this process the ice crystals displace unfrozen water. If a capillary void is above critical saturation (91.7% filled with water), hydraulic pressures will result as freezing progresses (Kosmatka et al., 2002). Theoretically, there should be no hydraulic pressure at lower water contents.

Powers (1965) first introduced the concept that osmotic pressure in concrete develops as a result of differential concentrations of alkali solutions in the cement paste. As pure water freezes, the alkali concentration in the adjacent unfrozen water increases. Through osmosis, this draws water from the lower-alkali solutions in the pores. The drawing of water towards the ice continues until equilibrium in the fluids' alkali concentration is reached. Osmotic pressures are said to be the major contributing factor in salt scaling.

As ice forms within capillaries or air voids within concrete, water is drawn from other pores due to hydraulic and osmotic pressures. Since many pores within concrete are too small for ice crystals to form, water tends to migrate towards a location that is large enough for it to freeze. If air voids are distributed throughout the concrete, the water will be able to move to the void and freeze, causing the concrete to remain intact. However, if the air voids are spaced too far apart, the water will freeze within the capillaries and pores of the concrete. With repeated freezing and thawing cycles, the ice expands within the small spaces and eventually destroys the concrete.

The type of AEA utilized to produce the air voids can also influence the frost durability of a concrete. It has been noted that AEAs like Vinsol resin and sodium oleate perform better than other agents like phenol ethoxylate in freezing and thawing durability (Chatterji, 2003). The ability of an AEA to change the restraining pressure acting on the ice crystals ultimately improves the freeze-thaw durability of a concrete. The hydrophobic components of an AEA reduce the strength of the ice-paste bond within the concrete, thus causing hydrostatic pressures to draw water out of the capillaries (Chatterji, 2003).

1.2.2 Requirements for Freeze-Thaw Durability

A key difference exists between intentionally entrained air bubbles and entrapped air voids, but all result from mixing, handling and placing concrete. Entrained air voids are extremely small in size, between 10 to 1000 μm in diameter, whereas entrapped air voids are generally 1 mm or larger in diameter, and often non-spherical in shape (Dodson, 1990). Additionally, in the case of conventional concrete, most entrapped air voids are usually removed through mechanical consolidation (vibration) during placement. More recently, the micro-air content has been recognized as an important factor in determining the frost durability of concrete (Brite/Euram Project, 1994). The micro-air content is defined in the European standard for determination of air void characteristics as the volume percentage of air voids 300 μm or less (EN 480-11, 1998).

1.2.2.1 Specific Surface and Spacing Factor of Air Voids

Entrained air that is evenly spaced throughout the paste is important in developing concrete that is resistant to freezing and thawing. The air bubbles act as a location where water can travel to when freezing conditions occur, thus relieving the pressure on

concrete. The spacing and size of air voids are the two critical factors contributing to the effectiveness of air-entrainment and freeze-thaw resistance of concrete. The spacing factor, \bar{L} , is an index related to the distance between the air bubbles, but is not the actual average spacing in a given air void system. The spacing factor is defined as the “maximum distance of any point in the paste or in the cement paste fraction of mortar or concrete from the periphery of an air void” (Dodson, 1990). Figure 1.5 illustrates the concept of the spacing factor – note both samples have the same percentage of air, but the one on the right has a better spacing factor.

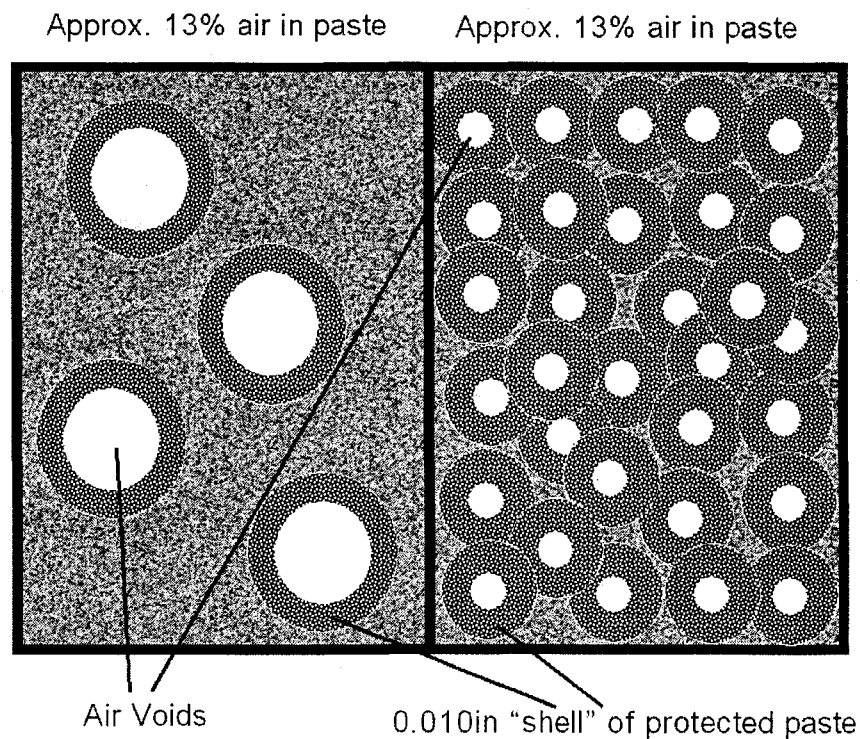


Figure 1.5 Illustration of spacing factor (Crawford, Wathne and Mullarky, 2003)

The spacing factor, \bar{L} , is calculated using the following equations:

$$\bar{L} = \frac{3}{\alpha} \left[1.4 \left(\frac{p}{A} + 1 \right)^{1/3} - 1 \right] \quad \text{where } p/A > 4.342 \quad \text{Eq. 1.1(a)}$$

$$\bar{L} = \frac{p}{400n} \quad \text{where } p/A \leq 4.342 \quad \text{Eq. 1.1(b)}$$

where: p = paste content (volume % of concrete), n = average number of air voids intersected per linear inch (or millimeter) of traverse, α = specific surface of air voids in inches (or mm), e = average chord length of air void in inches (or mm) traversed and equal to $A/100n$, and A = air content.

The specific surface, α , is a good indication of the air bubble size. Generally, smaller bubbles have a higher specific surface. The specific surface is calculated by dividing the surface area of voids by their volume:

$$\alpha = \frac{\text{Surface Area of Air Voids}}{\text{Volume of Air Voids}} \quad \text{Eq. 1.2}$$

While many current building codes do not specify the required air void characteristics, most research to date has considered the following air void characteristics representative of a system with adequate freeze-thaw resistance (Powers, 1964 and 1965):

1. Calculated spacing factor, \bar{L} , less than 0.2 mm (0.0079 in)
2. Specific surface, α , greater than 25 mm²/mm³ (635 in²/in³)

Additionally, freeze-thaw resistance is significantly increased with a good quality aggregate, a low water to cementitious materials ratio (maximum 0.45), a minimum cementitious materials content of 334 kg/m³ (564 lb/yd³), proper finishing and curing techniques, and a minimum compressive strength of 28 MPa (4000 psi) (Kosmatka et al., 2002).

1.2.2.2 Methods of Measuring Air in Concrete

As important as air void characteristics are to frost durability, designers do not usually specify requirements for the specific surface and spacing factor of the air voids in concrete. In cold weather climates, the total percentage of air in a concrete mixture is commonly specified. The American Concrete Institute (ACI) Standard 318-05, "Building Code Requirements for Structural Concrete and Commentary," specifies the total air content required for concrete based on the nominal aggregate size and the exposure condition, as seen in Table 1.2. In addition to the percentage of air required for frost durability, ACI 318-05 has specified maximum water-to-cementitious materials ratios and minimum compressive strengths required for concretes in certain exposure conditions, as depicted in Table 1.3.

Measurement of the total air volume of the concrete does not necessarily indicate the adequacy of the air void characteristics, but has been shown to present a general correlation, as seen in Figure 1.6.

Table 1.2 Total air content for frost-resistant concrete (ACI 318-05, Table 4.2.1.)

Nominal maximum aggregate size, mm (in.)	Air content (%)	
	Severe exposure	Moderate exposure
9.5 ($\frac{3}{8}$)	7.5	6
12.5 ($\frac{1}{2}$)	7	5.5
19.0 ($\frac{3}{4}$)	6	5
25.0 (1)	6	4.5
37.5 (1 $\frac{1}{2}$)	5.5	4.5
50 (2)	5	4
75 (3)	4.5	3.5

Table 1.3 Requirements for special exposure conditions (ACI 318-05, Table 4.2.2)

Exposure condition	Maximum water-cementitious material ratio, by weight, normalweight concrete	Minimum f'_c , normalweight and light-weight concrete, psi (MPa)
Concrete intended to have low permeability when exposed to water	0.50	4000 (27.6)
Concrete exposed to freezing and thawing in a moist condition or deicing chemicals	0.45	4500 (31.0)
For corrosion protection of reinforcement in concrete exposed to chlorides from deicing chemicals, salt, salt water, brackish water, seawater, or spray from these sources	0.40	5000 (34.5)

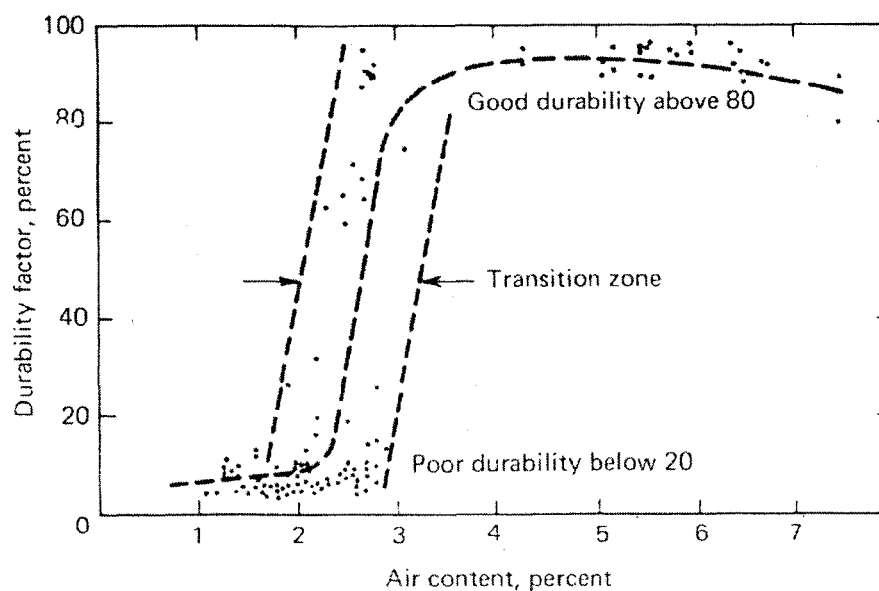


Figure 1.6 Correlation between freeze-thaw durability and air content (Cordon and Merrill, 1963)

1.2.2.2.1 Measuring Total Air Content

Currently, the American Society for Testing and Materials (ASTM) has outlined three methods for measuring the total air content of freshly mixed concrete. Each of these test methods has their drawbacks and benefits, but all are correlated to determine the total percentage of air in a given concrete mixture. The ASTM and American Association of State Highway and Transportation Officials (AASHTO) test methods for evaluating the air content of concrete are as follows:

1) Volumetric Method – ASTM C 173-08 “Standard Test Method for Air Content of Freshly Mixed Concrete by Volumetric Method” (AASHTO T 196) – This method relies on displacement of air with water in a vessel of pre-calibrated volume. Similar to the other air content tests, the sample should be a minimum size of 0.075 ft^3 (0.028 m^3).

2) Pressure Method – ASTM C 231-08 “Standard Test Method for Air Content of Freshly Mixed Concrete by the Pressure Method” (AASHTO T 152) – This method is based on the principle that the only significantly compressible ingredient in fresh concrete is air. This method should not be used with lightweight or highly porous aggregates.

3) Gravimetric Method – ASTM C 138-08 “Standard Test Method for Unit Weight, Yield, and Air Content [Gravimetric] of Concrete” (AASHTO T 121) – This is the oldest test method for determining air content in fresh concrete. The specific gravities of all materials are known to find the actual unit weight of concrete, which can be used to calculate air content.

4) Chace air indicator – AASHTO T 199 “Standard Method of Test for Air Content of Freshly Mixed Concrete by the Chace Indicator” – A simple and inexpensive

way to approximate air content of fresh concrete. The pocket-sized indicator is not a substitute for the three more accurate methods described above.

1.2.2.2.2 Measuring Air Void Characteristics

In the United States, there is currently one standardized method for determining the air void characteristics of concrete, ASTM C 457 “Standard Test Method for Microscopical Determination of the Air Void Content and Parameters of the Air Void System in Concrete,” which uses hardened concrete samples. A new method exists for air void evaluation called the Air Void Analyzer, which measures the spacing factor and specific surface of air voids in fresh concrete. This method does not yet have an ASTM standard designation, but its results are correlated to match that of ASTM C 457. Further detail on the Air Void Analyzer is presented in Chapter 2.

In the guidelines set forth by ASTM C 457, a hardened concrete sample is examined petrographically to ensure the air void system is adequate to resist damage from a freeze-thaw environment. Utilizing a polished section of concrete, the air void system is documented by making measurements using a microscope, as shown in Figure 1.7. The information obtained from this test includes the volume of entrained air and entrapped air, its specific surface (surface area of the air voids), the spacing factor and the number of voids per lineal distance.

Determining the air void specific surface and spacing factor using the ASTM C 457 method does have its drawbacks. It is a tedious method that requires trained personnel and expensive equipment, and is not designed for routine analysis (Mindess and Young, 1981). There can be differences in results between technicians and between laboratories, and the air void characteristics cannot be determined until the concrete is

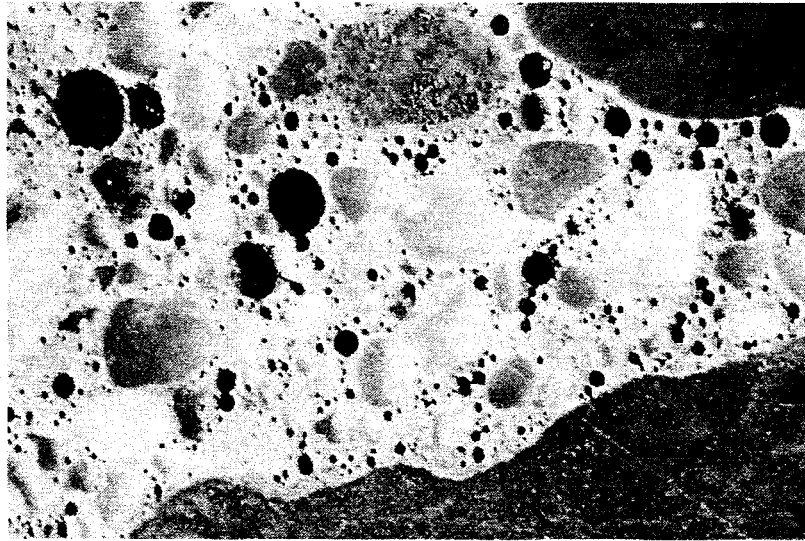


Figure 1.7 Polished section of air-entrained concrete as seen through a microscope (Kosmatka et al., 2002)

hardened. However, ASTM C 457 is currently the only test method approved to determine the air void characteristics of concrete in the United States.

It has been confirmed in numerous studies that SCC can be produced with adequate air void characteristics and good resistance to freeze-thaw cycles, with some case studies even indicating SCC mixtures slightly outperform conventional concrete mixtures in freeze-thaw durability (Nehdi, Pardhan and Koshowski, 2004; Khayat and Assaad, 2002; *ME 03-10*, 2003; Ozyildirim and Lane, 2003; Christensen and Ong, 2005; Beaupré, Lacombe and Khayat, 1999).

1.2.3 Air Void Production

The production of an adequate air void system in a concrete mixture chiefly requires an air-entraining admixture and mixing action. When added and subsequently dispersed throughout a mixture, some AEA molecules adsorb to cementitious materials, some remain in the liquid solution, and some concentrate at the air-water interfaces to stabilize bubbles (Bruere, 1971). The amount of surfactant added to a concrete mixture

can be described by the equation proposed by Du and Folliard (2005): $A = A_S + A_L + A_B$, where A is the amount of AEA added to the mixture, A_S is the amount of AEA adsorbed or absorbed on the solid surfaces, A_L is the amount of AEA in bulk liquid phase, and A_B is the amount of AEA concentrated at the liquid and air interface. Within the cement paste, the hydrophilic heads of the AEA (typically anionic) adsorb to the positively charged cement particles, while the hydrophobic tails stabilize the air bubbles, as seen in Figure 1.8. The hydrophobic tails of the AEA can also act as a bridge between air bubbles, creating a network structure that increases mixture cohesion and stability (Corr, Juenger, Monteiro and Bastacky, 2004).

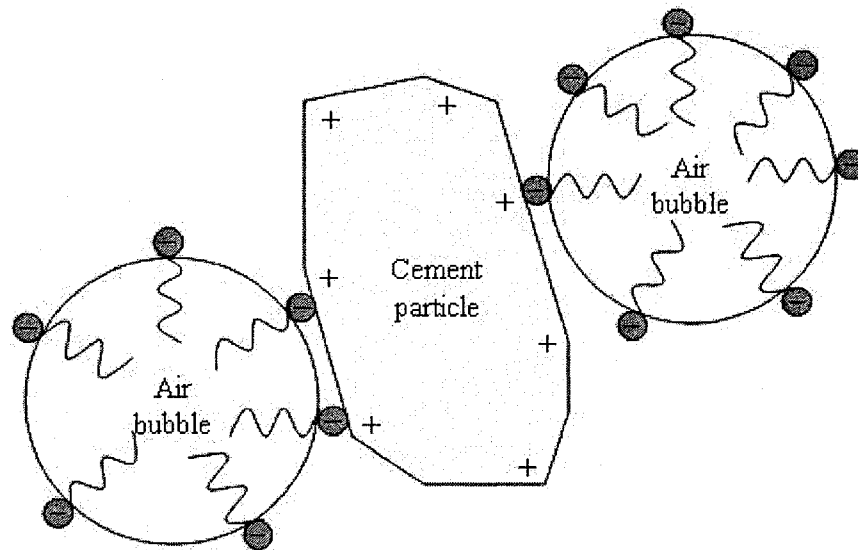


Figure 1.8 AEAs at the cement-air-water interface (adapted from Rixom and Mailvaganam, 1999)

1.2.3.1 Effect of AEA Type on Air Void Production

The type of AEA influences the size and rate of air bubbles produced, as outlined in Table 1.1. In SCC mixtures, tall oil AEAs have been found to produce a distribution

of smaller bubbles than natural AEAs (Christensen and Ong, 2005). The two types of AEAs used in this investigation are wood-derived acid salts and synthetic detergents. The chemical structures of a salt-type (containing wood resin) and detergent-type (orthododecylbenzene sulfonate) AEA can be seen in Figure 1.9.

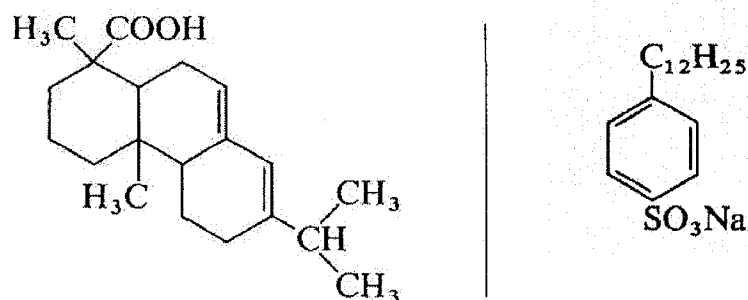


Figure 1.9 Chemical compositions of typical AEA agents: abietic acid, the primary component of wood-derived acid salts (left) and orthododecylbenzene sulfonate, the primary component of synthetic detergents (right) (Rixom and Mailvaganam, 1999)

A detergent-type AEA is a pure surfactant that quickly generates air within a mixture by reducing the surface tension of water. Through the action of mixing, the air bubble size and distribution is constantly changing. In order to prevent coalescence or complete rupture of air voids, a “healing” effect protects the bubbles against film thinning, which is caused by the combined Gibbs-Marangoni effects. The Marangoni effect of a surfactant attributes the reduction in surface tension at an interface to the balancing of forces in a moving fluid (Birikh, Briskman, Velards and Legros, 2003). Essentially, the combined Gibbs-Marangoni stabilization mechanism works in a complementary fashion. For example, when the film between two adjacent bubbles is stretched thin as a result of agitation, a new surface will be formed with a lower surfactant concentration and a higher surface tension. A surface tension gradient along

the film will form, causing liquid to flow from low-stress areas in the bulk liquid phase to the new stretched surface, “thereby opposing film thinning” (Myers, 1999). Additionally, diffusion of more surfactant molecules to the surface counters the thinning effect. Therefore, in order for a surfactant to effectively stabilize new bubbles, the concentration in bulk liquid phase, A_L , must be high enough to counteract disturbances caused by agitation or gravity.

Similar to the emulsion created by a surfactant, a salt-type AEA stabilizes air bubbles in concrete by accumulating at the interfaces between air, water, and cement (Du and Folliard, 2003). The key difference between salt-type and detergent-type AEAs is the immediate reaction of the salt-type with Ca^{2+} and Mg^{2+} ions found in the fresh concrete mixture. Salt-type AEAs also do not reduce the surface tension of water like surfactants. A salt-type AEA reacts directly with the calcium hydroxide ($\text{Ca}(\text{OH})_2$) solution in the cement paste to form insoluble calcium salts (Chatterji, 2003). The rate of precipitation between the AEA and calcium ions is much higher than the rate of adsorption onto cement and/or fly ash particles. As the AEA is adsorbed to particles, it is slowly replaced in solution through dissolution of the AEA-calcium salts until all AEA is adsorbed (Baltrus and LaCount, 2001). Salt-type AEAs are not as reliant on A_L as detergent-type AEAs to stabilize bubbles because they do not reduce the surface tension of water; however, the concentration of AEA in the liquid phase must be “sufficient to generate bubbles during mixing” (Rixom and Mailvaganam, 1999).

One other difference between the two types of AEAs used in this study is that the air voids generated by salt-type AEAs are adsorbed onto cement particles and/or calcium precipitates, whereas the surfactants stabilize bubbles in the bulk liquid phase. The mass

of the cement particles (or other adsorbent) acts like an anchor that stabilizes the air bubbles throughout the matrix. The tendency of air bubbles to float to the surface is also reduced if the bubble is adhered to a larger particle (Du and Folliard, 2005).

1.2.3.2 Effects of Slump Flow on Air Void Production

In conventional concrete there is a known relationship between the workability of a mixture (or slump) and the effectiveness of air-entrainment. Air-entrainment is more successful in a workable mix than in a very stiff mix (Saucier, Pigeon and Cameron, 1991). However, there is point when the concrete becomes too fluid to effectively entrain air. The published studies conflict on the exact slump value that optimizes air entrainment in conventional concrete – it is somewhere between 150 and 230 mm of slump (6 to 9 inches), and almost certainly depends on the specific properties of the components of the mixture (Saucier et al., 1991; Mindess and Young, 1981).

While it is established that increasing slump in conventional concrete generally increases the total air content up to a certain point, the available literature on SCC mixtures suggests contradictory findings (Saucier et al., 1991). Some studies state that there is a higher AEA demand with less-fluid SCC mixtures to secure a given air volume (Khayat and Assaad, 2002). This is thought to be caused by a “greater free-water content in the more fluid concrete, which increases the ability of the AEA to further reduce surface tension” (Khayat and Assaad, 2002). In turn, SCC with a high viscosity (low slump flow) will produce a less stable air void system, since the viscous cement paste increases internal pressure in the air bubbles, causing some to collapse (Khayat and Assaad, 2002). However, upon further investigation of the study in question, it appears

admixture interactions were most likely the cause of the higher AEA demand in less fluid mixtures. Admixture interactions will be discussed in the following section.

There are other studies that state increasing slump flow of an SCC mixture increases AEA demand due to a lower paste viscosity (Beaupré et al., 1999). This follows the trend indicated by highly flowable conventional concrete (slump > 230 mm) in that it is more difficult to entrain air in a more fluid mixture (Christensen and Ong, 2005). The high fluidity of the paste allows the air voids to move freely, increasing the occurrence of bubbles joining together or rupturing at the surface due to buoyant forces. Du and Folliard (2005) stated that a higher paste viscosity, present in lower slump flows, prevents bubbles from escaping or coalescing by creating a “cushion effect” for air bubbles to remain unaffected by disturbances. Thus, a smaller dosage of AEA is needed at lower slump flows to secure a certain percentage of air. In addition to the AEA demand increase with increasing slump flow to entrain a given amount of air, the air void characteristics, specifically the spacing factor in SCC, have been shown to increase (deteriorate) with an increase in slump flow (Khayat and Assaad, 2002). The high fluidity of SCC essentially facilitates the joining of air voids, thus increasing the spacing factor.

In summary, with high-slump conventional concrete (greater than 230 mm), and theoretically with SCC, a higher dosage of AEA is required as slump flow increases due to the increasing fluidity of the concrete. While comparing conventional concrete and SCC is outside the scope of this study, based on the literature review and the results of this investigation, the hypothesized relationship between air content and slump / slump flow can be seen in Figure 1.10.

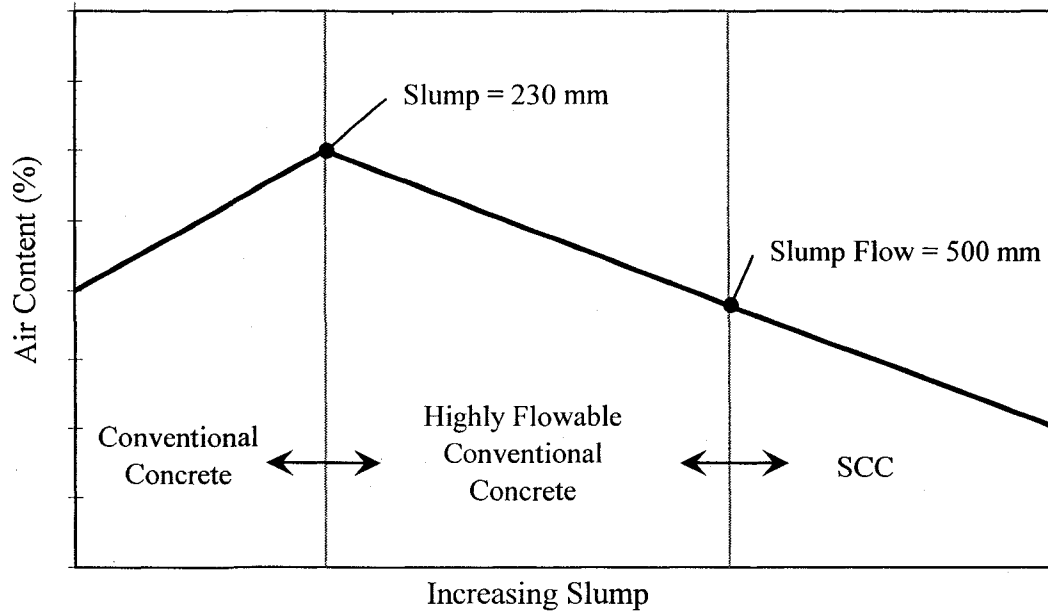


Figure 1.10 Theoretical relationship between air content and slump flow (not to scale)

1.2.3.3 Effects of Admixture Interactions on Air Void Production

The addition of a HRWR admixture will generally increase the demand of AEA. It is necessary for both the AEA and HRWR to adsorb to the cement to be effective. Therefore, competition between the two admixtures may cause reduced quantities of air entrained (Khayat and Assaad, 2002). Certain types of HRWR admixtures, specifically lingosulphonates, can sometimes entrain or entrap air, causing the spacing factor of the air void characteristics to increase (Malhotra, 1981). While the general effect of HRWR is to disrupt the air-entrainment mechanism, electrostatic repulsion between adjacent cement interfaces due to adsorption on the cement particle can inhibit bubble coalescence (Rixom and Mailvaganam, 1999).

As noted in the previous section, the study by Khayat and Assaad (2002) stated that a higher AEA demand was needed in less fluid SCC mixtures. However, the naphthalene-sulfonic acid formaldehyde condensate HRWR, welan gum VMA, and

synthetic detergent AEA dosages used by Khayat and Assaad (2002) were not optimized for the least admixture dosage. It appears that Khayat and Assaad (2002) added more VMA to achieve lower slump flows rather than decreasing the HRWR admixture. In both conventional and self-consolidating concrete mixtures, it has been noted that the addition of a VMA increased the required AEA dosage (Khayat and Assaad, 2002; Khayat, 1995; and Lachemi et al., 2004). The VMA essentially “locks up” the water particles; thus, if more VMA is added, there will be less water available in the mixture for the AEA to produce air bubbles. Synthetic detergent surfactants are more likely to be influenced by additional VMA dosages than salt-type AEAs, due to their high concentration at the air-water interface. While the effectiveness of most AEAs is influenced by the addition of a VMA, a higher VMA dosage will affect a synthetic detergent AEA to a higher degree.

The addition of supplementary cementitious materials, such as fly ash, also contributes to the production of an air void system. Class F fly ash has poor adsorption properties, and therefore reduces the effectiveness of an AEA to produce air voids (Baltrus and LaCount, 2001). The success of air-entrainment will also be poor if the AEA attaches to the carbon surface of the fly ash particle through the hydrophobic end, rather than the hydrophilic end.

1.3 Hauling Time and Air Void Stability

A differentiation must be made between the production and stability of the air void system, as per Saucier, Pigeon and Cameron (1991). Since the air void system is primarily influenced by the mechanical action of mixing, an adequate air void system may be initially produced, but then may gradually deteriorate with time and agitation. In

general, it has been noted in conventional and self-consolidating concretes that the total air content decreases with time, but is limited to 1-2% (Kosmatka et al., 2002; Khayat and Assaad, 2002). It cannot be overemphasized that the stability of the air voids in a particular concrete mixture depends on many interdependent factors including the nature of the materials, the admixture dosages and the chemical interactions among different admixture types. Additionally, the stability of the air voids and the stability of the air content are “very distinct trends that have little or no correlation” (Plante, Pigeon and Foy, 1989).

Concrete produced in the field is typically not placed as soon as it is batched. Hence, the effects hauling time, accompanied with continual agitation, on the air void characteristics of concrete is an important aspect of production. Initially, the concrete is incorporated in a ready-mixed truck for 70 to 100 revolutions at “mixing speed,” which is generally 6 to 18 rpm. The concrete usually spends a period of time in a ready-mixed truck at a lower speed, known as “agitating speed” to retain workability on its way to the construction site. Agitating speed is usually 2 to 6 rpm (Kosmatka et al., 2002).

1.3.1 Background on Slump Loss

Slump loss, or a reduction in fluidity and workability of concrete with time, is mainly caused by the chemical hydration of cement and the physical coagulation of cement particles (Hattori and Izumi, 1998). As the cement hydrates, the free water in the concrete mixture is absorbed by the products of hydration and the surface area of the cement particles themselves increase in size (Ravina and Soroka, 1994). The reduction in free water content increases friction between the cement and aggregate particles, causing grinding and breakage of the particles with continual agitation. The grinding of cement

particles causes the specific surface area of the mortar to increase. The cement particles tend to agglomerate together due to the attractive electrical forces between them. With time, the aggregates also abrade the surfaces of the cement particles, removing hydration products, thus increasing locations for adsorption of surface-acting agents.

The fluidity of SCC is developed primarily through the addition of a HRWR. Through adsorption to the cement particles, electrical repulsion, and physical obstruction (steric hindrance), the HRWR disperses the cement flocs, creating a flowable mixture. The mixing action breaks down the particles in the concrete, increasing the total specific surface area of the concrete mortar. The increase in cement surface area reduces the percentage of adsorption of the HRWR admixture. The mixture will be less fluid as a result of the lower HRWR adsorption, and because of possible breakage of the “comb” portion of the polycarboxylate molecule that is a physical barrier between the cement particles, as seen in Figure 1.2. As hauling time is increased, the SCC often transitions into high-slump conventional concrete due to the drastic loss in slump flow. While the present study measured slump loss in terms of hauling time, studies have shown that slump loss is more closely related to number of drum revolutions (thus, “applied shear energy”) than with elapsed time (Vickers, Farrington, Bury and Brower, 2005).

1.3.2 Effects of Hauling Time on Air Content

With increased hauling time, more air voids are entrained due to the decrease in competition with the HRWR molecules. The evolution of the AEA added to a concrete mixture with elapsed time and agitation can be described with the equation presented in Section 1.2.3: $A = A_s + A_L + A_B$ (Du and Folliard, 2005). As concrete is agitated, air bubbles are folded into the mixture, the cement is ground into finer particles by the

mixing action, and the products of hydration are abraded from the cement surface. Therefore, there are more locations for the newly created bubbles to adhere to in the paste. The amount of surfactant adsorbed onto the cement particles, A_S , increases as hauling time increases, partially due to the dissolution of precipitates if the AEA is a salt-type. The adsorption of the AEA to the cement particles is also accelerated by the decreasing electrostatic charge induced by the HRWR with time. As a result, the amount of surfactant in the bulk liquid phase, A_L , or the amount at the liquid-air interface, A_B , must decrease if no more AEA is added. There is increased bridging between air voids with hauling time, which also adds to their stability.

1.3.3 Definition of Air Void Stability

For the purposes of this study, air void stability shall be defined as the resistance to increase in spacing factor and decrease in specific surface with time. The deterioration of the air void characteristics degrade the ability of hardened concrete to resist damage by repeated freezing and thawing cycles. It is desirable for the air content and air void characteristics to remain the same or improve with time. However, mixing action creates an ever-changing air void system within a concrete mixture that can be difficult to predict.

1.3.4 Effects of Hauling Time on Air Void Stability

The effects of hauling time are intrinsically coupled with the effects of slump loss. With increasing hauling time (and decreasing slump flow) the air content of SCC increases. The effects of slump flow on air void production, as described previously in Section 1.2.3.2, occur whether slump loss is caused by hauling time or admixture dosage. With decreased fluidity, the air bubbles are not as free to move within the cement paste;

therefore, there is less rupturing of air voids at the surface and joining together of air voids within the paste. The mixing action enfolds more air voids into the concrete with time. The mixer also divides and disperses the air voids that are already present in the concrete, creating a more homogeneous mixture with the bubble size and spacing more consistent throughout. The increased viscosity of the SCC with hauling time creates a cushion effect, protecting the air voids within the matrix. It is conjectured that SCC behaves similarly to high-slump conventional concrete (vertical slump of 175 to 225 mm) with respect to air content and air void characteristics. The vertical slump of conventional concrete has been shown to influence the air content with respect to hauling time, as seen in Figure 1.11.

With increased hauling time, certain factors beyond the slump flow and admixture interactions can contribute to air void stability. A higher water-to-cementitious ratio has been shown to improve the air void stability with time (Khayat and Assaad, 2002). For a

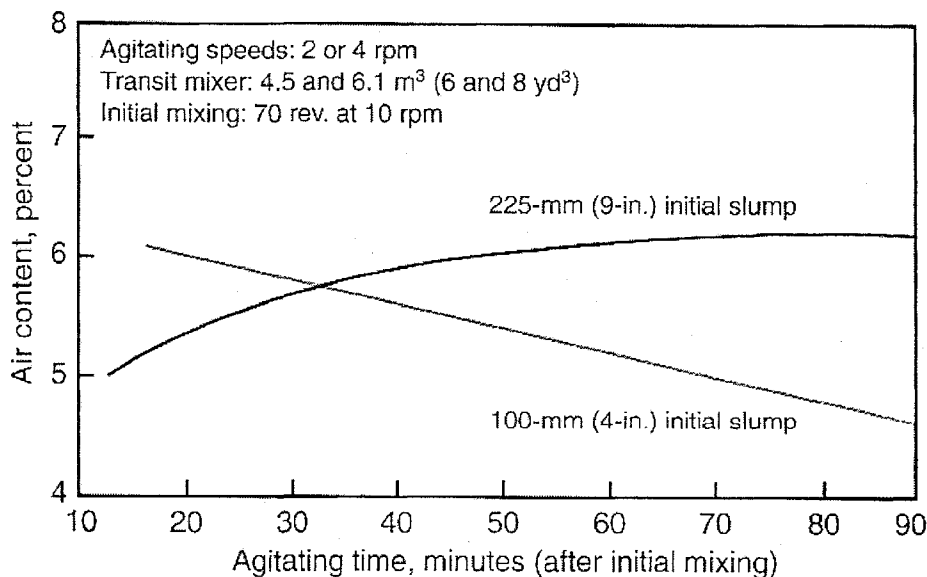


Figure 1.11 Relationship between time, air content and slump of concrete (Kosmatka et al., 2002)

given quantity of air-entrainment, only a definite quantity of surface can be stabilized (Saucier et al., 1991). The definite quantity of air is highly related to the amount present in the bulk liquid phase; a higher dosage of AEA has more potential to entrain air.

1.3.5 Effects of Retempering on Air Void Stability

Hauling time frequently produces slump loss, and occasionally the mixture must be remediated to achieve the desired flow characteristics. Remediation can be accomplished with various methods, but a common solution is the addition of supplemental admixtures after hauling time, which is known as retempering or redosing. Retempering prevents wasted concrete and is commonly utilized to restore the required flow properties of self-consolidating concrete.

Retempering with additional HRWR has been shown to damage the air void characteristics of conventional and self-consolidating concrete, but usually does not decrease the air content (Plante, Pigeon, and Saucier, 1989; Khayat and Assaad, 2002). Different types of HRWR alter the air content and air void characteristics of fresh concrete in varying degrees. In highly workable concrete, a superplasticizer typically entrains more air than a concrete without a water reducer (Rixom and Mailvaganam, 1999). However, with high cement content mixtures, the increase in air content will be minimal. The air bubbles entrained by HRWR tend to be larger than those entrained by an AEA; consequently, the addition of a HRWR can result in deteriorated air void characteristics (Plante, Pigeon and Saucier, 1989). The addition of a superplasticizer is normally linked with the increased fluidity of concrete, thus air void coalescence will be facilitated, degrading the air void characteristics (Plante, Pigeon and Saucier, 1989).

Besides adding more HRWR to achieve the desired workability, retempering can be done with water to increase slump or with additional AEA to improve the air content or air void characteristics. Retempering with water is not recommended due to the resulting strength reduction of the hardened concrete. However, research has shown that neither spacing factor nor specific surface is significantly altered with additional water (Pigeon, Saucier and Plante, 1990). Retempering with AEA results in an increase in air content, but does not necessarily improve the air void characteristics (Pigeon et al., 1990).

1.4 Research Objectives

The objectives of this research are to determine the influence of: 1) four different admixture sources, 2) three different slump flows, 3) eight different hauling times, and 4) two forms of remediation on the air void characteristics of self-consolidating concrete. The research was divided into two distinct phases. The Phase I of the study involved the effects of admixture source and slump flow on the fresh properties and air void characteristics of SCC. The Phase II of the investigation involved the effects of hauling time and the impact of hauling time remediation on the fresh properties and air void characteristics of the selected self-consolidating concretes.

Chapter 1 reviews the literature pertinent to self-consolidating concrete, mechanisms of air-entrainment, air void stability, and frost durability requirements.

Chapter 2 outlines the experimental procedures utilized for this investigation. Mixture proportioning, testing equipment, test methods, and target mixture properties are discussed.

Chapter 3 presents the results of the Phase I investigation. It provides the optimized admixture dosages of the four sources used to achieve the three target slump flows. The air void characteristics (specific surface and spacing factor), admixture dosages, and compressive strengths of the twelve developed mixtures are compared.

Chapter 4 presents the hauling time results of the Phase II investigation. It shows the effects of hauling time on the fresh properties and air void characteristics of three self-consolidating concrete mixtures.

Chapter 5 presents the results of two methods of remediation, overdosing and retempering, to achieve the target fresh properties at eight hauling times. The effects of remediation on the air void characteristics are discussed.

Chapter 6 includes conclusions from this investigation and provides recommendations for further research in this field.

1.5 Research Significance

This study is important for concrete construction in cold regions, as well as in Nevada since freezing conditions do occur in the northern part of the State. Deterioration due to repeated freezing and thawing cycles causes irreversible damage to concrete structures, foundations and roads. Ensuring that proper air void characteristics can be achieved in the field is important in creating a consistent quality concrete mixture. Knowledge of the properties of air voids in self-consolidating concrete as it is hauled in a ready-mixed truck is relevant to concrete producers who are required to deliver a quality product. Additionally, the effects of remediation are also important to ensure that a concrete mixture as expensive as SCC can be delivered to the site successfully or be re-dosed to achieve the intended characteristics.

With the increased use of SCC in structural and roadway applications, standards and characterization of mixtures must occur to increase awareness and knowledge on the benefits and costs associated with the production of self-consolidating concrete. This investigation contributes to the state-of-the-art knowledge, leading to a better understanding on the behavior of self-consolidating concrete in freezing and thawing regions, that ultimately benefits the concrete industry in the production of self-consolidating concrete.

CHAPTER 2

EXPERIMENTAL PROGRAM

The experimental program of the research study was divided into two distinct phases. The first phase investigated the effects of four different admixture manufacturers and three different slump flows on the air void characteristics of SCC. During this phase, admixture dosages were optimized; meaning, through trial-and-error, the minimum admixture dosages to achieve the target fresh properties were determined. Upon completion of the first phase, the second phase studied one admixture manufacturer and three slump flows to determine the effects of transportation time on air void characteristics of self-consolidating concretes. Additionally, two types of remediation, overdosing and retempering, were utilized in the Phase II of the investigation to determine their effects on the air void spacing factor and specific surface.

2.1 Mixture Proportioning

The SCC matrices developed in this investigation contained the same mixture proportions, with the exception of admixture dosages, to ensure isolation of the selected variables of admixture manufacturers and slump flows. A gravimetric water-to-cementitious materials ratio (w/cm) of 0.40 and an air content of 6% was selected, as per ACI 318-05 requirements for severe exposure to freezing and thawing cycles outlined in Chapter 1. Based on these parameters, the basic mixture proportions used in this investigation are shown in Table 2.1. Specific mixture proportions that include

admixture dosages are described in detail in Chapter 3 for Phase I, and Chapters 4 and 5 for Phase II.

Table 2.1 Basic mixture proportions (excluding admixtures)

Material	lb/yd³	kg/m³
Cement	658	390
Fly Ash	132	78
Coarse Aggregate	1458	865
Fine Aggregate	1340	795
Water	331	196

2.1.1 Cement and Fly Ash

The same source of cement and fly ash was used throughout the investigation. The cement used was ASTM C 150 Type V, due to the high occurrence of sulfates in the soil found in Southern Nevada. It is also customary and more economical in the local area to use fly ash in the concrete mixtures. Therefore, Class F fly ash was added at 20% by weight of cement in order to provide the trial self-consolidating concretes with sufficient cementitious materials. The fly ash used met the requirements set by ASTM C 618-08. The chemical composition and physical properties of the cement and fly ash can be seen in Table 2.2.

2.1.2 Aggregate

The aggregate used throughout the investigation was obtained from a quarry in Southern Nevada. The coarse aggregate had a nominal maximum size of $\frac{3}{8}$ inch (16 mm), and was required to meet the #7 gradation limits defined by ASTM C 33-07. The typical coarse aggregate gradation curve, an average of three sieve analyses, can be seen in Figure 2.1.

Table 2.2 Chemical and physical properties of Portland cement and fly ash

Chemical Composition	Portland Cement	Fly Ash
SiO ₂	20.64%	58.9%
Al ₂ O ₃	3.4%	20.5%
Fe ₂ O ₃	3.4%	5.6%
CaO	63.5%	7.5%
MgO	4.7%	-
SO ₃	2.4%	0.4%
Na ₂ O equivalent	0.46%	-
K ₂ O	-	-
C ₂ S	9%	-
C ₃ S	66%	-
C ₃ A	4%	-
Loss on Ignition	1.2	0.3
Insoluble residue	0.14	-
Moisture content	-	0
Blaine Fineness	3810 cm ² /gm	-
Autoclave expansion	0.18%	0.02%
Time of set		
Initial	96 minutes	-
Final	205 minutes	-
False Set	94%	-
Air Content	6.3%	-
Compressive Strength		
3-day	27.4 MPa	-
7-day	33.9 MPa	-
28-day	42.7 MPa	-
325 sieve passing	97.9%	23.5%
Specific Gravity	3.15	2.33

1 MPa = 145 psi, 1 kg/m³ = 0.0624 pcf

The aggregate was consistently dried to ensure a moisture content of 0.10% to 0.20%. However, due to slight variations in temperature and humidity, daily moisture content readings were taken during Phase II to ensure the proper amount of water added to the mixture. Due to the small batch size (typically 0.6 ft³), and sensitivity of the

admixture interactions with water, changes in the aggregate moisture content could cause significant changes in the slump flow (up to 3 in. (76 mm)).

The fine aggregate, obtained from the same quarry as the coarse aggregate, was required to meet ASTM C 33 gradation requirements. The typical gradation, an average of three aggregate sieve analyses, is seen in Figure 2.2. The moisture content of the fine aggregate varied from 0.10% to 0.20%, and was monitored daily during Phase II to ensure consistent results. The temperature and humidity during Phase I remained constant. Thus, there was a reduced amount of fluctuation in the aggregate moisture content. Other pertinent coarse and fine aggregate properties can be seen in Table 2.3.

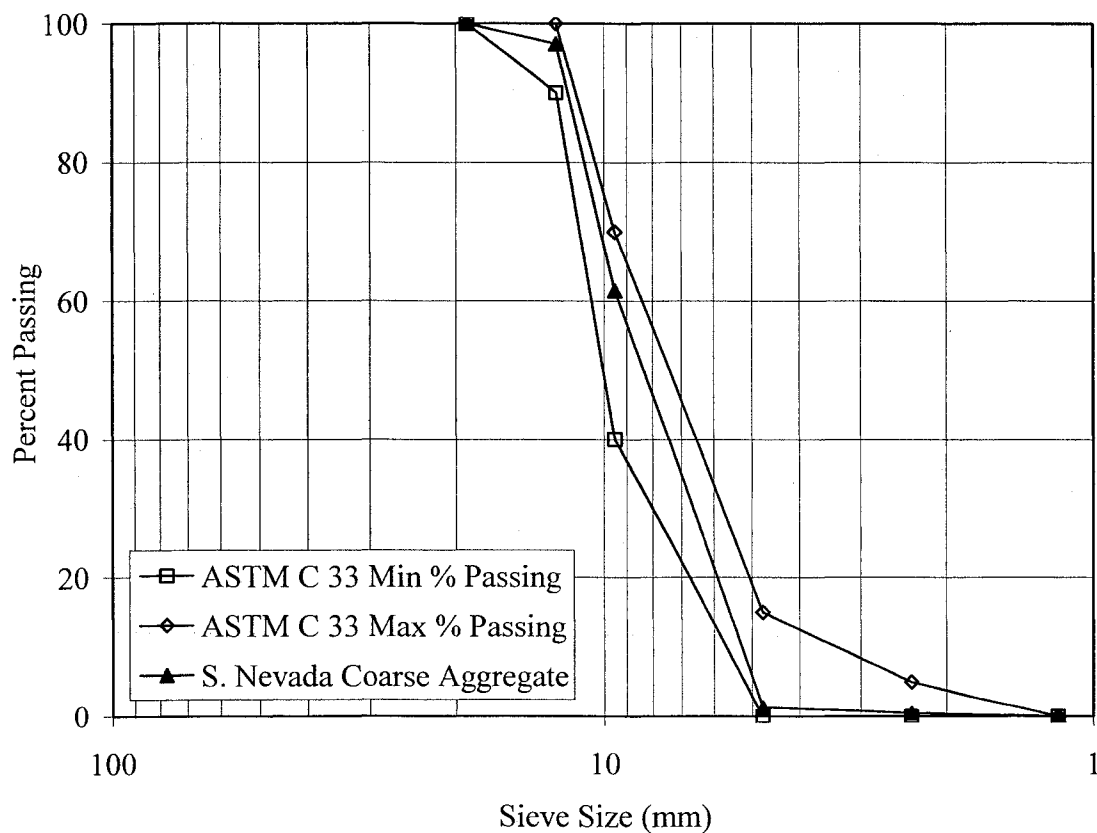


Figure 2.1 Coarse aggregate gradation

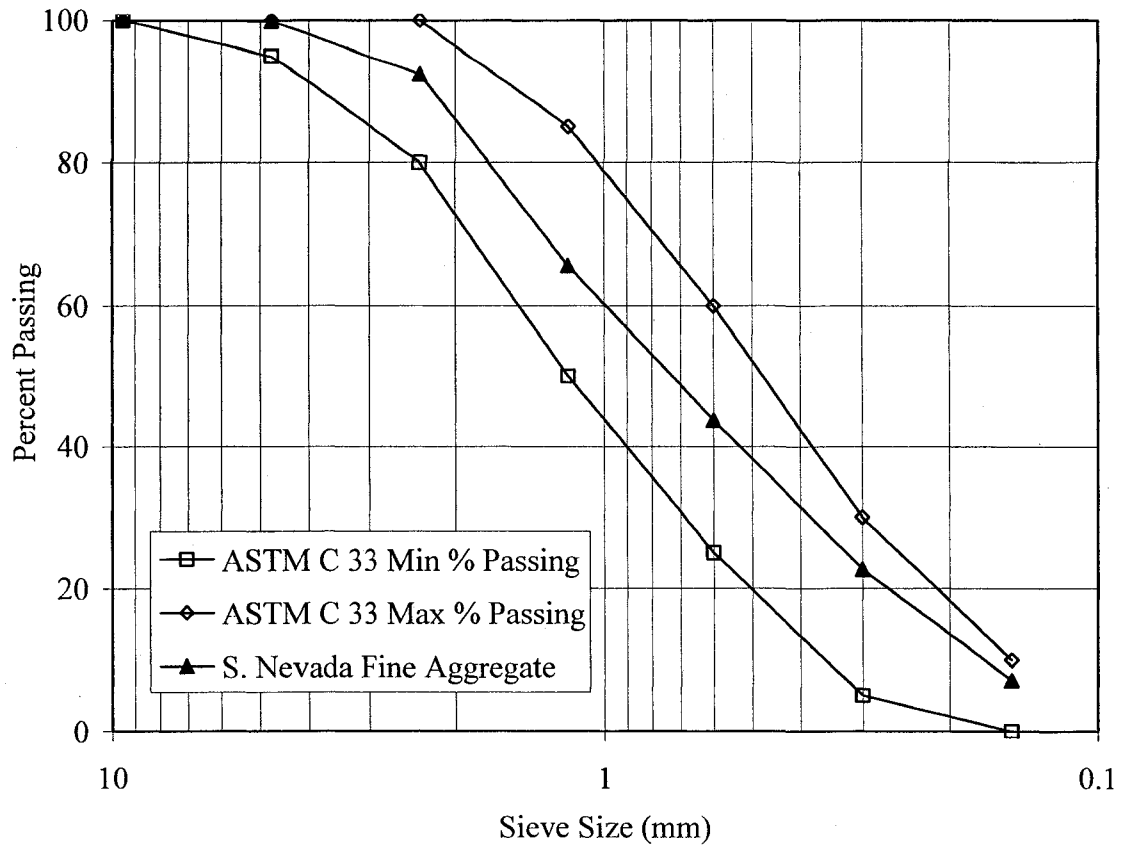


Figure 2.2 Fine aggregate gradation

Table 2.3 Aggregate physical properties

Property	Coarse	Fine
Absorption	0.60%	0.80%
Water Content (typical)	0.15%	0.10%
Specific Gravity	2.79	2.78
% Total Aggregate Volume	52%	48%
Dry rodded unit weight	1634 kg/m ³	-
Fineness Modulus	-	3.00

ASTM C 29-07 standard was utilized to determine the compacted unit weight and calculated void content using different ratios of the combined coarse and fine aggregates. The optimum volumetric coarse-to-fine aggregate ratio was determined to be 0.52/0.48 (1.083), as shown in Figure 2.3.

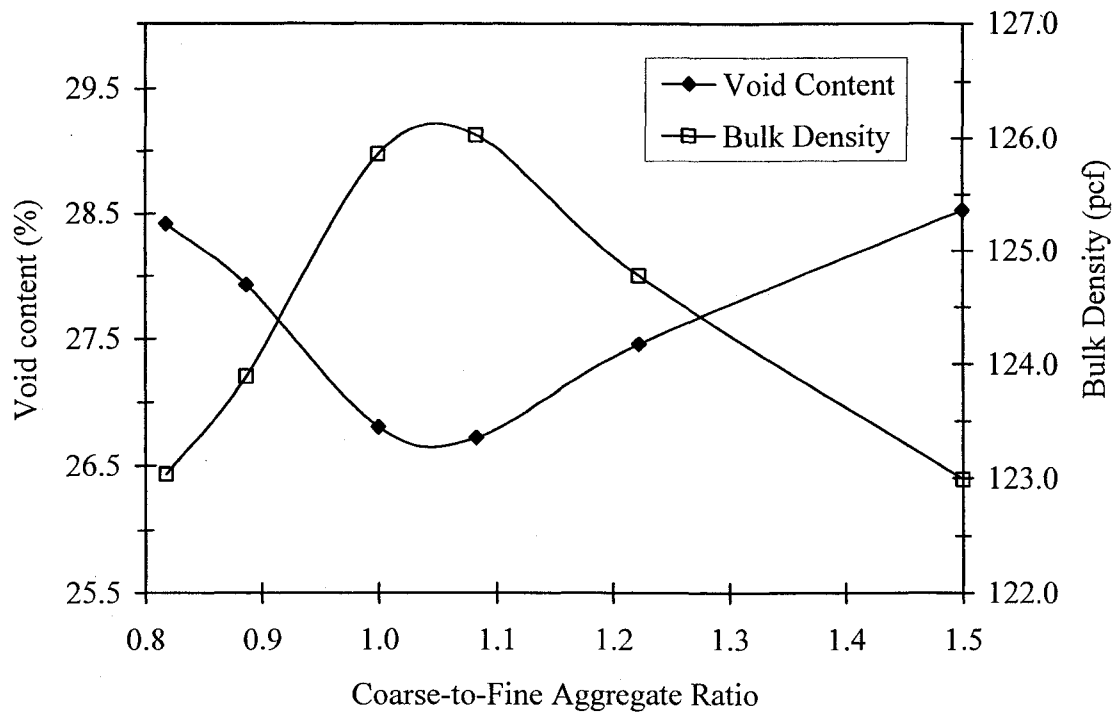


Figure 2.3 Optimum volumetric coarse-to-fine aggregate ratio

2.1.3 Admixtures

Admixtures were obtained from four different manufacturing sources, to be designated as “A”, “B”, “C” and “D.” Specific names of the companies were omitted to eliminate endorsement of one manufacturer over another. The admixtures can be classified under ASTM C 494-08 Type F.

2.1.3.1 High Range Water Reducing Admixtures (HRWR)

The high range water reducing admixtures selected from the four manufacturers are commonly used in the concrete industry in SCC applications. Only polycarboxylate type HRWRs were used in order to compare the difference in performance among this type of superplasticizer produced by various manufacturers. Three of the HRWRs were comprised of a polycarboxylate-acid (PCA), and one was a polycarboxylate-ester (PCE). The specific gravities and types of the HRWR admixtures are shown in Table 2.4.

Table 2.4 Selected high range water reducers

Manufacturer	Specific Gravity	Type
A	1.05	Polycarboxylate-ester
B	1.09	Polycarboxylate-acid
C	1.06	Polycarboxylate-acid
D	1.08	Polycarboxylate-acid

2.1.3.2 Viscosity Modifying Admixtures (VMA)

The types of viscosity modifying admixtures selected for this investigation varied in chemical composition and specific gravities, as seen in Table 2.5. The exact type of VMA was unknown in some cases, since the chemical structure was often proprietary information held by the manufacturer. However, it can be assumed they are non-adsorbent VMAs due to the recommendation by the manufacturer for use with a superplasticizer in SCC applications.

Table 2.5 Selected viscosity modifying admixtures

Manufacturer	Specific Gravity	Type
A	1.002	aqueous solution of polysaccharides
B	1.207	Naphthalene sulfonate 30-60%, Welan gum 7-13%
C	1.0	dispersed carbohydrate (sodium hydroxide, methyl alcohol)
D	1.23	sulfonated naphthalene and melamine polymer

2.1.3.3 Air-Entraining Admixtures (AEA)

The air-entraining agents selected ranged widely from natural resins to synthetic detergents, and came recommended to entrain air in SCC mixtures. The AEA types and specific gravities of the selected admixtures can be seen in Table 2.6.

Table 2.6 Selected air-entraining admixtures

Manufacturer	Specific Gravity	Type
A	1.0	alkybenzene sulfonic acid (synthetic detergent)
B	1.01	tall oil and glycol ether (stabilized modified resin surfactant)
C	1.02	saponified rosin (resin and rosin acid)
D	1.0	natural resin solution

2.2 Test Equipment

2.2.1 Concrete Mixer

The concrete mixer used during this study was a 1 ft³ (0.0283 m³) capacity laboratory pan mixer, as shown in Figure 2.4. The typical batch volume ranged from 0.6 to 0.8 ft³ (0.0170 to 0.0227 m³), depending on the number of tests conducted. The mixer employed a horizontal type mixing action, with a rotating cylindrical pan and rotating blade. The type of mixing action employed is critical in the process of air entrainment, because the size and quantity of air bubbles created is a function of the energy input to the mixture. The mixing action employed by a pan mixer is much different than a rotating drum mixer used in ready-mixed concrete trucks. A rotating drum imparts vertical action, allowing the concrete to fall on itself. To ensure consistent results throughout the investigation, the speed of the laboratory concrete mixer was kept

constant at 14.5 rpm. This was the only speed utilized during Phase I of the investigation. A control unit, as shown in Figure 2.5, was attached to the mixer to allow it to run at different speeds. The “agitating speed” used during Phase II (hauling time) of the program was 7.25 rpm.



Figure 2.4 Laboratory concrete mixer

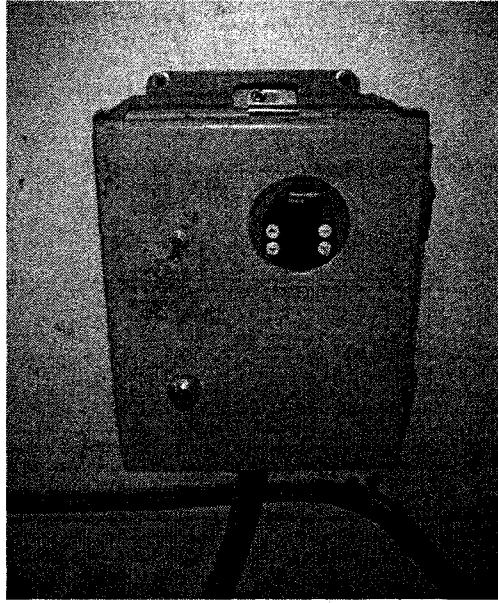


Figure 2.5 Concrete mixer speed control box

2.2.2 Air Void Analyzer

An Air Void Analyzer was used as the primary means of measuring the air void properties in fresh samples of air-entrained self-consolidating concrete. The test is based on the buoyancy principle and Stokes' Law, which states that larger bubbles will rise faster through water than smaller bubbles, as the rate of rise is a function of their size. The test apparatus measures the volume and size distributions of entrained air voids, and calculates the spacing factor, specific surface, and total amount of entrained air. Manufactured by Germann Instruments, the Air Void Analyzer was developed in Europe and validated to produce results that correlate with ASTM C 457 within a 95% confidence limit (Crawford et al., 2003). The purpose of this study was not to validate or prove the worth of this test equipment, but to use it to determine and compare the air void characteristics of freshly-mixed self-consolidating concrete.

2.2.2.1 AVA Testing Procedures

This section fully describes the step-by-step procedures to conduct the Air Void Analyzer test method (*Operation Manual*, 2005).

1) The test is controlled with computer software developed by Dansk Beton Teknik A/S (Series 2/2.0). The user first inputs information on the mixture proportions; specifically, the sample volume, percent mortar, percent paste and expected air content. The percent paste (by volume) of a concrete mixture is defined as % cement + % fly ash + % water + % admixtures. The percent mortar (by volume) is defined as % paste + % aggregate < 6mm. The AVA uses this information to calculate the spacing factor and specific surface once the air void distribution of the mixture has been measured.

2) A 20 cm³ sample of mortar is extracted using a vibrating drill attachment with a wire cage to sieve out any aggregate larger than 6 mm, as seen in Figure 2.6. For the case of SCC, the drill attachment is only used to remove large aggregate because vibration is not necessary to obtain a concrete sample.



Figure 2.6 Sampling SCC with attachment

3) The main component of the Air Void Analyzer is a plexiglass cylinder (known as the riser column) that is filled with de-aerated water and plugged at the bottom with a piston that doubles as a temperature gauge. The air bubbles are gently removed from the inside with a brush to ensure the test results will not be skewed, as seen in Figure 2.7. A magnetic stirring rod is placed at the bottom of the riser column. The mortar sample is attached to the piston and positioned inside the base of the cylinder, shown in Figure 2.8.

4) A blue glycerin-based viscous liquid is deposited at the base, which “releases” the air bubbles from the concrete, as shown in Figure 2.9. The viscous release liquid has properties that ensure the air voids do not coalesce or join together. The concrete must be stirred when the test is started, and the blue liquid allows the bubbles to retain the size distribution they had in the concrete. The temperature of the liquids must be regulated to ensure the viscous liquid properly releases the air bubbles.



Figure 2.7 Adding water (left) and removing air bubbles (right)

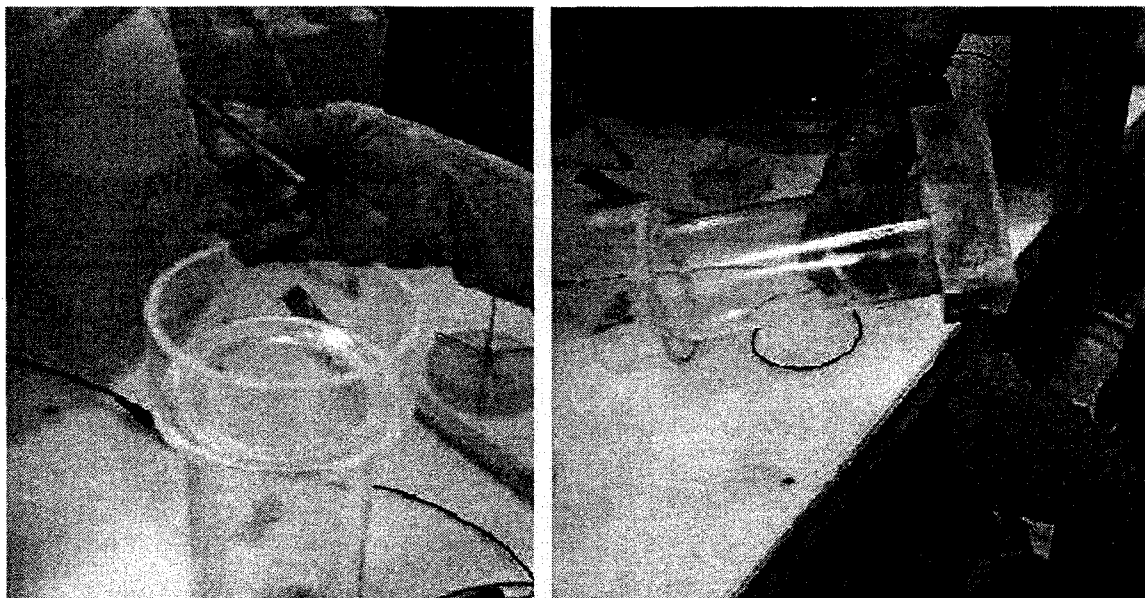


Figure 2.8 Magnetic stirring rod (left) and attaching mortar sample to piston (right)



Figure 2.9 Adding viscous release liquid to riser column

5) The mortar sample is injected with a syringe into the bottom of the riser column. The test is started on the computer, which runs a stirring rod in the mortar for 30 seconds. The entrained air is released from the mortar through this stirring action, which then floats to the top of the column, as seen in Figure 2.10. At the top of the riser column, the air bubbles are caught by an inverted Petri dish, which is connected to a balance. This balance measures the change in suspended mass with respect to time.

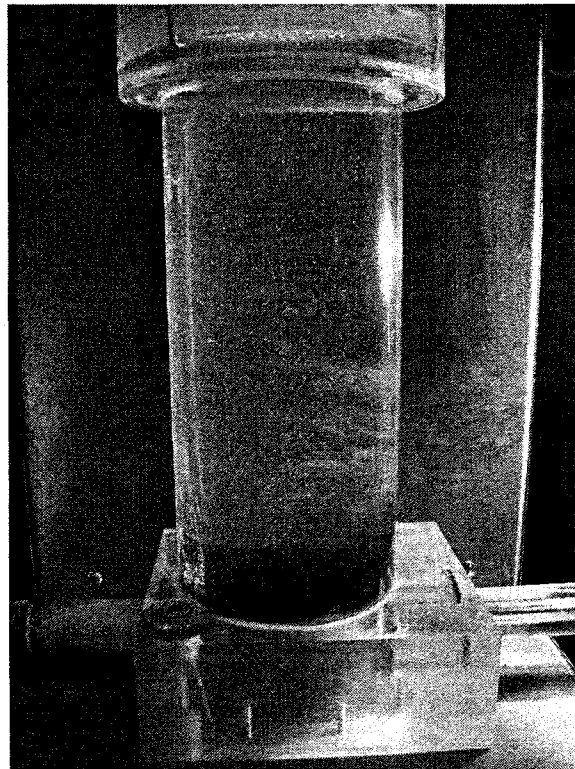


Figure 2.10 Bubbles rising in Air Void Analyzer

6) The program then creates a “gradation” of air bubbles based on the collected data from the balance and the information on mixture proportions provided by the user. The final result is the specific surface, spacing factor, an estimate of the total air content of voids < 2 mm and air content of voids < 0.35 mm (also referred to as “micro-air”

content (EN 480-11, 1998)). For calculation of the air void characteristics, air bubbles with a diameter greater than 2 mm (0.079 in) are considered to be entrapped air and excluded by the software program. The entire test set up can be seen in Figure 2.11.

The Air Void Analyzer (AVA) takes a maximum of 25 minutes to run, with the ability to conduct approximately two tests per hour, due to the test set up and the cleaning required between tests. The AVA is not meant to be a replacement for the current field tests for total air content, because the small sample size (20 cm^3) does not provide a representative cross-section of the concrete mixture.

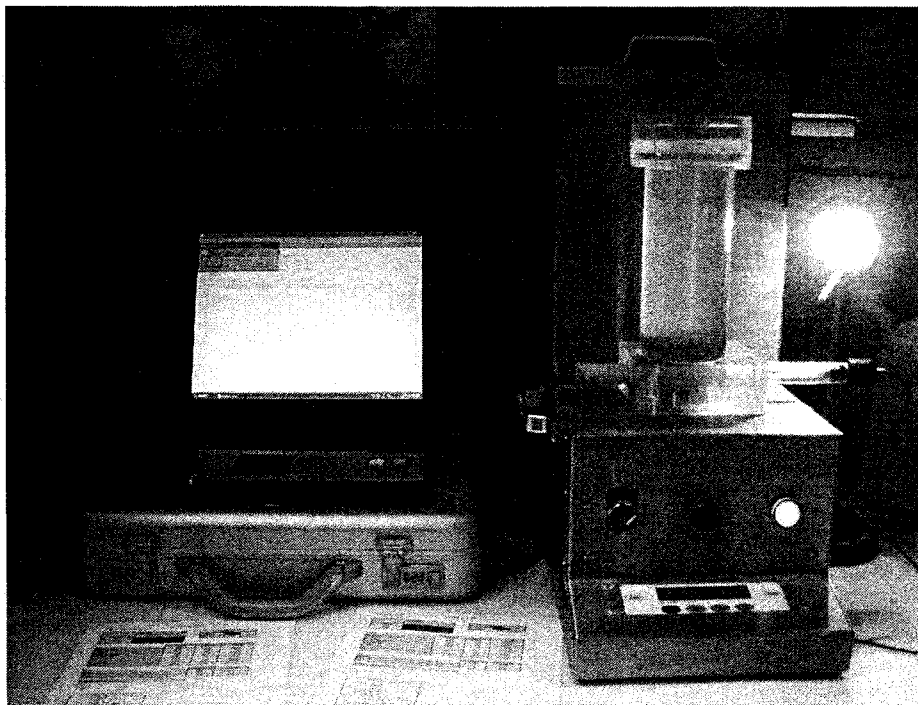


Figure 2.11 Air Void Analyzer test set up

2.2.2.2 Accuracy and Correlation of Results

Thirty-three tests on the air content and air void characteristics (using both ASTM C 457 and the AVA) on various air-entrained concretes were conducted for the Federal

Highway Administration (FHWA) across the United States (Magura, 1996). According to those tests, neither ASTM C 457 nor the air pressure methods were directly equivalent to the air content measured by the AVA. In fact, the AVA was always on the order of 2% less than the air content of the other two tests because of the exclusion of entrapped air voids greater than 2 mm (Magura, 1996). However, the AVA was only intended to measure air void characteristics, not to accurately measure the total air content of concrete. The spacing factor was about the same when tested by either the AVA or ASTM C 457, as depicted in Figure 2.12. The specific surface calculated by the AVA was found to be greater than that of ASTM C 457 tests (i.e. the AVA indicated smaller air voids than the ASTM procedure).

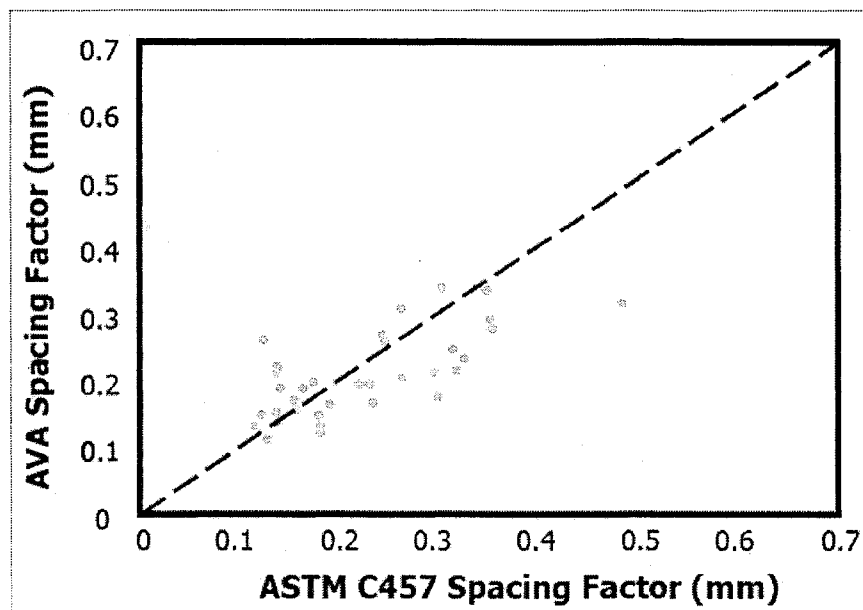


Figure 2.12 Spacing factor correlation between ASTM C 457 and AVA (Magura, 1996)

The AVA has an accuracy of $\pm 10\%$ when compared to the ASTM C 457 test method for air content, spacing factor and specific surface (Aarre, 1998). The $\pm 10\%$

average difference between the AVA and ASTM C 457 spacing factors appears to have significance, but in fact falls well within the range of average between-laboratory precision for two ASTM C 457 test results (Crawford et al., 2003). There has been a report of spacing factors from the same specimen determined using ASTM C 457 to be as much as 80% greater from one laboratory to another. While it can be concluded that the two methods measure the same parameters, the differences between AVA and ASTM C 457 spacing factors raises concern about the accuracy of the methods. However, it is “impossible to discern from this data set whether this variability is a result of AVA testing factors or ASTM C 457 testing factors” (Crawford et al., 2003).

In addition to the study by the Federal Highway Administration, Heinrichsen (2002) reported on the AVA, and determined that with 95% confidence the mean value of five performed AVA analyses will be within $\pm 2.96 \text{ mm}^{-1}$ of the mean specific surface and $\pm 0.014 \text{ mm}$ of the mean spacing factor determined by the ASTM C 457 method. For the same level of confidence, the individual AVA results will fall within $\pm 4.43 \text{ mm}^{-1}$ for the specific surface and $\pm 0.031 \text{ mm}$ of the average of five ASTM C 457 results.

2.2.2.3 Advantages and Disadvantages of the Air Void Analyzer

The Air Void Analyzer could help in the field to ensure that proper air void characteristics are present in the concrete before it is placed. In 9 out of the 14 cases tested by the FHWA where the concrete met total air volume requirements based upon the pressure tests (ASTM C 231), it did not meet the spacing factor durability requirements when tested with both the AVA and ASTM C 457 methods (Crawford et al., 2003). The general consensus is that there is definitely a place for the Air Void Analyzer in the current state of concrete practice in the field, based on the historical

inability to test air void parameters in concrete before placement (Saucier et al., 1990).

The approved ASTM tests that measure air void characteristics are performed on hardened concrete several days after the concrete is placed in the field. The Air Void Analyzer takes only 25 minutes to run and can be used at the concrete batch plant or transported to the job site to perform quick quality control of the air void characteristics of concrete.

The primary limitations of the AVA are: 1) the temperature of the liquids must be maintained between 21.1 and 25.6 °C (70 and 78 °F), and 2) the air content of the concrete must be between 3.5 and 10%. These limitations exist because of the specific calibration of the apparatus and its components. Additionally, in contrast to the air void measurement on hardened concrete, the AVA does not necessarily provide an accurate measurement of the total air content in the concrete.

2.2.3 Air Content Test

ASTM C 173, "Air Content of Freshly Mixed Concrete by the Volumetric Method," also referred to as the roll-a-meter, was employed to determine the total air content in the SCC mixtures, as seen in Figure 2.13.

2.3 Test Program

The test program consisted of two phases. Phase I aimed to evaluate the influence of four different admixture manufacturers for three distinct slump flows on the air void characteristics of the selected self-consolidating concretes. Phase II of the study included testing the influence of hauling time and two types of remediation on the trial self-consolidating concretes using a selected admixture manufacturer.

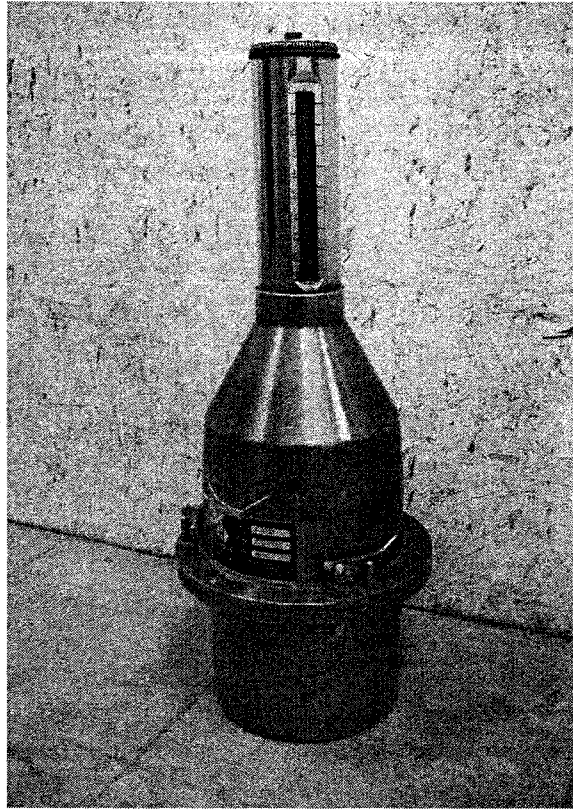


Figure 2.13 Volumetric air content roll-a-meter

2.3.1 Mixing Sequence

Following a consistent mixing sequence was critical for obtaining reproducible results with self-consolidating concrete. The mixing sequence selected for these experiments was based on ASTM C 192, but modified for self-consolidating concrete. The total mixing time was 14 minutes, with 10 minutes of mixing time from the initial cement-water contact to Phase I testing, as depicted in Figure 2.14. At the start of the investigation, the air-entrainment was added after seven minutes of mixing with the other admixtures. However, the air was insufficiently generated when the AEA was added with the other admixtures. Consequently, the mixing sequence was changed to follow most manufacturers' recommendations and add the AEA with first mixing water. Khayat

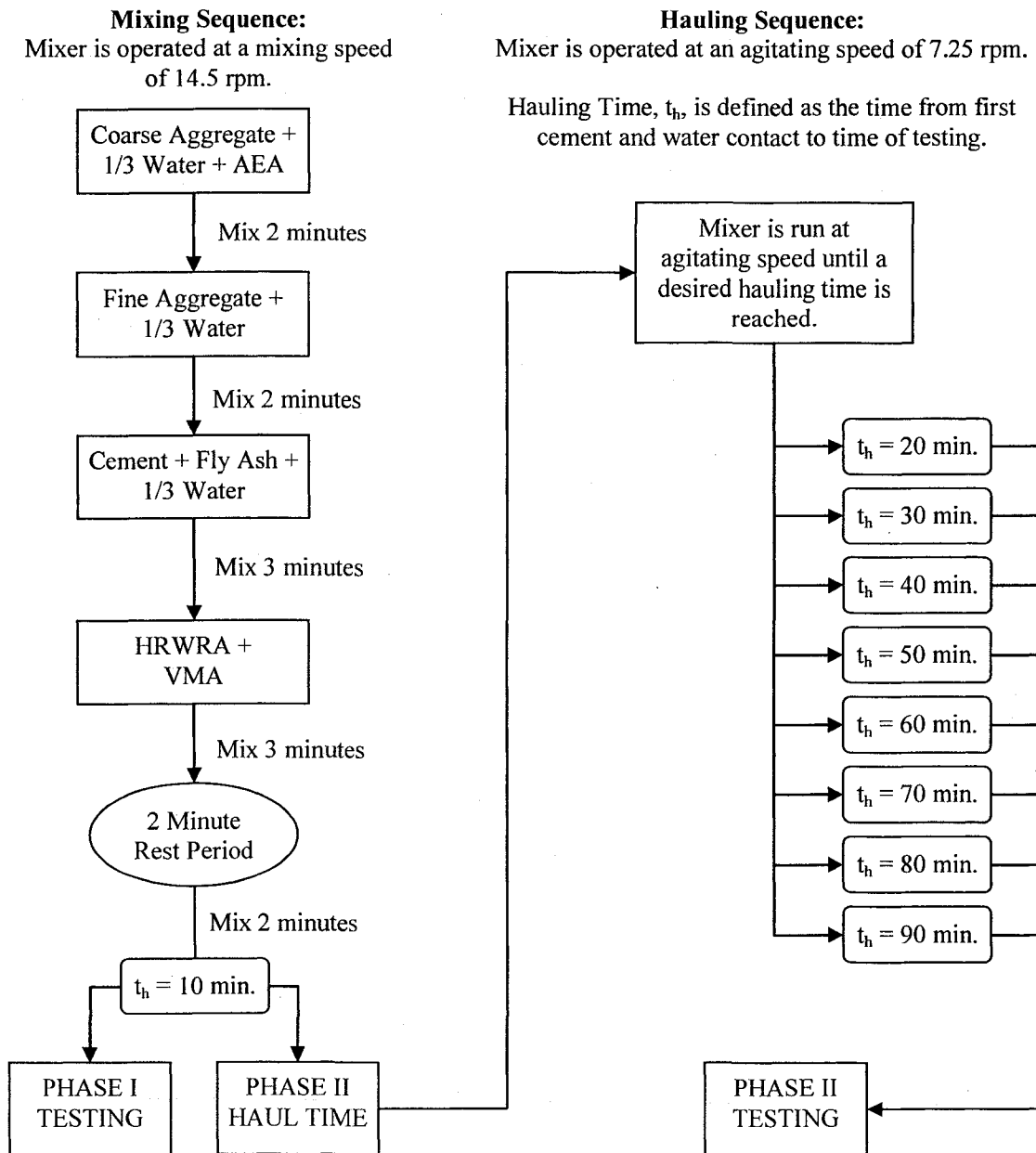


Figure 2.14 Mixing and hauling sequence

(2000) also noted that adding the AEA with the first mixing water was more efficient in entraining air when compared to adding AEA last.

2.3.2 SCC Test Methods

As stated in Chapter 1, test methods specific to SCC have been developed by researchers to classify and measure the flow ability, passing ability and resistance to dynamic segregation. The test methods employed in this research are outlined below.

2.3.2.1 Slump Flow and T_{50} Tests

The slump flow test, a measure of unconfined workability, is the most common method of determining the free flowing ability of a SCC mixture. A standard slump cone is used for the test; however, the diameter of the spread of concrete is measured instead of the height, as seen in Figure 2.15. ASTM C 1611 outlines the procedures for measuring slump flow. The procedure is similar to the slump test for conventional concrete without the mechanical consolidation at each layer to fill the cone. The average

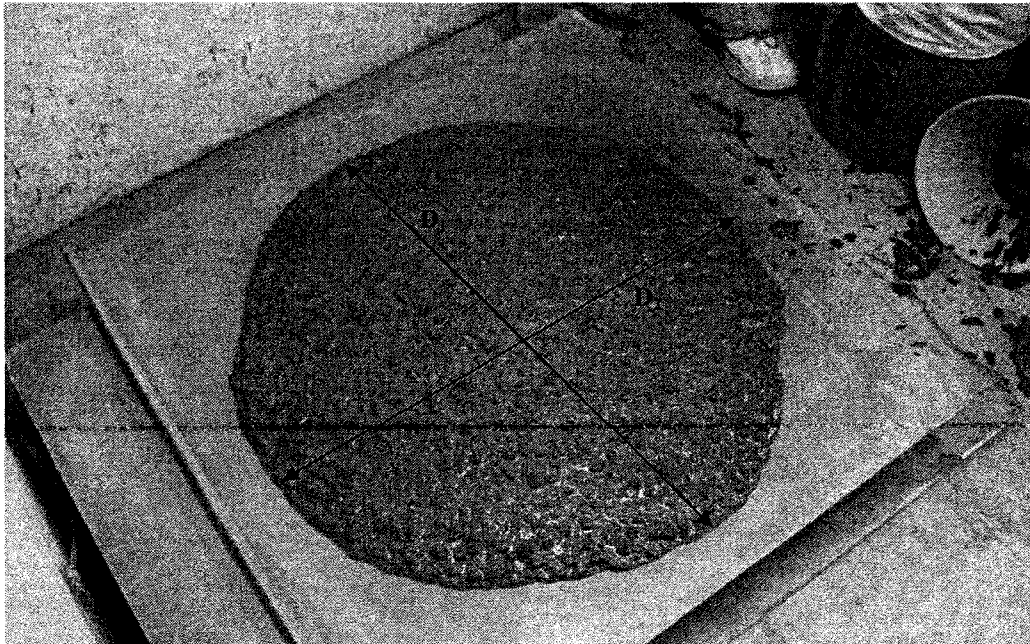


Figure 2.15 Slump flow measurement – average of D_1 and D_2 is taken

of two perpendicular measurements is recorded in the case of concrete flowing unevenly across the plate. The measured diameter is an indicator of the unobstructed flow ability of the concrete. In order to be classified as SCC, the slump flow must reach at least 500 mm (20 inches). The slump flow correlates with the yield stress of the concrete and evaluates the consistency of successive batches (Bonen and Shah, 2005).

The T_{50} , a measure of the flow rate or viscosity by inference, is the time elapsed from when the cone is lifted to when the concrete reaches a 50 cm circle. A T_{50} measurement in the range of 2 to 5 seconds is desirable to limit the impact a concrete mixture may impart when being placed against rebar and formwork. A higher T_{50} value indicates a concrete with higher viscosity. The T_{50} is sensitive due to the short duration of the timing, and therefore, is not the most accurate measurement. In the event of uneven flow of the concrete, the T_{50} measurement is taken when the majority ($\frac{3}{4}$) of the diameter has reached the 50 cm mark.

2.3.2.2 J-Ring Passing Ability Test

While the slump flow test measures the unobstructed flow ability of the concrete, the J-Ring test measures the obstructed flow ability and passing ability of a SCC mixture. The J-Ring test is typically conducted in conjunction with the slump flow test, and its procedure is outlined in ASTM C 1621. The conventional slump cone is used with a simulated reinforcement cage placed around it, as seen in Figure 2.16. When the cone is lifted, the SCC will flow around the rebar, and the final diameter of the spread is measured. Again, the average of two perpendicular measurements is taken due to the uneven spread of the concrete. The J-Ring measurement must be within 51 mm (2

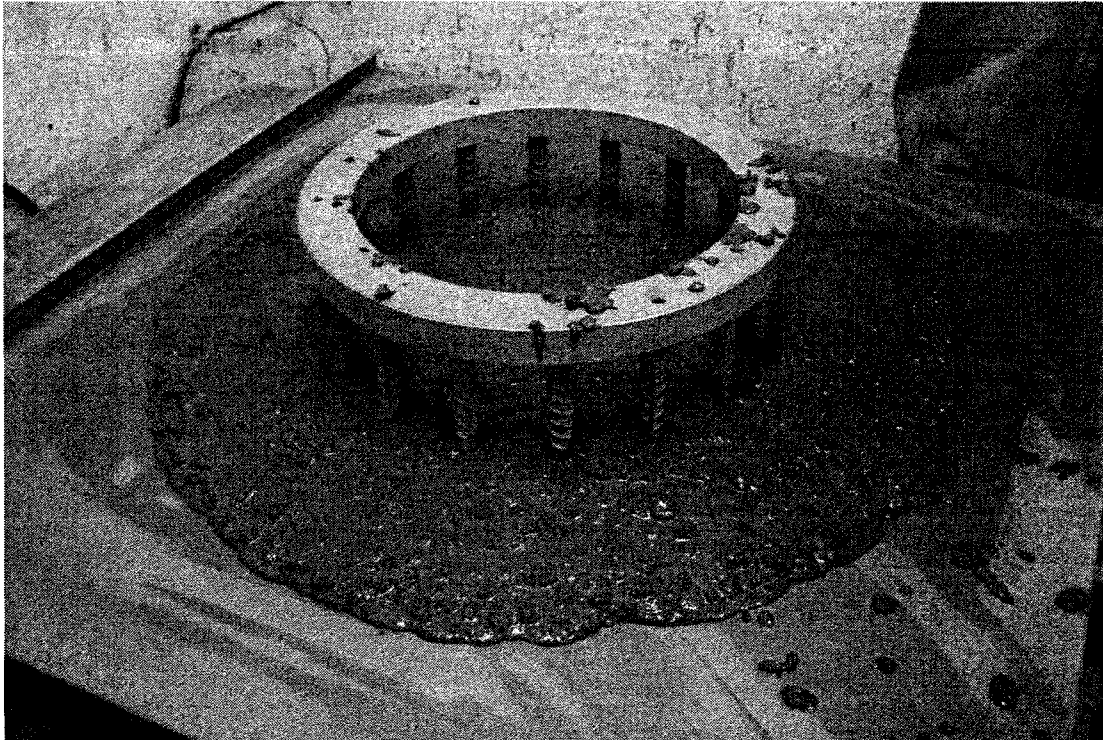


Figure 2.16 J-Ring test demonstrating good passing ability

inches) of the slump flow measurement to indicate adequate passing ability of the SCC mixture.

2.3.2.3 Dynamic Segregation Resistance Test

During the slump flow test, a SCC mixture's resistance to bleeding and segregation can be determined visually. This is quantified by the Visual Stability Index, or VSI, which ranges from a value of 0 to 3 (best to worst stability), and is outlined in Table 2.7. Mortar halo is a term for the cement paste that flows beyond the aggregate during a slump flow test. A highly stable or stable mixture, corresponding to a VSI of 0 or 1, is desirable, since segregation and bleeding of water can cause a decrease in the strength of concrete. The VSI indicates a mixture's stability and resistance to dynamic segregation.

Table 2.7 Visual Stability Index (ASTM C 1611)

VSI	Description
0	Highly Stable (no evidence of segregation or bleeding)
1	Stable (no evidence of segregation and slight bleeding observed as a sheen on concrete mass)
2	Unstable (slight mortar halo ≤ 0.5 in. (≤ 10 mm) and/or aggregate pile in center of the concrete mass)
3	Highly Unstable (clearly segregating by evidence of large mortar halo > 0.5 in. (> 10 mm) and/or large aggregate pile in the center of the concrete mass)

2.3.3 Phase I Procedures

During Phase I of the investigation, twelve mixtures were developed using four admixture sources and three target slump flows. Each mixture was labeled with an identification, where the first letter indicates the admixture manufacturing source, and the second two characters and number denote the slump flow (in inches). This identification system is shown in Table 2.8.

Table 2.8 Mixture identification

Mixture Identification	Slump Flow	Admixture Source
A-SF22	559 mm (22 in.)	A
B-SF22		B
C-SF22		C
D-SF22		D
A-SF25	635 mm (25 in.)	A
B-SF25		B
C-SF25		C
D-SF25		D
A-SF28	711 mm (28 in.)	A
B-SF28		B
C-SF28		C
D-SF28		D

2.3.3.1 Determination of Optimum Admixture Dosage

The procedures for obtaining the “optimum admixture dosage” were based on trial-and-error. The minimum amount of the admixture was used to obtain the target fresh properties, which are outlined in the following section. Optimization of admixture dosages typically involved a two-step process. The first step was to determine the HRWR and VMA dosages required to meet the flow properties of slump flow, T_{50} rate of flow ability, J-Ring passing ability, and resistance to dynamic segregation. Once the flow properties were within the acceptable range, the AEA dosage was determined to meet the required volumetric air content. The AEA dosage was then further corrected if the air void characteristics did not meet the minimum standards.

Once a certain mixture had successfully met all the target fresh properties, two validation batches were made to confirm the results and to produce cylinders for compressive strength testing. Five separate air void analyses were performed on each of the selected twelve mixtures to determine the fresh air void characteristics. Two AVA samples were taken from each of the two mixture validation batches for fresh properties, whereas the fifth sample was taken from the batch used to make cylinders. Five samples were taken to ensure a good level of confidence in the results presented, allowing an accurate comparison between the tested slump flows and admixture sources.

2.3.3.2 Target Fresh Properties

The target fresh properties and their corresponding accuracies are listed below in Table 2.9. During measurement of the T_{50} , often it was not possible to get a time more than 2 seconds, especially at the higher slump flows. It was considered uneconomical to

increase admixture dosages further in some cases; as a result, the T_{50} target window of 2 to 5 seconds was not always met.

Table 2.9 Phase I target fresh properties

Property	U.S. Units	SI Units	Method
Slump Flow	22, 25 or 28 ± 0.5 inches	559, 635 or 711 ± 13 mm	ASTM C 1611
T_{50}	2 to 5 seconds		ASTM C 1611
J-Ring	SF - J-Ring = 2 in.	SF - J-Ring = 51 mm	ASTM C 1821
VSI	0 or 1 (Highly Stable or Stable)		ASTM C 1611
Air Content	$6 \pm 0.5\%$		ASTM C 173
Spacing Factor	$\bar{L} < 0.0079$ in.	$\bar{L} < 200$ μm	AVA (correlated with ASTM C 457)
Specific Surface	$\alpha > 635$ in. ⁻¹	$\alpha > 25$ mm ⁻¹	

2.3.3.3 Hardened Properties

Compressive strength was the only hardened property tested of the twelve SCC mixtures. This test was conducted to characterize the mixtures and further compare the effects of admixture dosages and sources. Twelve 102 x 203 mm (4 x 8 inch) cylinders were prepared from a batch of each mixture once the target fresh properties had been achieved. They were demolded after one day and placed in a curing room (temperature of 70 ± 2 °F) with 100% humidity until they were tested. Compression tests were conducted after 7, 28 and 90 days of curing, following ASTM C 39, using a Gilson Company machine, which can be seen in Figure 2.17. The average of four cylinders was reported as the compressive strength of the mixture. On occasion, one measurement was not used if it was outside one standard deviation of the average result. There was no

specified target compressive strength required of the mixtures, although 34.5 MPa (5000 psi) is recommended for severe freezing and thawing exposure under ACI 318-05.

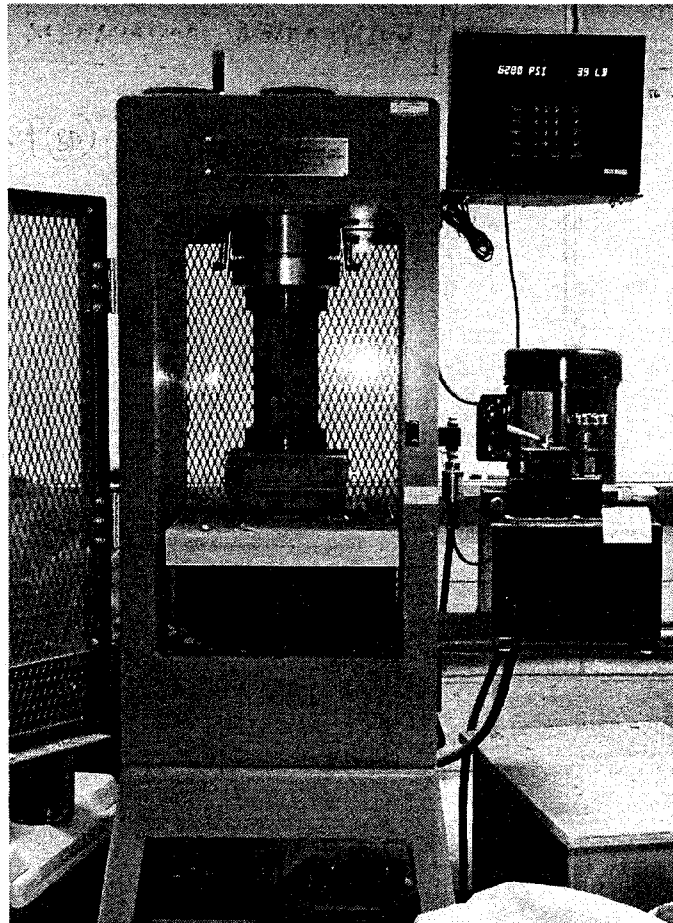


Figure 2.17 Compression test machine

2.3.4 Phase II Procedures

In the Phase II of the study, one admixture source and three different slump flows were tested to determine the effects of hauling time on the fresh properties and air void characteristics of self-consolidating concrete. There was no measurement of hardened properties for the mixtures developed during Phase II. The three mixtures designed in Phase I were further mixed at a designated agitation speed, as described in Section 2.2.1,

and then tested at eight hauling times of 20, 30, 40, 50, 60, 70, 80 and 90 minutes.

Hauling time is defined as the time from first water to cement contact to time of testing. After the initial mixing sequence depicted in Figure 2.14, the mixer was switched to the agitation speed until the desired hauling time was reached. One minute prior to the hauling time, the mixing action increased to the mixing speed (14.5 rpm), simulating the procedure a ready-mixed truck would follow upon arriving at a job site. At this point, the slump flow, T_{50} rate of flow ability, J-Ring passing ability, air content, and air void characteristics were tested to measure the change, if any, in the fresh properties recorded during the Phase I of the investigation. The procedures for hauling time were repeated at least once for each hauling time and each slump flow to validate results.

After each hauling time was validated for all three slump flows, remediation A (overdosing) and remediation B (retempering) were performed. Remediation A followed trial-and-error procedures. Based on the slump flow and air content loss (or gain) the admixtures were initially overdosed or under-dosed during the mixing sequence to obtain the target fresh properties. Then the mixer was run at the agitation speed until the desired hauling time was attained. Again, the speed was increased one minute before the hauling time was reached to ensure consistency. Finally, the slump flow, T_{50} rate of flow ability, J-Ring passing ability, air content and air void characteristics of the mixture were tested. If any of the target fresh properties did not adhere to the target limits, the admixture dosages were adjusted and the testing was repeated with a new batch. For remediation, only two AVA tests were conducted at each hauling time.

For the second type of remediation, known as retempering, the admixture dosages obtained in the Phase I were used for the initial mixing sequence. The mixer was run at

the agitation speed until the desired hauling time was met. At this point, the speed was increased to the mixing speed, and pre-measured admixtures were added to achieve the target fresh properties. The mixer was run for two minutes at the mixing speed, stopped to rest the concrete for 30 seconds, and then run again for 30 seconds. A total mixing time of three minutes is generally recommended for admixtures to impart their impact into a mixture. At this juncture, the mixture was tested in the same manner as remediation A.

2.3.4.1 Target Remediation Properties

The target properties were less stringent for remediation than for the mixture development of the Phase I. These properties are outlined in Table 2.10. The accuracy of slump flow was increased from 12 to 25 mm (0.5 to 1 inch), and the accuracy of the air content was increased from 0.5% to 1%. This was mainly due to time restrictions in the laboratory, but they are also more realistic thresholds for field applications when remediation is utilized.

Table 2.10 Phase II Remediation Target Fresh Properties

Property	U.S. Units	SI Units	Method
Slump Flow	22, 25 or 28 ± 1 inches	559, 635 or 711 ± 25 mm	ASTM C 1611
T ₅₀	2 to 5 seconds		ASTM C 1611
J-Ring	SF - J-Ring ≤ 2 inches	SF - J-Ring ≤ 51 mm	ASTM C 1821
VSI	0 or 1 (Highly Stable or Stable)		ASTM C 1611
Air Content	6 ± 1%		ASTM C 173
Spacing Factor	$\bar{L} < 0.0079 \text{ in.}$	$\bar{L} < 200 \text{ } \mu\text{m}$	AVA (correlated with ASTM C 457)
Specific Surface	$\alpha > 635 \text{ in.}^{-1}$	$\alpha > 25 \text{ mm}^{-1}$	

In summary, this chapter presented the properties of the constituents, mixture proportioning, test equipment, and test program developed for investigating various self-consolidating concrete mixtures. The SCC mixtures studied herein were developed using the HRWR, VMA and AEA from four admixture sources. The Air Void Analyzer was used for the determination of the air void characteristics of the fresh concrete. The mixing sequence, and SCC test methods and procedures were outlined for the investigation.

CHAPTER 3

PHASE I: MIXTURE OPTIMIZATION OF AIR-ENTRAINED SELF-CONSOLIDATING CONCRETES

The objectives of the first phase of the investigation are: 1) to determine the optimum dosage requirements of the four different admixture manufacturers in attaining the three target slump flows of 559 mm (22 in.), 635 mm (25 in.) and 711 mm (28 in.); and 2) to examine the influence of different admixture sources on air void characteristics of self-consolidating concrete. In addition to the required slump flow, other fresh properties such as J-Ring passing ability, resistance to dynamic segregation, T_{50} rate of flow ability, and total air content were evaluated. The air void characteristics were measured using the Air Void Analyzer (AVA) to obtain the specific surface and spacing factor. As outlined in Chapter 2, with the exception of the admixture dosages, the mixture proportions of the trial batches were held uniform. A total of 111 batches were tested and 107 concrete samples were analyzed with the Air Void Analyzer to achieve the objectives of the Phase I investigation.

3.1 Optimized HRWR and VMA Admixture Dosages

For the purposes of this study, the optimum HRWR and VMA admixture dosage was defined as the minimum amount of dosage required to achieve the target fresh properties. The optimized admixture dosages and mixture proportions are presented in Table 3.1.

Table 3.1(a) Phase I mixture constituents and proportions

Mixture Identification	Cement (kg/m ³)	Fly Ash (kg/m ³)	w/cm ¹	Water (kg/m ³)	Fine Aggregate (kg/m ³)	Coarse Aggregate (kg/m ³)
A-SF22	390	78	0.40	196	795	864
B-SF22	390	78	0.40	196	795	864
C-SF22	390	78	0.40	196	795	864
D-SF22	390	78	0.40	196	795	864
A-SF25	390	78	0.40	196	795	864
B-SF25	390	78	0.40	196	795	864
C-SF25	390	78	0.40	196	795	864
D-SF25	390	78	0.40	196	795	864
A-SF28	390	78	0.40	196	796	865
B-SF28	390	78	0.40	196	795	864
C-SF28	390	78	0.40	196	795	864
D-SF28	390	78	0.40	196	795	864

¹ water-to-cementitious materials ratio1 kg/m³ = 1.6856 lb/yd³

Table 3.1(b) Phase I mixture constituents and proportions

Mixture Identification	ml/kg cementitious materials			% Paste ⁵	% Mortar ⁶	% Air	% Vol. of Coarse Aggregate
	HRWR ²	AEA ³	VMA ⁴				
A-SF22	2.74	0.78	0.65	40.91	67.24	6.00	27.91
B-SF22	1.50	0.33	0.00	37.47	65.33	6.00	29.54
C-SF22	2.15	1.24	0.00	39.81	66.62	6.00	28.43
D-SF22	1.24	0.33	0.00	37.06	65.10	6.00	29.73
A-SF25	3.39	0.78	1.24	42.58	68.16	6.00	27.13
B-SF25	2.02	0.72	0.26	39.24	66.31	6.00	28.70
C-SF25	2.61	1.47	0.26	41.14	67.36	6.00	27.81
D-SF25	1.83	0.59	0.26	38.76	66.04	6.00	28.93
A-SF28	4.43	1.30	1.79	45.22	69.63	6.00	25.88
B-SF28	2.54	0.78	0.33	40.18	66.83	6.00	28.26
C-SF28	3.00	1.37	0.33	41.63	67.63	6.00	27.58
D-SF28	2.41	0.85	0.33	40.09	66.78	6.00	28.30

² high range water reducing admixture, ³ air-entraining admixture, ⁴ viscosity modifying admixture, ⁵ % paste by volume = % cement + % fly ash + % water + % admixtures, ⁶ % mortar by volume = (% paste) + (% aggregate < 6 mm)

1 ml/kg cementitious materials = 1.5338 ounces per 100 pounds cementitious materials

The overall ranking of sources from the most to the least economical admixture dosage by volume was D, B, C and A. Sources D, B and C tended to have relatively similar admixture dosages, whereas source A required a much higher amount to achieve the target fresh properties, as shown in Figure 3.1. Also, as shown in Figure 3.2, the required admixture dosages typically increased with increasing slump flow.

3.2 Fresh Properties

The actual slump flow, J-Ring passing ability, T_{50} rate of flow ability, VSI, and air content measured for each mixture design can be seen in Table 3.2. Most measurements reported are the average of two or three trials for each test, depending on the consistency between trial batches. In general, the 559 mm (22 in.) slump flow mixtures demonstrated less J-Ring passing ability than the higher slump flows, indicating a higher viscosity with a lower slump flow. One mixture, C-SF22, did not meet the maximum J-Ring passing ability requirement of 51 mm (2 in.). Four mixtures (A-SF25, D-SF25, A-SF28, and D-SF28) did not meet the T_{50} standard of greater than 2.0 seconds.

Table 3.2 Phase I fresh properties

Mixture Identification	Slump Flow (mm)	J-Ring (mm)	SF – J-Ring (mm)	T_{50} (sec.)	VSI	Air Content (%)
A-SF22	552	508	44	2.35	0	6.0
B-SF22	565	518	48	2.53	0	6.0
C-SF22	562	498	64	3.13	0	6.4
D-SF22	572	527	44	2.73	0	6.0
A-SF25	638	600	38	1.93	0	6.3
B-SF25	648	610	38	2.26	0	6.4
C-SF25	640	608	32	2.50	0	6.5
D-SF25	624	586	38	1.92	0	6.2
A-SF28	709	671	38	1.77	1	6.1
B-SF28	715	684	32	2.02	1	6.0
C-SF28	714	676	38	2.25	1	6.4
D-SF28	711	699	13	1.71	1	6.0

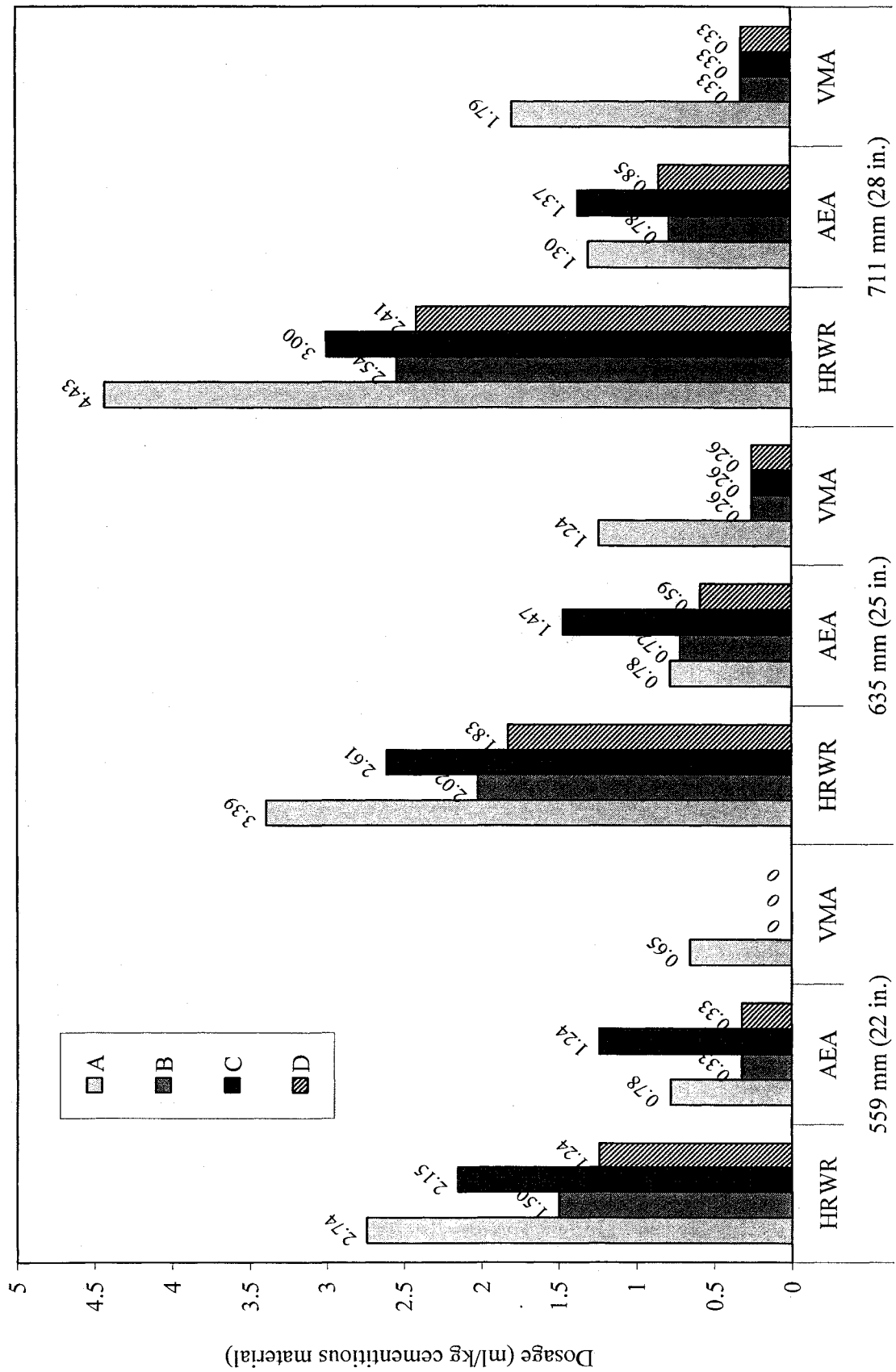


Figure 3.1 Phase I admixture dosages with respect to manufacturer

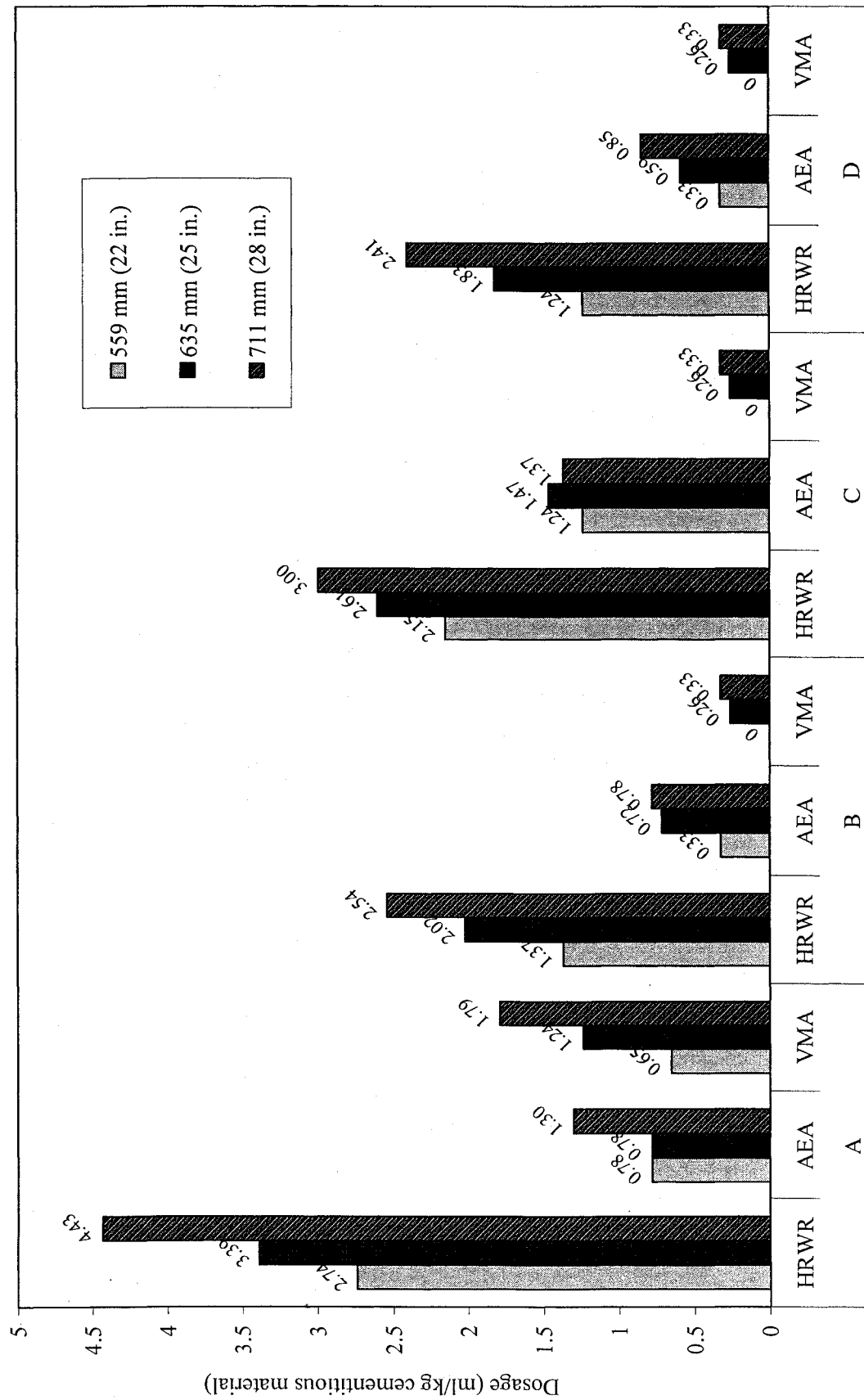


Figure 3.2 Phase I admixture dosages with respect to slump flow

However, these four mixtures were within 0.3 seconds of the lower range suggested for the rate of flow ability. Due to the high operator error associated with measuring the T_{50} , and the variance of data between batches, these mixtures were deemed acceptable. All mixtures met the VSI rating of 0 (highly stable) or 1 (stable), but only mixtures with a 711 mm (28 in.) slump flow received the rating of 1. In terms of total air content, the $6 \pm 0.5\%$ target was achieved in all mixtures.

3.2.1 Effects of Admixture Source

The SCC mixtures developed were primarily reliant on the dosages of HRWR and VMA to achieve the required flow properties and passing ability. Regardless of admixture manufacturer, the dosage of HRWR and VMA increased with increasing slump flow. Increasing the dosage of HRWR typically resulted in a less stable mixture, evidenced by more bleeding and segregation. These characteristics necessitated an increase in the VMA dosage in order to create a stable mixture with the required flow ability and resistance to segregation and bleeding.

SCC mixtures utilizing admixtures from source A always required VMA to create a stable SCC mixture ($VSI \leq 1$). This was especially evident at the lowest slump flow (559 mm) since sources B, C and D did not require any VMA. The HRWR used from source A had a slightly different chemical composition than the other three sources. Source A consisted of a polycarboxylate-ester (PCE) molecule, as opposed to a polycarboxylate-acid (PCA) molecule. In general, the PCE molecule contains less binding sites to adsorb to the cement particles, but more side chains that allow for better slump retention capability, as seen in Figure 3.3. On the other hand, a PCA molecule has

more binding sites which allows for more dispersion of the cement particles, thus imparting greater flow ability to a mixture.

Trial-and-error procedures were used to achieve the optimum admixture dosages of the SCC mixtures. However, upon inspection of the HRWR-VMA dosage combinations, there was an ideal VMA-to-HRWR ratio for each admixture source to produce air-entrained SCC, as shown in Table 3.3. Source A had an increase in VMA-to-HRWR ratio with increasing slump flow, from 0.24, 0.37 and 0.40 for the 559, 635 and 711 mm slump flows, respectively. Sources B, C and D had an optimum ratio of VMA-to-HRWR (when VMA was utilized) of 0.13, 0.11 and 0.14, respectively. Although the chemical differences between each admixture manufacturer may be small, an ideal relationship or trend between the HRWR and VMA had to be established for each source before incorporating into a mixture. The polycarboxylate-ester (PCE) HRWR of source A had a varying VMA-to-HRWR ratio; whereas the polycarboxylate-acid (PCA) HRWR

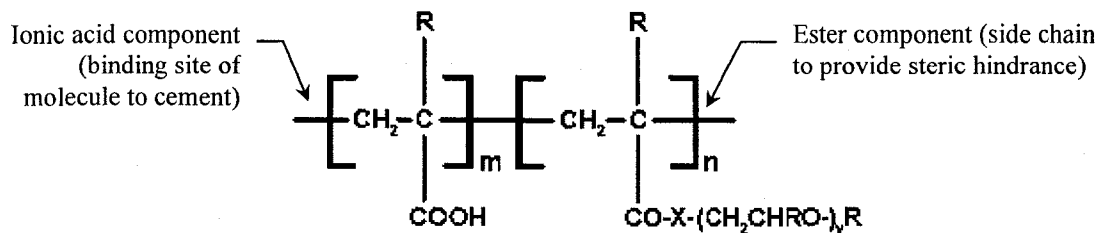


Figure 3.3 Chemical structure of a polycarboxylate polymer (SIKA ViscoCrete, 2008)

Table 3.3 VMA-to-HRWR dosage ratios

	Slump Flow (mm)		
	559	635	711
Source A	0.24	0.37	0.40
Source B	0	0.13	0.13
Source C	0	0.10	0.11
Source D	0	0.14	0.14

of sources B, C and D revealed that an ideal ratio exists. The immediate adsorption of the PCA to the cement causes less flocculation, bleeding and sedimentation of particles, thus a certain dosage of VMA is needed to slow down the flow of mixture. On the other hand, with PCE, the VMA is needed to both slow down the flow of mixture and decrease segregation and bleeding.

The different types of admixtures originating from each source significantly influenced the passing ability and flow ability of the mixtures. Source D exhibited the best J-Ring passing ability, and source C exhibited the best flow ability (T_{50} time). The average passing ability of the three slump flows, as evaluated by the difference between the slump flow and J-Ring tests, and the average T_{50} flow ability of the three slump flows are shown in Table 3.4. The admixture source with the highest average T_{50} rate of flow ability was source C, followed by B, D and A, which indicates the most viscous to least viscous mixtures by source.

Table 3.4 Average fresh properties by source

Average of Three Slump Flows	Admixture Source			
	A	B	C	D
Slump Flow - J-Ring (mm)	40	39	44	32
T_{50} (sec.)	2.02	2.27	2.62	2.12

3.2.2 Effects of Slump Flow

Slight differences in flow properties existed between the admixture sources; however, more marked differences in T_{50} , VSI and J-Ring passing ability values existed between slump flows. As stated earlier, both the HRWR and VMA dosage increased

with increasing slump flow. To facilitate dispersion of particles, the HRWR was increased, and to increase viscosity and reduce segregation and bleeding, the VMA was increased.

The T_{50} flow times, which indicate the flow ability and viscosity of a SCC mixture, generally decreased with increasing slump flow, as seen in Table 3.2. The average T_{50} decrease from 559 to 635 mm slump flow was 20%, and the average T_{50} decrease from 635 to 711 mm slump flow was 10%, signifying a greater decrease in viscosity from 559 to 635 mm than from 635 to 711 mm. All of the mixtures developed had a relatively low viscosity, evidenced by the T_{50} times remaining close to the lower limit of the suggested values.

The VSI rating determined for each of the twelve mixtures indicated the mixture's dynamic stability, or resistance to bleeding and segregation. A VSI rating of 1 was only given at the largest slump flow of 711 mm (28 inches) for the four admixture sources. This suggests that an increase in slump flow decreases stability.

The J-Ring test results of the SCC mixtures demonstrated that passing ability increased as the slump flow increased. On average, the differences between the measured slump flow and J-Ring passing ability values for 559, 635, and 711 mm slump flows were 50, 37 and 30 mm. This equates to a 27% increase in average passing ability between 559 and 635 mm flows, and 17% increase in average passing ability from the 635 and 711 mm slump flows. As the cohesion of a mixture increases, the more likely it is to be stopped by an obstruction like rebar. The J-Ring differences between the 559 and 635 mm slump flows were greater than the differences between the 635 and 711 mm slump flows. This distinction was also evident with the T_{50} flow times, as there appeared

to be more similar flow ability between the 635 and 711 mm slump flows than between then 559 and 635 mm slump flows.

3.2.3 Predictive Equations of Admixture Dosages

The HRWR and VMA dosages for all sources were correlated with the slump flow at a 95% confidence level using statistical analysis software, DataFit version 8.2, and the results are shown below in Table 3.5. The coefficients of determination (R^2), standard errors and t-test probabilities for the variables are shown in Table 3.6.

Table 3.5 HRWR and VMA predictive equations

Source	Admixture Dosage (ml/kg cementitious materials)	
A	$HRWR_A = \frac{1}{0.872 - 9.1 \times 10^{-4} SF}$	$VMA_A = -1.104 + 5.758 \times 10^{-6} SF^2$
B	$HRWR_B = 6.348 + \frac{-2756.0}{SF}$	$VMA_B = 0.914 + \frac{-288037}{SF^2}$
C	$HRWR_C = 6.1232 + \frac{-2237.2}{SF}$	$VMA_C = 0.905 + \frac{-280782}{SF^2}$
D	$HRWR_D = 7.214 + \frac{-3397.2}{SF}$	$VMA_D = 0.956 + \frac{-299616}{SF^2}$

where: SF = actual slump flow, $559 \leq SF \leq 711 \pm 13$ mm

Table 3.6 Statistical data for HRWR and VMA equations

Equation	R^2	Standard Error	T-Test Probability	
			Variable a	Variable b
$HRWR_A$	1.00	0.577	0.024	0.034
$HRWR_B$	0.98	0.931	0.055	0.081
$HRWR_C$	1.00	0.217	0.013	0.023
$HRWR_D$	0.99	0.743	0.043	0.057
VMA_A	1.00	0.001	0.001	0.000
VMA_B	0.97	0.398	0.083	0.103
VMA_C	0.96	0.498	0.104	0.129
VMA_D	0.87	0.902	0.196	0.239

Initially, the HRWR and VMA dosages were also predicted using a variable β , which indicated the mixture proportions by multiplying (% paste) x (% mortar) x (% coarse aggregate) by volume. However, after further analysis, it was determined that β did not play a significant role in the determination of the HRWR and VMA dosages since only one aggregate source was used in this investigation. The equations presented in Table 3.5 accurately represent the HRWR and VMA dosages, based on the coefficients of determination (R^2) close to 1. It can be noted that sources B, C and D utilized similar predictive equations for HRWR and VMA, whereas source A necessitated equations in a different form. Due to their similarity, predictive equations of the HRWR and VMA dosages of admixture sources B, C and D were attempted. The VMA dosage was successfully predicted for sources B, C and D, as seen in Equation 3.1. In fact, the R^2 value of Equation 3.1 is 0.98, and the standard error is 0.022, which predicts the VMA dosage significantly better than the equations presented in Table 3.5. However, the HRWR dosages could not be combined into one equation because the dosages of source C were 30% greater than source B and 47% greater than source D, on average. Actual VMA dosages and those calculated using Equation 3.1 can be seen in Appendix B.

$$VMA_{B,C,D} = -22.2 + \frac{1200.9}{\sqrt{SF}} + \frac{-16006.7}{SF} \quad \text{Eq. 3.1}$$

The required AEA dosage was predicted by the HRWR dosage, VMA dosage, and slump flow. The predictive equation for AEA dosages to produce $6 \pm 0.5\%$ entrained air, in ml/kg cementitious materials, can be seen in Equation 3.2. The values of variables a through g , as well as their individual t-test probabilities can be seen in Table 3.7. Equation 3.2 can be used for all four admixture sources, has a coefficient of determination of 0.97, and a standard error of 0.097.

$$AEA = \frac{a}{HRWR} + bVMA + cSF + \frac{d}{HRWR^2} + eVMA^2 + fSF^2 + g \frac{VMA}{HRWR} \quad \text{Eq. 3.2}$$

where: $HRWR$ = HRWR dosage, $1.2 \leq HRWR \leq 4.5$ ml/kg cementitious materials

VMA = VMA dosage, $0 \leq VMA \leq 1.8$ ml/kg cementitious materials

SF = actual slump flow, $559 \leq SF \leq 711 \pm 13$ mm

Table 3.7 Statistical data for AEA dosage predictive equation

Variable	a	b	c	d	e	f	g
Value	-23.58	-8.89	0.03	16.25	2.37	-2.4×10^{-5}	13.55
Prob(t)	0.003	0.011	0.001	0.005	0.009	0.001	0.028

Equation 3.2 demonstrates that the AEA dosage is affected by the HRWR and VMA dosages, as well as the slump flow. Increasing the HRWR and VMA dosage is accompanied by increasing slump flow, which generally increases the AEA dosage required. The AEA dosage required in a SCC mixture entrained with 6% air can be accurately predicted using Equation 3.2, based on the R^2 value close to 1, and statistically significant t-test probabilities of variables (not greater than 2.8%).

The actual admixture dosages were compared with the calculated dosages using the equations in Table 3.5 for HRWR and VMA, and Equation 3.2 for AEA. The calculated dosages and percent error for the HRWR, VMA and AEA dosages can be seen in Tables 3.8 and 3.9. The equations presented most accurately predict the dosages for admixture source A, evidenced by its low percent error. Predicting the dosage rates for sources B and D typically produced the most error in comparison to the actual admixture dosages. There was no trend evident in the error associated with predicting admixture dosages with respect to slump flow.

Table 3.8 Actual and calculated HRWR and VMA dosages (ml/kg cementitious materials)

Admixture Source	Actual SF (mm)	HRWR			VMA		
		Actual	Calculated	% Error	Actual	Calculated	% Error
A	552	2.74	2.71	1.0%	0.65	0.65	-0.2%
	638	3.39	3.44	-1.4%	1.24	1.24	-0.2%
	709	4.43	4.41	0.6%	1.79	1.79	0.3%
B	565	1.50	1.47	2.0%	0.00	0.01	-1.0%
	648	2.02	2.09	-3.5%	0.26	0.23	12.8%
	715	2.54	2.49	1.9%	0.33	0.35	-7.8%
C	562	2.15	2.14	0.4%	0.00	0.02	-1.0%
	640	2.61	2.63	-0.7%	0.26	0.22	16.0%
	714	3.00	2.99	0.3%	0.33	0.35	-8.8%
D	572	1.24	1.27	-2.5%	0.00	0.04	0.0%
	624	1.83	1.77	2.9%	0.26	0.19	28.1%
	711	2.41	2.44	-1.0%	0.33	0.36	-11.6%

Table 3.9 Actual and calculated AEA dosages (ml/kg cementitious materials)

Source	Actual SF (mm)	HRWR	VMA	AEA		
				Actual	Calculated	% Error
A	552	2.74	0.65	0.78	0.75	3.9%
	638	3.39	1.24	0.78	0.86	-9.9%
	709	4.43	1.79	1.30	1.29	1.2%
B	565	1.50	0.00	0.33	0.29	10.3%
	648	2.02	0.26	0.72	0.72	0.1%
	715	2.54	0.33	0.78	0.92	-18.1%
C	562	2.15	0.00	1.24	1.34	-7.8%
	640	2.61	0.26	1.47	1.37	6.5%
	714	3.00	0.33	1.37	1.37	0.0%
D	572	1.24	0.00	0.33	0.36	-9.4%
	624	1.83	0.26	0.59	0.58	1.6%
	711	2.41	0.33	0.85	0.82	3.8%

3.2.4 Air Content

The air content and required AEA dosage of the twelve mixtures were influenced by both the admixture source and slump flow. Similar to the flow properties, the admixture source dictated the dosage required to achieve the target air content of $6 \pm 0.5\%$. Conversely, the slump flow influenced the effectiveness of the AEA to produce the target air content.

3.2.4.1 Effects of Admixture Source on Air Content

Differences and similarities between the admixture sources are primarily linked to the AEA type: sources B, C and D are wood-derived acid salts, while source A is a synthetic detergent. The two classes of AEAs utilize different mechanisms to entrain air, and thus react differently with the other mixture constituents (i.e. cement, fly ash, HRWR and VMA). The type of AEA also dictated the dosage required to entrain the target air content. Indeed, source C necessitated the largest volume of AEA to entrain 6% air.

Sources B and D required similar AEA dosages to obtain the target air content. The dosage of AEA increased with increasing slump flow for sources B and D, but at different rates, as seen in Figure 3.2. The AEA dosage increase for source B was 54% and 8% from 559 to 635 mm and 635 to 711 mm, respectively. For source D, there was a more steady change in AEA dosage between the slump flows: from 559 to 635 mm the increase was 44%, and from 635 to 711 mm the increase was 31%. Along with the increased dosage of AEA from 559 to 635 mm for sources B and D, there was also an increase in HRWR and the introduction of a VMA. The increased fluidity (due to increased HRWR) and introduction of VMA increased the required AEA dosage. Source

B and D admixtures are both salt-type AEAs that typically bond at the air-water-cement interface. Greater HRWR adsorption to cement particles limits the adsorption locations available on the cement for AEA. The increased fluidity and decreased stability of the mixture allows for the air voids to coalesce and rupture at the surface more easily. Finally, the increased dosage of VMA absorbed more water, providing fewer locations for the AEA to bond with water, resulting in a greater demand of AEA to secure a certain air content.

The AEA dosage using source A remained constant from the 559 to 635 mm slump flow, but increased by 40% from 635 to 711 mm. The primary reasons as to why the AEA dosage did not change from 559 to 635 mm slump flows are linked with the viscosity of the mixtures. Mixture A-SF22 contained VMA, but at the same slump flow the other sources did not. The 0.78 ml/kg AEA dosage established in mixture A-SF22 was adequate to entrain 6% air in mixture A-SF25 because its effectiveness was bolstered by the increased VMA. Mixtures A-SF25 and A-SF28 were the only mixtures to contain more VMA than AEA by volume. The additional VMA prevented the air bubbles from moving freely in the paste. The viscosity of the 635 mm slump flow was sufficient to stabilize the air voids and prevent rupture at the surface, whereas the high fluidity of the cement paste at the 711 mm slump flow necessitated the 44% increase in AEA dosage. When the viscosity was significantly decreased, the air bubbles ruptured and coalesced more easily, resulting in additional demand for air-entrainment.

Source C air-entraining admixture dosages did not follow a trend similar to the other three sources. The source C AEA dosage increased by 18% from the 559 to 635 mm slump flow, but decreased by 7% from the 635 to 711 mm slump flow. The

chemical composition of this admixture is similar to Vinsol resin, which tends to form air voids more quickly than other wood-derived acid salts (VanderWerf and Watson, 2007). Additionally, of the sources with a polycarboxylate-acid HRWR and a salt-type AEA (sources B and D), the HRWR dosage from source C was an average of 30% greater than source B and 47% greater than source D. Due to the chemical and volumetric disparities between the admixture sources, it is not surprising that source C required a larger dosage of AEA to achieve 6% air content at the 635 mm slump flow than at the 711 mm slump flow.

3.2.4.2 Effects of Slump Flow on Air Content

Among all twelve SCC mixtures, there was an average increase of 0.2% in total air content from 559 to 635 mm slump flows. Likewise, there was a 0.2% average decrease in total air content from 635 to 711 mm slump flows. However, it is interesting to note that there was an average of 0.2 ml/kg increase in AEA dosage between each slump flow. When analysis of the total air content is coupled with the air void characteristics, it becomes evident that an increased AEA dosage is required due to the increased fluidity and increased HRWR dosage at higher slump flows, both of which reduce the effectiveness of the AEA to entrain air. For all admixture sources, the increase in air from 559 to 635 mm slump flows was accompanied with a deterioration in the air void characteristics. This confirms the observation by Plante, Pigeon and Foy (1989) that increased air content is not necessarily representative of improved air void characteristics.

Similar to the VMA-to-HRWR dosage ratio (introduced in Section 3.2.1), an AEA-to-HRWR dosage ratio can be established with respect to slump flow. The average

ratio (of all four sources) of AEA to HRWR dosage was 0.35, 0.36 and 0.35 for the 559, 635 and 711 mm slump flow, respectively. The higher AEA to HRWR ratio at the 635 mm slump flow contributed to the 0.2% air content increase. The higher ratio reduced competition between the AEA and HRWR, allowing the AEA to more effectively entrain air.

3.3 Air Void Characteristics

The results of the air void analyses can be seen in Figure 3.4. The full data set and typical Air Void Analyzer output from each mixture can be seen in Appendix B. Source A produced the smallest and most closely spaced air voids, followed by sources B, C, and D. These rankings were consistent at each of the three slump flow levels. The lowest slump flow (559 mm) generated better air void characteristics than the highest slump flow (711 mm). Source A showed a specific surface and spacing factor deterioration of 6 mm^{-1} and $20 \text{ }\mu\text{m}$, respectively, from the 635 mm to 711 mm slump flow. The air void characteristics of sources B, C and D showed a similar trend from 635 to 711 mm slump flows: the specific surface and spacing factors degraded an average of 0.9 mm^{-1} and $5.4 \text{ }\mu\text{m}$, respectively.

A minimum of five samples for each mixture design were tested by the Air Void Analyzer. Samples outside one standard deviation of the mean for that mixture design were not included in the data set. In some cases, more than five samples were tested if there was high variability of data. There was a correlation between the specific surface and spacing factor. Based on an analysis of variables, the t-test probability between the specific surface and spacing factor was 8.94×10^{-82} , signifying that a high specific surface value correlated well to a low spacing factor value.

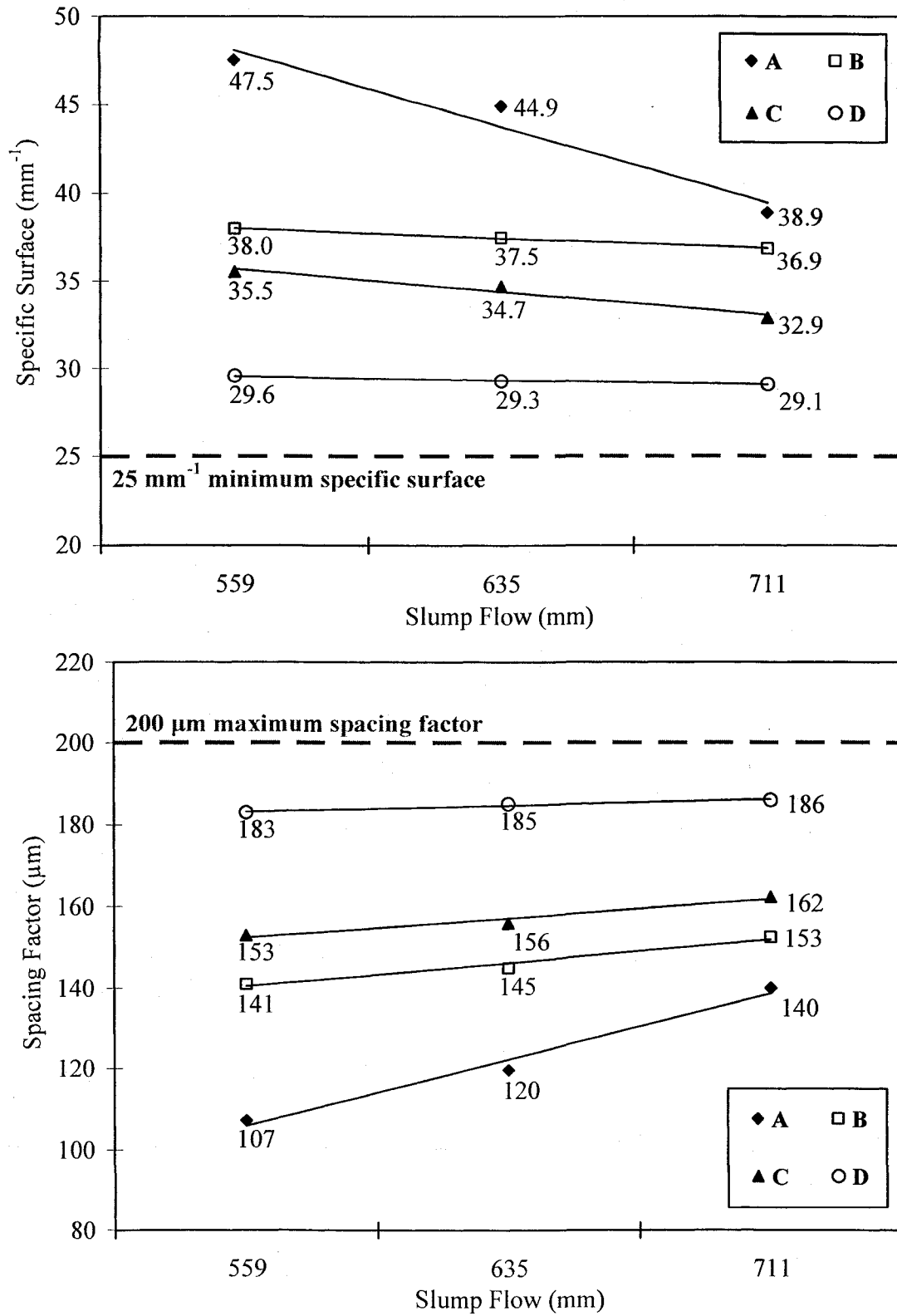


Figure 3.4 Phase I air void characteristics: specific surface (top) and spacing factor (bottom)

3.3.1 Effects of Admixture Source on Air Void Characteristics

The increases in spacing factors from the 559 to 711 mm slump flows were 33, 12, 9 and 3 μm for sources A, B, C and D, respectively. The decreases in specific surfaces were 8.6, 1.1, 2.6 and 0.5 mm^{-1} for sources A, B, C and D, respectively. The salt-type AEAs of sources B, C and D produced relatively similar air void characteristics amongst different slump flows when compared to those generated by source A.

The air-entraining agents from sources B, C and D were all forms of wood-derived acid salts. Source B developed the smallest air bubbles of the three salt-type AEA sources due to its tall oil component, as evidenced by the air void characteristics shown in Figure 3.4. Tall oil has been noted in many sources to generate the smallest air voids of all AEAs (Kosmatka et al., 2002; Christensen and Ong, 2005). The wood rosin and Vinsol resin components of the AEAs from sources C and D tended to develop mid-size bubbles, which are reflected in the moderate air void characteristics generated. Furthermore, the saponified wood rosin and resin combination of source C seemed to produce a superior air void system than the pure resin solution of source D. The air voids generated by salt-type AEAs are primarily adhered or bridged to the cement particles, resulting in similar air void characteristics regardless of slump flow. The mass of the cement particles acts like an anchor to consistently disperse the air bubbles throughout the matrix, regardless of the paste viscosity and fluidity. The tendency of air bubbles to float to the surface is also reduced if the bubble is adhered to a larger particle (Du and Folliard, 2005).

Among the four sources, the air void characteristics of source A tended to be the most influenced by slump flow. The AEA from source A is a synthetic detergent,

primarily constituted by alkybenzene sulfonic acid. These types of surfactants are influenced by increased fluidity due to their primary location at the air-water interface. Since the air voids are not necessarily anchored to cement particles, the bubbles produced by detergent AEAs can move about freely in the matrix. Therefore, source A produced bubbles that are more likely to rupture on the surface and coalesce than the bubbles produced by salt-type AEAs.

3.3.2 Effects of Slump Flow on Air Void Characteristics

Increasing slump flow deteriorated the air void characteristics of self-consolidating concrete. The high fluidity and low viscosity of the concrete at the higher slump flows made it more difficult to entrain and stabilize air bubbles. The high deformability allowed more coalescence of air bubbles, resulting in a decreased specific surface and increased spacing factor. Additionally, the increased dosage of HRWR and VMA at the higher slump flows interfered with the mechanisms of air-entrainment. Both the HRWR and AEA are surface-active agents that rely on adsorption to cement grains to cause dispersion of particles or entrainment of air. If more HRWR molecules are adhered to the surface of the cement particles, there is less surface area available for the AEA to function and entrain air voids.

The limits for specific surface (greater than 25 mm^{-1}) and spacing factor (less than $200 \text{ }\mu\text{m}$) were achievable at all slump flows. All mixture designs were initially designed to meet the required air content of 6% solely using the volumetric air meter. For the majority of the mixtures, the air void characteristics that resulted from the optimum AEA dosage met the air void standards. However, at the highest slump flow, the spacing factors measured from the initial AEA dosage (that achieved a total air content of $6 \pm$

0.5%) of mixtures A-SF28 and D-SF28 were greater than the 200 μm maximum. The specific surfaces met the target, but the spacing factors were 15 μm (0.0006 inches) and 17 μm (0.001 inches) higher than the standard for A-SF28 and D-SF28, respectively. Consequently, the mixtures A-SF28 and D-SF28 necessitated the addition of 0.2 and 0.06 ml/kg (0.3 and 0.1 oz/cwt) more AEA, respectively, to achieve the target air void characteristics. The addition of more AEA at the 711 mm slump flow indicated that with an increasing slump flow and fluidity of the mixture, the air void characteristics decreased. In fact, it was more difficult to achieve acceptable air void characteristics at the higher slump flows because the air bubbles moved more freely in the paste and rose more rapidly to the surface. Consequently, there was increased coalescence and rupturing of air voids, which increased the spacing factor and decreased the specific surface of the matrix.

3.3.3 Predictive Equations of Air Void Characteristics

Statistically, the air void characteristics of each admixture source can be correlated with the target slump flow with the linear equation: $Y = a \cdot SF + b$, where Y is the specific surface (mm^{-1}) or spacing factor (μm), and SF is the slump flow in mm. The regression is valid for SCC mixtures with $6 \pm 0.5\%$ air, and a slump flow between 559 and 711 mm (± 13 mm). The values of coefficients a and b for each admixture source, along with the coefficients of determination, R^2 , and t-test probabilities of the coefficients can be seen in Table 3.10.

The predictive equations for all admixture sources represent the data accurately, as seen by the R^2 values close to 1 and statistically significant t-test probabilities. Source A, however, exhibited the highest standard error of all sources, along with a t-test

Table 3.10 Statistical data for predictive equations of air void characteristics

Air Void Parameter	Value of coefficient		R^2	Std. Error	Prob(f)	Probability (t)	
	a	b				a	b
α , source A	-0.057	79.69	0.95	1.39	0.143	0.143	0.066
\bar{L} , source A	0.217	-15.53	0.98	2.85	0.078	0.078	0.526
α , source B	-0.007	42.06	0.99	0.04	0.033	0.033	0.004
\bar{L} , source B	0.079	96.20	0.96	1.63	0.121	0.121	0.064
α , source C	-0.017	45.23	0.95	0.41	0.140	0.140	0.034
\bar{L} , source C	0.059	119.40	0.96	1.23	0.121	0.121	0.039
α , source D	-0.003	31.42	0.98	0.04	0.073	0.073	0.005
\bar{L} , source D	0.020	172.13	0.96	0.41	0.121	0.121	0.009

probability of 0.526 for the variable b . There is a 50% probability that the intercept of the linear regression does not have a significant influence on the outcome of the spacing factor for source A. The actual air void characteristics are compared with the predicted values determined from the linear regressions in Table 3.11. In determination of both the spacing factor and specific surface, source A was the least predictable source by a linear equation. Additionally, on average, the air void characteristics of the 635 mm slump flow mixtures exhibited the least agreement with the predictive equations. In general, the calculated spacing factors had a lower percent error than the calculated specific surfaces.

3.3.4 Correlation of Total Air Content to AVA Air Content

A correlation was found between the total air content measured by ASTM C 173 and the Air Void Analyzer, which can be seen in Figure 3.5. The air content measured by the Air Void Analyzer was generally 3% lower than that measured by the volumetric method. The correlation is consistent with current literature that states the Air Void Analyzer tends to underestimate the total air content because of its exclusion of air voids

Table 3.11 Actual and calculated air void characteristics

Source	Target SF (mm)	Specific Surface (mm ⁻¹)			Spacing Factor (μm)		
		Actual	Calculated	% Error	Actual	Calculated	% Error
A	559	47.5	47.8	-0.7	107	106	1.3
	635	44.9	43.5	3.2	120	122	-2.2
	711	38.9	39.2	-0.7	140	139	0.9
B	559	38.0	38.1	-0.3	141	140	0.5
	635	37.5	37.6	-0.3	145	146	-0.9
	711	36.9	37.1	-0.5	153	152	0.2
C	559	35.5	35.7	-0.6	153	152	0.4
	635	34.7	34.4	0.8	156	157	-0.6
	711	32.9	33.1	-0.7	162	161	0.6
D	559	29.6	29.7	-0.5	183	183	-0.2
	635	29.3	29.5	-0.7	185	185	0.1
	711	29.1	29.3	-0.6	186	186	-0.2

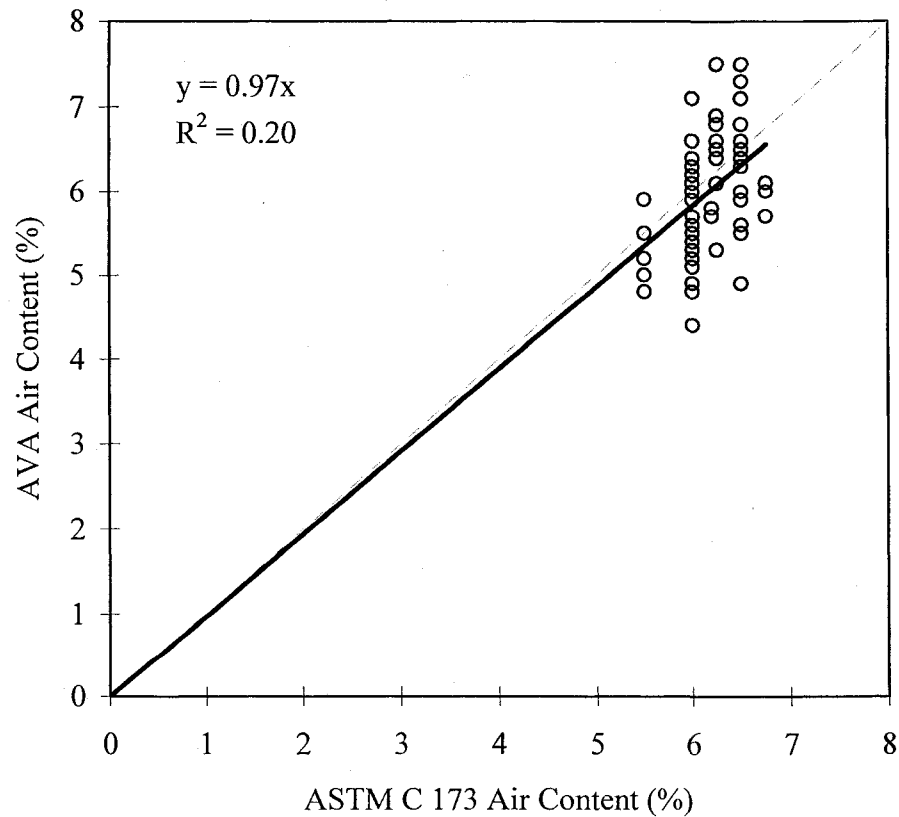


Figure 3.5 Phase I air content correlation between Air Void Analyzer and ASTM C 173

less than 2 mm in size (Magura, 1996). The coefficient of determination, R^2 , is only 0.20, indicating the relationship between the two air contents is not linear. However, the slope of the trend line shown in Figure 3.5 does indicate the general tendency of the Air Void Analyzer total air content data to be less than that from the ASTM C173 volumetric method.

3.4 Compressive Strength

The compressive strengths of 102 x 203 mm (4 x 8 inch) cylinders from each mixture design were tested after 7, 28 and 90 days of curing. Values reported in Table 3.12 represent the average of a minimum of three cylinders; however, in most cases the value is an average of four tests. All mixtures met the target 28-day compressive strength of 34.5 MPa (5000 psi), required by ACI 318-05 for freeze-thaw durability under severe conditions.

The admixture source and dosage amount influenced the 28-day strength of the concrete, as seen in Figure 3.6. With the water-to-cementitious materials ratio remaining

Table 3.12 Phase I compressive strength results

Mixture Identification	SI Units (MPa)			U.S. Units (psi)		
	7-day	28-day	90-day	7-day	28-day	90-day
A-SF22	28.6	40.5	50.4	4154	5872	7316
B-SF22	31.9	40.5	52.9	4625	5878	7672
C-SF22	30.2	39.7	49.7	4382	5759	7209
D-SF22	33.2	42.6	53.6	4809	6177	7773
A-SF25	32.6	41.9	55.5	4728	6071	8045
B-SF25	29.3	37.8	48.0	4245	5480	6957
C-SF25	29.7	39.5	48.6	4305	5728	7050
D-SF25	29.6	41.1	51.8	4291	5954	7511
A-SF28	28.5	38.2	50.7	4139	5542	7358
B-SF28	27.0	36.4	43.1	3922	5285	6250
C-SF28	31.7	41.3	51.6	4599	5983	7488
D-SF28	29.2	39.6	51.1	4230	5746	7410
Average	30.1	39.9	50.6	4370	5790	7340

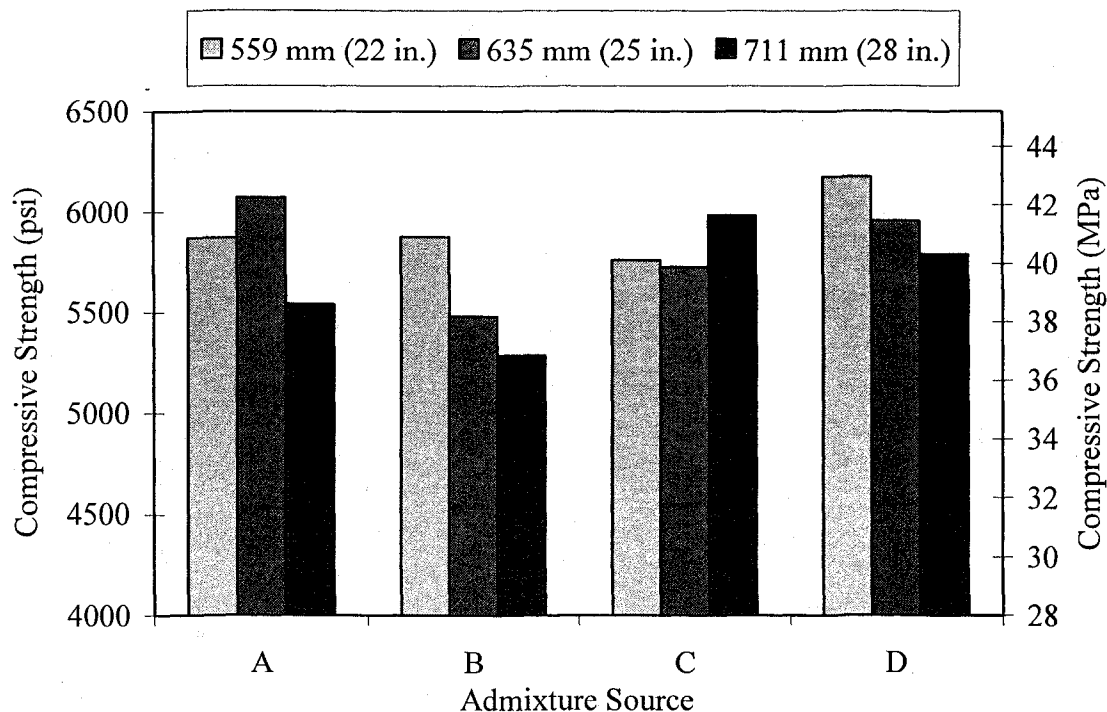


Figure 3.6 28-day average compressive strength results

constant for all mixtures, the primary factor influencing strength was the admixture dosage. For every source, there was an increase in HRWR and VMA dosages with increasing slump flow. With the increase in admixture dosage, there was an accompanying decrease in strength. However, this decrease was limited to 2-4 MPa (200-600 psi).

Sources B and D performed similarly in that the strength decreased with increasing slump flow. However, sources A and C displayed no evident trend in compressive strength with respect to slump flow. For source A, there was a distinct decrease in strength at the 711 mm slump flow. Source C, however, showed an increase in strength at the 711 mm slump flow. The lack of a noticeable trend in sources A and C can be clarified by the AEA dosage. For source A, the AEA dosage remained constant

from 559 to 635 mm slump flow, but then increased by 40% from 635 to 711 mm. The increase in AEA dosage caused a decrease in compressive strength. Likewise, with source C, the AEA dosage increased from 559 to 635 mm, causing a slight decrease in strength. From 635 to 711 mm, the AEA dosage actually decreased, causing an increase in strength.

The data was further analyzed to compare the average compressive strength for each source and each slump flow, which is depicted in Figure 3.7. The overall difference between admixture manufacturers was limited to 1.2, 2.8, and 4.2 MPa (180, 410, 613 psi) for the 7, 28 and 90 day strength results, shown in Figure 3.7 (a). Although the difference is minor, the ranking of the sources from strongest to weakest was D, A, C and B. The differences in strength were less pronounced between the slump flows than between the admixture manufacturers. However, there was a general trend in that there was decreasing strength with increasing slump flow. The decrease in strength from the 559 mm to 711 slump flow was limited to 2 MPa (300 psi), as seen in Figure 3.7 (b).

3.5 Conclusions

For the test results of the Phase I study, the following conclusions can be drawn about the optimization and performance of self-consolidating concrete mixtures:

- The admixture source primarily influenced the admixture dosage of a SCC mixture.

The rankings of the four selected admixture manufacturers in different categories are presented in Table 3.13. In terms of volumetric admixture dosage, source A required a higher dosage than the other three manufacturers, mainly due to the difference in chemical composition of the polycarboxylate-ester high range water reducer. The most

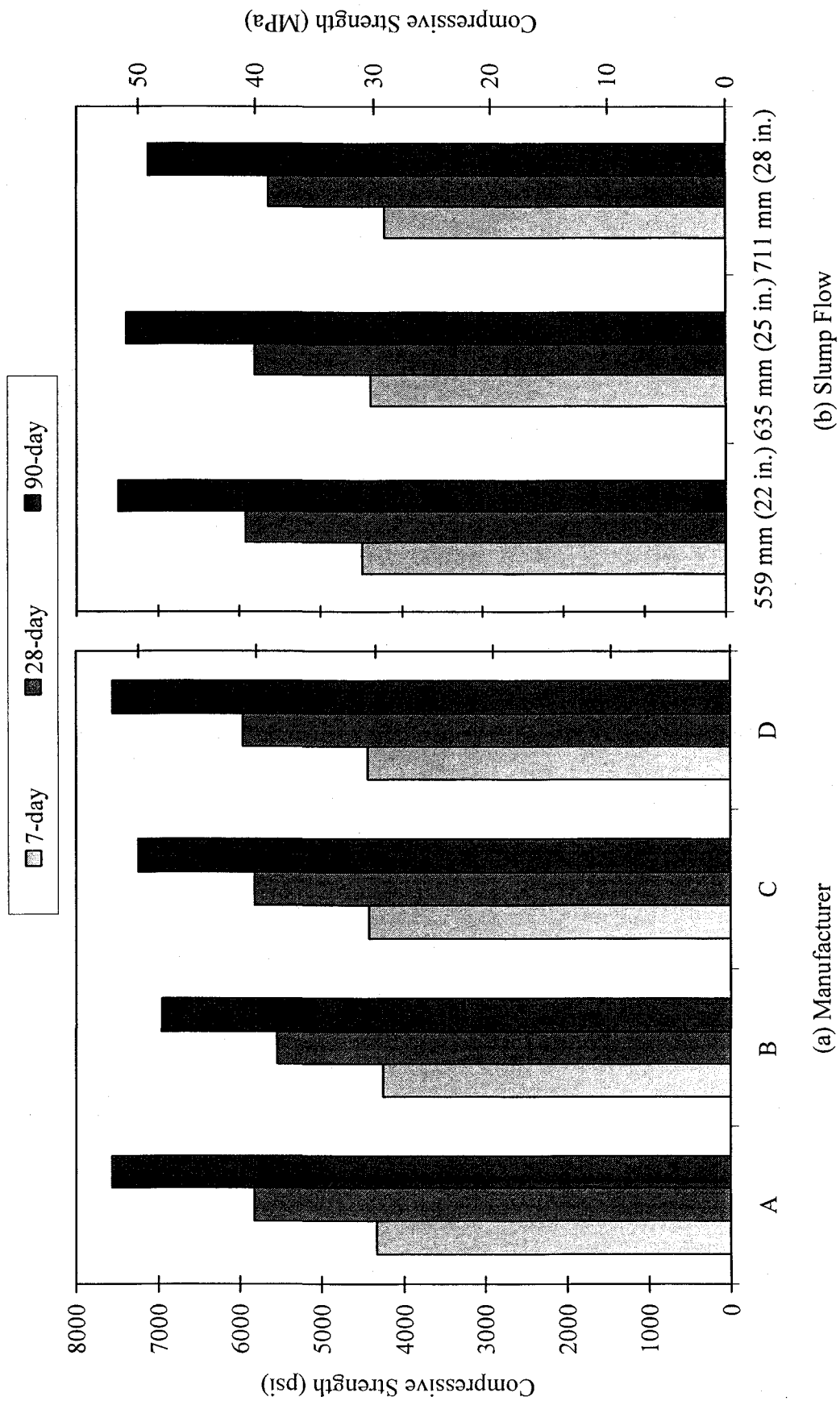


Figure 3.7 Average compressive strength results with respect to admixture manufacturer (a) and slump flow (b)

Table 3.13 Phase I comparison of admixture manufacturers

Category	Relative Ranking			
	Best	↔		Worst
Admixture Dosage	D	B	C	A
Air Void Characteristics	A	B	C	D
Compressive Strength	D	A	C	B

economic source in terms of admixture dosage produced the worst air void characteristics, and vice versa.

- The dosages of high range water reducer, viscosity modifying admixture and air-entraining admixture typically increased with increasing slump flow.
- The slump flow primarily influenced the flow properties of a SCC mixture.
 - The SCC mixtures with the most stability (resistance to segregation and bleeding) were produced with a 559 mm (22 in.) slump flow. However, the stability was sometimes compromised with a decrease in passing ability.
 - The differences in fresh properties of the SCC mixtures, specifically J-Ring passing ability and T_{50} flow ability, were greater from 559 to 635 mm (22 to 25 in.) slump flows than from 635 to 711 mm (25 to 28 in.) slump flows.
- Three main factors influenced the air content and air void characteristics of SCC:
 - 1) Competition with high range water reducer and viscosity modifying admixture: Increased dosages of high range water reducer competed with air-entrainment for adsorption to cement particles. Increased dosages of viscosity modifying admixture competed with air-entrainment by preventing water molecules from forming bubbles.

- 2) Slump Flow: Air void characteristics declined with increasing slump flow. The increased fluidity of the cement paste increased the coalescence and rupturing of air voids. Higher paste viscosity of SCC acted as a cushion to prevent air voids from rupturing.
- 3) Type of air-entraining admixture: Surfactant-type air-entrainment (i.e. synthetic detergents) secured the best air void characteristics, followed by salt-type air-entraining admixtures containing tall oil, and finally salt-type air-entraining admixtures containing Vinsol resin and wood rosin. However, the surfactant-type was more affected by slump flow than the salt-type AEA because all air bubbles were not anchored to cement particles.
- The compressive strengths of the selected self-consolidating concretes decreased with an increase in slump flow. A decrease in compressive strength was typically accompanied by an increased dosage of air-entraining admixture.

CHAPTER 4

PHASE II: EFFECTS OF HAULING TIME ON FRESHLY- MIXED SELF-CONSOLIDATING CONCRETE

This chapter presents the effects of hauling time on the fresh properties and air void characteristics of three SCC mixtures. Admixture manufacturer B was selected for this phase of the investigation due to its relatively economical dosage of admixtures. Therefore, only mixtures B-SF22, B-SF25 and B-SF28 were examined during this phase. The fresh properties of the three mixtures were tested at eight hauling times of 20, 30, 40, 50, 60, 70, 80 and 90 minutes. Each hauling time was compared to the fresh properties measured at 10 minutes (reference or control), as reported in Chapter 3. Hauling time, accompanied with prolonged agitation, can adversely affect fresh properties and the economy of an SCC mixture and its suitability for certain applications.

In the field, concrete is rarely placed immediately after the initial mixing period. Typically, a concrete mixture travels for a period of time in a ready-mixed concrete truck from the plant to the job site. While traveling, the drum rotates at a lower speed, known as the agitation speed, for hauling times typically not exceeding 90 minutes. SCC is known to have high slump flow losses with time, due to its heavy reliance on a superplasticizer for flow ability (Hanehara and Yamada, 1998). In this phase of investigation, the change in slump flow, T_{50} , VSI, air content, and air void characteristics

were measured at eight different hauling times for the three different mixtures prepared using three distinct slump flows.

4.1 Effects of Hauling Time on Flow Properties

For the purpose of this investigation, hauling time is defined as the elapsed time from the first cement and water contact to the time of testing. The slump flow of all mixtures decreased with increasing hauling time, as seen in Table 4.1 and Figure 4.1. For the mixture B-SF22, the average slump flow reduction was 27 mm for every 10 minutes of hauling time. This mixture experienced a maximum slump flow loss of 216 mm, or 39%, recorded at 90 minutes. For the mixture B-SF25, the average slump flow reduction with hauling time was similar to that of B-SF22. The slump flow of the 635 mm mixture decreased an average of 29 mm per 10 minutes of hauling time, with a maximum slump flow loss of 230 mm or 37%. While mixture B-SF28 lost slump flow, its rate of reduction was less than the concretes with lower initial slump flows. B-SF28 lost a

Table 4.1 Fresh properties of SCC with hauling time

Hauling Time (min.)	B-SF22			B-SF25			B-SF28		
	Slump Flow (mm)	T ₅₀ (sec.)	Air (%)	Slump Flow (mm)	T ₅₀ (sec.)	Air (%)	Slump Flow (mm)	T ₅₀ (sec.)	Air (%)
10	559	2.00	6.0	646	2.01	6.3	724	2.04	6.0
20	518	3.22	6.3	610	2.25	6.5	699	1.94	6.6
30	486	-	6.5	591	2.41	6.8	686	2.00	7.0
40	467	-	7.0	572	2.45	7.3	673	2.36	7.5
50	435	-	7.6	551	2.65	7.8	648	1.91	7.5
60	391	-	8.5	502	3.99	8.0	635	2.06	7.8
70	368	-	9.5	483	-	8.3	622	2.39	8.0
80	352	-	10.0	438	-	9.0	572	3.01	8.5
90	343	-	10.8	416	-	9.5	546	3.18	8.6

Note: A T₅₀ time could not be recorded for slump flows less than 500 mm.

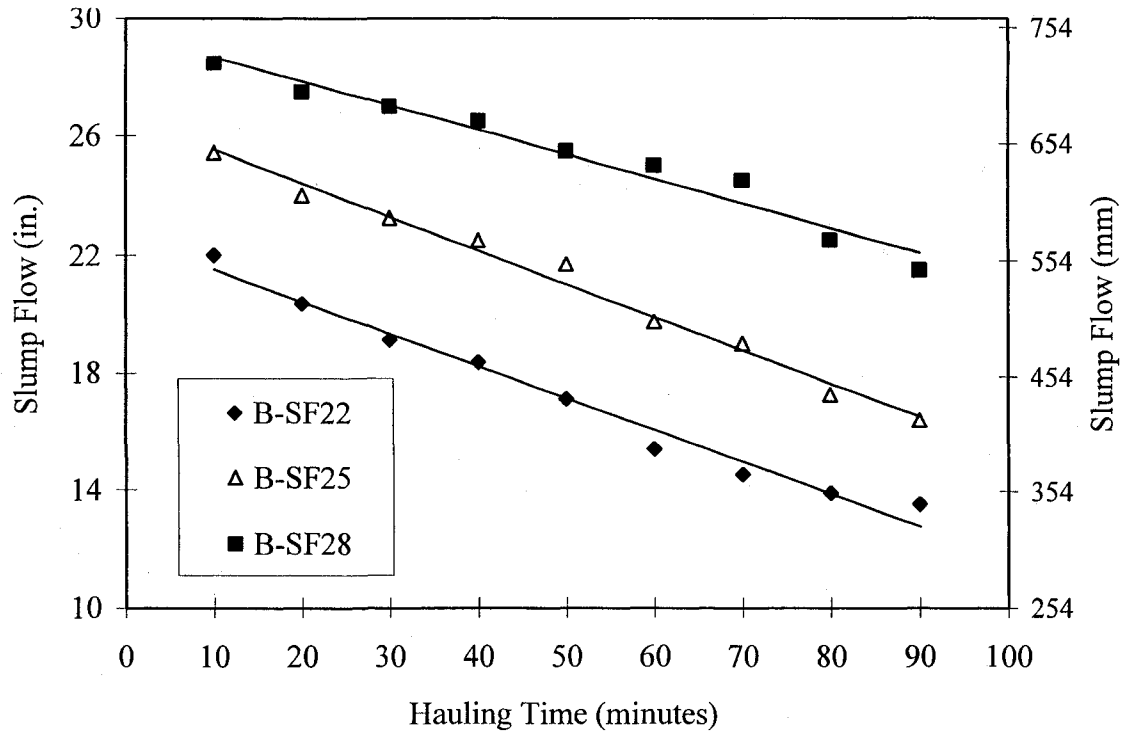


Figure 4.1 Effects of hauling time on slump flow

maximum of 178 mm at 90 minutes, or 25%, with an average loss of 22 mm per 10 minutes of hauling time. The higher HRWR dosage of mixture B-SF28 is the primary reason for the decreased rate of slump flow loss.

Accompanying the decrease in slump flow, the T_{50} times increased with hauling time for all mixtures, indicating an increase in viscosity, as seen in Table 4.1. For the mixtures B-SF22 and B-SF25, the T_{50} could not be recorded starting at 30 and 70 minutes of hauling time, respectively, since the slump flow did not reach the 50 cm mark. The increases in T_{50} times over the 90 minute hauling period were 1.22, 1.98 and 1.14 seconds for B-SF22, B-SF25 and B-SF28, respectively. At the point where the T_{50} could no longer be measured, the mixture could not technically be categorized as SCC. However, the slump flow was still measured if it was less than 500 mm. Throughout the investigation, regardless if the concrete mixture developed into high-slump conventional

concrete, SCC test methods continued to be followed for consistency among measurements.

All mixtures experienced an increased resistance to bleeding and segregation with respect to hauling time. Therefore, the Visual Stability Index (VSI) was 0 for all mixtures at all hauling times. The increased stability with hauling time can be attributed to both the increase in viscosity and the increase in air content. The increased viscosity is caused by the decrease in slump flow. The increase in air content, described in Section 4.1.2, also reduces bleeding (Rixom and Mailvaganam, 1999).

4.1.1 Predictive Equations of Slump Flow

The change in slump flow with respect to hauling time can be predicted with linear regressions of the data, as depicted in Figure 4.1. The linear regression equations conducted at a 95% confidence level and the corresponding coefficients of determination, or R^2 values, can be seen in Table 4.2. The coefficients of determination are close to 1, indicating an accurate representation of the data. For the three selected mixtures, the slump flow could be predicted using these equations to a high degree of accuracy. It is evident from the slope of these equations that B-SF-22 and B-SF25 lost slump flow at a similar rate, but B-SF28 retained more slump flow with time. B-SF22 and B-SF25 lost enough flow ability to be categorized as high-slump concrete, whereas B-SF28 retained the high slump flow expected from a self-consolidating concrete mixture.

Table 4.2 Predictive equations for final slump flow with hauling time

Mixture	B-SF22	B-SF25	B-SF28
Equation	$SF_f = -2.78t_h + 574.50$	$SF_f = -2.87t_h + 677.55$	$SF_f = -2.10t_h + 749.65$
R^2	0.98	0.99	0.96

where: SF_f = final slump flow in mm, t_h = hauling time, $10 \leq t_h \leq 90$ minutes

Additionally, Equation 4.1 was developed at a 95% confidence level using statistical analysis software to determine the final slump flow with respect to the hauling time and initial slump flow.

$$SF_{final} = -147.424 - 2.586t_h + 1.267SF_i \quad \text{Eq. 4.1}$$

where: SF_{final} = final slump flow, $340 \leq SF_{final} \leq 700 \pm 13$ mm

SF_i = initial slump flow, $559 \leq SF_i \leq 711 \pm 13$ mm

t_h = hauling time, 10 minutes $\leq t_h \leq$ 90 minutes

The coefficient of determination for Equation 4.1 is 0.98, with the t-test probability of all variables equal to zero, indicating the equation is an accurate predictor for slump flow. Tabulated values of the actual and calculated slump flows can be seen in Appendix B.

4.1.2 Effects of Hauling Time on Air Content

Past research indicates that the total air content of a conventional concrete mixture typically decreases by 1-2% with hauling time (Kosmatka et al., 2002). However, the air content of a high-slump conventional concrete mixture may increase with hauling time, as discussed in Section 1.3.2 (Kosmatka et al., 2002). In this study using self-consolidating concrete, the total air content of all selected mixtures increased with hauling time, as seen in Table 4.1. The absolute increase in air content from the initial mixing time to the 90 minute hauling time was 4.8%, 3.3% and 2.6% for the mixtures B-SF22, B-SF25 and B-SF28, respectively. Mixture B-SF22, which had the lowest initial slump flow, experienced a 79% increase in air content from 10 to 90 minutes, whereas B-SF25 and B-SF28 had a 52% and 44% increase in air content, respectively.

In addition to the difference in absolute increase in air content, mixtures B-SF28 and B-SF25 displayed dissimilar rates of change in air content when compared to B-

SF22. The 711 mm slump flow mixture experienced a rapid increase in air content at 20 minutes, followed by a slower rate of change as the hauling time increased. On the other hand, B-SF22 demonstrated a more gradual increase in air content initially, followed by a faster rate of change as the hauling time increased. After 40 minutes of hauling time, all three mixtures had approximately the same air content of 7%. At this point, the air content of mixture B-SF22 increased at a higher rate than the other two mixtures. B-SF28 increased at a lower rate than B-SF22 and B-SF25 due to its higher fluidity, which provided a less stable environment for the air voids.

The air content changed in a linear manner with respect to hauling time, as seen in Figure 4.2. The linear regression equations displayed in Figure 4.2 accurately represent the data, since the R^2 values are all above 0.95. The equations could be used to predict

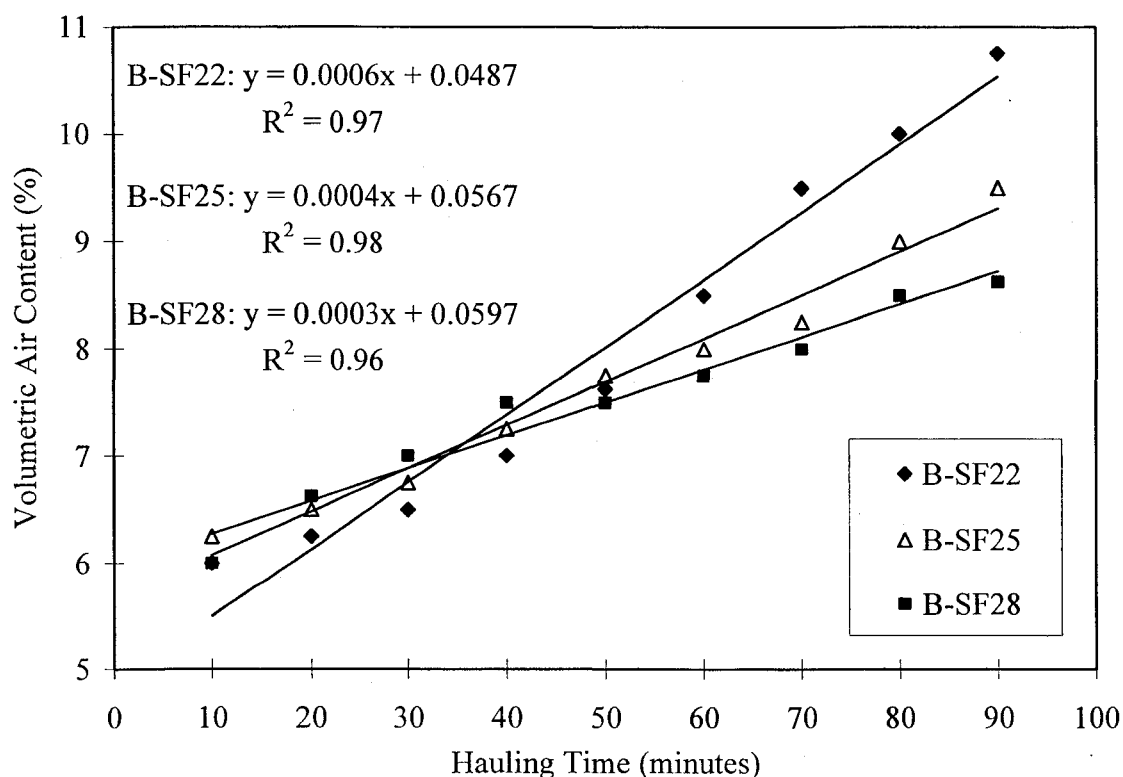


Figure 4.2 Air content with respect to hauling time

the air content for these SCC mixtures at a given hauling time. The increase in air content with hauling time, described in the following sections, is attributed to: 1) the decrease in slump flow, 2) the mechanism of action of the salt-type AEA of admixture manufacturer B, and 3) air entrapped during testing.

4.1.2.1 Effects of Slump Flow on Air Content

The air content increased with increasing hauling time, which can partially be attributed to the loss of slump flow. The increased viscosity of the concrete mixture with decreasing slump flow provided more stability, or cushioning, for the air voids distributed throughout the concrete. The air voids were met with more resistance from the concrete as the fluidity decreased, thus preventing the bubbles from joining together. Detailed effects of slump flow on air content were discussed in Chapter 1.

Based on the results of this investigation, a correlation can be established between air content (as measured by ASTM C 173) and slump flow for each mixture. In general, the air content increased as the slump flow decreased with hauling time. The three mixtures behaved in a slightly different manner, mainly due to when the concrete transitioned from SCC to high-slump concrete, as seen in Figure 4.3. The equations and coefficients of determination for the trend lines are listed in Table 4.3. For mixture B-SF22, the best-fit line predicting air content with slump flow was a concave-up 2nd order polynomial. Mixture B-SF25 behaved in a linear manner, with a decreasing air content as slump flow increased. The behavior of mixture B-SF28, which was the only concrete that remained SCC after 90 minutes of hauling time, can be described with a 2nd order polynomial that is concave-down. All of the coefficients of determination are greater than 0.97, indicating an accurate representation of the slump flow and air content data.

The trend line equations reflect the previous observation of an increased rate of change in air content with increasing hauling time for B-SF22, and a decreased rate of change for B-SF28 with increasing hauling time.

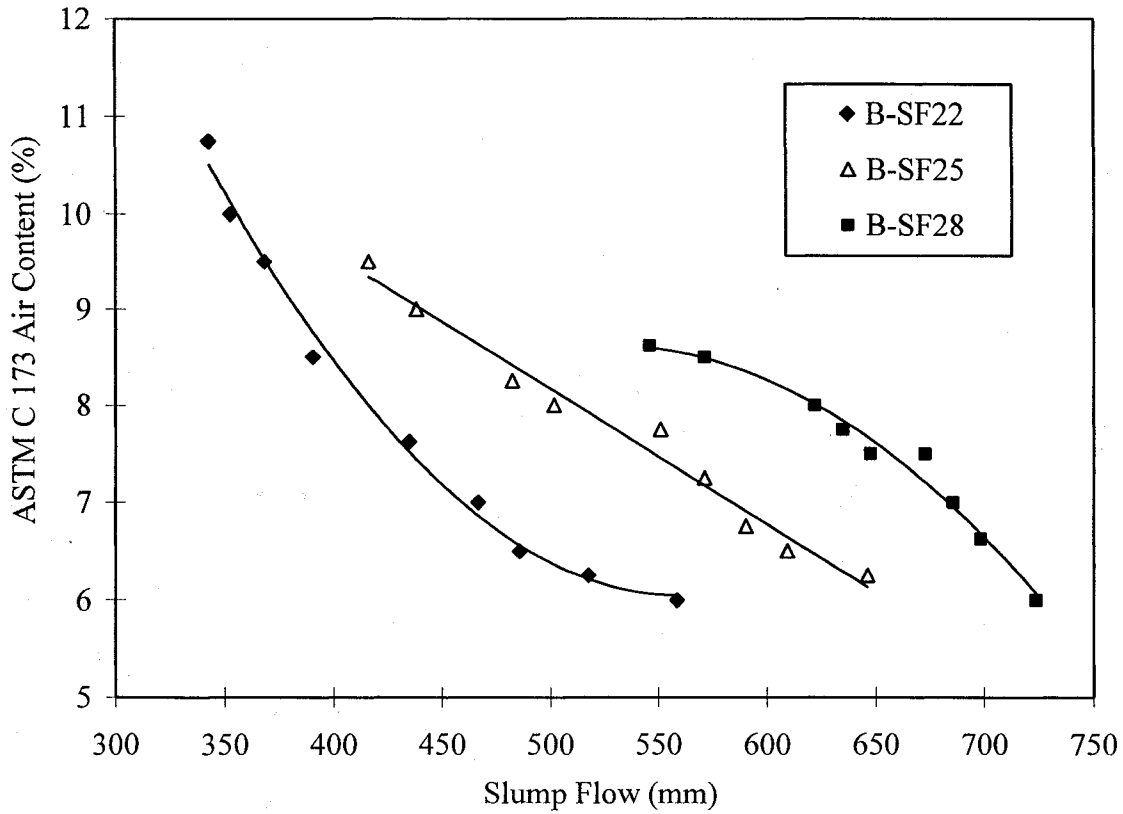


Figure 4.3 Volumetric air content versus slump flow

Table 4.3 Trend line equations for prediction of air content

Mixture ID	Trend line Equation	Coefficient of Determination, R^2
B-SF22	% Air = $0.0001 SF_f^2 - 0.107 SF_f + 35.95$	0.993
B-SF25	% Air = $-0.014 SF_f + 15.152$	0.978
B-SF28	% Air = $-6 \times 10^{-5} SF_f^2 + 0.0672 SF_f - 8.97$	0.978

where: SF_f = final slump flow, $340 \leq SF_f \leq 700 \pm 13$ mm

Additionally, the total air content can be statistically predicted with respect to hauling time and initial slump flow (assuming an initial air content of $6 \pm 0.5\%$), as seen in Equation 4.2.

$$\%Air = -9.9 \times 10^{-4} t_h + 8.56 \times 10^{-5} SF_i + 0.914 \left(\frac{t_h}{SF_i} \right) \quad \text{Eq. 4.2}$$

where: $\% Air$ = volumetric air content, $5\% \leq \% Air \leq 11\%$

t_h = hauling time, $10 \text{ minutes} \leq t_h \leq 90 \text{ minutes}$

SF_i = initial slump flow, $559 \leq SF_i \leq 711 \pm 13 \text{ mm}$

Equation 4.2 has an R^2 value of 0.97, and a t-test probability for each variable equal to zero, indicating a statistically significant influence of hauling time and initial slump flow on the final slump flow. Additionally, the standard error for an air content prediction is 0.0024, or 0.24%. Actual and calculated air contents are tabulated in Appendix B.

4.1.2.2 Mechanism of the Salt-Type AEA

The 711 and 635 mm slump flows necessitated a higher initial AEA dosage than the 559 mm slump flow to entrain $6 \pm 1\%$ air. The higher AEA dosage caused the 711 and 635 mm mixtures to experience an accelerated increase in air content at the beginning of hauling time, and stabilization when the AEA had been maximized. The air content increase of mixture B-SF22 is primarily attributed to excessive entrapped air, rather than the dosage of AEA, as described in the following section.

The type of AEA utilized in this phase is a contributing factor to the increase in air content with continued agitation over the hauling time. Source B AEA is a stabilized resin solution containing tall oil, which is known to have slower air generation, and can increase the total air content with mixing time (see Table 1.1). The rate of adsorption of a tall oil AEA is slower than the rate of salt precipitation (due to the reaction calcium ions

and AEA), which occurs almost immediately when the AEA is added to the concrete mixture. The precipitates created initially are dissolved with time, until all AEA is adsorbed onto cement or fly ash particles (Baltrus and LaCount, 2001). The gradual dissolution of precipitates causes slow production of air voids within the concrete, and an increase of air content with time.

4.1.2.3 Entrapped Air

Throughout the investigation, all concrete was tested as if it was SCC, even if the slump flow indicated that it was high-slump conventional concrete (slump flow less than 500 mm). Hence, the ASTM C 173 volumetric air content test and the Air Void Analyzer sampling were done without mechanical consolidation (such as rodding or vibration). Large air bubbles entrapped during mixing or sampling could have erroneously increased the air content when the slump flow was less than 500 mm.

The notion of increased quantity of entrapped air can be confirmed by the results from the Air Void Analyzer. The AVA reports both the total air content of the concrete as voids less than 2 mm and as voids less than 0.35 mm. The difference is an indication of the percentage of the entrapped air content of the concrete mixture. Table 4.4 presents the entrapped air with respect to hauling time. Mixture B-SF22 had 1.0%, 1.2%, and 2.1% entrapped air at 70, 80 and 90 minutes of hauling time, respectively, which indicates increased entrapped air with increased hauling time. The increase in entrapped air voids is related mainly to the decrease in slump flow, as the 559 mm slump flow mixture should have been vibrated or rodded for complete consolidation. Mixture B-SF25 had a slump flow of less than 500 mm after 60 minutes of hauling time, signifying that only the last three measurements required mechanical consolidation. In contrast, the

Table 4.4 Percent entrapped air (AVA % air > 0.35 mm)

Hauling Time (min.)	B-SF22 (%)	B-SF25 (%)	B-SF28 (%)
10	0.5	0.5	0.5
20	0.5	0.4	0.5
30	0.6	0.4	0.4
40	0.7	0.4	0.4
50	0.6	0.5	0.4
60	0.6	0.5	0.4
70	1.0	0.6	0.4
80	1.2	0.5	0.4
90	2.1	0.7	0.5

711 mm mixture always retained a slump flow greater than 500 mm during hauling time, and therefore the air content measurements contained less entrapped air. The percentage of entrapped air is plotted against slump flow in Figure 4.4. As the slump flow decreased past a threshold of approximately 500 mm, the entrapped air content rose sharply.

4.2 Effects of Hauling Time on Air Void Characteristics

Coupled with the increase in total air content, the air void characteristics of all three trial mixtures improved with hauling time, as seen in Figure 4.5 and Table 4.5. B-SF28 had the highest rate of improvement in air void characteristics in the first 20 minutes of hauling time, whereas B-SF25 and B-SF22 initially experienced more gradual air void improvements. All three mixtures experienced a peak in air void specific surface at 70 minutes of hauling time, followed by a gradual deterioration. Likewise, the spacing factors of all three mixtures declined after 80 minutes of hauling time. The increase in specific surfaces of the air voids from the initial mixing period to the 70 hauling time (α_{\max}) were 16%, 21% and 24%, for B-SF22, B-SF25 and B-SF28, respectively. The

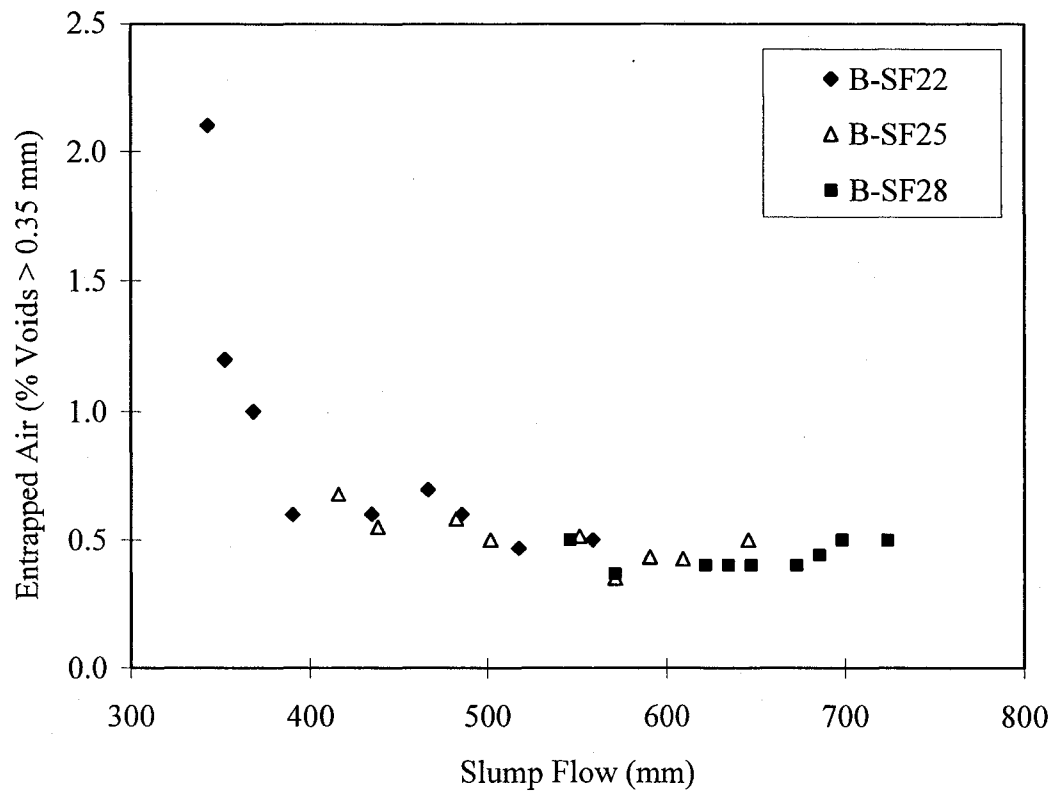


Figure 4.4 Entrapped air content with respect to slump flow

Table 4.5 Air void characteristics with respect to hauling time

Hauling Time (minutes)	B-SF22		B-SF25		B-SF28	
	Specific Surface (mm ⁻¹)	Spacing Factor (μm)	Specific Surface (mm ⁻¹)	Spacing Factor (μm)	Specific Surface (mm ⁻¹)	Spacing Factor (μm)
10	38.0	141	37.0	145	37.0	153
20	40.1	129	41.8	113	42.1	104
30	41.8	125	43.9	106	44.4	98
40	42.6	115	45.3	104	45.7	92
50	43.8	110	46.2	101	46.9	90
60	44.8	104	46.5	91	48.0	87
70	45.1	92	47.0	86	48.4	83
80	44.6	84	47.0	84	48.0	80
90	41.8	86	44.8	85	46.5	83

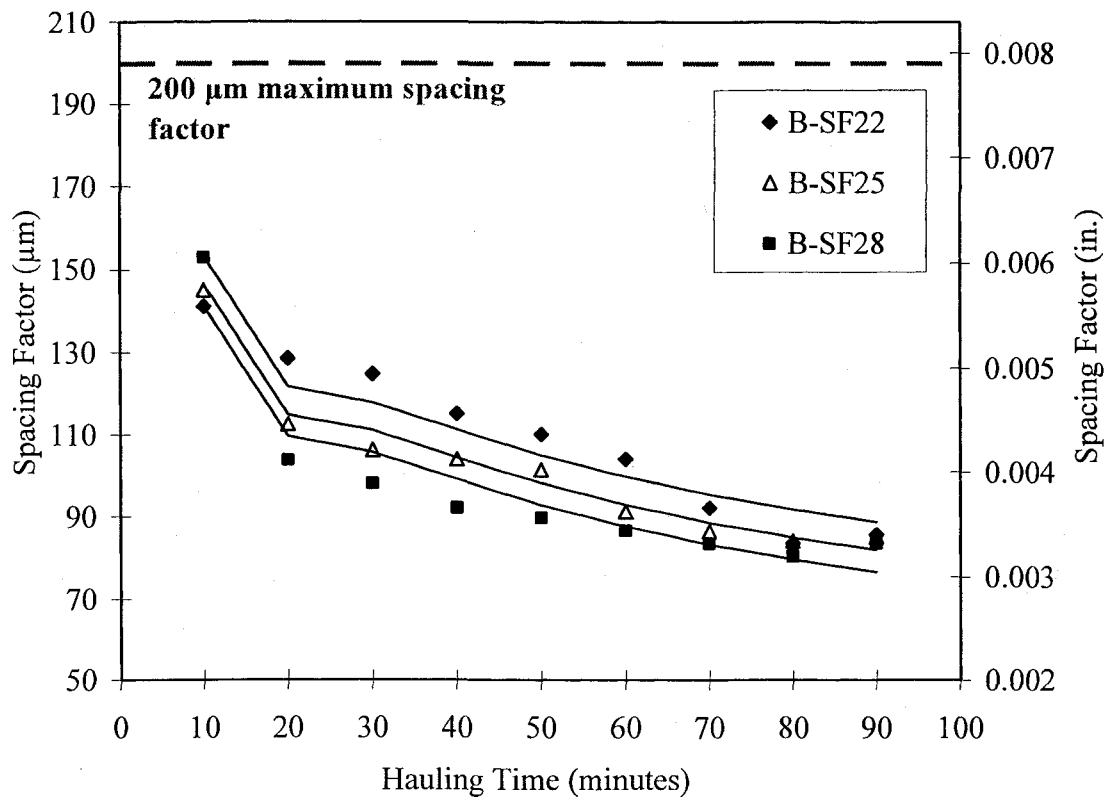
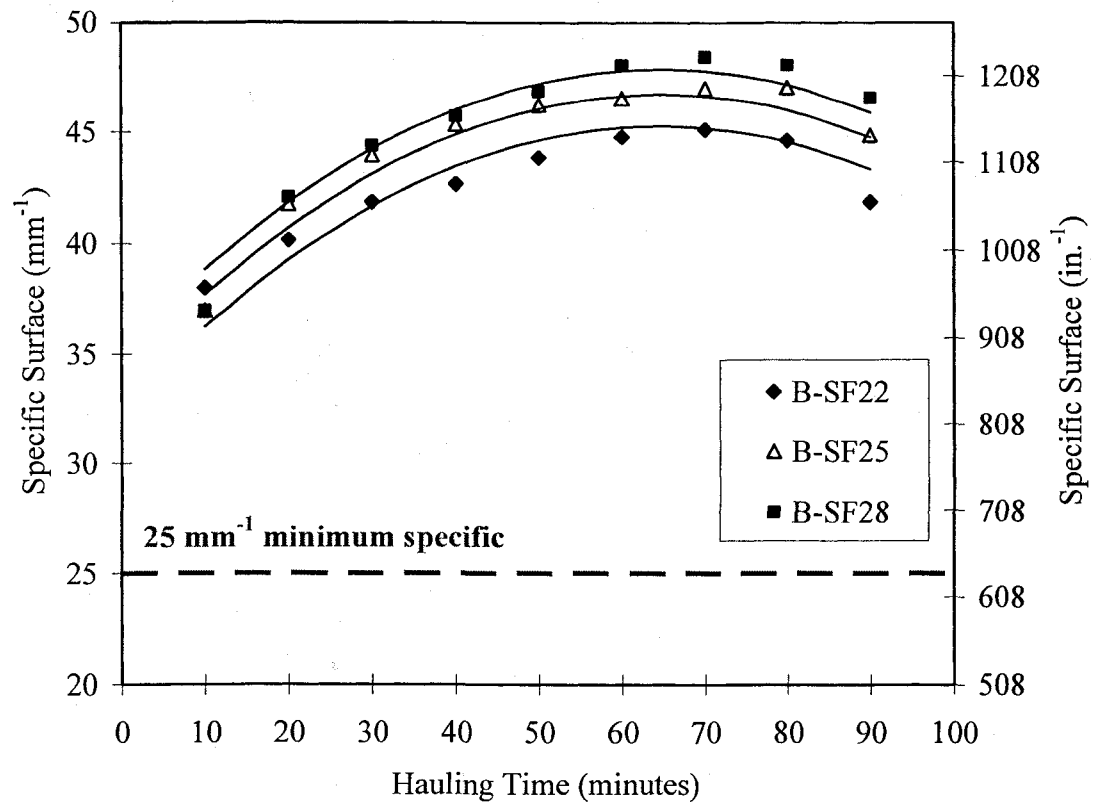


Figure 4.5 Effects of hauling time on air void characteristics

decrease in spacing factors from the initial mixing period to the 80 minute hauling time (\bar{L}_{\min}) was 59%, 58% and 53%, for B-SF22, B-SF25 and B-SF28, respectively.

4.2.1 Air Void Distributions

Regardless of slump flow, the air voids in the concrete mixtures decreased in size and became more uniformly dispersed with hauling time, as indicated by the improvement in air void characteristics. The reasons for the improvement in air void characteristics are linked to the reasons for the increase in total air content of the concrete. Over time, the agitation and mixing action forms new bubbles, distributes existing bubbles more evenly throughout the mixture, and breaks up the bubbles into increasingly smaller sizes. A decrease in fluidity and slump flow of the concrete prevents coalescence and rupturing of air voids. The increase in cement surface area due to grinding of particles produces more locations for the AEA to stabilize newly formed air bubbles.

The difference in air void distributions between the initial mixing period ($t_h = 10$ min.) and final hauling time ($t_h = 90$ min.) is remarkable, as seen in Figures 4.6, 4.7 and 4.8, for the mixtures B-SF22, B-SF25, and B-SF28, respectively. A typical air void distribution produced by the Air Void Analyzer for the mixture B-SF22 after the initial mixing period tended to be evenly distributed, as seen in Figure 4.6 (left). Specifically, the quantity of air voids at 10 minutes was uniformly allocated from 75 μm to 2 mm, with no voids smaller than 75 μm . In contrast, after 90 minutes of hauling time, the air voids reduced in size and increased in quantity. Seventy-five percent of the air voids at 90 minutes were less than 200 μm in size, as opposed to 63% less than 200 μm at 10 minutes. At 90 minutes, there was also 7% of air voids less than 75 μm . The other

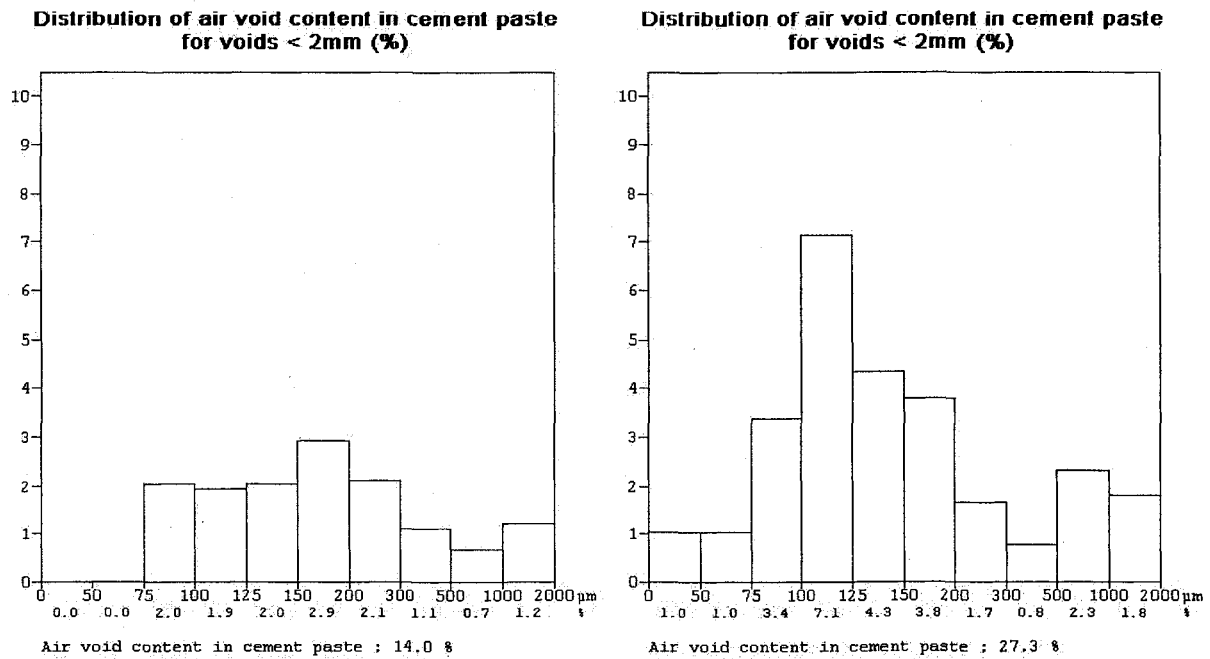


Figure 4.6 Typical air void distribution of B-SF22 at 10 minutes (left) and at 90 minutes (right)

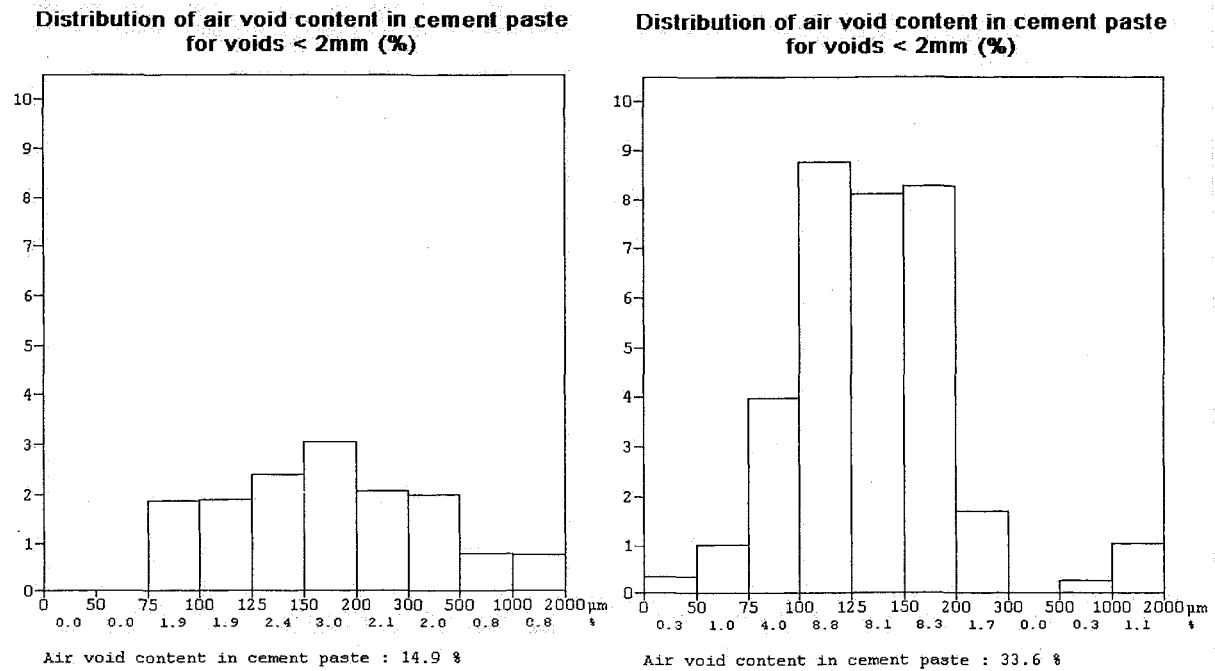


Figure 4.7 Typical air void distribution of B-SF25 at 10 minutes (left) and at 90 minutes (right)

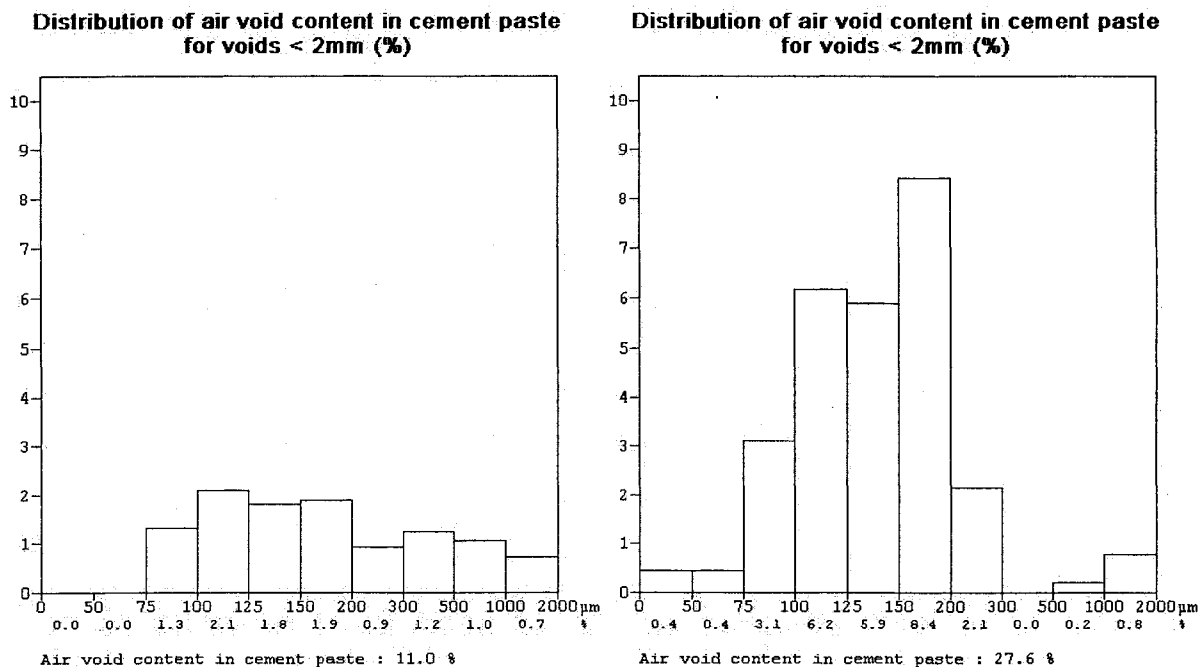


Figure 4.8 Typical air void distribution of B-SF28 at 10 minutes (left) and at 90 minutes (right)

mixtures, B-SF25 and B-SF28, produced air void distributions similar to B-SF22 at 10 and 90 minutes. Both distributions had an increasing quantity of smaller air voids, and an overall increase in air content with increasing hauling time.

4.2.2 Effect of AEA Dosage on Air Void Characteristics

The AEA dosage was the primary reason that mixture B-SF28 produced better air void characteristics than B-SF25 and B-SF22. The AEA dosage for B-SF28 was 58% greater than B-SF22 and 8% greater than B-SF25. The more air-entrainment admixture added to the concrete, the more potential it has to entrain air bubbles. Initially, B-SF28 necessitated a higher AEA dosage to obtain 6% air due to its high fluidity, but with time and agitation was able to produce and stabilize more air bubbles because there was more air-entrainment available. B-SF25 had a similar dosage in air entrainment to B-SF28, and therefore closely mimicked its air void distribution.

4.2.3 Effect of Slump Flow on Air Void Characteristics

In comparing the different slump flows, the increase in total air content did not correlate with the improvement in air void characteristics. For example, B-SF22 experienced the greatest increase in air content, but the least improvement in air void characteristics. B-SF28 had the least increase in air content with the most improved air void characteristics. There is a greater possibility of entrapped air in the lower-slump concrete, and therefore a deteriorated air void system is produced. Without manual consolidation, air was entrapped in the mixture during testing, giving an errantly inflated value for total air content. However, the air void characteristics reflected the larger size and spacing of the entrapped air, correlating to a lower specific surface and higher spacing factor. The fact that there is more entrapped air in the mixtures with the lower slump flows can be seen in the AVA air void distributions, Figures 4.6 through 4.8. The AVA air void distributions demonstrate the increased occurrence of entrapped air (voids greater than 0.35 mm) after 90 minutes of hauling time for the lower slump flow concretes.

The decrease in specific surface after 70 minutes of hauling time, and the increase in spacing factor after 80 minutes of hauling time can be attributed to both the increase in entrapped air bubbles and the maximization of the AEA potential. The specific surface values decreased by 3.3, 2.1 and 1.9 mm^{-1} for the mixtures B-SF22, B-SF25 and B-SF28, respectively, from 70 to 90 minutes. B-SF22 experienced the greatest decrease in specific surface from 70 to 90 minutes because more air became entrapped throughout the mixture due the mixture's high viscosity. The spacing factors increased an average of 2 μm from 80 to 90 minutes. A given dosage of AEA can only entrain a finite amount of

air, and after that point the air voids may rupture or coalesce, causing the spacing factor to increase.

4.2.4 Predictive Equations of Air Void Characteristics

The specific surface and spacing factor of the mixtures developed can be statistically predicted with respect to hauling time and initial slump flow, as seen in Equations 4.3 and 4.4.

$$\alpha = 44.73 + 0.389t_h - 0.00301t_h^2 + \frac{-6730.97}{SF_i} \quad \text{Eq. 4.3}$$

$$\bar{L} = \frac{3530.7}{t_h} + \frac{-63633.6}{t_h^2} + \frac{379710.4}{t_h^3} + \frac{31733.01}{SF_i} \quad \text{Eq. 4.4}$$

where: α = specific surface (mm^{-1})

\bar{L} = spacing factor (μm)

t_h = hauling time, $10 \leq t_h \leq 90$ minutes

SF_i = initial slump flow, $559 \leq SF_i \leq 711 \pm 13$ mm

The coefficients of determination for Equations 4.3 and 4.4 are 0.94 and 0.93, respectively, indicating an accurate representation of the gathered data. In addition, the t-test probabilities of all variables are 0 or very close to 0, and the standard errors are 0.832 and 5.89 for α and \bar{L} , respectively, both of which demonstrate that hauling time and initial slump flow are statistically significant predictors of the air void characteristics. The actual and calculated values of spacing factor and specific surface, as well as percent error, can be seen tabulated in Appendix B.

4.3 Conclusions

Hauling times up to 90 minutes can adversely affect the flow properties of self-consolidating concrete. Slump flow loss in self-consolidating concrete mixtures occurs

due to: 1) decreased adsorption of high range water reducer on cement particles, 2) increased surface area of mortar due to mixing and grinding action, and 3) growth of cement hydration products. The slump flow losses of the selected SCC mixtures increased with decreasing initial slump flow. The slump flow losses were measured at 39%, 37% and 25% for the mixtures with an initial slump flow of 559, 635 and 711 mm, respectively. Decreasing slump flow loss with increasing initial slump flow can mainly be attributed to the higher dosage of HRWR present in the higher slump flow mixtures. Other flow properties, such as T_{50} rate of flow ability and resistance to dynamic segregation, were found to improve with increased hauling time.

In the air-entrained SCC mixtures selected for this study, hauling time and continual agitation increased the total air content. The air content increase over the 90 minute hauling period was found to be 79%, 52% and 44% for the mixtures with a 559, 635 and 711 mm initial slump flow. The primary factors that triggered the increasing air content were:

- 1) Decreased slump flow: The viscosity of a mixture increased with a decreasing slump flow which provided a greater cushioning effect, and thus stability, for the air voids.
- 2) Type of air-entraining admixture: The salt-type air-entraining admixture containing tall oil slowly generated air voids. The calcium precipitates slowly dissolved with increasing hauling time, allowing increased adsorption of air-entrainment on cement particles.

- 3) Increased entrapped air: Without mechanical consolidation, such as rodding or vibration, air voids larger than 1 mm were entrapped throughout the mixture, increasing the total air content.

Additionally, a relationship was established between the air content and slump flow. The air content increased more rapidly with slump flows less than 500 mm. If the flow ability of a mixture was maintained within the range of SCC, the air content increased more slowly.

The air void characteristics of the three SCC mixtures improved with increasing hauling time. The measured spacing factors of the mixtures decreased by 57%, on average, after 80 minutes of hauling time. The specific surface of the air voids increased an average of 20% over 70 minutes of hauling time. The air void characteristics did not continually improve over the entire 90 minute hauling time period because of the increased occurrence of entrapped air and the maximization of the potential of the air-entraining admixture. The change in air void characteristics of a SCC mixture with respect to hauling time was dictated by:

- 1) Air-entrainment dosage: An increased initial dosage of air-entraining admixture produced a greater improvement in air void characteristics with respect to hauling time. The higher air-entrainment dosage available in the mixture allowed a larger quantity of smaller air voids to be stabilized.
- 2) Slump loss: Decreased slump flow with hauling time increased the occurrence of entrapped air (without mechanical consolidation). The larger entrapped air bubbles (voids > 1 mm) caused the air void characteristics, specifically the specific surface, to deteriorate over time.

CHAPTER 5

PHASE II: EFFECTS OF REMEDIATION ON SELF-CONSOLIDATING CONCRETE

Field applications of self-consolidating concrete frequently necessitate long hauling times between batching and placing. The effects of hauling time such as loss of slump flow, documented in Chapter 4, are typically counteracted using various methods of remediation. The first form of remediation utilized in this investigation is overdosing or under-dosing admixtures initially to achieve the desired fresh properties at the end of a stipulated hauling time. This shall henceforth be referred to as overdosing or remediation A. The second form of remediation employed in this study begins with the initial mixture design (developed in Phase I) and then following a certain hauling time, retempering the concrete by adding more admixtures to achieve the desired fresh properties. This shall be referred to as retempering or remediation B.

Concrete mixtures with three target slump flows (559, 635 and 711 mm) utilizing one admixture manufacturer (source B) were investigated on the effects of the two forms of remediation. In completing remediation A, the concrete admixtures were overdosed or under-dosed to meet the target fresh properties at hauling times of 20, 30, 40, 50, 60, 70, 80 and 90 minutes after first cement and water contact. For remediation B, the concrete was retempered with admixtures after 20, 40, 60 and 80 minutes of hauling time to meet the target fresh properties. The target fresh properties during this phase of investigation

are outlined in Table 5.1. The performance criteria were altered from the first phase to reflect irregularities that occur when batching concrete in the field.

Throughout the discussion on remediation, the values recorded at the specific hauling times shall be compared to the initial mixtures developed in Chapter 3, and subjected to hauling times in Chapter 4. Mixtures B-SF22, B-SF25 and B-SF28 are the reference batches to which all remediated mixtures shall be compared to.

Table 5.1 Target fresh properties for Phase II remediation

Property	U.S. Units	SI Units	Method
Slump Flow	22, 25 or 28 ± 1 inch	559, 635 or 711 ± 25 mm	ASTM C 1611
T ₅₀	2 to 5 seconds		ASTM C 1611
J-Ring	SF - J-Ring ≤ 2 in.	SF - J-Ring ≤ 51 mm	ASTM C 1821
VSI	0 or 1 (Highly Stable or Stable)		ASTM C 1611
Air Content	$6 \pm 1\%$		ASTM C 173
Spacing Factor	$\bar{L} < 0.0079$ in.	$\bar{L} < 200$ μm	AVA (correlated with ASTM C 457)
Specific Surface	$\alpha > 635$ in. ⁻¹	$\alpha > 25$ mm ⁻¹	

5.1 Remediation A: Overdosing and Under-Dosing Admixtures

5.1.1 Mixture Proportioning and Fresh Properties

Determination of the admixture dosages for remediation A was accomplished through trial-and-error. The aggregates, cementitious materials and water proportions of the mixtures remained the same as those used in Phase I. For each hauling time, the three mixtures (B-SF22, B-SF25 and B-SF28) were remediated for decreasing slump flow and increasing air content by overdosing and under-dosing of admixtures to achieve the target fresh properties, as seen in Tables 5.2 through 5.4.

Table 5.2(a) B-SF22 Phase II remediation A mixture constituents and proportions

Hauling Time (min.)	Cement (kg/m ³)	Fly Ash (kg/m ³)	w/cm ¹	Water (kg/m ³)	Fine Aggregate (kg/m ³)	Coarse Aggregate (kg/m ³)
10	390	78	0.40	197	795	864
20	390	78	0.40	197	795	864
30	390	78	0.40	197	795	864
40	390	78	0.40	197	795	864
50	390	78	0.40	197	795	864
60	390	78	0.40	197	795	864
70	390	78	0.40	197	795	864
80	390	78	0.40	197	795	864
90	390	78	0.40	197	795	864

¹ water-to-cementitious materials ratio1 kg/m³ = 1.6856 lb/yd³

Table 5.2(b) B-SF22 Phase II remediation A mixture constituents and proportions

Hauling Time (min.)	ml/kg cementitious materials			% Paste ⁵	% Mortar ⁶	% Air	% Vol. of Coarse Aggregate
	HRWR ²	AEA ³	VMA ⁴				
10	1.50	0.33	0	37.47	65.33	6.00	29.54
20	1.63	0.33	0	37.67	65.44	6.00	29.44
30	1.76	0.33	0	37.87	65.55	6.00	29.35
40	1.89	0.33	0	38.07	65.66	6.00	29.26
50	1.96	0.33	0	38.17	65.71	6.00	29.21
60	2.02	0.33	0	38.27	65.77	6.00	29.16
70	2.09	0.33	0	38.37	65.82	6.00	29.12
80	2.12	0.33	0	38.41	65.85	6.00	29.09
90	2.15	0.33	0	38.46	65.88	6.00	29.07

² high range water reducing admixture, ³ air-entraining admixture, ⁴ viscosity modifying admixture, ⁵ % paste by volume = % cement + % fly ash + % water + % admixtures, ⁶ % mortar by volume = (% paste) + (% aggregate < 6 mm)

1 ml/kg cementitious materials = 1.5338 ounces per 100 pounds cementitious materials

Table 5.3(a) B-SF25 Phase II remediation A mixture constituents and proportions

Hauling Time (min.)	Cement (kg/m ³)	Fly Ash (kg/m ³)	w/cm ¹	Water (kg/m ³)	Fine Aggregate (kg/m ³)	Coarse Aggregate (kg/m ³)
10	390	78	0.40	196	795	864
20	390	78	0.40	196	795	864
30	390	78	0.40	196	795	864
40	390	78	0.40	196	795	864
50	390	78	0.40	196	795	864
60	390	78	0.40	196	795	864
70	390	78	0.40	196	795	864
80	390	78	0.40	196	795	864
90	390	78	0.40	196	795	864

¹ water-to-cementitious materials ratio1 kg/m³ = 1.6856 lb/yd³

Table 5.3(b) B-SF25 Phase II remediation A mixture constituents and proportions

Hauling Time (min.)	ml/kg cementitious materials			% Paste ⁵	% Mortar ⁶	% Air	% Vol. of Coarse Aggregate
	HRWR ²	AEA ³	VMA ⁴				
10	2.02	0.72	0.26	39.24	66.31	6.00	28.70
20	2.15	0.72	0.26	39.43	66.41	6.00	28.61
30	2.28	0.72	0.26	39.62	66.52	6.00	28.52
40	2.35	0.72	0.26	39.71	66.57	6.00	28.48
50	2.41	0.65	0.26	39.71	66.57	6.00	28.48
60	2.44	0.59	0.26	39.66	66.54	6.00	28.50
70	2.48	0.52	0.26	39.62	66.52	6.00	28.52
80	2.51	0.46	0.26	39.57	66.49	6.00	28.55
90	2.54	0.39	0.26	39.52	66.47	6.00	28.57

² high range water reducing admixture, ³ air-entraining admixture, ⁴ viscosity modifying admixture, ⁵ % paste by volume = % cement + % fly ash + % water + % admixtures, ⁶ % mortar by volume = (% paste) + (% aggregate < 6 mm)

1 ml/kg cementitious materials = 1.5338 ounces per 100 pounds cementitious materials

Table 5.4(a) B-SF28 Phase II remediation A mixture constituents and proportions

Hauling Time (min.)	Cement (kg/m ³)	Fly Ash (kg/m ³)	w/cm ¹	Water (kg/m ³)	Fine Aggregate (kg/m ³)	Coarse Aggregate (kg/m ³)
10	390	78	0.40	196	795	864
20	390	78	0.40	196	795	864
30	390	78	0.40	196	795	864
40	390	78	0.40	196	795	864
50	390	78	0.40	196	795	864
60	390	78	0.40	196	795	864
70	390	78	0.40	196	795	864
80	390	78	0.40	196	795	864
90	390	78	0.40	196	795	864

¹ water-to-cementitious materials ratio1 kg/m³ = 1.6856 lb/yd³

Table 5.4(b) B-SF28 Phase II remediation A mixture constituents and proportions

Hauling Time (min.)	ml/kg cementitious materials			% Paste ⁵	% Mortar ⁶	% Air	% Vol. of Coarse Aggregate
	HRWR ²	AEA ³	VMA ⁴				
10	2.54	0.78	0.33	40.18	66.83	6.00	28.26
20	2.61	0.78	0.33	40.27	66.88	6.00	28.22
30	2.67	0.78	0.33	40.36	66.93	6.00	28.17
40	2.77	0.78	0.39	40.59	67.06	6.00	28.06
50	2.84	0.72	0.39	40.59	67.06	6.00	28.06
60	2.87	0.65	0.39	40.55	67.03	6.00	28.09
70	2.93	0.59	0.46	40.64	67.08	6.00	28.04
80	2.97	0.52	0.46	40.59	67.06	6.00	28.06
90	3.00	0.46	0.46	40.55	67.03	6.00	28.09

² high range water reducing admixture, ³ air-entraining admixture, ⁴ viscosity modifying admixture, ⁵ % paste by volume = % cement + % fly ash + % water + % admixtures, ⁶ % mortar by volume = (% paste) + (% aggregate < 6 mm)

1 ml/kg cementitious materials = 1.5338 ounces per 100 pounds cementitious materials

The fresh properties of the mixtures remediated during hauling time using the overdosing procedures can be seen in Tables 5.5, 5.6 and 5.7 for mixtures with a 559, 635 and 711 mm target slump flow, respectively. The average passing ability (measured by the difference between the slump flow and J-Ring) increased from the initial mixing time by 23, 10 and 15 mm for mixtures B-SF22, B-SF25 and B-SF28, respectively. The increased passing ability is based on the average passing abilities of all hauling times 20 through 90 minutes compared to the control (reference) mixture at 10 minutes. The average values do not necessarily indicate that the passing ability improved with hauling time, since the passing ability at a particular hauling time was, on occasion, less than or equal to that of the reference mixture.

The stability of the remediated mixtures, as indicated by the VSI, was typically equal to the VSI recorded at 10 minutes. In the case of the 711 mm slump flow, the VSI improved from 1 to 0 (stable to very stable) for 7 out of 8 hauling times, as seen in Table 5.7. The agitation and decreased effectiveness of the HRWR with time generally increased the stability, homogeneity and resistance to bleeding of the mixtures.

Table 5.5 B-SF22 Remediation A fresh properties

Hauling Time (min.)	SF (mm)	J-Ring (mm)	SF - J-Ring (mm)	T ₅₀ (sec.)	VSI	Air Content (%)
10	572	522	50	2.00	0	6.00
20	565	521	44	2.47	0	6.25
30	572	546	25	2.05	0	6.25
40	572	572	0	2.56	0	6.25
50	578	565	13	2.00	0	6.25
60	546	508	38	2.85	0	6.50
70	565	546	19	2.00	0	6.25
80	559	533	25	2.75	0	6.25
90	533	483	50	3.00	0	6.50
AVG ₂₀₋₉₀	561	534	27	2.46	0	6.31

Table 5.6 B-SF25 Remediation A fresh properties

Hauling Time (min.)	SF (mm)	J-Ring (mm)	SF - J-Ring (mm)	T₅₀ (sec.)	VSI	Air Content (%)
10	645	610	36	1.99	0	6.30
20	610	591	19	2.47	0	6.75
30	648	598	50	2.28	0	6.50
40	654	654	0	2.22	0	7.00
50	648	616	32	2.41	0	6.75
60	641	616	25	2.78	0	6.50
70	648	629	19	2.10	0	6.50
80	622	597	25	2.29	0	6.25
90	622	584	38	3.18	0	6.00
AVG₂₀₋₉₀	637	611	26	2.47	0.00	6.53

Table 5.7 B-SF28 Remediation A fresh properties

Hauling Time (min.)	SF (mm)	J-Ring (mm)	SF - J-Ring (mm)	T₅₀ (sec.)	VSI	Air Content (%)
10	715	684	32	2.02	1	6.00
20	692	679	13	1.68	0	6.25
30	711	699	13	1.28	1	6.00
40	718	705	13	2.81	0	6.50
50	711	686	25	2.18	0	6.25
60	711	699	13	1.81	0	6.50
70	711	699	13	1.53	0	6.25
80	692	667	25	1.66	0	6.50
90	686	667	19	1.88	0	6.25
AVG₂₀₋₉₀	704	687	17	1.85	0.13	6.31

The average flow ability decreased with hauling time for the remediated 559 and 635 mm slump flow mixtures. The average T₅₀ times from 20 to 90 minutes increased by 0.46 and 0.48 seconds for mixtures B-SF22 and B-SF25, respectively. The slower T₅₀ times indicate increased viscosity with hauling time, even though the slump flow is comparable to that of the control mixture. The same mechanisms that cause slump loss, such as particle grinding, chemical hydration of cement, and coagulation of particles,

occur in all mixtures with continual agitation, but the overdosed HRWR maintains the desired slump flow level. Increased surface area of the particles (or increased fineness) increases the viscosity of the mixture. In contrast to the mixtures with lower slump flows, the average T_{50} flow ability time for the 711 mm target slump flow mixtures decreased by 0.17 seconds. Although the VMA was increased at 40 minutes, the flow ability of the 711 mixtures did not always meet the T_{50} requirement of 2 to 5 seconds.

5.1.2 Admixture Dosages

The HRWR dosage was overdosed an average of 0.08, 0.07 and 0.06 ml/kg per 10 minutes of hauling time to achieve the 559, 635 and 711 mm slump flows, respectively. However, the change in HRWR from the initial dosage was not always linear, as seen in Figure 5.1. For the target slump flow of 559 mm, the first 30 minutes of hauling time necessitated an average dosage of 0.13 ml/kg, whereas a dosage of 0.03 ml/kg per 10 minutes were needed beyond 60 minutes of hauling time. The HRWR dosage for the 635 mm slump flow behaved similarly to the 559 mm slump flow in that the rate of dosage increase decreased with hauling time.

The predictive equations of the HRWR dosage with respect to hauling time and target slump flow can be seen in Table 5.8. The actual versus calculated HRWR dosages are tabulated in Appendix B. The HRWR dosage for both the 559 and 635 mm slump flows can be characterized by a second-order polynomial. Unlike the other slump flows, the SCC mixture with a 711 mm slump flow necessitated a HRWR dosage that increased linearly with hauling time. Using the initial admixture dosage developed in Phase I, the B-SF28 mixture retained more slump flow with hauling time than the other two mixtures.

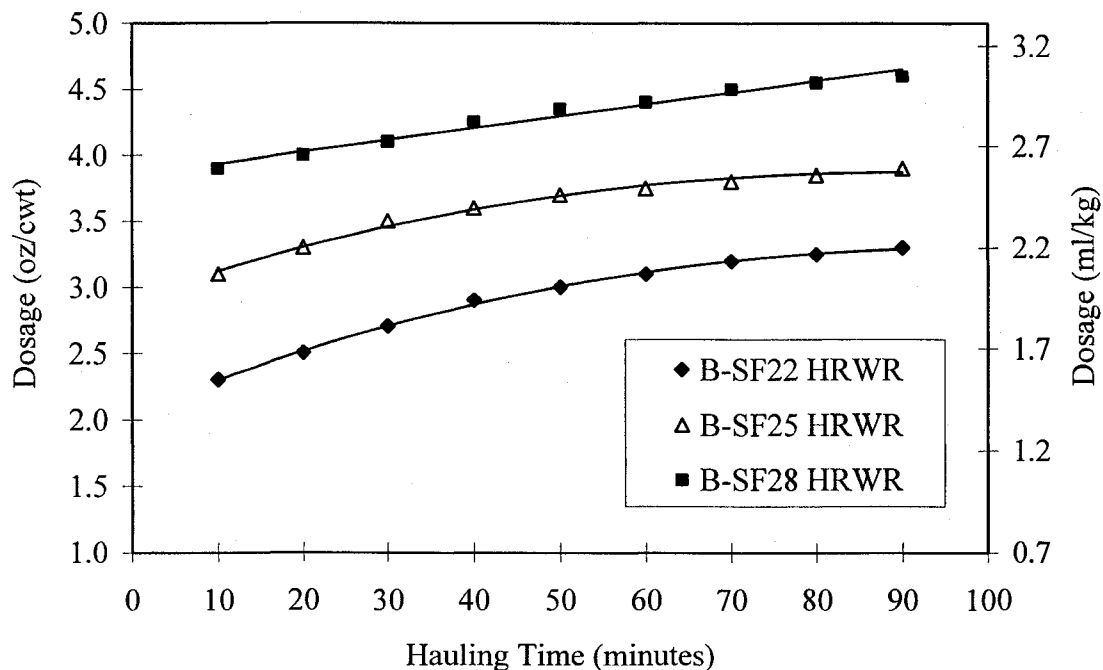


Figure 5.1 Remediation A dosage of HRWR admixture with hauling time

Table 5.8 Predictive equations for overdosing HRWR from source B

Target Slump Flow	Trend line Equation	R ²
559 mm (22 in.)	$HRWR_B = -9 \times 10^{-5} t_h^2 + 0.0167 t_h + 1.3397$	1.00
635 mm (25 in.)	$HRWR_B = -8 \times 10^{-5} t_h^2 + 0.0141 t_h + 1.904$	0.99
711 mm (28 in.)	$HRWR_B = 0.0059 t_h + 2.5065$	0.98

where: $HRWR_B$ = dosage in ml/kg cementitious materials

t_h = hauling time, $10 \leq t_h \leq 90$ minutes

Therefore, it follows that this mixture necessitated less HRWR per 10 minutes of hauling time to counteract the effects of slump loss.

The overdosing of HRWR to overcome slump loss follows a predictable trend regardless of target slump flow, as seen in Figure 5.2. The slump loss due to hauling time recorded in Chapter 4 correlates to the overdose in HRWR with a probability of 1.4×10^{-11} that the relationship is due to chance. The coefficient of determination of the second-

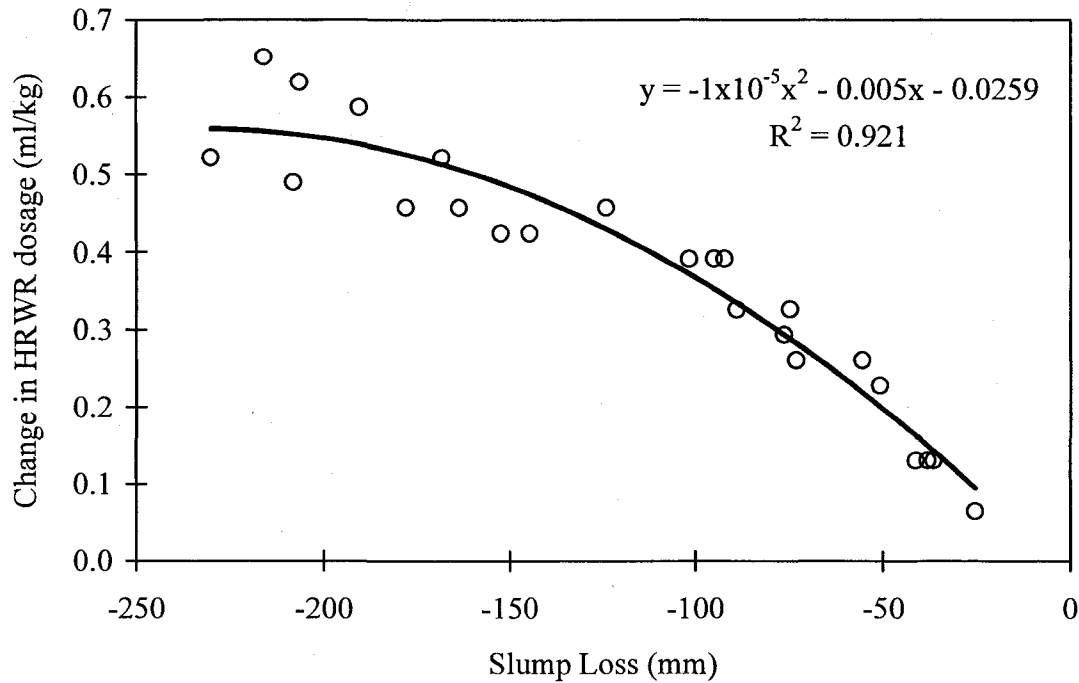


Figure 5.2 Remediation A: change in HRWR vs. slump loss of all mixtures

order polynomial fit line in Figure 5.2 is 0.921, signifying an accurate representation of all of the data from remediation A. Therefore, from one particular admixture source there is a correlation between the magnitude of slump loss and the additional quantity of HRWR needed for remediation.

Remediation by overdosing the VMA was only necessary in achieving the 711 mm slump flow beyond 30 minutes of hauling time, as seen in Figure 5.3. Adequate viscosity was met for the two lower slump flows without increasing the initial dosage of VMA. For the 711 mm slump flow, the VMA dosage was increased incrementally after 30 and 60 minutes of hauling time. At 40 and 70 minutes, the VMA was increased by 0.07 ml/kg (0.1 oz/cwt).

In contrast to losing slump flow with hauling time, the air content increased with hauling time, as documented in Chapter 4. Therefore, in order to remediate the air

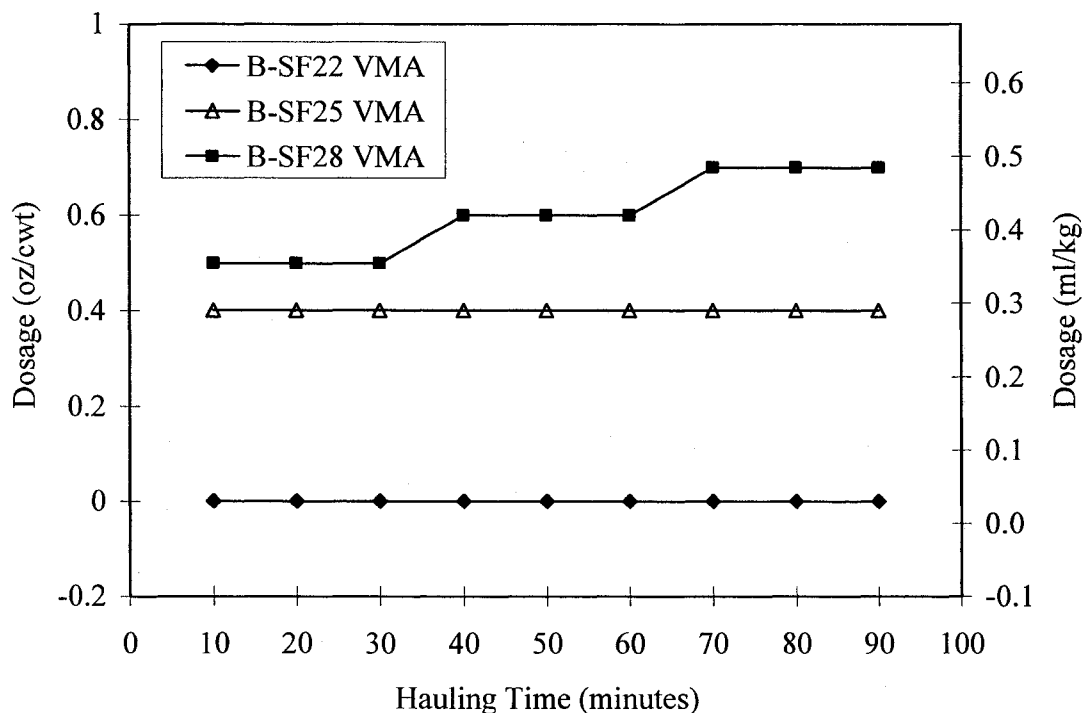


Figure 5.3 Remediation A dosage of VMA with hauling time

content, the AEA was under-dosed to counteract the natural tendency of the mixture to generate air. With remediation of slump flow through a larger dosage of HRWR, the AEA dosage required for the 559 mm slump flow remained constant for all hauling times, as seen in Figure 5.4. It is interesting to note that mixture B-SF22 experienced a more significant increase in air content than mixtures B-SF25 and B-SF28 during hauling time (without remediation), but did not require under-dosing with remediation. The dosage utilized for mixture B-SF22 (0.33 ml/kg), was established in Chapter 3 as a minimum required dosage to initially generate 6% air. The remediation results substantiate the notions that: 1) the air content of SCC increases with decreasing slump flow partially due to the increased occurrence of entrapped air, and 2) a higher AEA dosage has the potential to entrain more air.

Mixtures with the 635 and 711 mm target slump flow necessitated under-dosing of the AEA to achieve $6 \pm 1\%$ air content at the specified hauling times, as seen in Figure 5.4. After 40 minutes of hauling, the AEA was reduced by 0.07 ml/kg (0.1 oz/cwt) for every 10 minute increment. At 90 minutes, the AEA dosages dropped to 0.39 and 0.46 ml/kg for the 635 and 711 mm slump flows, respectively. It is evident that much of the increase in air content with hauling time was due to slump loss and resulting entrapped air. However, because the AEA needed to be under-dosed, the slow air generation by the tall oil AEA and constant agitation with hauling time also had a significant contribution to the increasing air content.

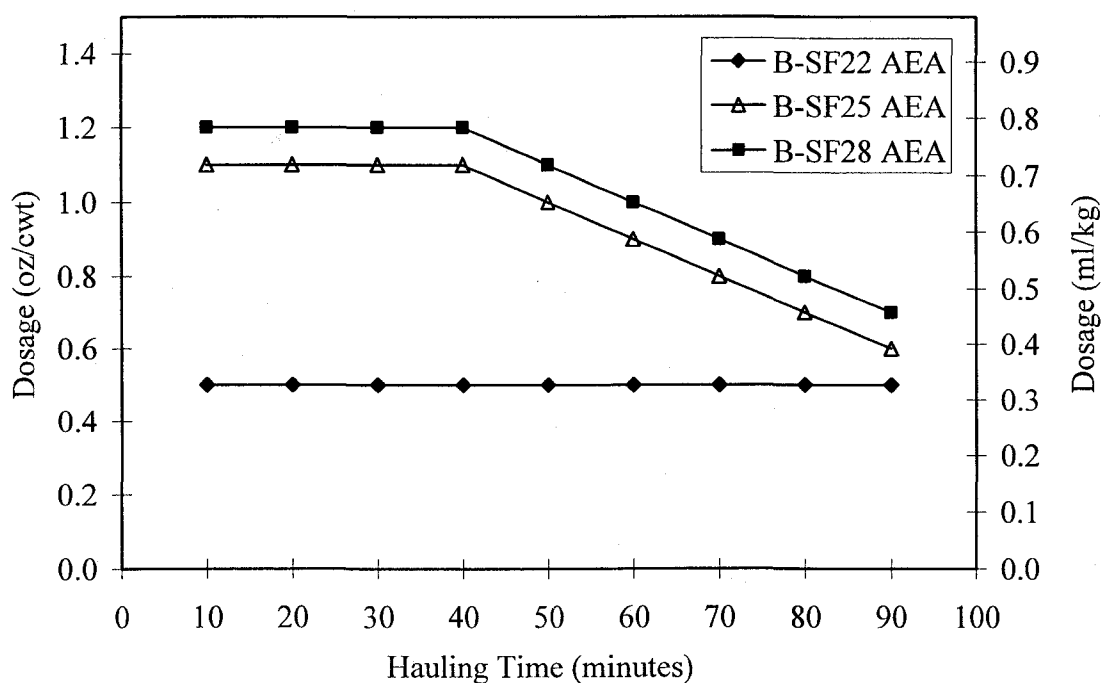


Figure 5.4 Remediation A dosage of AEA with hauling time

5.1.3 Air Void Characteristics

The AVA results of remediation presented herein are the average of two samples taken from the same batch of SCC. The results presented in Chapters 3 and 4 are typically the average of five samples from two batches; therefore, the air void characteristics for remediation are not as precise, and generally contain more scatter of data. However, the results will indicate if a mixture departs significantly from the initial air void characteristics (measured at 10 minutes), or if the mixture is no longer within the acceptable range of air void characteristics presented in Table 5.1.

The air void characteristics of the mixtures tested after overdosing of admixtures and hauling time can be seen in Figure 5.5. The air void systems measured for all mixtures remained within the acceptable range of specific surface $> 25 \text{ mm}^{-1}$ and spacing factor $< 200 \text{ }\mu\text{m}$. Similar to the effects of hauling time on the air void characteristics, the average spacing factor, \bar{L} , of all slump flows improved from the initial characteristics measured at 10 minutes, as seen in Table 5.9. However, the average specific surface, α , improved only for the 635 and 711 mm slump flows, while the 559 mm slump flow decreased an average of 1.9 mm^{-1} . The anomalous decrease in air void specific surface area for the 559 mm slump flow mixtures can be attributed to the lower AEA dosage and higher HRWR dosage. The AEA dosage for the 559 mm slump flow mixture remained constant for all hauling times, in contrast to the 635 and 711 mm slump flow mixtures, which were initially 2.2 and 2.4 times greater than the 559 mm AEA dosage. When coupled with an increased amount of HRWR, the low AEA dosage was not able to produce the same air void system initially. The increased fluidity of the overdosed mixture caused bubble coalescence, thus increasing the average size of the voids.

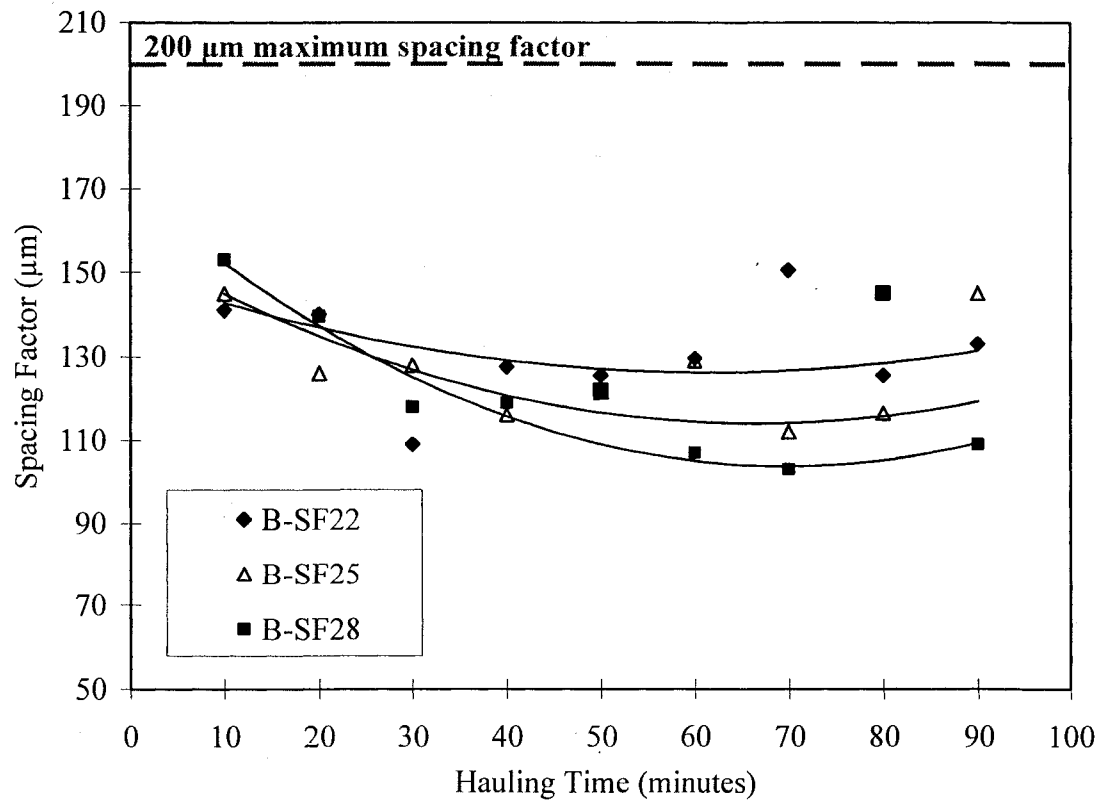
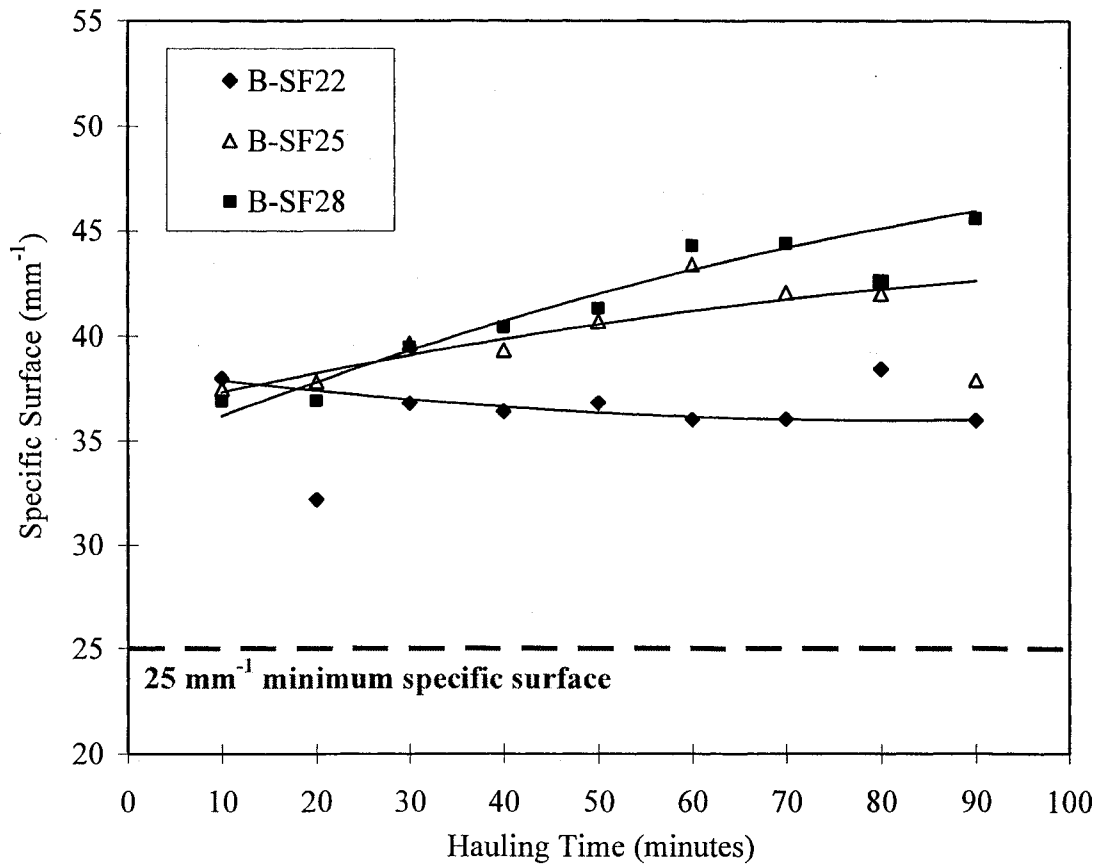


Figure 5.5 Remediation A air void characteristics

Table 5.9 Remediation A: Change in air void characteristics from $t_h = 10$ min.

t_h (min.)	559 mm (22 in.)			635 mm (25 in.)			711 mm (28 in.)		
	α (mm ⁻¹)	\bar{L} (μ m)	Air % < 2mm	α (mm ⁻¹)	\bar{L} (μ m)	Air % < 2mm	α (mm ⁻¹)	\bar{L} (μ m)	Air % < 2mm
20	-5.8	-1.0	2.9	-0.2	-19.0	2.5	-1.1	-1.5	1.6
30	-1.2	-32.0	2.8	1.7	-13.0	2.2	1.5	-23.0	2.4
40	-1.6	-13.5	2.5	1.3	-25.0	2.3	2.4	-22.0	2.3
50	-1.2	-15.5	1.5	2.7	-19.5	2.9	3.3	-31.0	1.2
60	-2.0	-11.5	2.4	5.9	-16.0	3.3	6.3	-34.0	1.9
70	-2.0	9.5	1.4	4.0	-29.0	2.6	6.4	-38.0	1.8
80	0.4	-15.5	1.4	4.0	-24.5	1.8	5.7	-8.0	2.5
90	-2.0	-8.0	2.0	0.4	0.0	1.7	7.6	-32.0	1.1
AVG	-1.9	-10.9	2.1	2.5	-18.3	2.4	4.0	-23.7	1.8

Note: $+\alpha$ / $-\bar{L}$ = improvement. $-\alpha$ / $+\bar{L}$ = deterioration

Therefore, the increased fluidity of the SCC overwhelmed the ability of the tall oil AEA to produce and stabilize air voids over time. Another interesting trend with remediation A is the increased stability of air voids with increasing slump flow, as seen in Table 5.9, which is due to the decreased rate of change in the HRWR dosage.

The air void characteristics of the remediated mixtures can be compared to the air void characteristics of the non-remediated mixtures at their respective hauling times (documented in Chapter 4), as seen in Table 5.10. In contrast to the change from the initial air void characteristics generated at 10 minutes, the air void characteristics of the overdosed mixtures were weaker than those of the non-remediated mixtures. The specific surface decreased an average of 5.4 mm⁻¹ between the remediated and non-remediated mixtures. The spacing factor increased an average of 24.6 μ m from the hauling time without remediation to the overdosed mixtures. Additionally, the AVA air content of the remediated mixtures was an average of 1.4% less than the corresponding hauling time. This comparison indicates that when a mixture is remediated for a

Table 5.10 Remediation A: Change in air void characteristics from respective hauling times

t_h (min.)	559 mm (22 in.)			635 mm (25 in.)			711 mm (28 in.)		
	α (mm ⁻¹)	\bar{L} (μ m)	Air % <2mm	α (mm ⁻¹)	\bar{L} (μ m)	Air % <2mm	α (mm ⁻¹)	\bar{L} (μ m)	Air % <2mm
20	-8.0	11.5	2.1	-3.9	13.5	0.1	-5.2	35.8	-2.1
30	-5.0	-15.8	1.9	-4.3	21.8	-0.4	-4.9	20.0	-1.5
40	-6.2	12.5	1.1	-6.0	12.0	-0.5	-5.3	27.0	-1.5
50	-7.0	15.5	-0.3	-5.5	20.2	-0.5	-5.5	32.3	-2.8
60	-8.8	25.5	0.3	-3.1	37.8	-0.5	-3.8	20.4	-2.3
70	-9.1	58.5	-1.8	-4.9	25.6	-2.2	-4.0	19.6	-2.5
80	-6.2	42.0	-3.6	-5.0	32.5	-3.6	-5.5	64.6	-1.8
90	-5.9	54.0	-4.2	-6.9	67.3	-3.9	-0.9	25.7	-3.4
AVG	-7.0	25.5	-0.6	-5.0	28.8	-1.4	-4.4	30.7	-2.2

Note: $+\alpha$ /- \bar{L} = improvement. $-\alpha$ /+ \bar{L} = deterioration

designated slump flow and air content by adjusting the initial admixture dosage, the air void system becomes less effective than when non-remediated. As numerated earlier, in order to maintain the volumetric air content of $6 \pm 1\%$, the higher initial slump flow and decreasing AEA dosage contribute to the relative degradation of the air void characteristics.

Predictive equations were developed at a 95% confidence interval for the air void characteristics produced by overdosing admixtures with respect to hauling time and slump flow, as seen in Equations 5.1 and 5.2.

$$\alpha_A = 0.127SF - 0.522t_h - 1.07 \times 10^{-4} SF^2 + 5.1 \times 10^{-4} t_h^2 + 8.53 \times 10^{-4} SF \cdot t_h \quad \text{Eq. 5.1}$$

$$\bar{L}_A = 220.64 - 0.183SF - \frac{879.01}{t_h} - \frac{4836.07}{t_h^2} + 2.796 \frac{SF}{t_h} \quad \text{Eq. 5.2}$$

where: t_h = hauling time, $10 \leq t_h \leq 90$ minutes

SF = actual slump flow, $559 \leq SF \leq 711 \pm 25$ mm

Statistical data for Equations 5.1 and 5.2 can be seen in Table 5.11, and calculated values at each hauling time can be seen in Appendix B. Due to the variability of data, outliers significantly outside the trend line were removed from the regression analysis in order to obtain a more suitable statistical correlation. It would have been preferable to validate the data recognized as outliers to increase the accuracy; however, time constraints limited the data available. Nonetheless, most suitable predictions of the air void properties with respect to unconfined workability and hauling time of different remediation techniques were generated.

Table 5.11 Statistical data for predictive equations for remediation A air void characteristics

Specific Surface , α (mm ⁻¹)			Spacing Factor, \bar{L} (μm)		
R ² = 0.95			R ² = 0.95		
Standard Error = 0.7403			Standard Error = 3.258		
T-Test Probabilities					
	a	b	c	d	e
α	0	0	0	0.07737	0
\bar{L}	0	0	0.00681	0.0008	0.00001

5.2 Remediation B: Retempering

Retempering the three trial mixtures after hauling time yielded acceptable flow characteristics, but typically the air content could not be maintained at $6 \pm 1\%$. The procedures set did not account for increasing air content with hauling time; therefore, the AEA admixture dosages optimized in Phase I had to be utilized to follow true retempering methodology. The slump flow was able to be retempered by adding supplementary doses of HRWR and VMA, but the air content could not be reduced by the simple addition of more admixtures. In the field, courses of action that eliminate air

voids would be to add a defoaming agent or apply mechanical consolidation, such as vibration. However, both of these options are risky in that they would: 1) potentially destroy the air void system necessary for freeze-thaw durability, 2) negate the benefits of SCC, namely, the obsolescence of manual consolidation, and 3) increase the production cost of the concrete. It would be more effective to reduce the AEA dosage initially than try to retemper if the air content was known to increase to an unacceptable level with hauling time. However, for the purposes of comparison, the AEA dosages optimized in Chapter 3 were utilized in this portion of the study.

5.2.1 Mixture Proportioning and Fresh Properties

Retempering procedures began with the mixture proportions optimized in Phase I for B-SF22, B-SF25 and B-SF28, as seen in Table 3.1. The mixing sequence was followed with the mixer operating at mixing speed, 14.5 rpm, until 10 minutes after initial water and cement contact. At this point, the mixer was run at a lower agitating speed, 7.25 rpm, until the desired hauling time was met. At the specified hauling time, the mixer speed was increased to 14.5 rpm, and the supplementary admixtures were incorporated. The mixer was run for 2 minutes at mixing speed, followed by a 30 second resting period, and concluded with 30 seconds of mixing. At this juncture, the SCC mixture was tested for its fresh “retempered” properties. The fresh properties of the retempered mixtures can be seen in Tables 5.12, 5.13 and 5.14 for the target slump flows of 559, 635 and 711 mm, respectively. The intervals between hauling times were 20 minutes, as opposed to the 10 minute intervals for remediation A, because the admixture dosages needed for retempering were too diminutive for practical application at smaller time intervals.

Table 5.12 B-SF22 Remediation B fresh properties

Hauling Time (min.)	SF (mm)	J-Ring (mm)	SF - J-Ring (mm)	T₅₀ (sec.)	VSI	Air Content (%)
10	572	521	50	2.00	0	6.0
20	565	533	32	2.19	0	6.5
40	561	514	47	2.56	0	7.0
60	546	483	64	2.04	0	8.3
80	552	475	77	2.48	0	9.5

Table 5.13 B-SF25 Remediation B fresh properties

Hauling Time (min.)	SF (mm)	J-Ring (mm)	SF - J-Ring (mm)	T₅₀ (sec.)	VSI	Air Content (%)
10	645	610	36	1.99	0	6.3
20	641	625	17	2.54	0	6.8
40	648	616	32	1.53	0	7.3
60	660	629	32	1.44	0	7.8
80	648	616	32	1.59	0	8.3

Table 5.14 B-SF28 Remediation B fresh properties

Hauling Time (min.)	SF (mm)	J-Ring (mm)	SF - J-Ring (mm)	T₅₀ (sec.)	VSI	Air Content (%)
10	724	699	25	2.04	1	6.0
20	711	699	13	1.71	0	6.3
40	718	667	50	1.22	1	6.5
60	730	699	32	1.64	1	6.8
80	724	686	38	2.25	0	7.0

The fresh flow properties of the three mixtures were not consistent following retempering. When mixture B-SF22 was retempered, it exhibited adequate viscosity to maintain T₅₀ flow ability times within the 2 to 5 second standard, as seen in Table 5.12. However, the J-Ring passing abilities of the retempered mixtures at 60 and 80 minutes of

hauling time were not sufficient, as indicated by the difference between the slump flow and J-Ring greater than 50 mm. When the 635 and 711 mm slump flow mixtures were retempered, the passing abilities obtained were adequate, but the flow of the mixtures was typically not viscous enough to attain a T_{50} time between 2 and 5 seconds. The HRWR increased the flow of the mixtures, but decreased the viscosity and, at 40 and 60 minutes, caused slight bleeding on the surface of the SCC.

The chief shortfall of the retempered mixtures was that the air content exceeded the target of $6 \pm 1\%$ for 6 out of the 12 hauling times, as seen in Figure 5.6. The trend of increasing air content with hauling time of the retempered mixtures closely follows that of the non-remediated mixtures. However, retempering did decrease the total air content by an average of 0.1%, 0.2% and 1.0% for the 559, 635 and 711 mm slump flows,

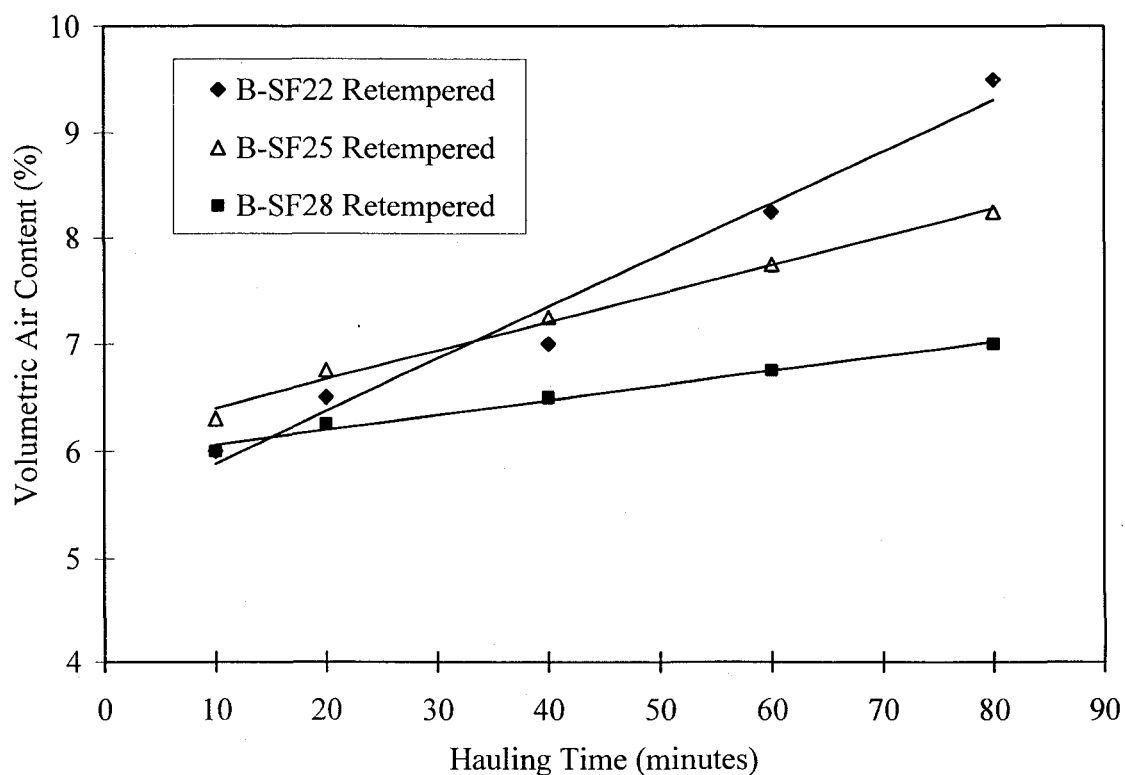


Figure 5.6 Remediation B volumetric air content

respectively, when compared to the non-remediated mixtures at the same hauling time. Retempering caused increased fluidity of the concrete and increasing competition between the admixtures, which decreased the total air content by destabilizing the air voids. A greater retempering dosage of admixtures typically caused a greater reduction in air content. However, the reduction was typically not substantial enough to bring the air content to the acceptable range of $6 \pm 1\%$. The air content of all retempered mixtures increased linearly with respect to hauling time, as seen in Figure 5.6 and Table 5.15. The retempered mixture B-SF28 retained an air content less than or equal to 7% throughout hauling time, whereas the air content of mixtures B-SF22 and B-SF25 increased to 9.5% and 8.3%, respectively. Tabulated values of the calculated air content based on the equations in Table 5.15 can be seen in Appendix B.

Table 5.15 Remediation B predictive equations of air content

Mixture	Equation	R ²
B-SF22	<i>Air Content</i> = $0.0489 t_h + 5.395$	0.98
B-SF25	<i>Air Content</i> = $0.0270 t_h + 6.128$	0.99
B-SF28	<i>Air Content</i> = $0.0137 t_h + 5.924$	0.99

where: t_h = hauling time, $10 \leq t_h \leq 90$ minutes

5.2.2 Admixture Dosages

The initial admixture dosages and supplementary retempering dosages can be seen in Tables 5.16, 5.17 and 5.18 for mixtures with a 559, 635 and 711 mm slump flow, respectively. In Tables 5.16, 5.17 and 5.18, a “+” indicates the dosage added at the specified hauling time, which can be seen graphically in Figure 5.7. Only mixture B-SF28 necessitated the addition of VMA to enhance its stability and viscosity. Mixtures B-SF22 and B-SF25 experienced a similar slump loss (approximately 207 mm) during 80

Table 5.16 B-SF22 retempered admixture dosages

Hauling Time (min.)	ml/kg cementitious materials			% Paste	% Mortar
	HRWR	VMA	AEA		
10	1.50	0	0.33	37.47	65.33
20	+ 0.13	0	0	37.67	65.44
40	+ 0.20	0	0	37.77	65.49
60	+ 0.33	0	0	37.97	65.60
80	+ 0.52	0	0	38.27	65.77

Table 5.17 B-SF25 retempered admixture dosages

Hauling Time (min.)	ml/kg cementitious materials			% Paste	% Mortar
	HRWR	VMA	AEA		
10	2.02	0.26	0.72	39.24	66.31
20	+ 0.13	0	0	39.43	66.41
40	+ 0.20	0	0	39.52	66.47
60	+ 0.33	0	0	39.71	66.57
80	+ 0.46	0	0	39.90	66.67

Table 5.18 B-SF28 retempered admixture dosages

Hauling Time (min.)	ml/kg cementitious materials			% Paste	% Mortar
	HRWR	VMA	AEA		
10	2.54	0.33	0.78	40.18	66.83
20	+ 0.07	0	0	40.27	66.88
40	+ 0.26	+ 0.07	0	40.64	67.08
60	+ 0.33	+ 0.07	0	40.73	67.13
80	+ 0.46	+ 0.13	0	41.00	67.29

minutes of hauling. However, mixture B-SF25 had a higher initial HRWR dosage, and therefore necessitated a smaller dosage at 80 minutes. Mixture B-SF28 experienced a slower rate of slump loss than mixtures B-SF22 and B-SF25. The HRWR retempering dosage needed to achieve the 711 mm slump flow was initially less than the other two slump flows because of the lower rate of slump loss, but increased with hauling time because VMA was added to maintain the required stability.

The volumetric quantity of HRWR needed for retempering is proportional to slump loss, as seen in Figure 5.8. However, the coefficient of determination of the linear regression is only 0.835, indicating a higher variability of data through retempering than through overdosing. The correlation between slump loss and the amount of HRWR needed for retempering is not as close as that between slump loss and HRWR needed for overdosing, as seen in Figure 5.2.

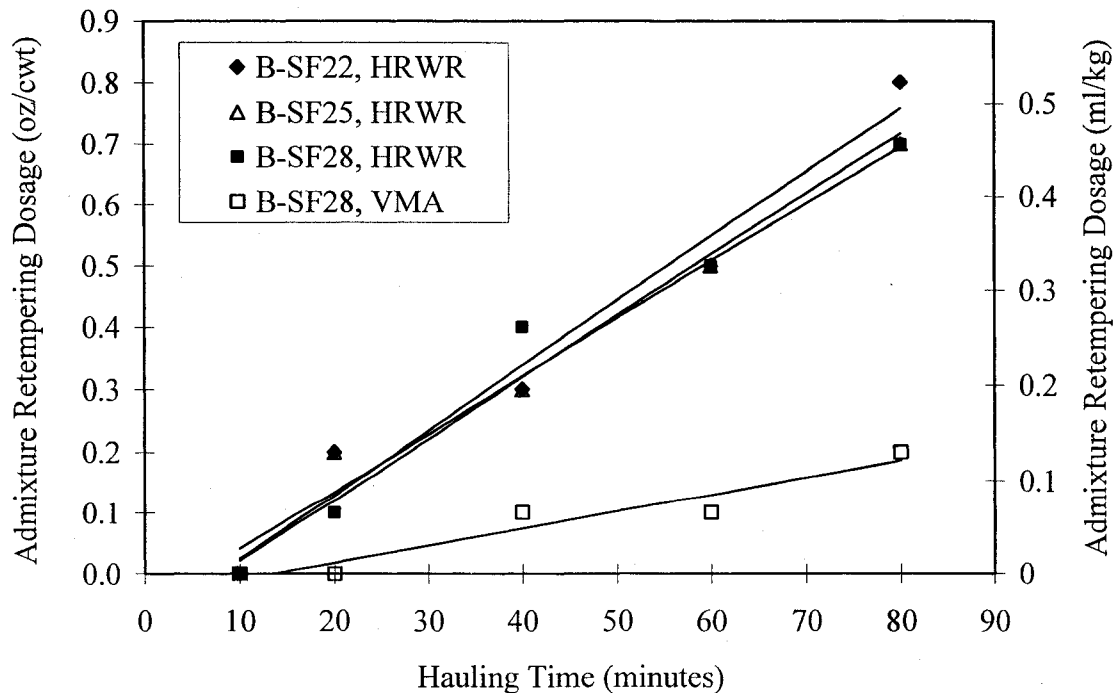


Figure 5.7 Remediation B admixture dosages

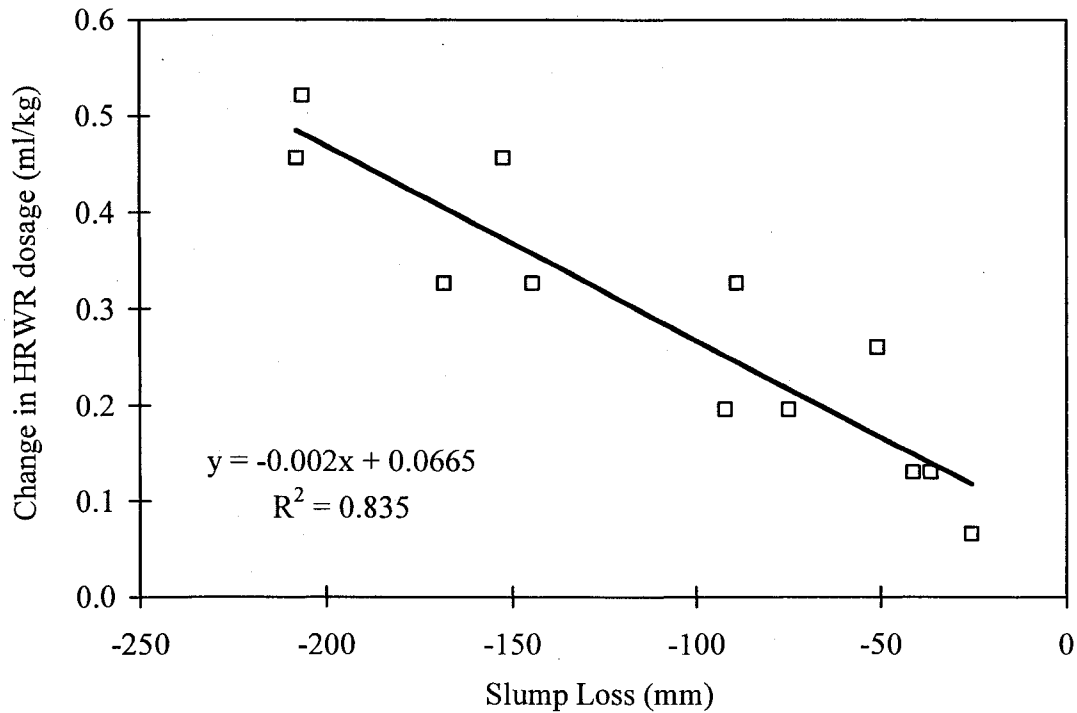


Figure 5.8 Remediation B: change in HRWR dosage vs. slump loss of all mixtures

5.2.3 Air Void Characteristics

The air void characteristics of the three retempered SCC mixtures exhibited a trend similar to that produced by overdosing, as seen in Figure 5.9. Hauling time has been shown to increase the air content and improve the air void characteristics of the SCC mixtures, while retempering with a HRWR has been shown to destabilize the air voids (Khayat and Assaad, 2002). Additional HRWR has the potential to disrupt the air voids because: 1) the increased fluidity of the concrete allows for more coalescence and rupturing of air voids, and 2) the increased adsorption of the HRWR on cement particles can dislocate the AEA particles and air voids already adsorbed.

The air void characteristics of the retempered mixtures were typically improved from the initial mixtures ($t_h = 10$ minutes), as seen in Table 5.19. From the initial 10

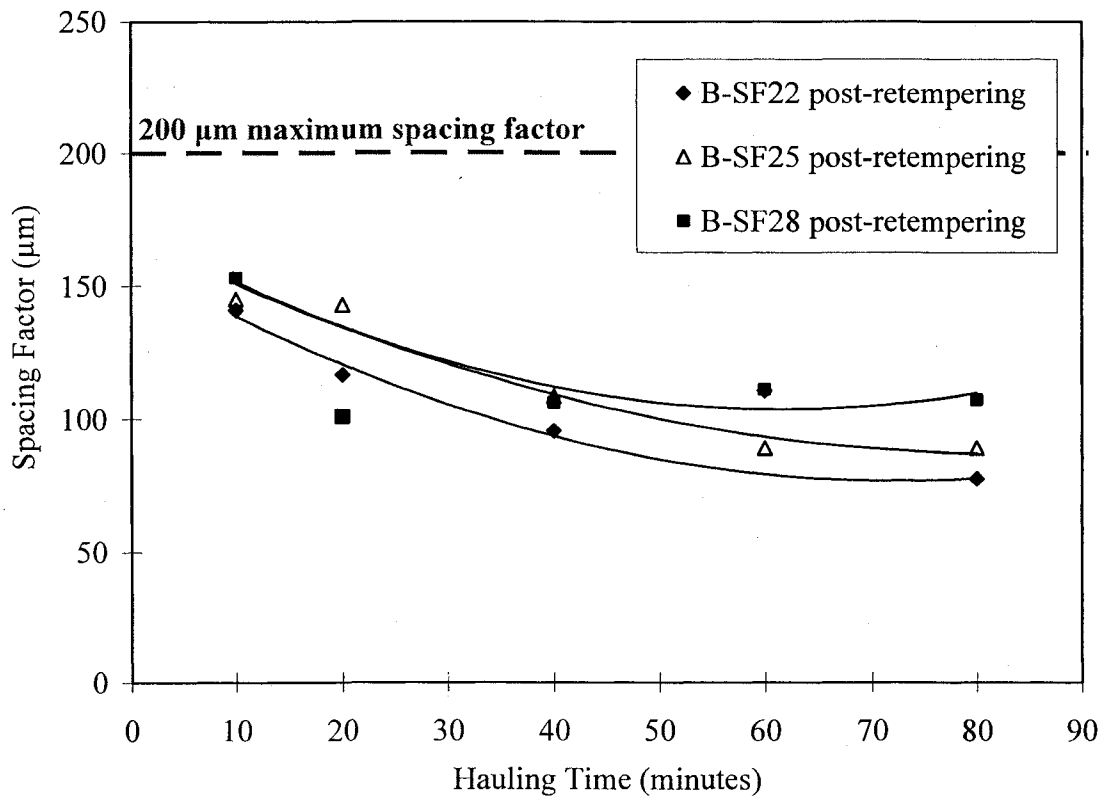
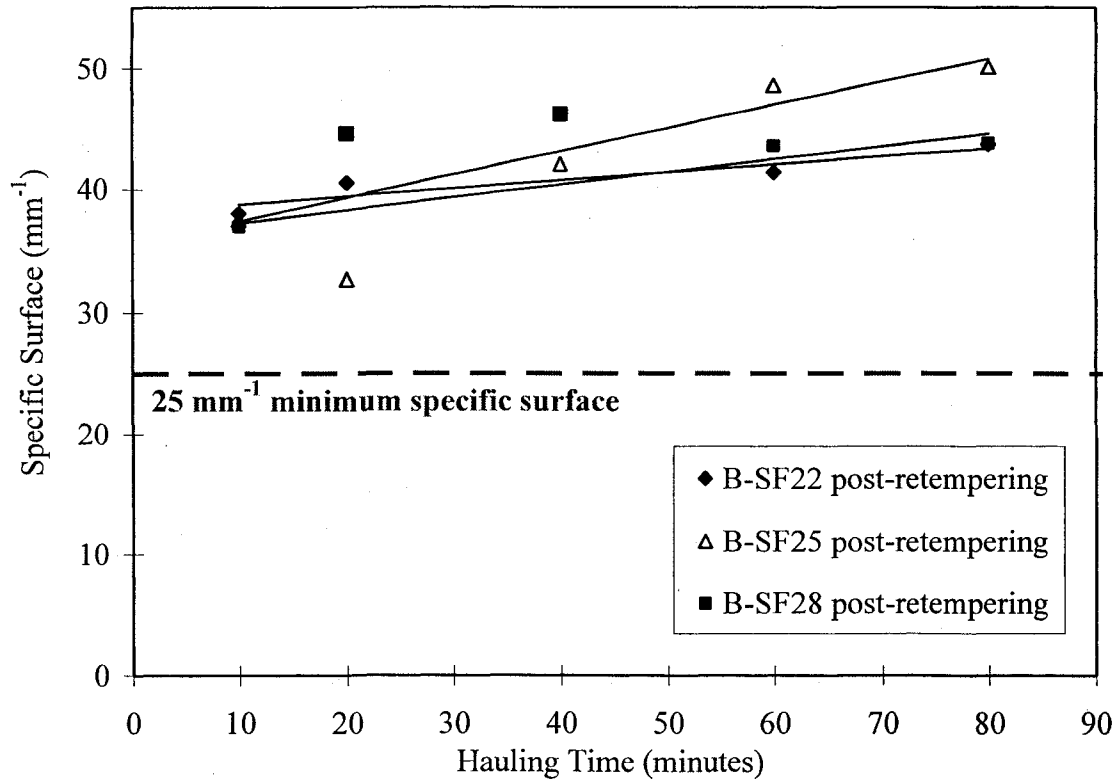


Figure 5.9 Remediation B air void characteristics

minute hauling time, the specific surface, α , increased an average of 6.1 mm^{-1} , and the spacing factor, \bar{L} , decreased an average of $41.8 \text{ }\mu\text{m}$. The air content measured by the AVA indicated an average increase of 2.9% from the initial time. There was one case of deterioration of the air void characteristics with retempering, the specific surface of mixture B-SF25 at 20 minutes, as shown in Table 5.19. The one instance of decreasing specific surface can be considered an anomaly specific to the particular batch, and would most likely improve if more tests were conducted. Additionally, the flow characteristics of the batches were not retempered to match one another exactly. The slight differences in slump flow, which varied up to 20 mm, contribute to the variation in air void characteristics. Overall, the effects of slump loss and hauling time, which improve the air void characteristics, dominated over the destabilizing effects of retempering on the air void system of SCC.

Table 5.19 Remediation B: Change in air void characteristics from $t_h = 10 \text{ min}$.

t_h (min.)	559 mm (22 in.)			635 mm (25 in.)			711 mm (28 in.)		
	α (mm^{-1})	\bar{L} (μm)	Air % <2mm	α (mm^{-1})	\bar{L} (μm)	Air % <2mm	α (mm^{-1})	\bar{L} (μm)	Air % <2mm
20	2.5	-24.5	2.0	-4.9	-2.0	1.5	7.7	-52.0	3.1
40	8.2	-45.5	2.4	4.5	-36.5	2.1	9.2	-47.0	3.6
60	3.4	-30.5	2.7	11.1	-56.0	2.4	6.7	-42.0	2.6
80	5.7	-63.5	6.0	12.6	-55.8	4.1	6.9	-45.8	2.0
AVG	5.0	-41.0	3.3	5.8	-37.6	2.5	7.6	-46.7	2.8

Note: $+\alpha$ / $-\bar{L}$ = improvement. $-\alpha$ / $+\bar{L}$ = deterioration

In comparing the effects of hauling and retempering against the benchmark of the initial mixing time, the air void characteristics generally improved. However, when the air void characteristics at each hauling time are compared against the benchmark of the

non-remediated mixtures, retempering typically causes a marked deterioration. The specific surface and spacing factor of all slump flows depreciated from their respective hauling times by an average of 1.43 mm^{-1} and $5.8 \text{ }\mu\text{m}$, respectively, as seen in Table 5.20.

Plante, Pigeon and Saucier developed a stability index in 1989 to quantify the acceptability of a change in air void spacing factor due to hauling time or retempering.

The equation $\Delta\bar{L} = \bar{L}_{\max} - \bar{L}_{\min}$ quantifies the overall change in spacing factor, with a maximum acceptable stability index, $\Delta\bar{L}$, of 100. Throughout their investigation, Plante, Pigeon and Saucier (1989) typically measured deterioration of air void characteristics; therefore this index is not applicable in cases where the spacing factor decreases.

Due to the instability caused by retempering, the air void systems of mixtures B-SF22, B-SF25 and BSF28 had a stability indices, $\Delta\bar{L}$, of 6.5, 30.5 and 26.8 μm , respectively.

Although it is arbitrary, past research indicates that the increase of spacing factor greater than 100 μm implies an unstable air void system. Therefore, the magnitude of increase in air void spacing factors due to retempering can be considered acceptable. The slump flow played a significant role in the air void stability of SCC mixtures. The lowest slump

Table 5.20 Remediation B: Change in air void characteristics from respective hauling times

t_h (min.)	559 mm (22 in.)			635 mm (25 in.)			711 mm (28 in.)		
	α (mm^{-1})	\bar{L} (μm)	Air % <2mm	α (mm^{-1})	\bar{L} (μm)	Air % <2mm	α (mm^{-1})	\bar{L} (μm)	Air % <2mm
20	0.4	-12.0	1.2	-9.1	30.5	0.1	2.5	-2.8	-0.4
40	3.6	-19.5	0.9	-3.3	4.5	0.4	0.4	14.0	-0.1
60	-3.4	6.5	0.6	2.1	-2.2	-0.5	-4.5	24.4	-1.4
80	-0.9	-6.0	1.0	3.1	5.2	-0.2	-4.2	26.8	-2.2
AVG	-0.1	-7.8	1.0	-1.8	9.5	-0.1	-1.4	15.6	-1.0

Note: $+\alpha$ / $-\bar{L}$ = improvement. $-\alpha$ / $+\bar{L}$ = deterioration

flow of 559 mm was more resistant to retempering, and thus produced a more stable air void system than the higher slump flows of 635 and 711 mm.

Predictive equations of the air void characteristics were developed at a 95% confidence interval, shown in Equations 5.3 and 5.4. Due to the scatter of the data collected for retempering, outliers were excluded from the regression analysis to obtain a better statistical correlation. The statistical data for the predictive equations of the specific surface and spacing factor for the three slump flows can be seen in Table 5.21. In general, the retempering trend lines of the air void characteristics did not fit the data as well as the overdosing trend lines, as evidenced by the average R^2 value of 0.91. The accuracy of the equations may have been compromised because less data was gathered for retempering. The calculated values for air void specific surfaces and spacing factors using Eq. 5.3 and 5.4 are tabulated in Appendix B.

$$\alpha_B = -173.003 + \frac{266475.2}{SF} - \frac{8.4 \times 10^7}{SF^2} + 0.13133t_h \quad \text{Eq. 5.3}$$

$$\bar{L}_B = 250.8 - \frac{53083.2}{SF} - 2.158t_h + 0.0151t_h^2 \quad \text{Eq. 5.4}$$

where: t_h = hauling time, $10 \leq t_h \leq 80$ minutes

SF = actual slump flow, $559 \leq SF \leq 711 \pm 25$ mm

5.3 Comparison of Remediation Techniques

Both remediation techniques produce similar flow properties, but utilize different admixture dosages and generate different air contents and air void characteristics. In producing SCC for a certain field application, there are advantages of using one remediation procedure over the other. Construction management issues are one factor:

Table 5.21 Statistical data of predictive equations for remediation B air void characteristics

Specific Surface , α (mm ⁻¹)		Spacing Factor, \bar{L} (μm)		
R ² = 0.86		R ² = 0.96		
Standard Error = 1.937		Standard Error = 6.916		
T-Test Probabilities				
	a	b	c	d
α	0.0515	0.02387	0.02304	0.00047
\bar{L}	0	0.00197	0.00014	0.00281

overdosing does not require trained and qualified personnel on the job site to assess the flow ability of the concrete like retempering does. Additionally, with overdosing, a concrete batch plant can guarantee their product and increase quality control if it is not altered after it leaves the plant. In contrast, there is increased flexibility with retempering. The hauling time for a ready-mixed concrete truck is often unpredictable, which affects the flow properties. Thus, a designated person on the job site can add the appropriate amount of admixture to retemper the concrete. The ability to retemper a mixture to achieve the desired flow potentially reduces the amount of concrete wasted.

5.3.1 Admixture Dosages

The volumetric quantity of admixtures incorporated into a mixture is important in determining the economic preference of one form of remediation over another. A comparison of the total admixture dosages (HRWR + VMA + AEA) can be seen in Figure 5.10. Likewise, these values are tabulated in Tables 5.22, 5.23 and 5.24. For short hauling times of 20 minutes, the two forms of remediation utilize equivalent admixture dosages for all slump flows. However, at 40 minutes of hauling time, with remediation B, both mixtures B-SF22 and B-SF25 use 0.1 and 0.2 ml/kg less admixtures,

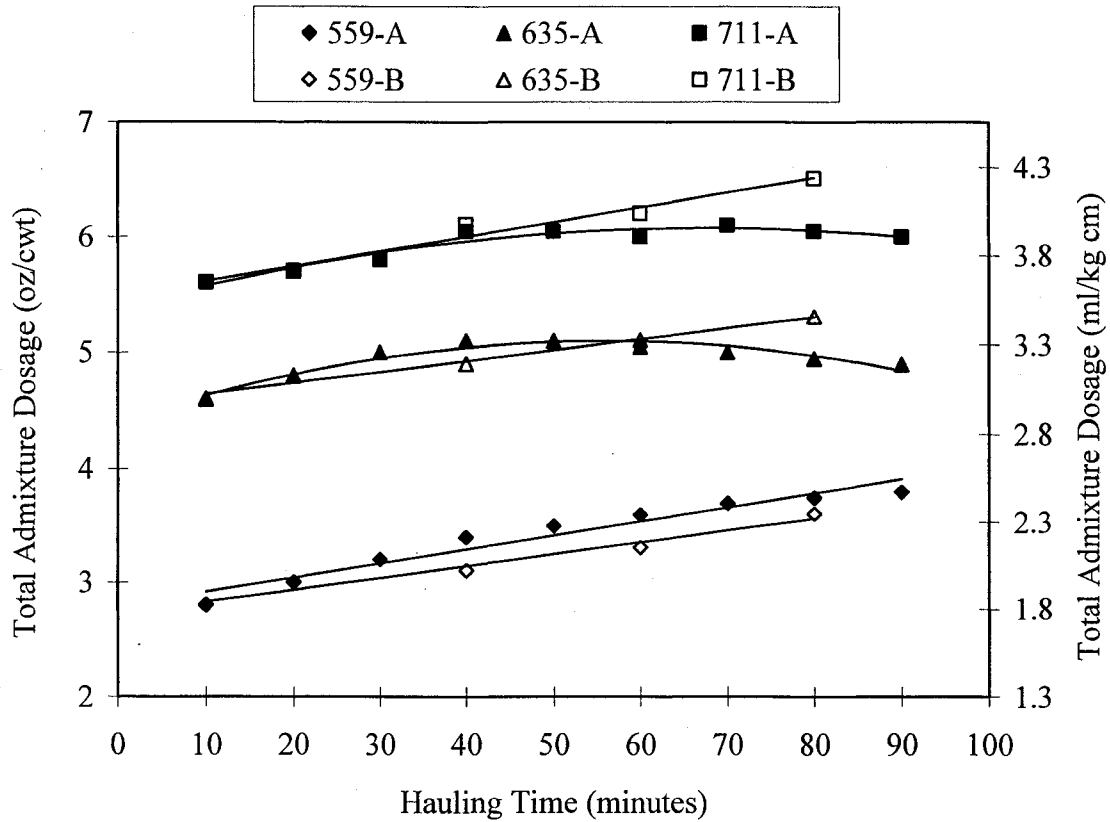


Figure 5.10 Comparison of total admixture dosages of remediation techniques A and B

Table 5.22 559 mm slump flow remediation dosage comparison (ml/kg cm)

Hauling Time (min.)	HRWR		AEA		VMA		TOTAL	
	A	B	A	B	A	B	A	B
10	1.50	1.50	0.33	0.33	0	0	1.83	1.83
20	1.63	1.63	0.33	0.33	0	0	1.96	1.96
30	1.76	-	0.33	-	0	-	2.09	-
40	1.89	1.70	0.33	0.33	0	0	2.22	2.02
50	1.96	-	0.33	-	0	-	2.28	-
60	2.02	1.83	0.33	0.33	0	0	2.35	2.15
70	2.09	-	0.33	-	0	-	2.41	-
80	2.12	2.02	0.33	0.33	0	0	2.44	2.35
90	2.15	-	0.33	-	0	-	2.48	-

Table 5.23 635 mm slump flow remediation dosage comparison (ml/kg cm)

Hauling Time (min.)	HRWR		AEA		VMA		TOTAL	
	A	B	A	B	A	B	A	B
10	2.02	2.02	0.72	0.72	0.26	0.26	3.00	3.00
20	2.15	2.15	0.72	0.72	0.26	0.26	3.13	3.13
30	2.28	-	0.72	-	0.26	-	3.26	-
40	2.35	2.22	0.72	0.72	0.26	0.26	3.33	3.19
50	2.41	-	0.65	-	0.26	-	3.33	-
60	2.44	2.35	0.59	0.72	0.26	0.26	3.29	3.33
70	2.48	-	0.52	-	0.26	-	3.26	-
80	2.51	2.48	0.46	0.72	0.26	0.26	3.23	3.46
90	2.54	-	0.39	-	0.26	-	3.19	-

Table 5.24 711 mm slump flow remediation dosage comparison (ml/kg cm)

Hauling Time (min.)	HRWR		AEA		VMA		TOTAL	
	A	B	A	B	A	B	A	B
10	2.54	2.54	0.78	0.78	0.33	0.33	3.65	3.65
20	2.61	2.61	0.78	0.78	0.33	0.33	3.72	3.72
30	2.67	-	0.78	-	0.33	-	3.78	-
40	2.77	2.80	0.78	0.78	0.39	0.39	3.94	3.98
50	2.84	-	0.72	-	0.39	-	3.94	-
60	2.87	2.87	0.65	0.78	0.39	0.39	3.91	4.04
70	2.93	-	0.59	-	0.46	-	3.98	-
80	2.97	3.00	0.52	0.78	0.46	0.46	3.94	4.24
90	3.00	-	0.46	-	0.46	-	3.91	-

respectively. To achieve a 559 mm slump flow, remediation B was always more economical than remediation A after 20 minutes of hauling. In contrast, to achieve a 711 mm slump flow, remediation A was always more economical after 20 minutes of hauling. The economy of mixture B-SF25 depended on the length of hauling time: after 60 minutes, remediation A became the method that used a smaller admixture dosage overall.

Remediation A developed into the more economical method with hauling time because of the decrease in AEA dosage after 40 minutes (for 635 and 711 mm slump flows). The AEA could have been under-dosed initially for the retempered mixtures to meet the target air content; however, this method would not necessarily be more economical than remediation A. For example, for the retempered mixture B-SF28, the air content at 80 minutes was 7.0%, which meets the $6 \pm 1\%$ target. It is difficult to hypothesize whether or not the AEA dosage could have been significantly decreased initially and still endure the detrimental effects of retempering on the air void system and air content. Since the fluidity of the SCC affects the ability of the AEA to secure an air void system, perhaps mixtures with a high slump flow (711 mm) require a higher initial dosage to withstand retempering.

Predictive equations at a 95% confidence level were developed for the HRWR dosages of each remediation technique, as seen in Equations 5.5 and 5.6 for remediation A and B, respectively. The coefficients of determination, standards of error and F-test probabilities can be seen in Table 5.25.

$$HRWR_A = -1.7335 + 0.0067t_h + 0.00591SF \quad \text{Eq. 5.5}$$

$$HRWR_B = -2.3196 + 0.0065t_h + 0.00676SF \quad \text{Eq. 5.6}$$

where: $HRWR_x$ = HRWR dosage (ml/kg cementitious materials)

t_h = hauling time, $10 \leq t_h \leq 90$ minutes (Eq. 5.5), $10 \leq t_h \leq 80$ minutes (Eq. 5.6)

SF = target slump flow, $559 \leq SF \leq 711 \pm 25$ mm

The accuracy of these equations was tested by comparing the actual dosages used for remediation versus the calculated HRWR dosages, as seen in Tables 5.26, 5.27 and

5.28 for 559, 635 and 711 mm slump flows, respectively. The equations produced an error an average of 0.7% higher in remediation A than remediation B. Additionally, the errors decreased with increasing target slump flow by 2.1% and 1.1% for remediation A and B, respectively, from 559 to 711 mm slump flows.

Table 5.25 Statistical data for predictive equations of HRWR remediation dosages

Remediation	R ²	Standard Error	Prob(F)
A: Eq. 5.5	0.985	0.054	0
B: Eq. 5.6	0.996	0.054	0

Table 5.26 559 mm slump flow - calculated versus actual HRWR remediation dosages

Hauling Time (min.)	Remediation A (ml/kg cm)			Remediation B (ml/kg cm)		
	Actual	Calculated	% Error	Actual	Calculated	% Error
10	1.50	1.64	-9.0	1.50	1.53	-1.8
20	1.63	1.70	-4.4	1.63	1.59	2.4
30	1.76	1.77	-0.5	-	-	-
40	1.89	1.84	2.9	1.70	1.72	-1.5
50	1.96	1.90	2.7	-	-	-
60	2.02	1.97	2.5	1.83	1.85	-1.4
70	2.09	2.04	2.4	-	-	-
80	2.12	2.10	0.7	2.02	1.98	2.0
90	2.15	2.17	-0.9	-	-	-
Average			2.9			1.8

Table 5.27 635 mm slump flow - calculated versus actual HRWR remediation dosages

Hauling Time (min.)	Remediation A (ml/kg cm)			Remediation B (ml/kg cm)		
	Actual	Calculated	% Error	Actual	Calculated	% Error
10	2.02	2.08	-3.1	2.02	2.04	-0.9
20	2.15	2.15	0.0	2.15	2.11	2.2
30	2.28	2.22	2.8	-	-	-
40	2.35	2.28	2.7	2.22	2.24	-0.8
50	2.41	2.35	2.5	-	-	-
60	2.44	2.42	1.1	2.35	2.37	-0.8
70	2.48	2.49	-0.3	-	-	-
80	2.51	2.55	-1.7	2.48	2.50	-0.7
90	2.54	2.62	-3.0	-	-	-
Average			1.9			1.1

Table 5.28 711 mm slump flow - calculated versus actual HRWR remediation dosages

Hauling Time (min.)	Remediation A (ml/kg cm)			Remediation B (ml/kg cm)		
	Actual	Calculated	% Error	Actual	Calculated	% Error
10	2.54	2.53	0.4	2.54	2.55	-0.4
20	2.61	2.60	0.3	2.61	2.62	-0.4
30	2.67	2.67	0.2	-	-	-
40	2.77	2.73	1.3	2.80	2.75	1.9
50	2.84	2.80	1.2	-	-	-
60	2.87	2.87	0.0	2.87	2.88	-0.4
70	2.93	2.93	0.0	-	-	-
80	2.97	3.00	-1.2	3.00	3.01	-0.3
90	3.00	3.07	-2.3	-	-	-
Average			0.8			0.7

5.3.2 Air Content

The total air content of the two remediation techniques with respect to hauling time are compared in Figure 5.11. Remediation A mitigates the increase in air content by decreasing the AEA dosage after 40 minutes for the 635 and 711 mm slump flows.

Therefore, the mixtures remained at the target air content of $6 \pm 1\%$. However, the air

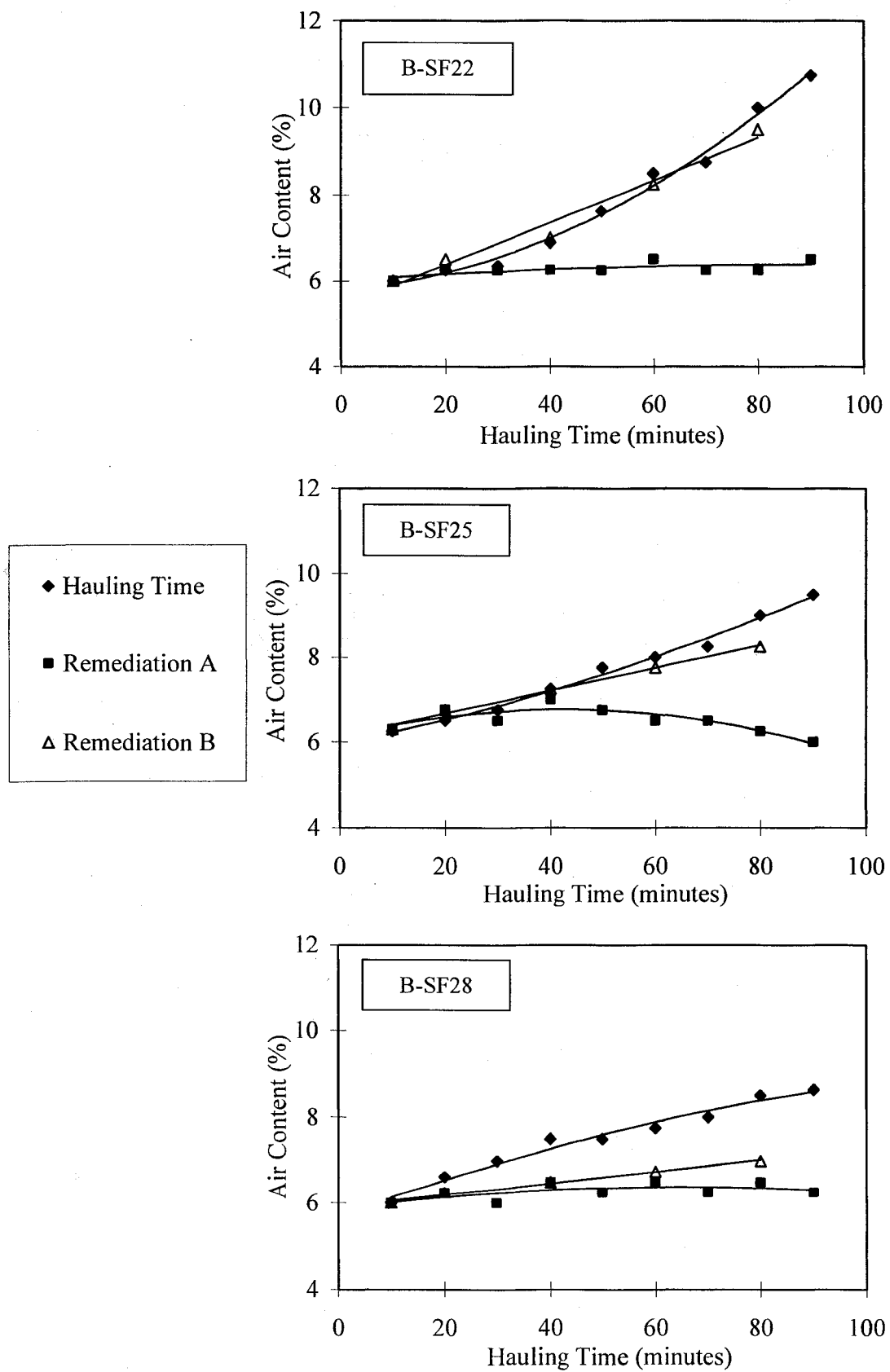


Figure 5.11 Air content comparison of remediation techniques

could not be eliminated by retempering the concrete, and thus the air content in remediation B typically mimicked the increase that occurred during hauling. The average decrease in volumetric air content due to retempering with HRWR and VMA to achieve the target flow properties was 1.5%, compared to the non-remediated mixtures at the same hauling time. The fluidity of the concrete and admixture dosages affected the air content in that increasing slump flow and increasing HRWR through retempering decreased the quantity of air entrained.

5.3.3 Air Void Characteristics

Irrespective of slump flow or remediation method, the average spacing factors improved from the initial characteristics measured at 10 minutes, as seen in Table 5.29. With the exception of the 559 mm slump flow in remediation A, the average specific surfaces also improved from the initial characteristics. The improvement in overall air void characteristics with hauling time can be attributed to the factors outlined in Chapter 4, such as slump loss and the type of AEA utilized. The increase in air content, coupled with the division and dispersion of the air voids with hauling time exceeded the

Table 5.29 Change in air void characteristics from initial mixing time ($t_h = 10$ min.) to average of all hauling times

Remediation Technique	Slump Flow (mm)	α (mm ⁻¹)	\bar{L} (μm)	Air % < 2 mm
A	559	-1.9	-10.9	2.1
	635	2.5	-18.3	2.4
	711	4.0	-23.7	1.8
B	559	5.0	-42.4	3.3
	635	5.8	-37.6	2.5
	711	7.6	-46.7	2.8
Average A		1.5	-17.6	2.1
Average B		6.1	-42.2	2.9

destabilizing affects of remediation. Thus, the air void characteristics and air content typically increased with hauling time, regardless of remediation method.

Remediation B produced a better overall air void system than remediation A throughout hauling time. The lower dosage of AEA utilized in remediation A (for 635 and 711 mm slump flows after 40 minutes) was not able to produce as many air voids as the AEA dosages incorporated with remediation B. Also, the initial slump flows of the overdosed mixtures (remediation A) were highly fluid and caused more bubble coalescence than the lower initial slump flows used in retempering. Therefore, the lower slump flows could entrain more air with hauling time, causing the air void characteristics of the retempered mixtures to more closely resemble those of the non-remediated mixtures.

The air void characteristics of the non-remediated mixtures were also compared with and found superior to those of the remediated mixtures at their respective hauling times, as seen in Table 5.30. Remediation A caused the average specific surface to decrease by 5.5 mm^{-1} and the average spacing factor to increase by $28.3 \text{ }\mu\text{m}$. With remediation B, the average specific surface decreased by 1.1 mm^{-1} and the average

Table 5.30 Change in air void characteristics from respective hauling times

Remediation Technique	Slump Flow (mm)	$\alpha \text{ (mm}^{-1}\text{)}$	$\bar{L} \text{ (}\mu\text{m)}$	Air % < 2 mm
A	559	-7.0	25.5	-0.6
	635	-5.0	28.8	-1.4
	711	-4.4	30.7	-2.2
B	559	-0.1	-9.1	1.0
	635	-1.8	9.5	-0.1
	711	-1.4	15.6	-1.0
Average A		-5.5	28.3	-1.4
Average B		-1.1	5.3	0.0

spacing factor increased by 5.3 μm . The two main factors that contributed to inferior air void stability of remediation A were: 1) decreased AEA dosage, and 2) higher initial slump flow. The decreased AEA was unable to produce and stabilize as many bubbles as a higher dosage, and the higher initial slump flow increased the occurrence of bubble coalescence, causing the size of the air voids in the fresh matrix to increase.

The air void characteristics of the two forms of remediation are further compared in Figure 5.12, which shows the predictive equations of overdosing (A) and retempering (B) at each slump flow. The specific surfaces and spacing factors of remediation A follow the same trend as the non-remediated mixtures with respect to slump flow: the 711 mm mixture produced the best air void system, followed by the 635 and 559 mm mixture. However, remediation B does not exhibit the same trend, evidenced by the 635 mm mixture producing the best specific surface and the 559 mm mixture producing the best spacing factor. In fact, the spacing factors of remediation B exhibit the opposite trend as the non-remediated and overdosed mixtures. The inconsistent trend of remediation B may stem from the variability of data and lack of sufficient population. It is possible that with more retempering data, the air void system would follow a similar trend to that of the non-remediated mixtures.

5.4 Conclusions

Remediation of self-consolidating concrete mixtures is a complex process that requires extensive testing prior to application in order to yield satisfactory results. The effects of hauling most certainly vary according to the mixture proportioning and the types of admixtures used. A general rule of thumb for successful remediation of air-entrained SCC is to keep the paste-to-mortar ratio approximately the same as the initial

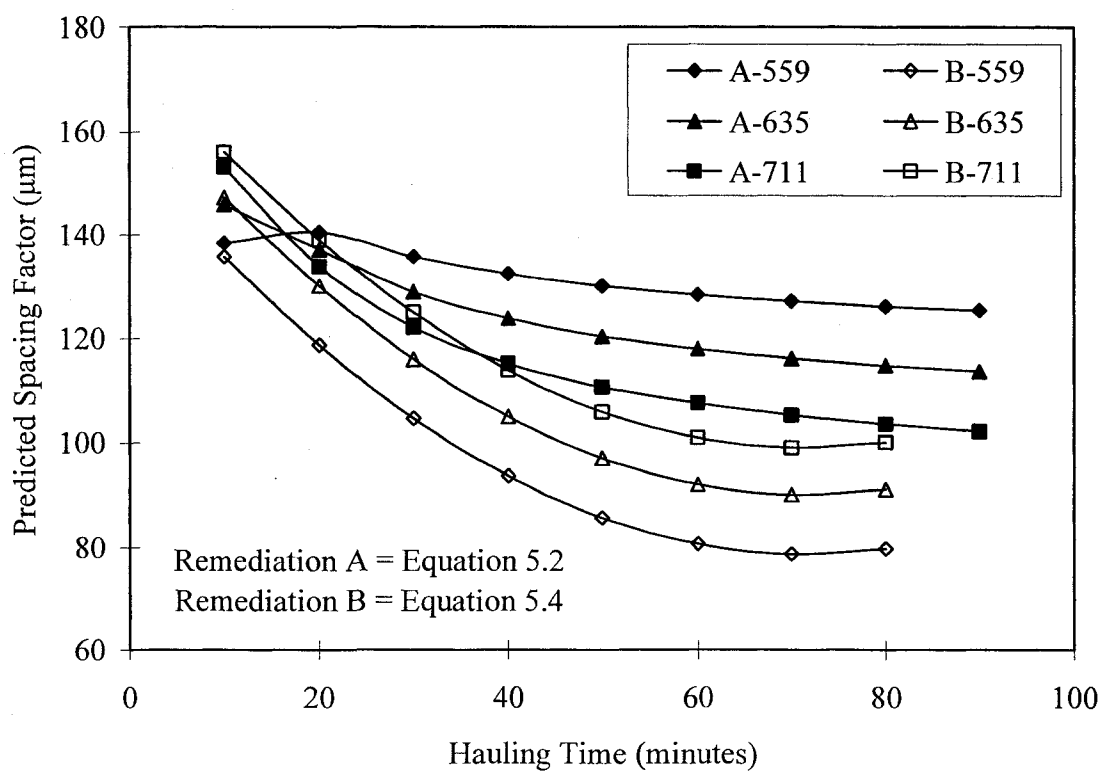
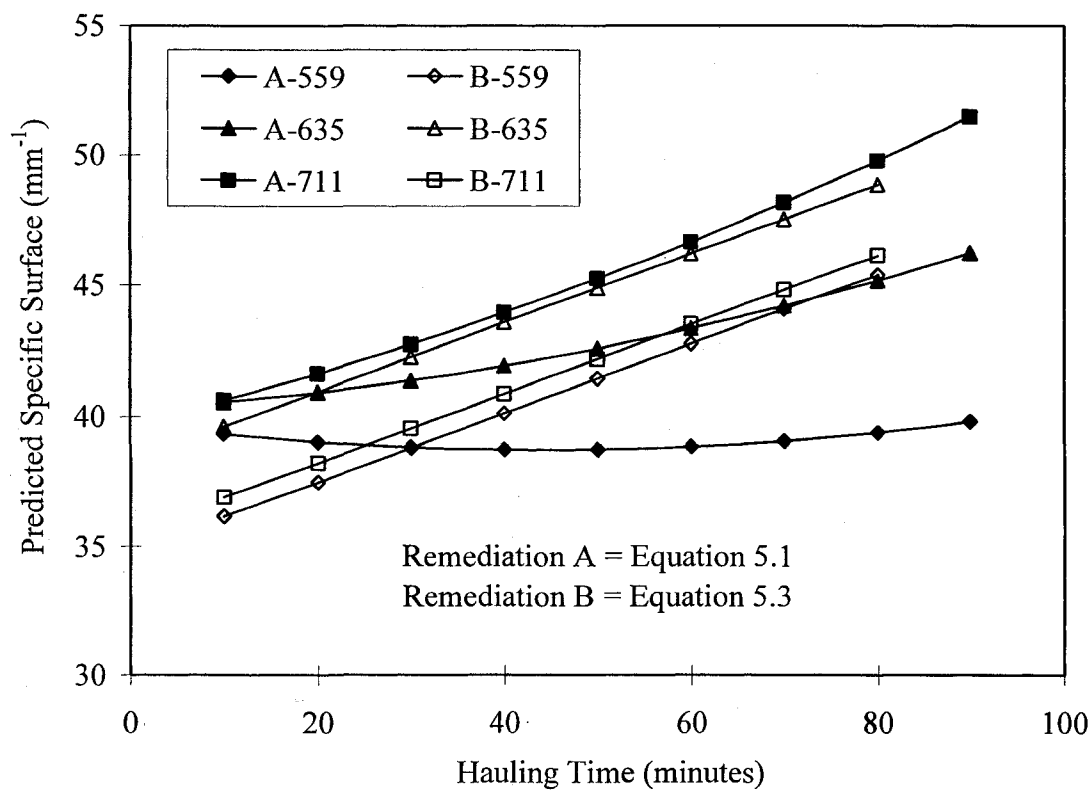


Figure 5.12 Comparison of remediation techniques: predictive equations of air void specific surface (top) and spacing factor (bottom)

mixture design by adjusting the admixture dosages up or down. However, the tendencies of a specific admixture must be tested to determine its performance during long hauling times and remediation.

In selecting the most economical form of remediation, the primary factors to consider are the slump flow and hauling time. In this study, for a low slump flow (~559 mm), retempering was typically be more economical. However, for a high slump flow (~711 m), overdosing was more economical. The preferred method for the mid-range slump flows (~635 mm) depends on the length of hauling time, as outlined in Table 5.31.

Table 5.31 Comparison of remediation techniques

Category		Form of Remediation	
		A: Overdosing	B: Retempering
Construction Management Issues		Better quality control	More flexibility, but need trained personnel on job site
Economy of Admixture Dosage	SF = 559 mm		✓
	SF = 635 mm	✓ (for $t_h \geq 60$ min)	✓ (for $t_h < 60$ min.)
	SF = 711 mm	✓	
Air Content		Better (more control of initial AEA dosage)	Preferred if air ↓ with hauling time
Air Void Characteristics	compared to $t_h = 10$ min.	α , \bar{L} improve	α , \bar{L} improve
	compared to respective t_h	α , \bar{L} degrade	α , \bar{L} degrade

The two forms of remediation utilized in this investigation, overdosing and retempering, were typically able to produce SCC mixtures that met the target fresh properties. Both forms of remediation necessitated an increased dosage of HRWR with increasing hauling time. The HRWR dosage could be predicted based on the hauling

time and target slump flow for both overdosing and retempering. A viscosity modifying admixture was added in both forms of remediation for only the 711 mm slump flow mixtures, which increased with increasing hauling time. The AEA was under-dosed after 40 minutes for remediation A because of the tendency of the air content to increase with hauling time; however, the AEA was held constant for retempering.

Due to the decreasing AEA dosage, remediation A produced SCC mixtures with the target air content, while remediation B typically produced mixtures with an elevated air content. For this reason, remediation A may be the desirable technique when the air content increases with hauling time, and remediation B may be preferred if a mixture experiences a decreasing air content with hauling time.

The air void characteristics behaved similarly regardless of remediation technique. The air void characteristics produced as a result of both forms of remediation surpassed the target specific surface of 25 mm^{-1} and spacing factor of $200 \text{ }\mu\text{m}$. Additionally, for both forms of remediation, the air void characteristics produced throughout hauling time surpassed those produced initially at 10 minutes. The air voids produced by retempering were superior to those produced by overdosing, compared to the initial air void characteristics produced at 10 minutes after initial cement and water contact. Moreover, when compared to the initial hauling time, the stability of the air voids increased with decreasing slump flow for both remediation techniques. At a specific hauling time, the air void system produced in remediated concrete was inferior to the air voids produced without remediation. The flow ability imparted by additional dosages of HRWR was the primary reason for the deteriorated air void characteristics of

the remediated mixtures. Retempering degraded the air void characteristics less than overdosing, compared to the change from respective hauling times.

In summary, as there are many variables that contribute to selecting one form of remediation over another, as outlined in Table 5.31. A detailed cost analysis, combined with the mixture specifications and job site limitations, would have to be conducted by the construction manager to determine the best method for remediation.

CHAPTER 6

CONCLUSIONS AND RECOMMENDATIONS

This investigation on self-consolidating concrete (SCC) consisted of two phases. The first phase aimed at determining the optimum admixture dosage requirements for three slump flows and four admixture manufacturers in order to establish the effects of slump flow and admixture source on the fresh properties and air void characteristics of SCC. The second phase studied the effects of eight different hauling times and two forms of remediation on the fresh properties and air void characteristics of SCC.

6.1 Effects of Admixture Source and Slump Flow on SCC

The results of this study indicated that the types of high range water reducer (HRWR) and air-entraining admixture (AEA) utilized in developing self-consolidating concrete play a significant role in the volumetric economy of the admixture dosages and the production of entrained air voids. Additionally, the slump flow was found to influence the stability, air void characteristics and compressive strength of SCC mixtures.

6.1.1 Effects of Admixture Source

6.1.1.1 High Range Water Reducing Admixture Source

The two types of high range water reducers (HRWRs) used in this study were a polycarboxylate-ester (PCE) from admixture source A, and polycarboxylate-acid (PCA) from admixture sources B, C and D. The two types of polycarboxylate HRWRs chemically vary in the number of anionic binding sites available and in the number side

chains on the molecule. The PCE molecule contains more side chains, creating greater slump retention, and the PCA molecule contains more anionic binding sites, allowing greater dispersion capability. In this study, mixtures utilizing PCE always necessitated the addition of a viscosity modifying admixture (VMA) to reduce bleeding and segregation. In contrast, mixtures utilizing PCA did not require the addition of VMA at the lowest slump flow of 559 mm to obtain a stable matrix. Another difference between the PCE and PCA HRWRs was the VMA-to-HRWR ratio. The mixtures incorporating the PCE HRWR had an increasing VMA-to-HRWR ratio with increasing slump flow. The mixtures incorporating the PCA HRWR had an optimum VMA-to-HRWR ratio that existed regardless of slump flow (as long as VMA was utilized).

The dosages of HRWR and VMA could be predicted based on the target slump flow, although among HRWRs with similar chemical compositions, the dosages were not necessarily the same. The mixtures utilizing a PCE HRWR necessitated a significantly higher dosage of HRWR than the mixtures utilizing a PCA HRWR. The HRWR and VMA indirectly influenced the air void characteristics. Irrespective of admixture types, the increase in HRWR and VMA dosages resulted in an increased required dosage of air-entraining admixture. While the target volumetric air content was maintained through proper alteration of the required air-entraining agent, with increased HRWR and VMA dosages, the slump flow increased, which typically deteriorated the air void characteristics.

6.1.1.2 Air-Entraining Admixture Source

The two main types of air-entraining admixtures (AEAs) utilized during this study were synthetic detergents (source A) and wood-derived acid salts (sources B, C and D).

The primary difference between these two types of AEAs is the mechanism of air-entrainment. The synthetic detergents reduce the surface tension of water to form and stabilize air bubbles primarily at the air-water interface. In contrast, the salt-type AEAs form precipitates that help stabilize the air voids at the air-cement-water interface. While the air void characteristics of both types of AEAs are affected by slump flow, the synthetic detergent types produce bubbles that are more influenced by slump flow in SCC mixtures. The air voids produced by the salt-types are all anchored to cement or fly ash particles, and therefore are more resistant to rupturing and coalescence caused by an increasing fluidity.

The smallest and most closely spaced air voids were produced by the synthetic detergent type AEA of source A. In order of decreasing air void characteristics, the other sources were ranked B, C and D. Among the salt-types, the AEA containing tall oil (source B) produced the best air void characteristics, followed by the saponified wood rosin/resin-acid combination (source C), and the natural wood rosin (source D).

6.1.2 Effects of Slump Flow

Three slump flows of 559, 635 and 711 mm (22, 25 and 28 inches) were tested during the first phase of the investigation. The HRWR, VMA and AEA dosages typically increased with increasing slump flow. There was also decreased mixture stability with increasing slump flow, evidenced by the increased dosage of VMA required and the Visual Stability Index (VSI) rating of 1 (stable) for high slump flows of 711 mm. The fluidity of the mixtures with the 711 mm slump flows caused increased segregation and bleeding, resulting in a change of matrix stability from highly stable to stable.

6.1.2.1 Air Void Characteristics

The air void characteristics deteriorated with increasing slump flow. The specific surface decreased an average of 3.2 mm^{-1} from the 559 to 711 mm slump flow. The spacing factor increased an average of $14.2 \text{ }\mu\text{m}$ from the 559 to 711 mm slump flow. The deterioration of the air void characteristics with respect to slump flow was attributed to: 1) competition with increased dosages of HRWR and VMA, and 2) increased fluidity of the paste. Increased slump flow is accompanied by increased dosages of HRWR and VMA. An increased dosage of HRWR competes with the AEA for adsorption on the cement and fly ash particles, and an increased dosage of VMA competes with the effectiveness of the AEA to entrain air by locking up water molecules, thus preventing them from aiding in the formation of air voids. Additionally, the increased dosages of HRWR and VMA may cause the wrong end of the AEA molecule (the hydrophobic end) to adhere to the admixture, rather than contribute to bubble formation. The increased fluidity of the mixtures caused the air void characteristics to deteriorate because of increased ability of the air voids to move about in the cement paste, causing bubble coalescence.

There was a significant difference between the synthetic detergent and wood-derived acid salt AEAs on the effect of slump flow on the air void characteristics. Source A, a synthetic detergent AEA, experienced a specific surface decrease of 8.6 mm^{-1} and a spacing factor increase of $33 \text{ }\mu\text{m}$ from the 559 to 711 mm slump flows. In contrast, the specific surfaces of the air voids produced by sources B, C and D decreased an average of 1.4 mm^{-1} and the spacing factors increased an average of $8 \text{ }\mu\text{m}$. The air voids produced by salt-type AEAs are anchored to cement or fly ash particles, thus preventing the paste

fluidity to cause bubble coalescence. The decreased stability with increasing slump flow of the air voids produced by synthetic detergent AEAs could adversely affect its suitability where air-entrained self-consolidating concrete with a high slump flow is required.

6.1.2.2 Compressive Strength

The average compressive strength of the trial self-consolidating concrete mixtures decreased with increasing slump flow. An increased slump flow was typically accompanied by an increased HRWR, VMA and AEA dosage. The increased quantity of admixtures, particularly air-entrainment, caused the compressive strength of the mixtures to decrease by approximately 2 MPa (300 psi) from the 559 to 711 mm slump flows.

6.2 Effects of Hauling Time on SCC

In this investigation, eight hauling times of 20, 30, 40, 50, 60, 70, 80 and 90 minutes were tested to determine the influence of continual agitation over time on the fresh properties and air void characteristics of self-consolidating concrete. During this phase of the investigation, only admixtures from source B were tested; thus, only a polycarboxylate-acid HRWR and wood-derived acid salt AEA containing tall oil were utilized.

6.2.1 Fresh Properties

The selected self-consolidating concretes experienced slump flow loss with hauling time. The slump flow losses increased with decreasing initial slump flow. The losses incurred over the 90 minute hauling time were 39%, 37% and 25% for the 559, 635 and 711 mm slump flows, respectively. The highest slump flow maintained its flow ability better than the other mixtures due to its higher dosage of HRWR, which allowed

for greater dispersion capability. The stability of all tested mixtures improved with increasing hauling time. The T_{50} rate of flow ability increased (slowed) and the resistance to dynamic segregation (VSI) improved.

The fresh air content of the selected mixtures increased with increasing hauling time. Additionally, the air content increased with decreasing initial slump flow. For example, the total air content increased by 79%, 52% and 44% for the 559, 635 and 711 mm mixtures, respectively. The primary reasons for the increasing air content with respect to hauling time can be attributed to three factors:

- 1) Tall oil AEA: The salt-type AEA that contains tall oil has the tendency to generate more air during continual agitation and hauling time due to its mode of action. In general, the precipitates that are immediately formed when the AEA is added to the mixture dissolve over time, allowing more AEA molecules to be available for adsorption to cement particles and air void stabilization.
- 2) Slump flow loss: The loss of slump flow that occurs with hauling time causes the mixture to exhibit increased viscosity. The increased viscosity of the mixture provides a greater cushion, or stabilizing effect, on the air voids produced. Additionally, with decreased fluidity, there is more resistance to bubble coalescence and rupture.
- 3) Entrapped air: Throughout the investigation, the mixtures were tested as though they were self-consolidating concrete. Thus, there was no rodding or vibration when samples were taken to conduct the volumetric air content test and air void analysis. In the absence of mechanical consolidation, for the mixtures that had a slump flow of less than 500 mm, it can be assumed that air voids larger than 1

mm became entrapped throughout the mixture. Entrapped air is also responsible for the higher air content for the mixtures of lower slump flow and those with a slump flow of less than 500 mm.

6.2.2 Air Void Characteristics

The air void characteristics improved with increasing hauling time from the initial air void characteristics measured at 10 minutes. The specific surfaces of the air voids increased an average of 20% until 70 minutes of hauling time, indicating smaller air voids, at which point the specific surfaces decreased. The spacing factors of the air voids in the selected mixtures decreased an average of 57% until 80 minutes of hauling time, indicating more closely spaced air voids, at which point they typically increased slightly. The 711 mm slump flow produced the best air void characteristics, followed by the 635 and 559 mm slump flow. The 711 mm slump flow mixture contained a higher initial dosage of AEA than the other two mixtures, and therefore had the potential to entrain a larger volume of air voids. The 559 mm slump flow mixture had the lowest initial AEA dosage, which prevented it from entraining as much air as the 711 mm slump flow mixture. The 559 mm mixture also lost the most slump flow throughout hauling time, causing it to contain excessive entrapped air, which reduced the air void characteristics.

6.3 Effects of Hauling Time and Remediation on SCC

In order to counter the effects of long hauling times, two types of remediation were tested in the second phase of the investigation: overdosing (remediation A) and retempering (remediation B). In overdosing, the admixtures were overdosed or underdosed from their initial optimum dosages to produce the target fresh properties at the eight designated hauling times of 20, 30, 40, 50, 60, 70, 80 and 90 minutes. In

retempering, the three selected mixtures optimized in the first phase of the investigation were subjected to hauling times of 20, 40, 60 and 80 minutes, at which point more admixtures were added to obtain the target fresh properties.

6.3.1 Remediation A: Overdosing

With the overdosing remediation technique, the HRWR admixture was overdosed in all mixtures to obtain the desired flow properties. The HRWR was overdosed an average of 0.08, 0.07 and 0.06 ml/kg cementitious material per 10 minutes of hauling for the 559, 635 and 711 mm slump flows, respectively. The decreased dosage with increasing slump flow is related to the rate of slump flow loss, in that the lowest slump flow experienced the greatest reduction in slump flow overall. The VMA only had to be overdosed for the 711 mm slump flow. In contrast, the AEA was under-dosed initially for the 635 and 711 mm slump flows after 40 minutes of hauling, due to the increasing air content with hauling time typical of the tall oil AEA. As such, the air content remained within the acceptable range of $6 \pm 1\%$ throughout the hauling time.

In general, overdosing the admixtures to maintain flow ability resulted in self-consolidating concretes with adequate air void characteristics to ensure freeze-thaw durability in a severe environment. When compared to the initial air void characteristics measured at 10 minutes, the specific surfaces increased an average of 1.5 mm^{-1} and the spacing factors decreased an average of $17.6 \text{ }\mu\text{m}$ for all slump flows and hauling times. Additionally, the air content measured by the Air Void Analyzer increased an average of 2.1% for all slump flows and hauling times. This improvement in air void characteristics indicates that even if the AEA is under-dosed, the beneficial effects of hauling time

overwhelm any of the negative effects (such as air void destabilization) associated with remediation.

While the air void characteristics of the remediated mixtures improved from their initial state, they generally deteriorated when compared to the non-remediated self-consolidating concretes of the same hauling time. On average, the specific surfaces of all slump flows and hauling times of the overdosed mixtures decreased by 5.5 mm^{-1} when compared to the specific surfaces of the non-remediated mixtures at their respective hauling times. Likewise, the spacing factors increased an average of $28.3 \text{ }\mu\text{m}$ from their respective hauling times after remediation.

In summary, while the air void characteristics of the overdosed mixtures improved from their initial state obtained at the control hauling time of 10 minutes, remediation by overdosing resulted in minor deterioration of air void characteristics when compared to the non-remediated mixtures of the same hauling time. However, the air void systems of the overdosed self-consolidating concretes remained well above the acceptable limits for freeze-thaw durability in a severe environment.

6.3.2 Remediation B: Retempering

The second form of remediation utilized in this investigation was to retemper with additional admixtures after the mixture had reached the desired hauling time. The admixture dosages that were optimized in the first phase of the investigation were utilized in the initial mixing period, with supplementary admixtures added after hauling time. HRWR was added for retempering the slump flow of all mixtures, but additional VMA was only needed at the highest slump flow of 711 mm. Since the air content increased with hauling time, no additional AEA was added to the mixtures for retempering. The

chief shortfall of this remediation technique was that the air content typically exceeded the target of $6 \pm 1\%$. Hauling time and continual agitation caused the air content to increase, and no amount of admixture could remove the air voids that had become entrained/entrapped throughout the mixture. Retempering was successful in terms of restoring the desired slump flow. In turn, the fluidity of the self-consolidating concrete lowered the volumetric air content an average of 1.4% when compared to the non-remediated concretes. However, the reduction in air typically resulted in a mixture that remained above the target volumetric air content, particularly for the mixtures with a lower slump flow. The reduction in volumetric air content can be attributed to the increased fluidity of the mixture imparted by the HRWR.

The effects of retempering on the air void characteristics were similar to the effects of remediation by overdosing. The specific surfaces increased an average of 6.1 mm^{-1} from the initial hauling time to after retempering. The spacing factors decreased an average of $42.2 \text{ }\mu\text{m}$ from the initial hauling time to after retempering. The improvement in air void characteristics indicates that, similar to overdosing, the effects of hauling time (such as increasing air content) overwhelm any negative or destabilizing effects of remediation. However, the air void characteristics were typically more improved with retempering than with overdosing, due to the fact that the AEA was under-dosed with remediation A and was unable to entrain as many air voids. Also similar to overdosing, the air void characteristics resulting from retempering were worse than the air void characteristics obtained at the same hauling time. On average, the specific surfaces and spacing factors of the retempered self-consolidating concrete deteriorated by 1.1 mm^{-1} and $5.3 \text{ }\mu\text{m}$, respectively, when compared to those of the equivalent non-remediated

matrices. The change in air void characteristics from hauling time are less pronounced for retempering than they were for overdosing.

6.3.3 Comparison of Remediation Techniques

The two forms of remediation, overdosing and retempering, were both able to produce the desired fresh flow properties. However, the air content resulting from retempering typically exceeded the target air content, since the AEA dosage could not be initially under-dosed. In choosing one form of remediation over another, consideration must be given to construction management issues as well as performance. For example, overdosing may give a concrete batch plant more quality control over the final product, but retempering may impart more flexibility if the exact hauling time is unknown.

6.3.3.1 Admixture dosages

The volumetric economy of the admixture dosages can contribute to the desirability of one form of remediation over the other. In this study, retempering was more economical for producing a SCC mixture with a 559 mm slump flow. In producing a mixture with a 711 mm slump flow, overdosing was more economical because the AEA dosage was reduced with increasing hauling time. In creating a mixture with a 635 mm slump flow, the preference of one form of remediation over the other depended on the hauling time. For hauling times greater than or equal to 60 minutes, retempering was more economical, whereas with hauling times less than 60 minutes, overdosing was more economical.

6.3.3.2 Air Content

The trend with mixtures utilizing the salt-type AEA containing tall oil was that the air content increased with increasing hauling time. Therefore, only the overdosing

remediation technique could prevent the air content from going beyond the target limit. With mixtures where the air content increases with hauling time, such as those evaluated in this study, remediation A is preferable because the air-entraining admixture can be suitably under-dosed. However, other variables such as admixture type, mixture constituents and proportioning, and applied mixing action, may cause the air content to decrease with increasing hauling time, in which case remediation B may be more desirable because more air-entrainment can be added to increase the air content.

6.3.3.3 Air Void Characteristics

Both forms of remediation produced mixtures at all hauling times that met the target air void characteristics for freeze-thaw durability. For overdosing and retempering, the specific surfaces and spacing factors of all mixtures improved with increased hauling time from the initial air void characteristics (at 10 minutes). However, retempering typically produced better air void characteristics than overdosing due to its un-remediated AEA dosage. Likewise, for both forms of remediation, the specific surfaces and spacing factors of all mixtures deteriorated from those air void characteristics measured at their respective hauling times without remediation. The air void characteristics of overdosing generally depreciated more than the air void characteristics produced after retempering. It should still be noted that the deterioration caused by either form of remediation was not great enough to be considered destabilizing.

6.4 Recommendations on Future Research

Future studies on air-entrained self-consolidating concrete should include the effects of air-entrainment admixture type and high range water reducer type on hauling time and remediation behavior of SCC. In the first phase of the investigation, it was

discovered that the type of AEA and HRWR significantly influenced the air void characteristics and behavior with respect to slump flow. However, in the second phase of this investigation, only one admixture source was studied on the effects of hauling time and remediation. In future studies, a polycarboxylate-acid and polycarboxylate-ester should be investigated with hauling time, since the PCE is believed to have better slump retention capabilities than the PCA type. Additionally, a salt-type or tall oil AEA should be compared to a synthetic detergent AEA under hauling time, because significant differences were encountered on the AEA performance with increasing slump flow. Also, a study on the change in air content and air void characteristics of SCC mixtures with respect to hauling time should be conducted with a synthetic detergent AEA, since the tall oil AEA tends to increase the air content with hauling time.

In terms of remediation, the retempering technique should be studied further to include under-dosing the AEA in conjunction with retempering after hauling time. Field tests utilizing ready-mixed concrete trucks may provide more realistic information for concrete producers due to the difference in mixing action between a laboratory pan mixer and a rotating drum mixer. As such, further studies pertaining to air void characteristics of self-consolidating concrete need to be conducted to obtain appropriate correlations between field and laboratory results.

APPENDIX A
CONVERSIONS

$$1 \text{ mm} = 0.03937 \text{ inches}$$

$$1 \text{ }\mu\text{m} = 0.00003937 \text{ inches}$$

$$1 \text{ kg/m}^3 = 1.6856 \text{ lb/yd}^3$$

$$1 \text{ ml/kg} = 1.5338 \text{ ounces/100 pounds}$$

$$1 \text{ MPa} = 145 \text{ lb/in}^2$$

$$1 \text{ kg/m}^3 = 0.0624 \text{ lb/ft}^3$$

$$1 \text{ m}^3 = 35.3147 \text{ ft}^3$$

APPENDIX B

ADDITIONAL TABLES AND FIGURES

Table B.3.1 Calculated versus actual VMA dosages based on Eq. 3.1

Source	SF (mm)	ml/kg cementitious materials		% Error
		Actual	Calculated	
B	565	0.00	-0.01	-1.0
	648	0.26	0.27	-4.9
	715	0.33	0.32	0.6
C	562	0.00	-0.02	-1.0
	640	0.26	0.26	0.8
	714	0.33	0.32	0.6
D	572	0.00	0.03	0.0
	624	0.26	0.22	14.2
	711	0.33	0.32	0.5

Table B.3.2 Phase I air void characteristics

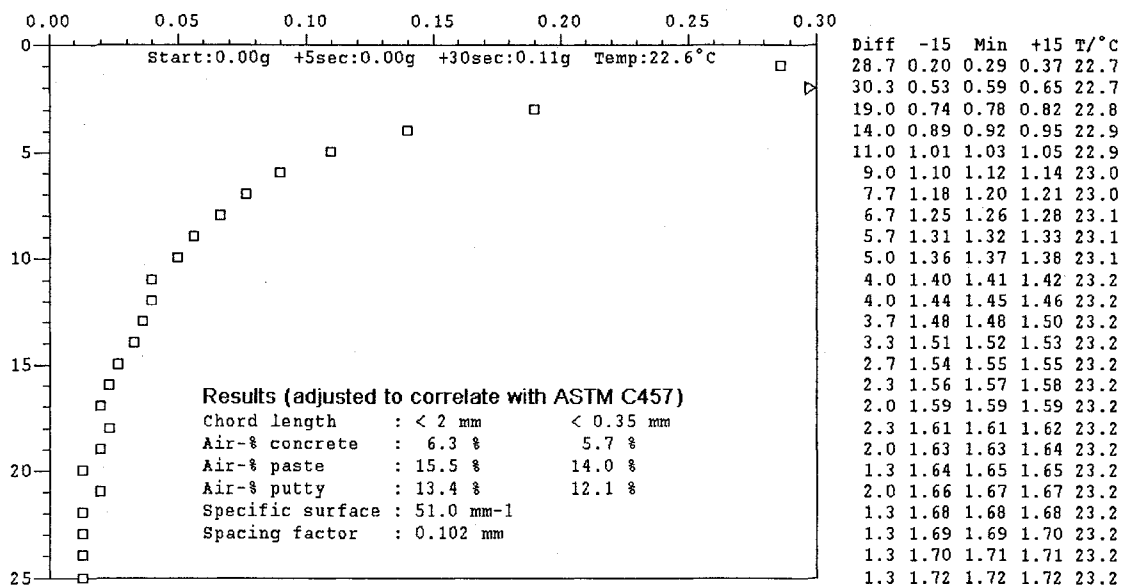
Mixture Identification	Specific Surface (mm ⁻¹)	Spacing Factor (μm)	Air % Concrete < 2mm	Air % Concrete < 0.35mm
A-SF22	50.0	102	6.6	5.9
	51.0	102	6.3	5.7
	49.6	100	7.1	6.2
	45.8	108	7.1	6.0
	41.1	124	6.6	5.6
B-SF22	35.4	150	5.6	5.0
	40.8	125	6.1	5.3
	36.3	149	5.3	4.6
	39.6	139	5.1	4.6
C-SF22	42.8	111	7.5	6.6
	34.7	153	5.9	5.1
	32.6	168	5.5	4.6
	32.0	181	4.9	4.1
D-SF22	28.6	186	5.5	4.1
	30.4	182	5.0	3.9
	30.9	176	5.2	4.0
	28.4	186	5.6	4.1
A-SF25	47.4	111	6.4	5.6
	46.6	120	5.6	5.0
	49.3	100	7.3	6.4
	46.9	109	6.8	5.9
	34.3	158	6.0	4.8
B-SF25	37.2	135	6.6	5.8
	35.0	151	5.8	5.1
	36.3	147	5.7	4.9
	36.2	152	5.3	4.7
	39.4	137	5.5	5.0
	37.8	137	6.1	5.2
	32.4	153	6.8	6.0
C-SF25	39.4	143	5.4	4.8
	32.0	177	5.3	4.3
	34.0	151	6.5	5.5
	33.5	153	6.5	5.5

Mixture Identification	Specific Surface (mm⁻¹)	Spacing Factor (μm)	Air % Concrete < 2mm	Air % Concrete < 0.35mm
D-SF25	31.6	158	6.6	4.8
	28.7	178	6.3	4.4
	27.6	191	5.9	4.1
A-SF28	42.6	136	5.5	4.7
	37.3	139	7.1	6.1
	35.4	152	6.5	5.5
	40.3	133	6.6	5.8
B-SF28	39.2	141	5.5	4.8
	35.9	164	4.8	4.1
	37.0	141	6.2	5.3
	39.2	140	5.6	5.0
	33.2	177	4.8	4.0
C-SF28	32.7	161	6.3	5.0
	32.6	160	6.4	5.1
	33.3	160	6.1	5.0
	33.2	163	6.0	4.8
	32.8	168	5.7	4.7
D-SF28	30.4	190	4.9	3.4
	28.2	188	6.0	4.1
	28.8	181	6.2	4.3

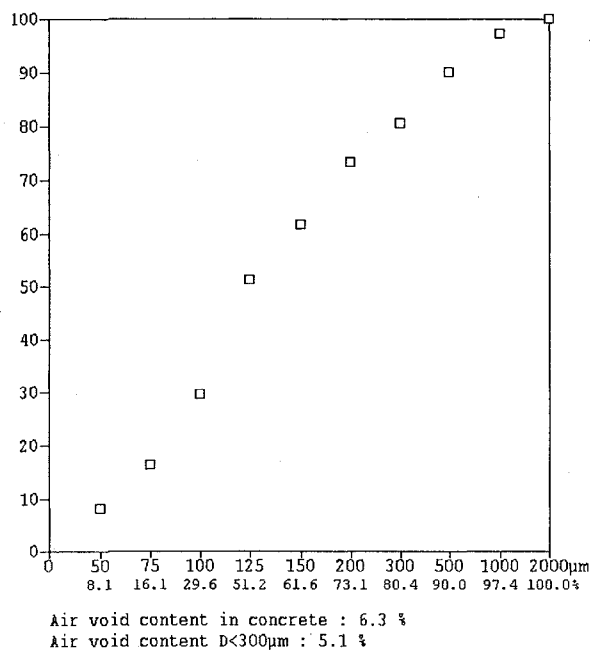
Measurement of 2007-08-18 14:49

Comments

Sampler : MBD Mortar<6mm : 67.2 % > batch 1, trial 2
 Ordered by : - Exp. air : 6.0 % >
 Sample loc. : UNLV Paste : 40.9 % >
 Case no. : A-SF22 Sample vol : 20.0 cm3 >
 Sample no. : 2



Distribution of air void content
 for voids < 2mm (%)



Distribution of air void content in cement paste
 for voids < 2mm (%)

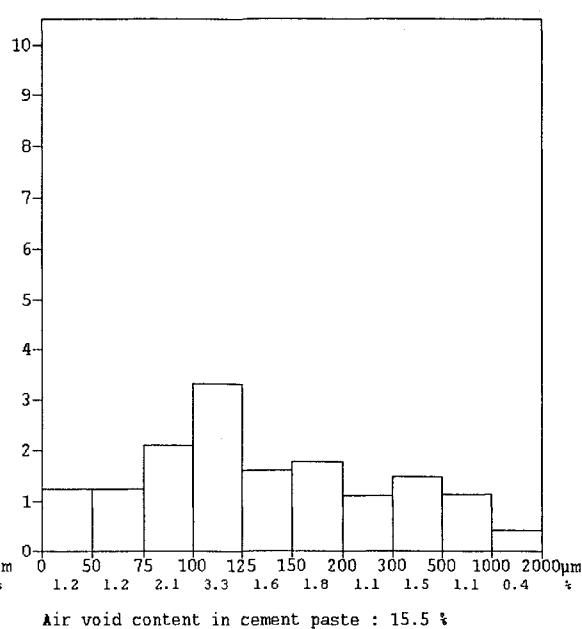
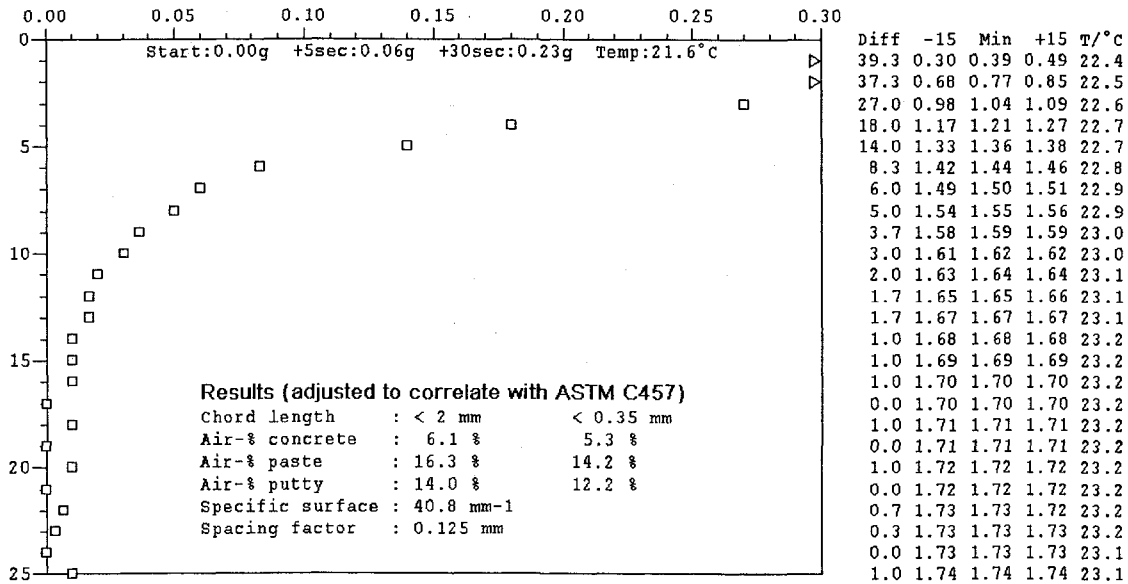


Figure B.3.1 A-SF22 Typical Air Void Analysis

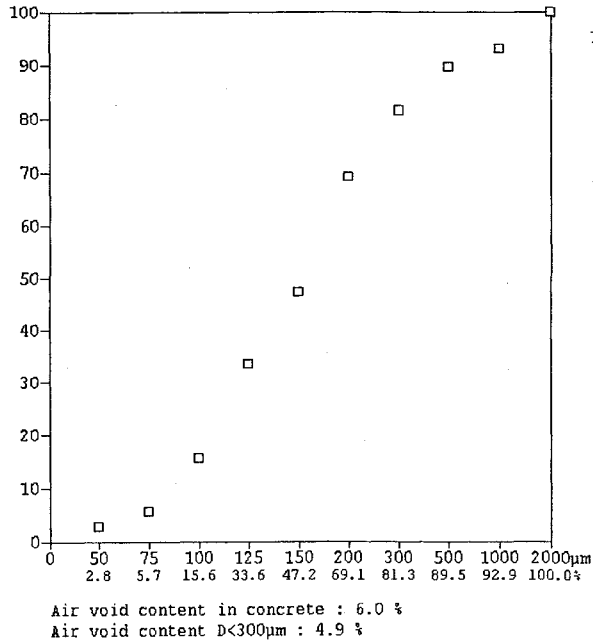
Measurement of 2008-01-23 13:52

Comments

Sampler : MEB Mortar<6mm : 65.3 % > 22 inch 10 minute trial 1
 Ordered by : - Exp. air : 6.0 % >
 Sample loc. : UNLV Paste : 37.5 % >
 Case no. : B-SF22 Sample vol : 20.0 cm3 >
 Sample no. : 1



Distribution of air void content
for voids < 2mm (%)



Distribution of air void content in cement paste
for voids < 2mm (%)

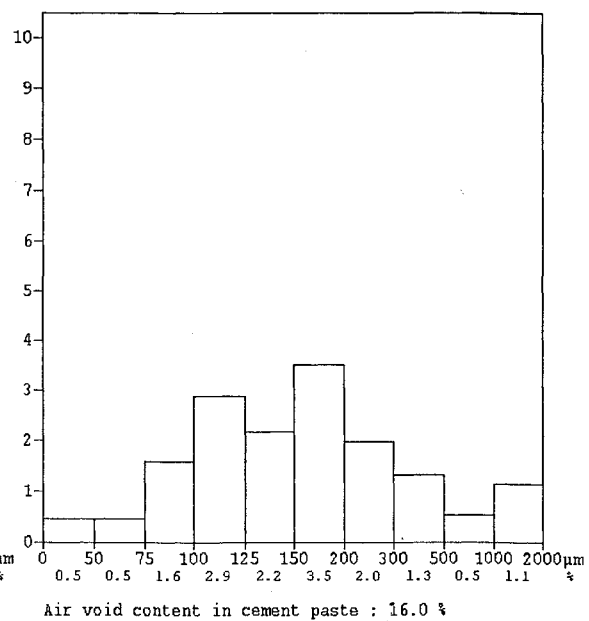


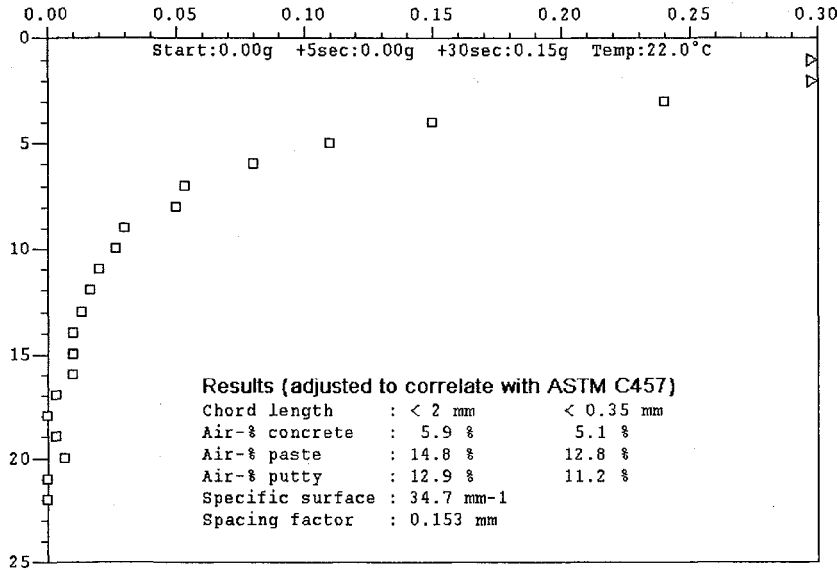
Figure B.3.2 B-SF22 Typical Air Void Analysis

Measurement of 2007-11-16 14:25

Sampler : MBB Mortar<6mm : 66.6 %
 Ordered by : - Exp. air : 6.0 %
 Sample loc. : UNLV Paste : 39.8 %
 Case no. : C-SF22 Sample vol : 20.0 cm3
 Sample no. : 5

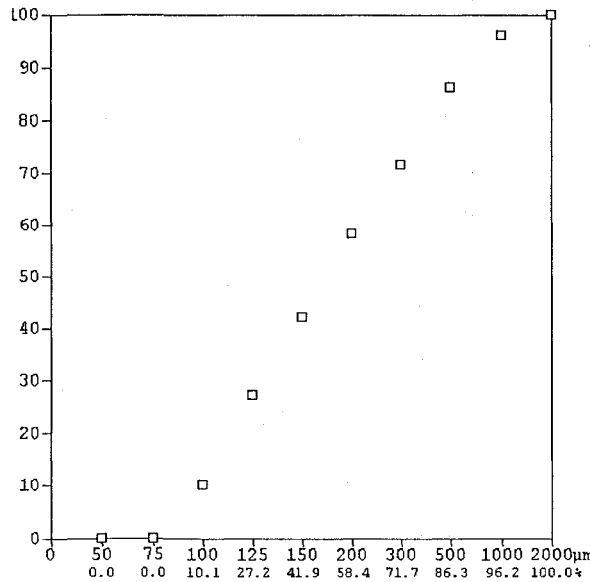
Comments

> batch 1, trial 1



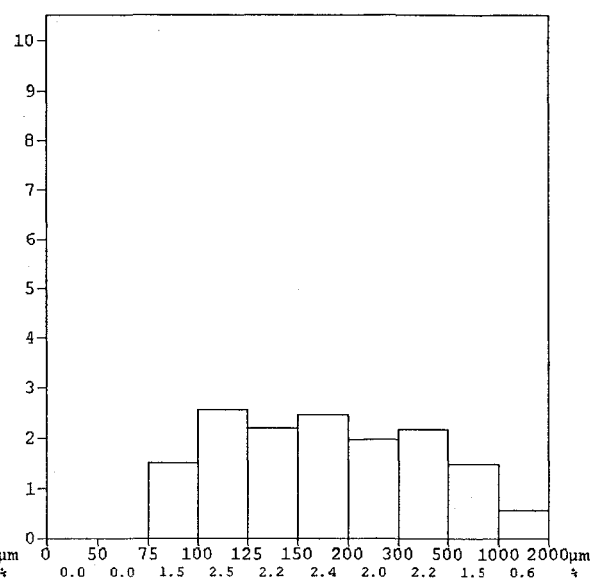
Diff	-15	Min	+15	T/°C
38.7	0.26	0.39	0.51	22.1
41.0	0.72	0.80	0.87	22.1
24.0	0.99	1.04	1.08	22.2
15.0	1.15	1.19	1.22	22.3
11.0	1.27	1.30	1.32	22.3
8.0	1.36	1.38	1.39	22.4
5.3	1.42	1.43	1.44	22.4
5.0	1.47	1.48	1.49	22.5
3.0	1.50	1.51	1.52	22.6
2.7	1.53	1.54	1.54	22.6
2.0	1.55	1.56	1.56	22.6
1.7	1.57	1.57	1.58	22.7
1.3	1.58	1.59	1.59	22.7
1.0	1.59	1.60	1.60	22.8
1.0	1.60	1.61	1.61	22.8
1.0	1.61	1.62	1.62	22.9
0.3	1.62	1.62	1.62	22.9
0.0	1.62	1.62	1.62	23.0
0.3	1.62	1.62	1.63	23.0
0.7	1.63	1.63	1.63	23.1
0.0	1.63	1.63	1.63	23.1
0.0	1.63	1.63	1.63	23.2

Distribution of air void content for voids < 2mm (%)



Air void content in concrete : 5.9 %
 Air void content D<300µm : 4.2 %

Distribution of air void content in cement paste for voids < 2mm (%)



Air void content in cement paste : 14.8 %

Figure B.3.3 C-SF22 Typical Air Void Analysis

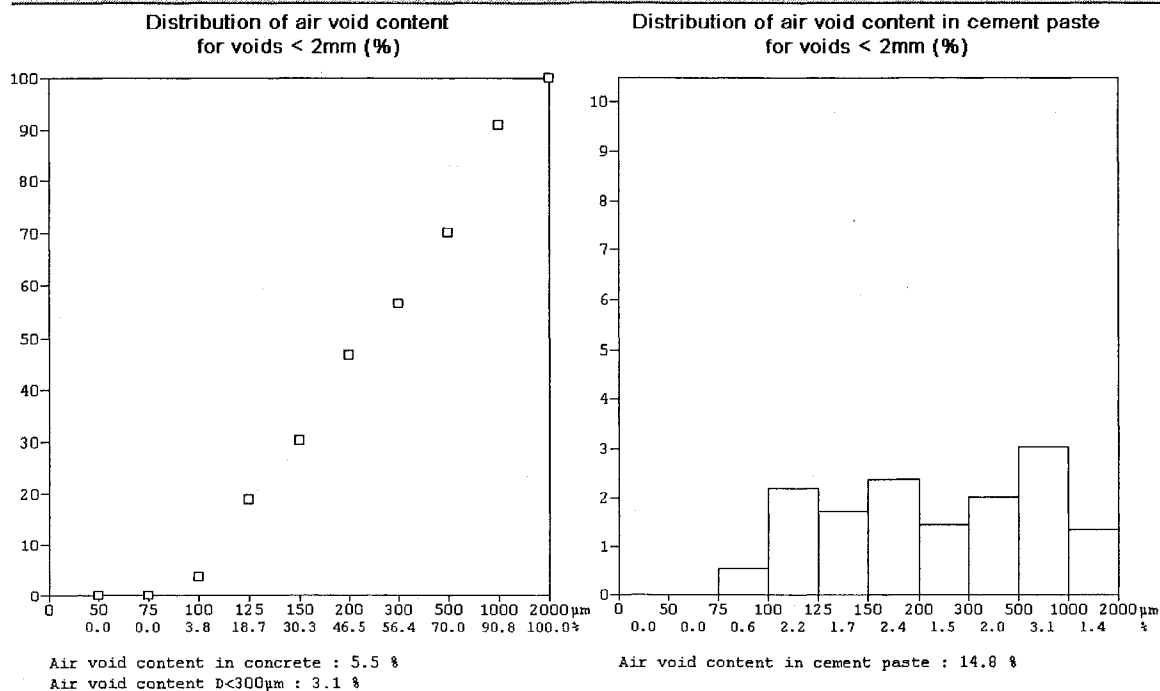
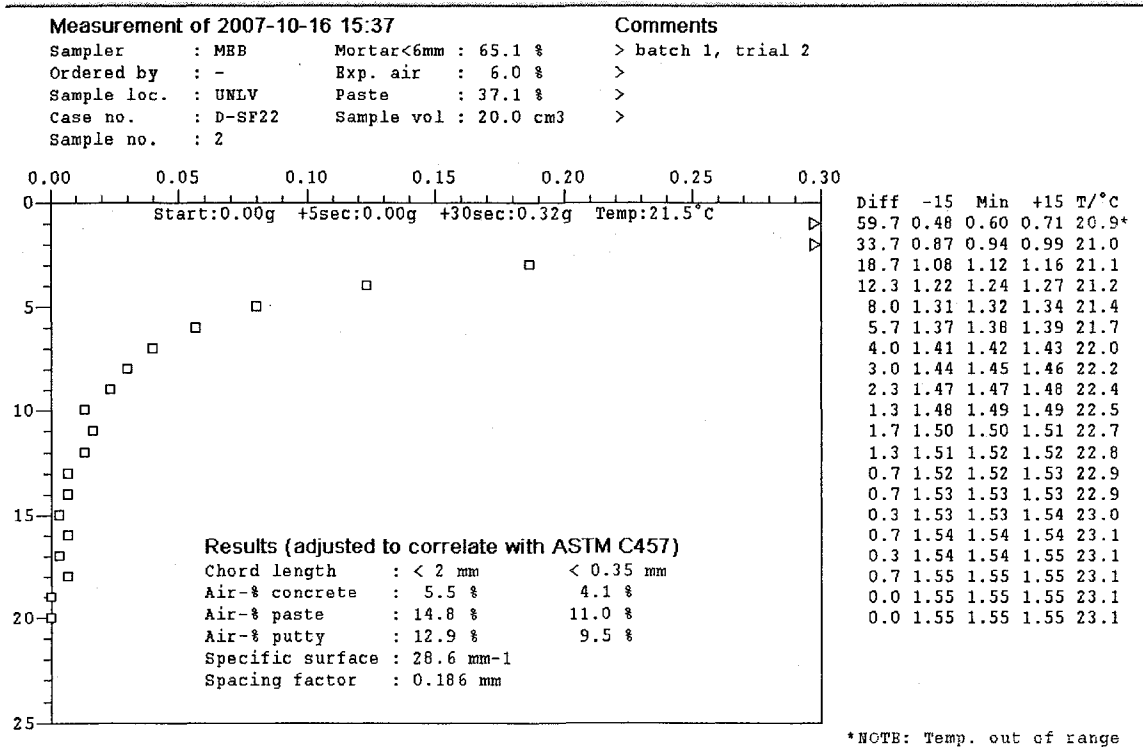


Figure B.3.4 D-SF22 Typical Air Void Analysis

Measurement of 2007-08-27 15:38

Sampler : MEB Mortar<6mm : 68.2 %
 Ordered by : - Exp. air : 6.0 %
 Sample loc. : UNLV Paste : 42.6 %
 Case no. : A-SF25 Sample vol : 20.0 cm3
 Sample no. : 2

Comments

> batch 1, trial 2
 >
 >
 >

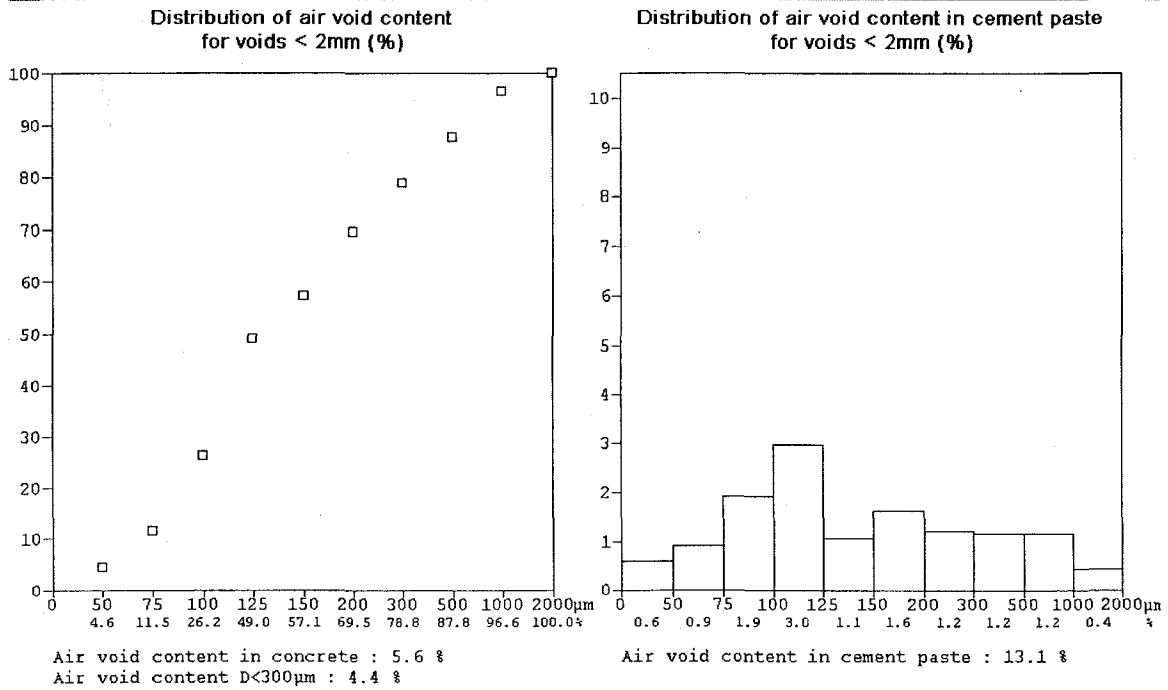
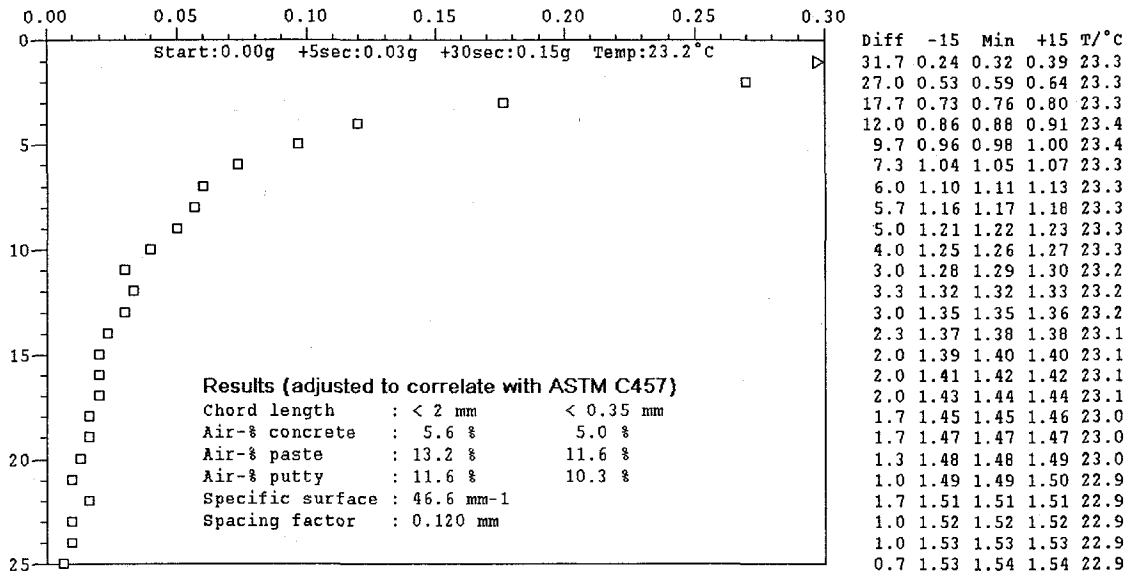


Figure B.3.5 A-SF25 Typical Air Void Analysis

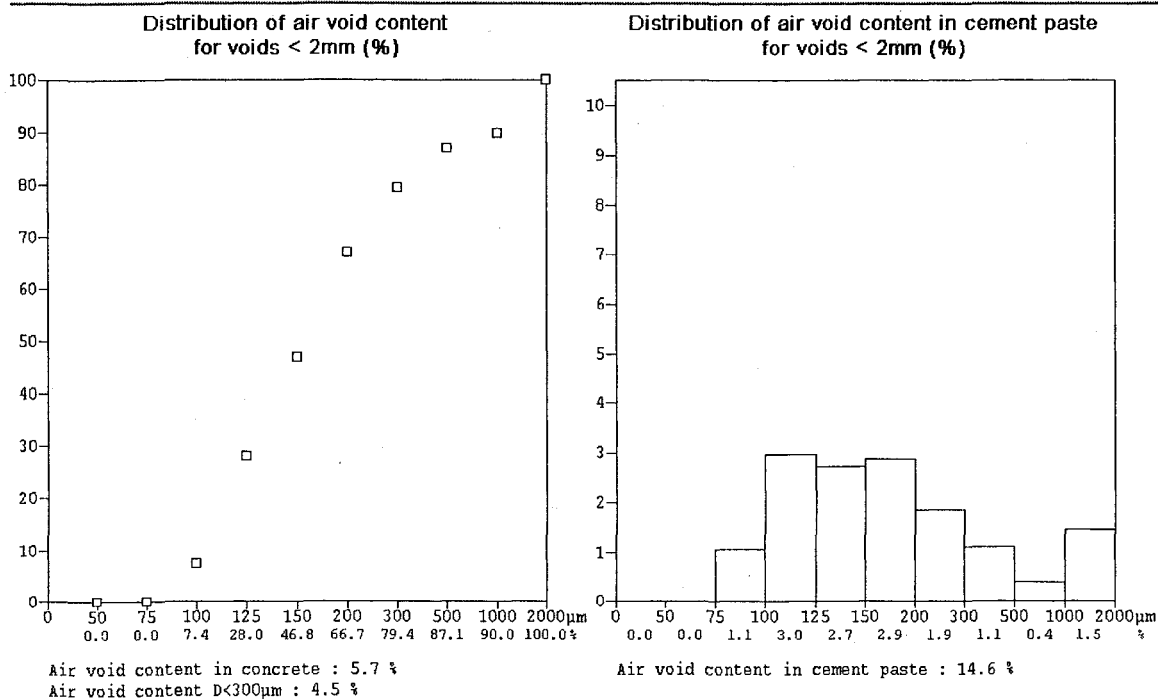
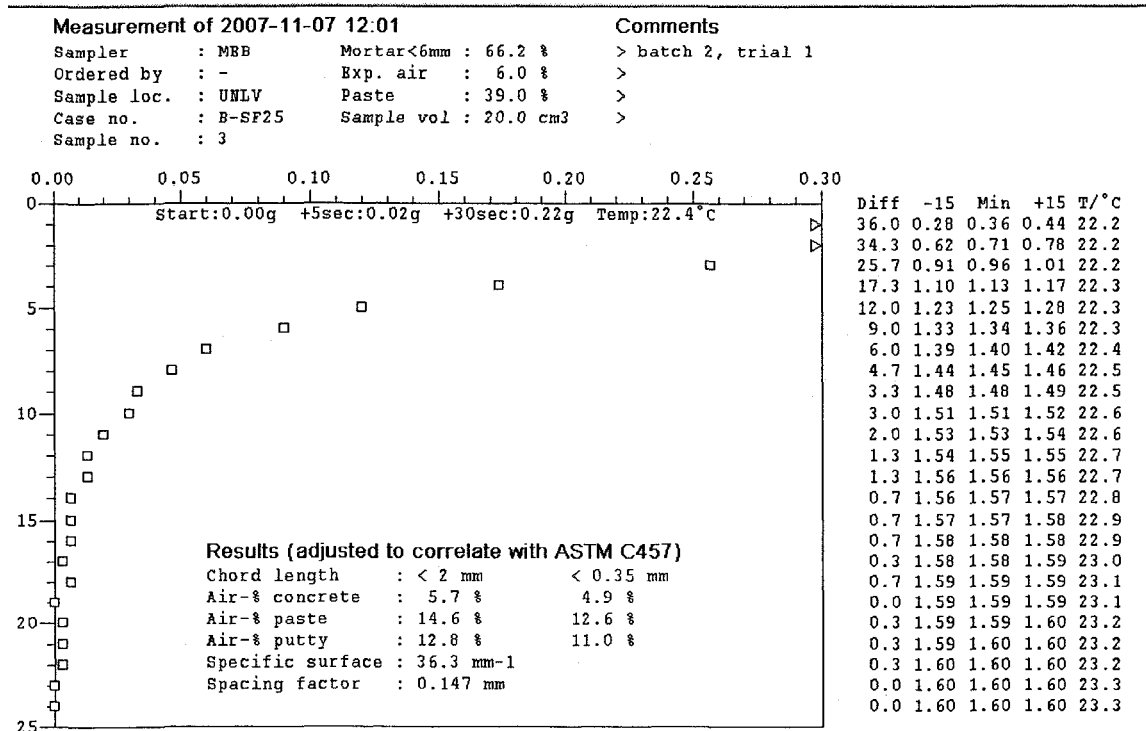


Figure B.3.6 B-SF25 Typical Air Void Analysis

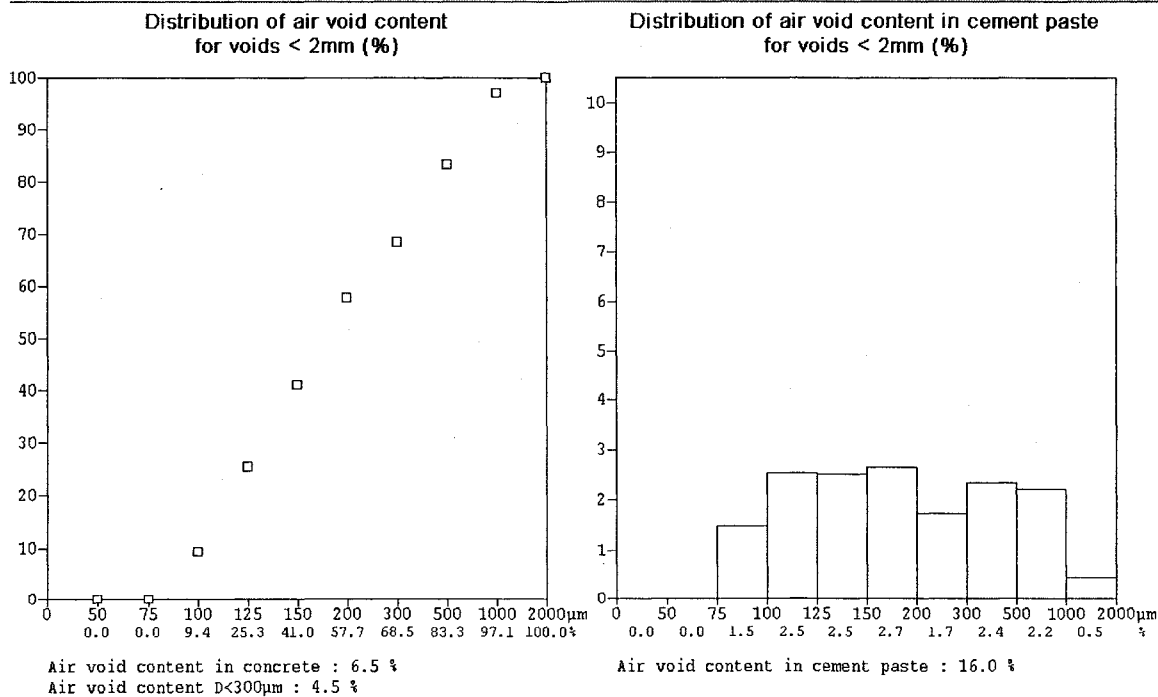
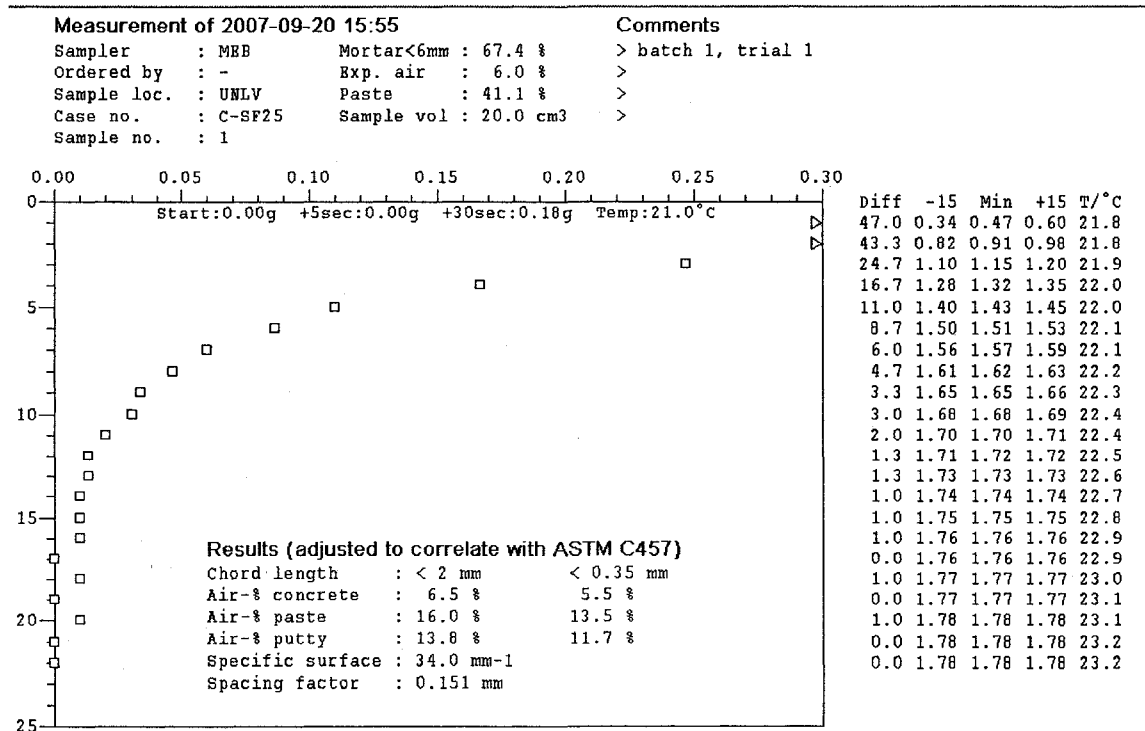
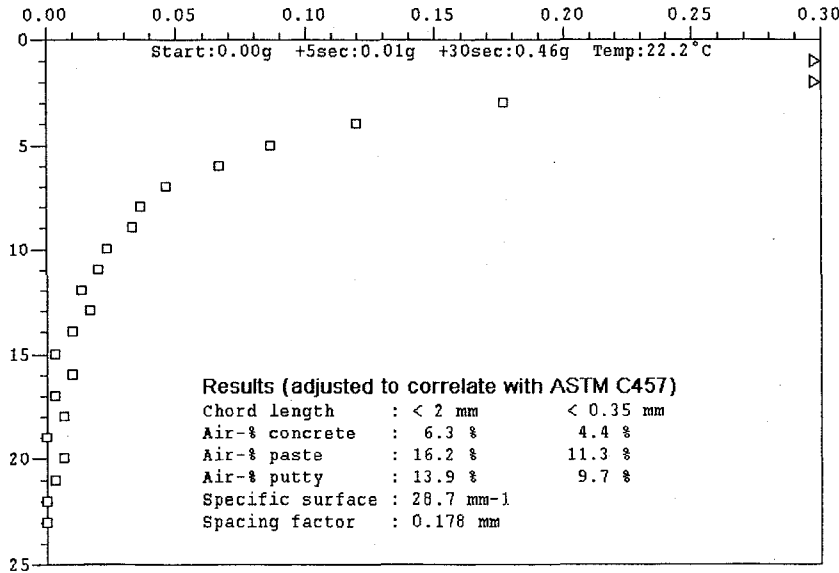


Figure B.3.7 C-SF25 Typical Air Void Analysis

Measurement of 2007-09-22 13:47

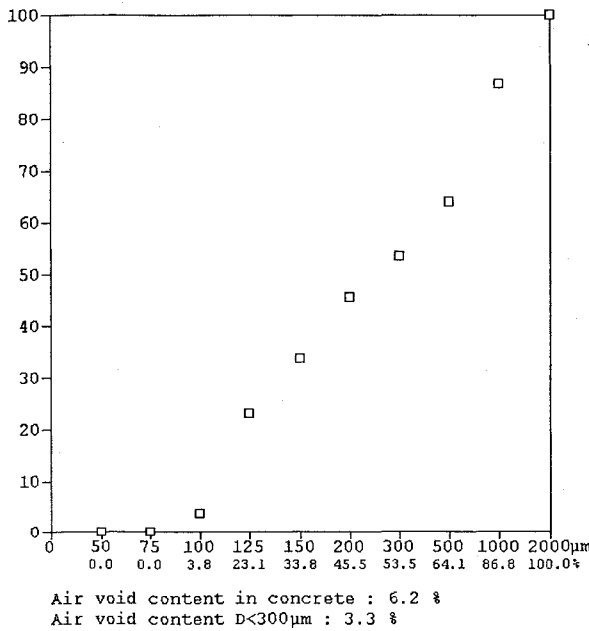
Comments

Sampler : MRB Mortar<6mm : 66.0 %
 Ordered by : - Exp. air : 6.0 %
 Sample loc. : UNLV Paste : 38.8 %
 Case no. : D-SF25 Sample vol : 20.0 cm3
 Sample no. : 2



Diff	-15	Min	+15	T/°C
75.0	0.63	0.76	0.86	21.8
30.7	1.00	1.06	1.11	21.9
17.7	1.20	1.23	1.27	21.9
12.0	1.33	1.35	1.38	22.0
8.7	1.42	1.44	1.46	22.0
6.7	1.49	1.51	1.52	22.1
4.7	1.54	1.55	1.57	22.2
3.7	1.58	1.59	1.60	22.3
3.3	1.62	1.62	1.63	22.3
2.3	1.64	1.65	1.65	22.4
2.0	1.66	1.67	1.67	22.5
1.3	1.68	1.68	1.68	22.6
1.7	1.69	1.70	1.70	22.7
1.0	1.70	1.71	1.71	22.8
0.3	1.71	1.71	1.71	22.8
1.0	1.72	1.72	1.72	22.9
0.3	1.72	1.72	1.73	23.0
0.7	1.73	1.73	1.73	23.0
0.0	1.73	1.73	1.73	23.1
0.7	1.73	1.74	1.74	23.1
0.3	1.74	1.74	1.74	23.2
0.0	1.74	1.74	1.74	23.2
0.0	1.74	1.74	1.74	23.2

Distribution of air void content
for voids < 2mm (%)



Distribution of air void content in cement paste
for voids < 2mm (%)

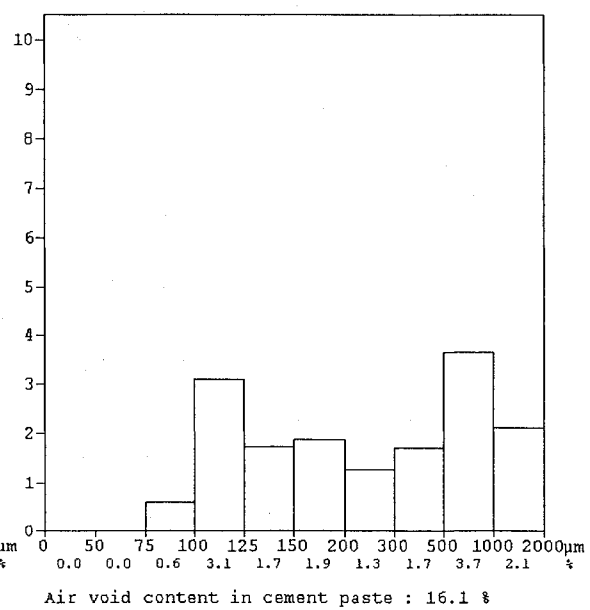


Figure B.3.8 D-SF25 Typical Air Void Analysis

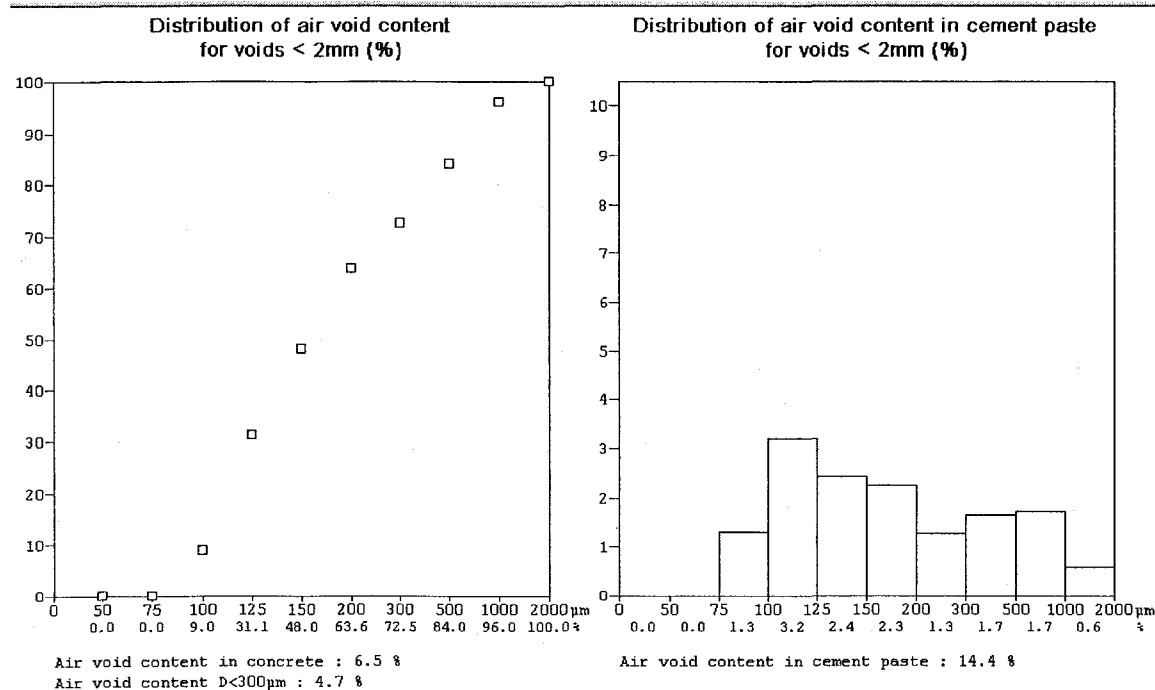
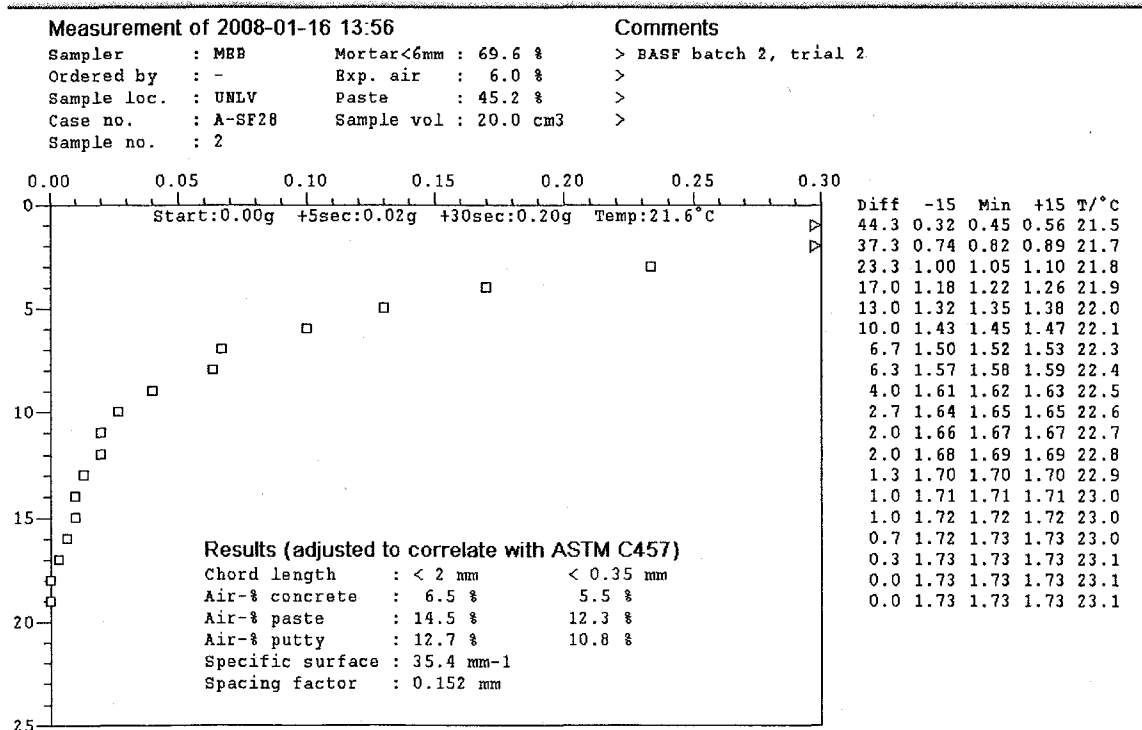


Figure B.3.9 A-SF28 Typical Air Void Analysis

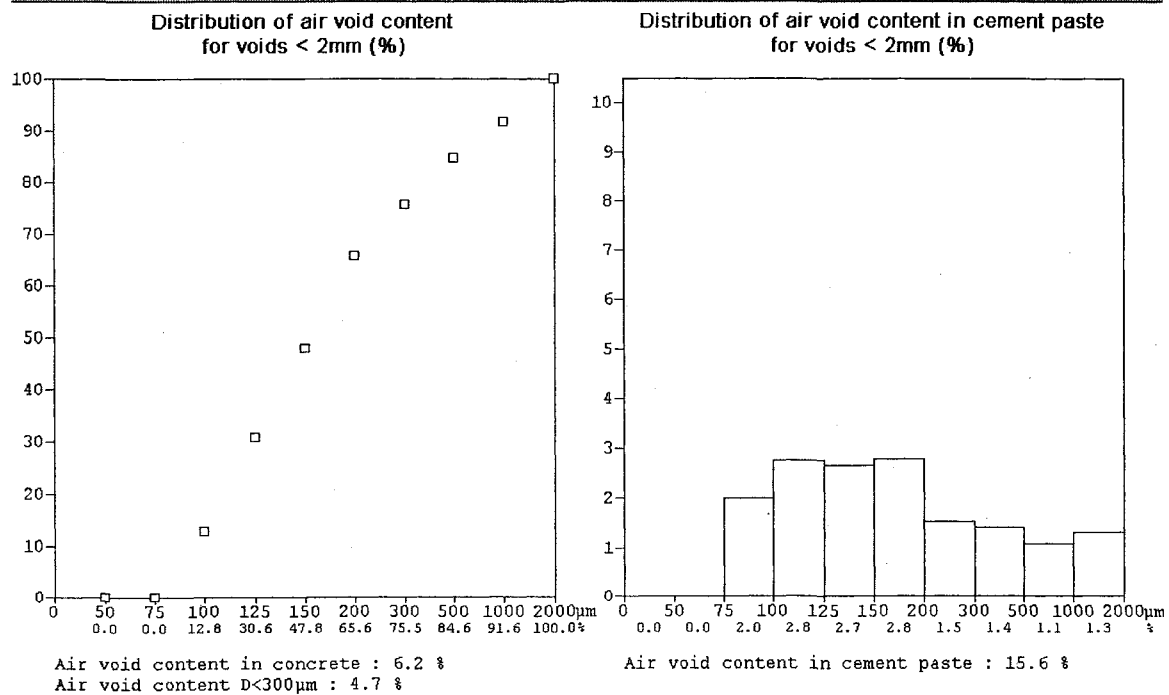
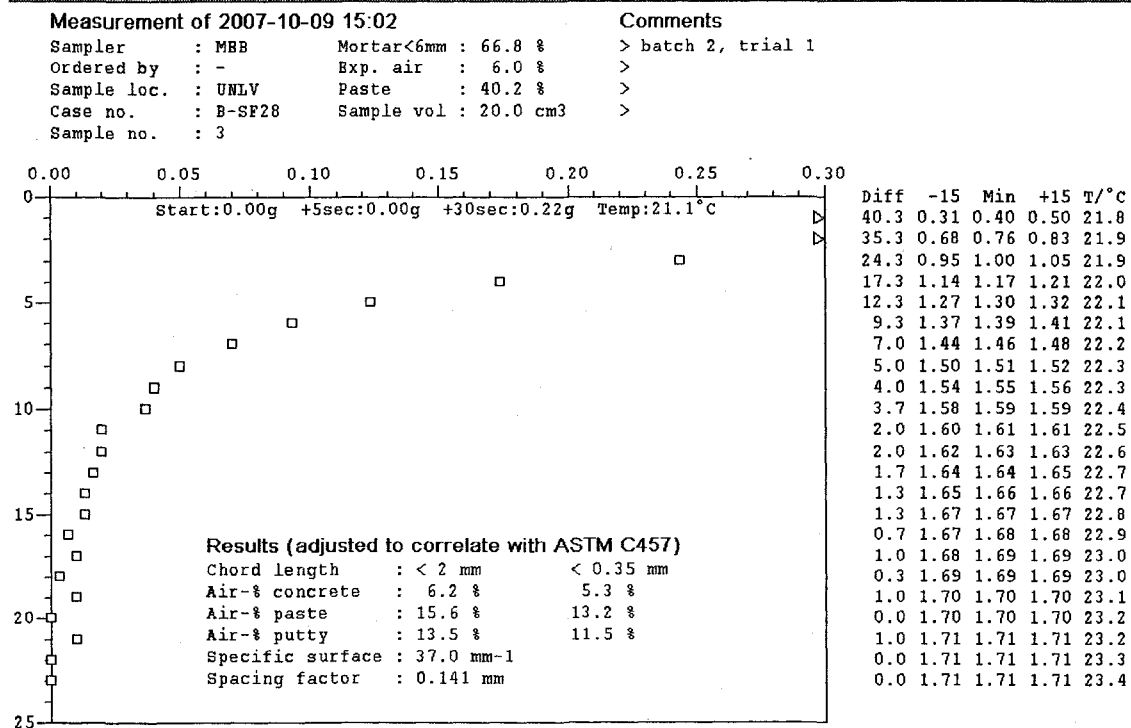


Figure B.3.10 B-SF28 Typical Air Void Analysis

Measurement of 2007-09-25 15:59

Sampler : MEB Mortar<6mm : 67.6 %
 Ordered by : - Exp. air : 6.0 %
 Sample loc. : UNLV Paste : 41.6 %
 Case no. : C-SF28 Sample vol : 20.0 cm3
 Sample no. : 3

Comments

> batch 2, trial 1
 >
 >
 >

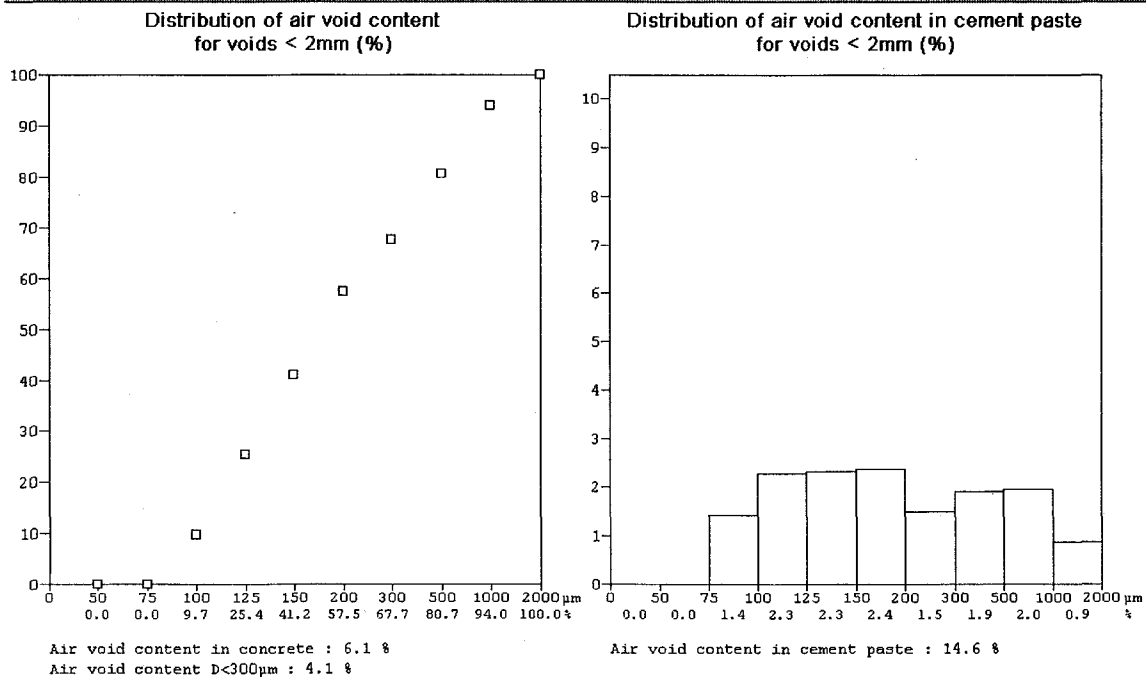
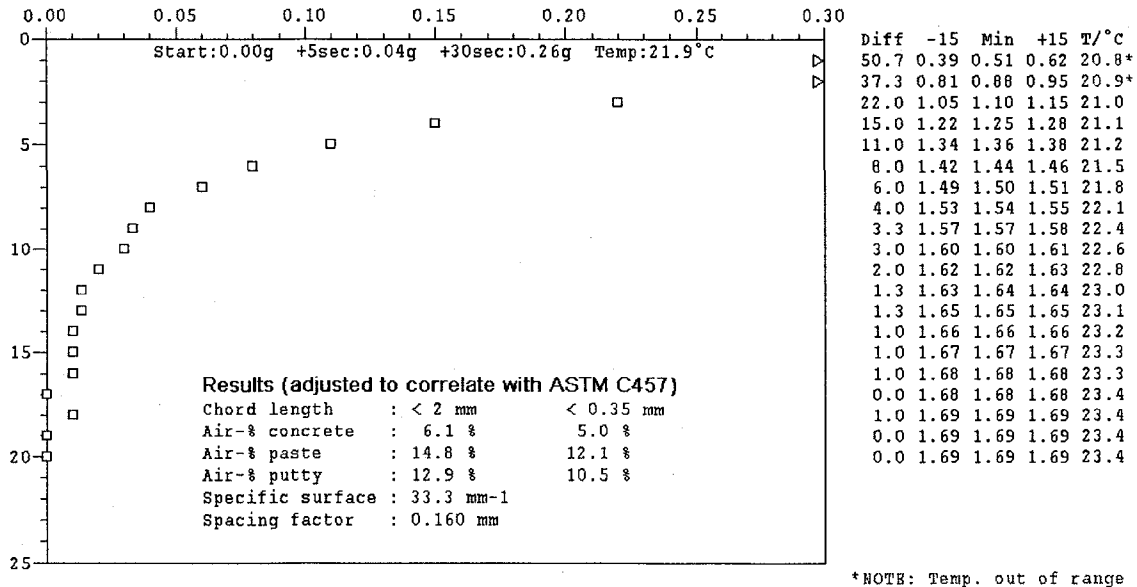


Figure B.3.11 C-SF28 Typical Air Void Analysis

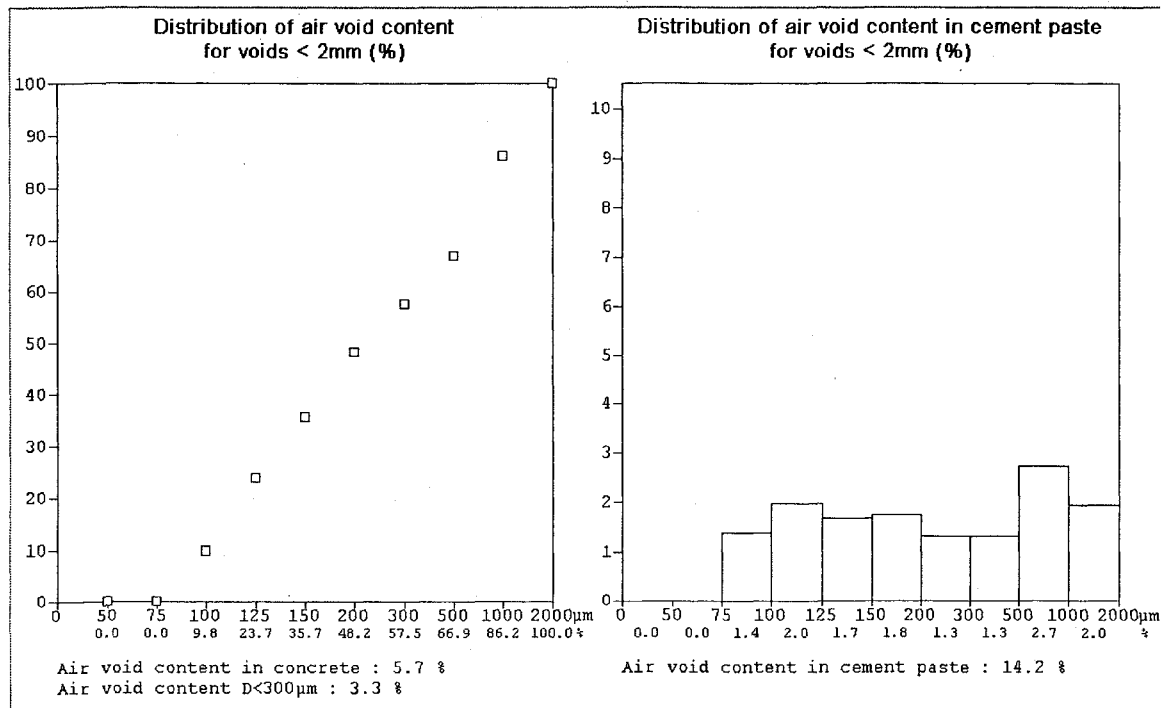
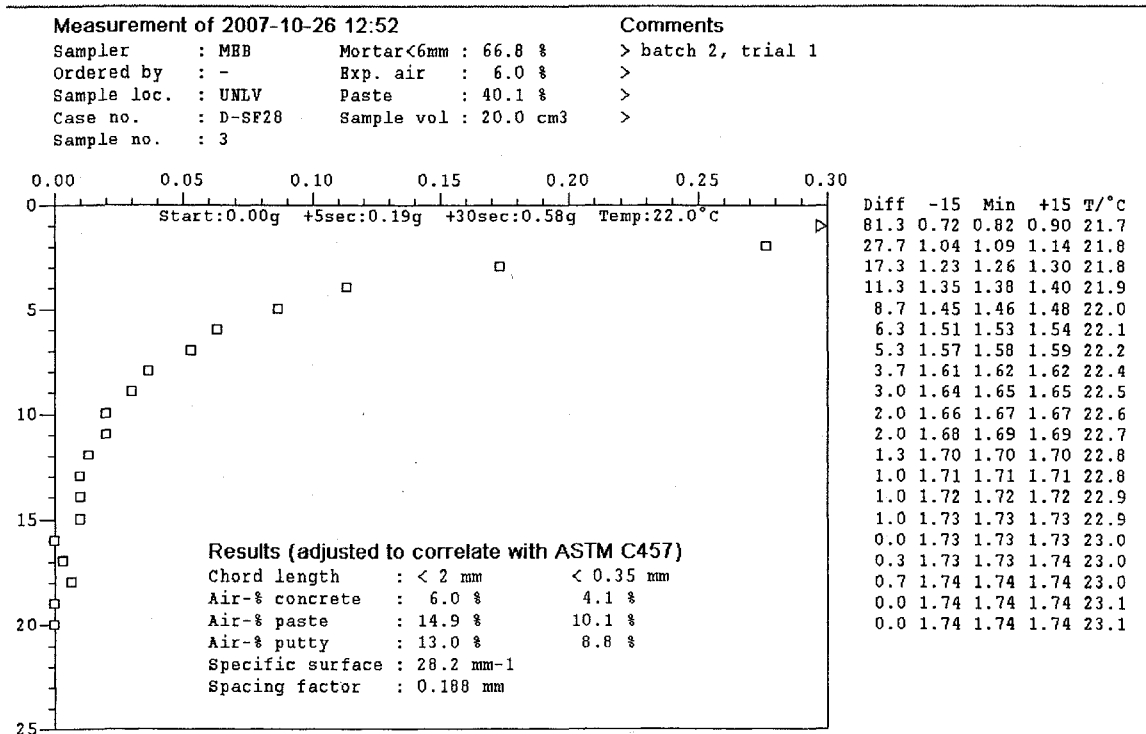


Figure B.3.12 D-SF28 Typical Air Void Analysis

Table B.4.1 Calculated and actual values of slump flow, based on Eq. 4.1

Hauling Time (min.)	SF_i (mm)	Final Slump Flow (mm)		Absolute % Error
		Actual	Calculated	
10	559	559	535	4.2
20	559	518	509	1.6
30	559	486	484	0.5
40	559	467	458	1.9
50	559	435	432	0.7
60	559	391	406	3.9
70	559	368	380	3.2
80	559	352	354	0.5
90	559	343	328	4.2
10	646	646	646	0.1
20	646	610	620	1.6
30	646	591	594	0.5
40	646	572	568	0.6
50	646	551	542	1.7
60	646	502	516	2.9
70	646	483	490	1.6
80	646	438	464	6.0
90	646	416	439	5.5
10	724	724	744	2.8
20	724	699	719	2.9
30	724	686	693	1.0
40	724	673	667	0.9
50	724	648	641	1.0
60	724	635	615	3.1
70	724	622	589	5.3
80	724	572	563	1.4
90	724	546	537	1.6

Table B.4.2 Calculated and actual values of air content, based on Eq. 4.2

Hauling Time (min.)	SF_i (mm)	Air Content (%)		Absolute % Error
		Actual	Calculated	
10	559	6.0	5.4	9.5
20	559	6.3	6.1	2.8
30	559	6.5	6.7	3.4
40	559	7.0	7.4	5.2
50	559	7.6	8.0	5.1
60	559	8.5	8.7	1.9
70	559	9.5	9.3	2.1
80	559	10.0	9.9	0.5
90	559	10.8	10.6	1.4
10	646	6.3	6.0	4.7
20	646	6.5	6.4	1.8
30	646	6.8	6.8	0.8
40	646	7.3	7.2	0.3
50	646	7.8	7.7	1.2
60	646	8.0	8.1	1.0
70	646	8.3	8.5	3.1
80	646	9.0	8.9	0.8
90	646	9.5	9.4	1.5
10	724	6.0	6.5	7.8
20	724	6.6	6.7	2.2
30	724	7.0	7.0	0.2
40	724	7.5	7.3	2.8
50	724	7.5	7.6	0.8
60	724	7.8	7.8	0.4
70	724	8.0	8.1	1.3
80	724	8.5	8.4	1.4
90	724	8.6	8.7	0.3

Table B.4.3 Phase II: Calculated and actual values of specific surface, based on Eq. 4.3

Hauling Time (min.)	SF_i (mm)	Specific Surface (mm^{-1})		Absolute % Error
		Actual	Calculated	
10	559	38.0	36.3	4.5
20	559	40.1	39.3	2.2
30	559	41.8	41.6	0.5
40	559	42.6	43.4	1.9
50	559	43.8	44.6	1.8
60	559	44.8	45.2	0.9
70	559	45.1	45.1	0.1
80	559	44.6	44.5	0.2
90	559	41.8	43.3	3.4
10	646	37.0	37.9	2.4
20	646	41.8	40.9	2.1
30	646	43.9	43.3	1.5
40	646	45.3	45.0	0.6
50	646	46.2	46.2	0.0
60	646	46.5	46.8	0.6
70	646	47.0	46.8	0.5
80	646	47.0	46.1	1.9
90	646	44.8	44.9	0.1
10	724	37.0	39.0	5.5
20	724	42.1	42.0	0.2
30	724	44.4	44.4	0.0
40	724	45.7	46.2	1.0
50	724	46.9	47.3	1.0
60	724	48.0	47.9	0.3
70	724	48.4	47.9	1.0
80	724	48.0	47.2	1.6
90	724	46.5	46.0	1.1

Table B.4.4 Phase II: Calculated and actual values of spacing factors, based on Eq. 4.4

Hauling Time (min.)	SF_i (mm)	Spacing Factor (μm)		Absolute % Error
		Actual	Calculated	
10	559	141	153	8.7
20	559	129	122	5.3
30	559	125	118	5.6
40	559	115	111	3.3
50	559	110	105	4.6
60	559	104	100	4.1
70	559	92	95	3.6
80	559	84	92	9.8
90	559	83	89	6.8
10	646	145	146	0.4
20	646	113	114	1.4
30	646	106	110	3.7
40	646	104	104	0.4
50	646	101	97	4.0
60	646	91	92	0.9
70	646	86	88	1.5
80	646	84	84	0.1
90	646	85	81	4.7
10	724	153	140	8.3
20	724	104	109	4.8
30	724	98	105	7.0
40	724	92	98	6.8
50	724	90	92	2.6
60	724	87	87	0.2
70	724	83	82	1.2
80	724	80	79	2.0
90	724	83	76	9.1

Table B.5.1 Actual and calculated values of HRWR dosages of remediation A, based on equations in Table 5.8

559 mm (22 in.) HRWR Dosage			
Hauling Time (min.)	ml/kg cementitious materials		% Error
	Actual	Calculated	
10	1.50	1.50	0.12
20	1.63	1.64	-0.47
30	1.76	1.76	0.04
40	1.89	1.86	1.43
50	1.96	1.95	0.32
60	2.02	2.02	0.17
70	2.09	2.07	0.89
80	2.12	2.10	0.91
90	2.15	2.11	1.76
635 mm (25 in.) HRWR Dosage			
Hauling Time (min.)	ml/kg cementitious materials		% Error
	Actual	Calculated	
10	2.02	2.04	-0.78
20	2.15	2.15	-0.11
30	2.28	2.26	1.18
40	2.35	2.34	0.30
50	2.41	2.41	0.14
60	2.44	2.46	-0.70
70	2.48	2.50	-0.87
80	2.51	2.52	-0.39
90	2.54	2.53	0.70
711 mm (28 in.) HRWR Dosage			
Hauling Time (min.)	ml/kg cementitious materials		% Error
	Actual	Calculated	
10	2.54	2.5655	-0.90
20	2.61	2.6245	-0.64
30	2.67	2.6835	-0.39
40	2.77	2.7425	1.03
50	2.84	2.8015	1.22
60	2.87	2.8605	0.29
70	2.93	2.9195	0.49
80	2.97	2.9785	-0.40
90	3.00	3.0375	-1.28

Table B.5.2 Remediation A: Actual versus calculated air void characteristics, based on Eq. 5.1 and 5.2

Hauling Time (min.)	Slump Flow (mm)	Specific Surface (mm ⁻¹)			Spacing Factor (μm)		
		Actual	Calculated	% Error	Actual	Calculated	% Error
10	559	38.0	39.3	-3.54	141	138	1.86
20	559	32.2	39.0	-21.39	140	140	-0.32
30	559	36.8	38.8	-5.59	109	136	-24.56
40	559	36.4	38.8	-6.50	128	132	-3.86
50	559	36.8	38.8	-5.30	126	130	-3.66
60	559	36.0	38.9	-7.96	130	128	0.85
70	559	36.0	39.1	-8.49	150	127	15.53
80	559	38.4	39.4	-2.52	126	126	-0.51
90	559	36.0	39.8	-10.69	133	125	5.76
10	635	37.5	40.6	-8.19	145	146	-0.50
20	635	37.8	40.9	-8.15	126	137	-8.86
30	635	39.7	41.4	-4.32	128	129	-0.74
40	635	39.3	41.9	-6.60	116	124	-6.74
50	635	40.7	42.6	-4.62	122	120	0.88
60	635	43.4	43.3	0.14	129	118	8.50
70	635	42.0	44.2	-5.11	112	116	-3.80
80	635	42.0	45.2	-7.50	117	115	1.39
90	635	37.9	46.2	-21.98	145	114	21.52
10	711	36.9	40.6	-10.14	153	153	-0.04
20	711	36.9	41.6	-12.87	140	134	4.03
30	711	39.5	42.7	-8.20	118	122	-3.49
40	711	40.4	43.9	-8.67	119	115	3.17
50	711	41.3	45.2	-9.50	122	111	9.20
60	711	44.3	46.6	-5.33	107	108	-0.62
70	711	44.4	48.2	-8.44	103	105	-2.31
80	711	42.6	49.8	-16.91	145	104	28.53
90	711	45.6	51.5	-12.94	109	102	6.19

Table B.5.3 Remediation B: Actual air content versus values calculated using equations in Table 5.15

Slump Flow (mm)	Hauling Time (min.)	Air Content (%)		% Error
		Actual	Calculated	
559	10	6.0	5.9	1.9
	20	6.5	6.4	2.0
	40	7.3	7.4	-0.7
	60	8.3	8.3	-0.3
	80	9.5	9.3	2.0
635	10	6.3	6.4	-1.6
	20	6.8	6.7	1.2
	40	7.3	7.2	0.6
	60	7.8	7.7	0.0
	80	8.3	8.3	-0.3
711	10	6.0	6.1	-1.0
	20	6.3	6.2	0.8
	40	6.5	6.5	0.4
	60	6.8	6.7	0.1
	80	7.0	7.0	-0.3

Table B.5.4 Remediation B: Actual versus calculated air void characteristics, based on Eq. 5.3 and 5.4

Hauling Time (min.)	Slump Flow (mm)	Specific Surface (mm^{-1})			Spacing Factor (μm)		
		Actual	Calculated	% Error	Actual	Calculated	% Error
10	559	38.0	36.2	4.75	141	136	3.71
20	559	40.5	37.5	7.42	117	119	-1.90
40	559	46.2	40.1	13.10	96	94	1.91
60	559	41.4	42.8	-3.34	111	81	26.95
80	559	43.7	45.4	-3.76	78	80	-3.02
10	635	37.5	39.6	-5.70	145	147	-1.47
20	635	32.6	40.9	-25.47	143	130	9.03
40	635	42.0	43.6	-3.63	109	105	3.18
60	635	48.6	46.2	4.90	89	92	-3.47
80	635	50.1	48.8	2.57	89	91	-2.25
10	711	36.9	36.9	-0.09	153	156	-2.01
20	711	44.6	38.2	14.18	101	139	-37.64
40	711	46.1	40.9	11.42	106	114	-7.53
60	711	43.6	43.5	0.19	111	101	8.99
80	711	43.8	46.1	-5.27	107	100	6.59

REFERENCES

- Aarre, T. (1998). "Air Void Analyzer." *Concrete Technology Today*, Portland Cement Association, 19(1), 1-3.
- AASHTO T 121. (2005). "Mass per Cubic Meter (Cubic Foot), Yield, and Air Content (Gravimetric) of Concrete," American Association of State Highway and Transportation Officials, www.aashto.org.
- AASHTO T 152. (2005). "Air Content of Freshly Mixed Concrete by the Pressure Method," American Association of State Highway and Transportation Officials, www.aashto.org.
- AASHTO T 196. (2005). "Air Content of Freshly Mixed Concrete by the Volumetric Method," American Association of State Highway and Transportation Officials, www.aashto.org.
- AASHTO T 199. (2006). "Air Content of Freshly Mixed Concrete by the Chace Indicator," American Association of State Highway and Transportation Officials, www.aashto.org.
- ACI Committee 318. (2005). *Building Code Requirements for Structural Concrete and Commentary: ACI 318-05*. ACI Committee Report, Farmington Hills, Michigan: American Concrete Institute.
- ASTM C 29-07. "Test Method for Bulk Density ("Unit Weight") and Voids in Aggregate," American Society for Testing and Materials, www.astm.org.
- ASTM C 33-07. "Specification for Concrete Aggregates," American Society for Testing and Materials, www.astm.org.
- ASTM C 39-05. "Standard Test Method for Compressive Strength of Cylindrical Concrete Specimens," American Society for Testing and Materials, www.astm.org.
- ASTM C 138-08. "Standard Test Method for Density (Unit Weight), Yield, and Air Content (Gravimetric) of Concrete," American Society for Testing and Materials, www.astm.org.
- ASTM C 150-07. "Specification for Portland Cement," American Society for Testing and Materials, www.astm.org.

- ASTM C 173-08. "Standard Test Method for Air Content by the Volumetric Method," American Society for Testing and Materials, www.astm.org.
- ASTM C 192-07. "Practice for Making and Curing Concrete Test Specimens in the Laboratory," American Society for Testing and Materials, www.astm.org.
- ASTM C 231-08. "Standard Test Method for Air Content of Freshly Mixed Concrete by the Pressure Method," American Society for Testing and Materials, www.astm.org.
- ASTM C 457-08. "Standard Test Method for Microscopical Determination of Parameters of the Air-Void System in Hardened Concrete," American Society for Testing and Materials, www.astm.org.
- ASTM C 494-08. "Specification for Chemical Admixtures in Concrete," American Society for Testing and Materials, www.astm.org.
- ASTM C 618-08. "Specification for Coal Fly Ash and Raw or Calcined Natural Pozzolan for Use in Concrete," American Society for Testing and Materials, www.astm.org.
- ASTM C 1611-05. "Standard Test Method for Slump Flow of Self-Consolidating Concrete," American Society for Testing and Materials, www.astm.org.
- ASTM C 1621-06. "Standard Test Method for Passing Ability of Self-Consolidating Concrete by J-Ring," American Society for Testing and Materials, www.astm.org.
- Baltrus, J. P., and LaCount, R.B. (2001). "Measurement of adsorption of air-entraining admixture on fly ash concrete and cement." *Cement and Concrete Research*, 31, 819-824.
- Beaupré, D., Lacombe, P., and Khayat, K.H. (1999). "Laboratory investigation of rheological properties and scaling resistance of air entrained self-consolidating concrete." *Materials and Structures*, 32, 235-240.
- Birikh, R., Briskman, V., Velards, M., and Legros, J.-C. (2003). *Liquid Interfacial Systems: Oscillations and Instability*. New York: Marcel-Dekker, Inc.
- Bonen, D., and Shah, S.P. (2005). "Fresh and hardened properties of self-consolidating concrete." *Progressive Structural Engineering Materials*, 4, 14-26.
- Bosilijkov, B., Duh, D., and Žarnić, R. (2005). "Salt Frost Scaling of Different SCCs Made From Locally Available Materials." *Proceedings from the 4th International RILEM Symposium on Self-Compacting Concrete*.

- Brite/Euram Project No: BE-3376-89, (1991-1994). "Quality assurance of concrete based on testing of the fresh, still plastic concrete."
- Bruere, G.M. (1971). "Air-entraining actions of anionic surfactants in portland cement pastes." *Journal of Applications in Chemical Biotechnology*, 21, 61-64.
- Chatterji, S. (2003). "Freezing of air-entrained cement-cased materials and specific actions of air-entraining agents." *Cement and Concrete Research*, 25(7), 759-765.
- Christensen, B., and Ong, F. (2005). "The Resistance of Self-Consolidating Concrete (SCC) to Freezing and Thawing Cycles." *Proceedings from the 4th International RILEM Symposium on Self-Compacting Concrete*.
- Cordon, W.A. and Merrill, D. (1963). "Requirements for Freezing and Thawing Durability of Concrete." *Proceedings of the ASTM*, 63.
- Corr, D.J., Juenger, M.C.G., Monteiro, P.J.M., and Bastacky, J. (2004). "Investigating entrained air voids and Portland cement hydration with low-temperature scanning electron microscopy." *Cement & Concrete Composites*, 26, 1007-1012.
- Crawford, G.L., Wathne, L.G., and Mullarky, J. I. (2003). "A 'Fresh' Perspective on Measuring Air in Concrete." *2003 Bridge Conference*, U.S.A.
- Daczko, J.A. and Kerns, M. (2008). "The New Variety of Polycarboxylate Dispersants." *Concrete Construction*, 53(1), 62-66.
- Dodson, V.H. (1990). *Concrete Admixtures*, New York: Van Nostrand Reinhold.
- Du, L., and Folliard, K.J. (2005). "Mechanisms of air entrainment in concrete." *Cement and Concrete Research*, 35, 1463-1471.
- EN 480-11 European Committee for Standardization. (1998). *Admixtures for concrete, mortar and grout – test methods – Part 11: Determination of air void characteristics in hardened concrete*. European Standard EN 480-11.
- Hanehara, S., and Yamada, K. (1999). "Interaction between cement and chemical admixture from the point of cement hydration, adsorption behaviour of admixture, and paste rheology." *Cement and Concrete Research*, 29, 1159-1165.
- Hattori, K., and Izumi, K. (1998). "Calculation of viscosities of cement pastes based on a new rheological theory." In *Electrical Phenomena at Interfaces* (467-483). New York: Marcel Dekker, Inc.
- Henrichsen, A. (2002). "Air-entraining and frost resistance properties of concrete," *ACI Fall Convention*, Phoenix, U.S.A.

- Khayat, K. H., and Assaad, J. (2002). "Air Void Stability in Self-Consolidating Concrete." *ACI Materials Journal*, 99(4), 408-416.
- Khayat, K. H. (2000). "Optimization and Performance of Air-Entrained, Self-Consolidating Concrete." *ACI Materials Journal*, 97(5), 526-535.
- Khayat, K.H. (1995). "Effects of Anti-Washout Admixtures on Fresh Concrete Properties," *ACI Materials Journal*, 92(2), 164-171.
- Kosmatka, S.H., Kerkhoff, B., and Panarese, W.C. (2002). *Design and Control of Concrete Mixtures*, Skokie, Illinois: Portland Cement Association.
- Lachemi, M., Hossain, K.M.A., Lambros, V., Nkinamubanzi, P.-C., and Bouzoubaâ, N. (2004). "Self-consolidating concrete incorporating new viscosity modifying admixtures." *Cement and Concrete Research*, 34, 917-926.
- Magura, D. (1996). "Evaluation of the Air Void Analyzer," *Concrete International*, 18(8), 55-59.
- Malhotra, V. M. (1981). "Effect of repeated dosages of superplasticizers on slump, strength and freeze-thaw resistance of concrete." *Materials and Structures*, 12(2), 79-89.
- ME 03-10 Technical Memorandum. (2003). "Experimental Use of Self-Consolidating Concrete for Precast Prestressed Box Beams." Maine Department of Transportation.
- Mindess, S., and Young, J.F. (1981). "Concrete." Englewood Cliffs, New Jersey: Prentice-Hall, Inc.
- Myers, D. (1999). *Surfaces, Interfaces, and Colloids*, New York: John Wiley & Sons.
- Nehdi, M., Pardhan, M., and Koshowski, S. (2004). "Durability of self-consolidating concrete incorporating high-volume replacement composite cements." *Cement and Concrete Research*, 34, 2103-2112.
- Operation Manual for DBT Air Void Analyzer: AVA Manual, AVA-2230. (2005). Copenhagen, Denmark: Germann Instruments A/S.
- Ozyildirim, C., and Lane, D.S. (2003). "Evaluation of Self-Consolidating Concrete," Virginia Transportation Research Council.
- Pigeon, M., Saucier, F., and Plante, P. (1990). "Air Void Stability Part IV: Retempering." *ACI Materials Journal*, 87(3), 252-259.

- Plante, P., Pigeon, M., and Foy, C. (1989). "The Influence of Water-Reducers on the Production and Stability of the Air Void System in Concrete." *Cement and Concrete Research*, 9, 621-633.
- Plante, P., Pigeon, M., and Saucier, F. (1989). "Air Void Stability, Part II: Influence of Superplasticizers and Cement." *ACI Materials Journal*, 86, 581-589.
- Powers, T.C. (1964). "Topics in Concrete Technology 3: Mixtures Containing Intentionally Entrained Air," *Journal of the PCA Development Laboratories*, 6(3), 19-42.
- Powers, T.C. (1965). "Topics in Concrete Technology 3: Characteristics of Air-Void Systems." *Journal of the PCA Development Laboratories*, 7(1), 23-41.
- Ravina, D., and Soroka, I. (1994). "Slump loss and compressive strength of concrete made with WRR and HRWR admixtures and subjected to prolonged mixing." *Cement and Concrete Research*, 24(8), 1455-1462.
- Rixom, R., and Mailvaganam, N. (1999). *Chemical Admixtures for Concrete*, New York: E & F.N. Spon Ltd.
- Saucier, F., Pigeon, M., and Cameron, G. (1991). "Air Void Stability, Part V: Temperature, General Analysis, and Performance Index." *ACI Materials Journal*, 88, 25-36.
- Saucier, F., Pigeon, M., and Plante, P. (1990). "Air Void Stability, Part III: Field Tests of Superplasticized Concretes." *ACI Materials Journal*, 87(1), 3-11.
- SIKA ViscoCrete. (2008). "Self-Consolidating Concrete." Technology & Concepts Brochure.
- VanderWerf, P.A. and Watson, D. (2007). "Reliable Air Entrainment." *Concrete International*, 29(11), 42-46.
- Vickers, M., Jr., Farrington, S.A., Bury, J.R., and Brower, L.E. (2005). "Influence of dispersant structure and mixing speed on concrete slump retention." *Cement and Concrete Research*, 35, 1882-1890.

VITA

Graduate College
University of Nevada, Las Vegas

Mary Ellen Barfield

Local Address:

2721 San Lago Ct.
Las Vegas, NV 89121

Home Address:

4701 Sunflower Dr.
Rockville, MD 20853

Degrees:

Bachelor of Science, Civil Engineering, 2004
United States Air Force Academy

Special Honors and Awards:

Army Commendation Medal, 2006
Air Force Achievement Medal, 2006
Afghanistan Campaign Medal, 2006
Tau Beta Pi Engineering Honor Society, 2003

Thesis Title: Air Void Characteristics of Air-Entrained Self-Consolidating Concrete

Thesis Examination Committee:

Chairperson, Dr. Nader Ghafoori, Ph. D.
Committee Member, Dr. Samaan Ladkany, Ph. D.
Committee Member, Dr. Aly Said, Ph. D.
Committee Member, Dr. Ying Tian, Ph. D.
Graduate Faculty Representative, Mr. Alfredo Fernández-González, M. Arch.